Phenotypic heterogeneity and preclinical change in familial Alzheimer's disease

SUBMITTED TO UNIVERSITY COLLEGE LONDON FOR
THE DEGREE OF
DOCTOR OF PHILOSOPHY

NATALIE SARAH RYAN

INSTITUTE OF NEUROLOGY, UNIVERSITY COLLEGE LONDON

2017

DECLARATION STATEMENT

I, Natalie Sarah Ryan, confirm that the work presented within this thesis is my own. Where information has been derived from other sources, I confirm that this has been indicated in the thesis.

Natalie Sarah Ryan

ABSTRACT

This thesis investigates relationships between clinical, neuroimaging and neuropathological features in autosomal dominant familial Alzheimer's disease (FAD), with the aim of studying phenotypic heterogeneity and preclinical change.

Chapters 1 and **2** introduce the background to the problem to be addressed in this thesis with an emphasis on current understanding of clinical and imaging changes in AD, and specifically in FAD. The FAD phenotype can be highly variable and, although it shares many clinical features with sporadic AD, it also possesses important differences. The clinical spectrum of FAD is first investigated, through analysis of all symptomatic cases studied at our research centre over the past twenty-five years **(Chapter 3)**. Associations between phenotypic and pathological heterogeneity are then explored, with a study investigating genetic determinants of white matter hyperintensities and cerebral amyloid angiopathy (CAA) in FAD **(Chapter 4)**. CAA is a common but variable feature of AD that appears to be an important factor in amyloid-modifying therapy and the term 'ARIA' has been coined to describe amyloid-related imaging abnormalities, thought to relate to vascular amyloid, that have been observed in a variety of amyloid-modifying therapy trials. Spontaneous changes of ARIA in FAD and the genetic risk factors that may provoke them are then described **(Chapter 5)**. The recent launch of preclinical treatment trials for FAD necessitates better understanding of the trajectory of biomarker changes early in the disease. Observations from amyloid imaging studies, of presymptomatic amyloid deposition in the thalamus and striatum, motivated the final study, which examines changes in volume and diffusivity of these subcortical structures and their connecting white matter tracts in symptomatic and presymptomatic FAD mutation carriers **(Chapter 6)**.

Together, these studies demonstrate that exploring phenotypic heterogeneity and preclinical imaging changes can illuminate aspects of the underlying disease process, informing our understanding of FAD and potential effects of treatment.

TABLE OF CONTENTS

1 Introduction 9

1.1 History and conceptualisation of Alzheimer's disease 9

1.2 Alzheimer's disease pathogenesis and the role of genetic mutations 19

1.3 Clinical manifestations of Alzheimer's disease 22

1.4 Future perspectives 38

2 Imaging biomarkers in Alzheimer's disease 41

2.1 Introduction 41

2.2 Imaging in Clinical Practice 42

2.3 Imaging in Research 46

2.4 Imaging presymptomatic Alzheimer's disease 51

3 Clinical phenotype and genetic associations in autosomal dominant familial Alzheimer's disease: a case series 60

3.1 Introduction 60

3.2 Materials and methods 61

3.3 Results 64

3.4 Discussion 81

4 Genetic determinants of white matter hyperintensities and amyloid angiopathy in familial Alzheimer's disease 86

4.1 Introduction 86

4.2 Materials and methods 88

4.3 Results 91

4.4 Discussion 105

5 Amyloid-related imaging abnormalities (ARIA) in familial Alzheimer's disease 112

5.1 Cerebral microbleeds (ARIA-H) in familial Alzheimer's disease 113

5.2 Spontaneous ARIA-E and cerebral amyloid angiopathy related inflammation in *PSEN1*-associated familial Alzheimer's disease 117

6 MRI evidence for presymptomatic change in thalamus and caudate in familial Alzheimer's disease 125

6.1 Introduction 125

6.2 Materials and methods 128

6.3 Results 133

6.4 Discussion 144

7 Thesis summary and conclusions 151

7.1 Summary 151

7.2 Imaging manifestations of familial Alzheimer's disease pathology 153

7.3 White matter involvement in familial Alzheimer's disease 157

7.4 Heterogeneity in the familial Alzheimer's disease phenotype 159

7.5 Limitations 160

7.6 Clinical implications 161

7.7 Directions for future research 163

7.8 Implications for clinical trials 165

7.9 Applying findings from familial Alzheimer's disease to sporadic Alzheimer's disease 166

8 Publications 168

9 Division of labour 175

10 Acknowledgements 178

11 Appendix 179

11.1 Neurological presentations of familial Alzheimer's disease 179

11.2 Genetics methods 180

11.3 Immunohistochemical methods in the pathology cohort 182

11.4 Grading system used to assess severity of cerebral amyloid angiopathy. 182

11.5 Semi-quantitative assessment of myelin loss, gliosis and microglial expression 182

12 Bibliography 184

13 Glossary 229

TABLES

Table 1.1 Clinical and pathological features of autosomal dominant *APP* mutations lying within the Aβ coding domain....35
Table 3.1 Mutations carried by the individuals in the cohort 65
Table 3.2 Mutations associated with atypical phenotypes and additional neurological features in our cohort 72
Table 4.1 Subjects' characteristics and total age-related white matter change (ARWMC) scores....93
Table 4.2 Mean total white matter hyperintensity score for each *PSEN1* mutation in the cohort....94
Table 4.3. Autopsy cohort subject demographics and results of CAA grading and blood vessel analysis 98
Table 4.4 Semi-quantitative assessment of white matter pallor, gliosis and microglial expression in parietal and occipital deep white matter 102
Table 6.1 Subject demographics, neuropsychological and clinical data.....135
Table 6.2 Mean ± sd volumes and diffusivity indices in the grey matter regions of interest. 140
Table 6.3. Mean ± sd diffusivity indices in the white matter tracts of interest. 142

FIGURES

Figure 1.1 Neurofibrillary tangles drawn by Alzheimer above the caption 'Peculiar fibrillary changes of the nerve cells. Progressed stage of disease' 12
Figure 1.2 Recombinant events in DRC Family 23 localised the AD locus to a region that included *APP* 16
Figure 1.3 *APP* gene with mutations indicated 21
Figure 2.1 Medial temporal lobe atrophy on MRI; a sensitive marker of neurodegeneration in AD. 45
Figure 2.2. Amyloid imaging with PIB-PET can be positive early in AD and may predict conversion from MCI to AD 48
Figure 2.3 PIB-PET imaging showing prominent striatal amyloid deposition in a presymptomatic *PSEN1* mutation carrier approximately three years prior to anticipated age at onset. 53
Figure 2.4 Hypothetical model of dynamic biomarkers of AD expanded to explicate the preclinical phase, ... 55
Figure 3.1 Familial Alzheimer's disease study participants 62
Figure 3.2 Age at onset for individuals with mutations involving each exon of the *PSEN1* gene. 69
Figure 3.3 Location of the mutations present in our cohort of *PSEN1* mutation carriers, shown according to age-at-onset quartiles 70
Figure 3.4 Cognitive presentations in *APP* and *PSEN1* mutation carriers in our cohort, with presenting symptoms in the *PSEN1* group shown by exon 71
Figure 3.5 Proportion of cases with each neurological feature for mutations involving each of the exons of *PSEN1* 75
Figure 3.6 Neuropathological findings in a 70 year old man with the novel *PSEN1* p.Ser132Ala mutation presenting with a Dementia with Lewy bodies phenotype . 78
Figure 3.7 Neuropathological findings in a 42 year old man with a *PSEN1* double substitution, p.Thr291Ala and p.Ala434Thr, presenting with cognitive impairment, pyramidal and extrapyramidal signs 80
Figure 4.1: Example MR images from subjects with (A) p.Glu120Lys (B) Intron 4 (g.23024delG) (C) p.Met139Val (D) p.Ile202Phe (E) p.Leu235Val (F) p.Glu280Gly (G) and (H) p.Arg278Ile and (I) p.Pro264Leu mutations, whose location within the *PSEN1* gene is indicated. 95

Figure 4.2 Mean density of immunohistochemical staining in parietal and occipital white matter. 99
Figure 4.3 Pathological analysis of familial Alzheimer's disease with *PSEN1* mutations. 103
Figure 5.1 3T T2-weighted FLAIR coronal MRI shows white matter lesions, but no significant medial temporal lobe atrophy in a patient with the p.Arg269His *PSEN1* mutation. 115
Figure 5.2 3T T2* MRI shows multiple lobar hypointensities consistent with microbleeds in a patient with the p.Arg269His *PSEN1* mutation. 116
Figure 5.3 Serial MRI scans demonstrating the appearance and then subsequent partial resolution of ARIA 119
Figure 5.4 Neuropathological analysis 120
Figure 6.1 Regions of interest 130
Figure 6.2 Mean and standard error z scores for presymptomatic and symptomatic mutation carriers on standard neuropsychological tests. 134
Figure 6.3 VBM results showing (top left) areas of grey matter reduction in PMCs compared with controls after correction for multiple comparisons at FWE < 0.1 and the effect-map for the PMC versus control group comparison. 137
Figure 6.4. VBM results showing (top) grey matter reduction and (bottom) white matter reduction in SMCs compared with controls. 138
Figure 6.5 TBSS results demonstrating areas of significantly decreased FA and significantly increased axial, radial and mean diffusivity in SMCs compared to controls. 139

1 Introduction

1.1 History and conceptualisation of Alzheimer's disease

It is just over one hundred years since the death of Aloysius "Alois" Alzheimer (1864-1915). In that time the disease that bears his name has gone from being considered a rare condition only affecting younger people to a major public health priority as Governments face ever-increasing numbers of people with dementia (Fox and Petersen, 2013). Worldwide some 40 million people have dementia and AD is the most important cause (Prince *et al.*, 2013). A recent UK poll identified AD as the greatest concern about later life for British people over 60 years old, more feared even than cancer or the death of family and friends [1]. Whilst AD may now be at the forefront of the public imagination, it was not always thus. Over the past century, concepts of what AD is, who it affects and how common it may be have undergone a number of dramatic shifts. As the historian of medicine and psychiatry Erwin Ackerknecht has argued, if any science is to chart new and reliable paths, it must continually re-examine its essential premises, which can best be understood by studying its origins. In this first section of the Introduction, I therefore examine the diverse factors that have contributed to the evolution of the concept of AD that exists today. The study of families affected by genetic forms of AD and developments in neuroimaging emerge as two of the major driving forces behind the modern conceptualisation of AD and form key themes of this thesis. These topics: familial AD (FAD) and neuroimaging, are then each discussed in detail, providing the background to the data chapters that follow.

The metaphor of 'framing' has been used to describe the dynamic process by which schemes for explaining and classifying disease are created and evolve (Rosenberg and Golden, 1992). Defining a disease involves first putting a name to the symptoms of an underlying biological event and creating a disease concept; a process that is dependent on the nature of the biological event and the forms of knowledge and technology available at the time to explain it. However, the definition is framed in a way that makes sense to, and serves wider objectives of, the groups it concerns. Disease frames therefore reflect and incorporate values of the society and culture that created them and provide a means for projecting, legitimizing and enforcing these ideas. They are constructed and refined through negotiations between all groups interested in the

disease and as the number of groups interested in a disease grows, these negotiations become more complex and multi-layered. Doctors and scientists, governments, research institutions and pharmacological companies and patients and their families may all play a role in shaping how a disease is framed. Each of these parties has contributed to the changing conceptualisation of AD over the past century.

1.1.1 Alzheimer, Auguste D., and the defining of a disease

On 25th November 1901, a 51 year old woman was admitted to the Municipal Asylum for Lunatics and Epileptics in Frankfurt. The patient was Auguste D. and the admitting psychiatrist Alois Alzheimer. Mislaid for years, the original file describing her case with her admission clerking handwritten by Alzheimer was found in 1995. It contains a detailed description of her clinical presentation: she had been well until March 1901 when she developed unprovoked paranoia that her husband was having an affair with a neighbour. Soon after, she was noticed to have difficulty remembering things and was making mistakes preparing meals and dealing with money. She became progressively disoriented to time and place and paranoid that people were talking about her. Alzheimer gives examples of the deficits he observes on cognitive assessment, including severely impaired recall memory of objects she has just seen and correctly named. On reading, she omits sentences, and she is unable to progress with writing, repeating "I have lost myself". Her spontaneous speech is "full of paraphrasic derailments and perseverations". Later in her admission, he notes "she behaves as if blind, touching other patients on their faces while they fight her." Auguste D. remained in the institution until her death in 1904. By this time, Alzheimer had moved to Munich to continue his medical and scientific work at the Royal Psychiatric Clinic, under the directorship of Emil Kraepelin. Alzheimer headed the neuroanatomic laboratory and requested that Auguste D.'s file and brain be sent to him so that he could study the neuropathological features of her disease. As a physician-researcher, he believed that clinical practice and laboratory research complemented each other in the quest to understand the diseases that afflicted his patients, once writing "Why should not the physician improve his competence by enlarging scientific knowledge of psychiatry besides doing his daily clinical practice?" (Whitehouse *et al.*, 2000)

Alzheimer presented the clinical and pathological findings from Auguste D.'s case at the meeting of Southwest German Psychiatrists held in Tübingen, in 1906 and his lecture was published under the title 'A Characteristic Disease of the Cerebral Cortex' the following year. He described and beautifully recorded (Figure 1.1) characteristic changes in the neurofibrils revealed by the Bielschowsky silver stain at autopsy. Thick fibrils accumulated in apparently normal-appearing cells until "eventually, the nucleus and cytoplasm disappeared, and only a tangled bundle of fibrils indicated the site where once the neuron had been located." Severe neuronal loss was observed and "…over the entire cortex, and in large numbers especially in the upper layers, miliary foci could be found which represented the sites of deposition of a peculiar substance." Many years later, hyperphosphorylated tau was found to be the key component of the tangles and amyloid-beta (Aβ) the 'peculiar substance' that formed the core of the plaques. Psychoanalytic studies presented at the meeting received more attention than Alzheimer's paper and were the ones to get reported in the local press. However, in 1910 Kraepelin coined the term 'Alzheimer's disease' in the eighth edition of his *Handbook of Psychiatry,* declaring it to be a specific clinical-pathological disease entity.

Examining the historical context in which these events occurred reveals a number of disparate factors that enabled the observations to be made by Alzheimer and may have influenced Kraepelin in defining them soon after as an eponymous disease. As often is the case, technological advances laid the ground for novel insights: the growth of German industry in the second half of the nineteenth century was revolutionizing histology. Improved microscopes had been developed and the creation of the aniline dye industry brought a plethora of new dyes and advances in staining methods, some of which found applications in histopathology. Alzheimer had worked closely with the neurologist and histopathologist Franz Nissl and could not have made his observations without the silver staining techniques developed by Bielschowsky in 1902, which allowed alterations to the neuronal cytoskeleton to be seen in such remarkable detail. Another important factor was the evolution of concepts around psychiatric disease. For Kraepelin, the explanation for mental disorders lay in organic changes in the brain and clinical delineation of distinct disease entities was the route to understanding the relationship between mind and brain. The clinical-pathological syndrome described by Alzheimer provided Kraepelin with a strong example of his approach; naming it a

"disease" after a colleague who shared his belief in an organic basis for psychiatric illness can perhaps be seen as putting down a marker for his theory over rival psychoanalytic ideologies.

Figure 1.1 Neurofibrillary tangles drawn by Alzheimer above the caption 'Peculiar fibrillary changes of the nerve cells. Progressed stage of disease'

in Alzheimer, Alois "Über eigenartige Krankheitsfälle des späteren Alters." Zeitschrift für die gesamte Neurologie und Psychiatrie: Originalen vol. 4 (1910-1911): 356–385. Reprinted from (Ryan *et al.*, 2015), with permission.

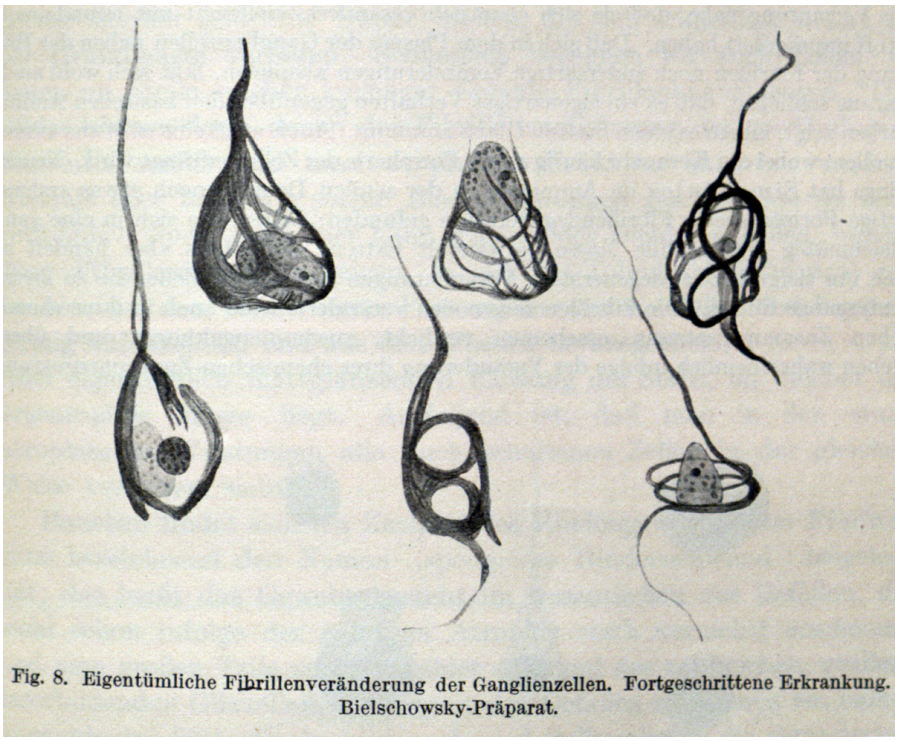

Fig. 8. Eigentümliche Fibrillenveränderung der Ganglienzellen. Fortgeschrittene Erkrankung. Bielschowsky-Präparat.

There was, however, a fundamental issue with Kraepelin's concept of AD, which was evident when he defined it and has remained a source of ambiguity and contention ever since. This was the relationship with senile dementia and normal ageing. Plaques and tangles had both been described previously, but in the brains of elderly patients with dementia. Extraneuronal plaques had been observed by Beljahow (1887), Redlich (1898) and Fischer (1907) and were renamed 'senile plaques' in 1910 by Simchowitz when he found they could also be present in non-demented elderly people, but in lower numbers. In 1906, 'destruction of the neurofibrillae' and 'neurofibrillary bundles' were

noted in senile dementia patients by Bianchi and Fuller respectively (Huppert *et al.*, 1994). However, the prevailing notion at the time was that senile dementia was an inevitable consequence of aging. "Senile dementia is that mental impairment which is a direct result of cerebral deterioration from old age," wrote the psychiatrist William Pickett in 1904. Over thirty years later, there had been little change to this view of aging. British neurologist MacDonald Critchley commented in 1939 that "frontiers between healthy and abnormal old age – between senescence and senility – [are] so ill-defined as to be scarcely recognizable."

A key feature that allowed Kraepelin to define AD as a discrete disease entity was the young age of the patients. In his 1910 *Handbook of Psychiatry*, he drew on Alzheimer's original description of Auguste D, a subsequent case report by Bonfiglio (1908) of a 60 year old Italian patient with similar clinical and histopathological findings and a case series (at the time unpublished) by his colleague Perusini (1910), which added two further young onset patients. Kraepelin felt that there were clinical features in addition to age that also distinguished these patients from those with senile dementia, including rapid progression, language disturbance, seizures and focal signs. Kraepelin however acknowledged that "The clinical interpretation of this Alzheimer's disease is still confused. Whilst the anatomical findings suggest that we are dealing with a particularly serious form of senile dementia, the fact that this disease sometimes starts already around the age of 40 does not allow this supposition." Age was therefore such a central parameter in Kraepelin's classification system and the idea that senile dementia was related to aging so entrenched in the thinking of the time that young patients were, by definition, precluded from being categorized together with senile dementia. Being so closely tied to normal aging, it was unclear whether senile dementia was a disease at all. AD as defined by Kraepelin, on the other hand, clearly fell within the realm of psychiatry and the dominant view in the decades that followed was that it represented a rare "pre-senile" condition.

1.1.2 Alzheimer's disease redefined as a 'major killer'

It was not until the second half of the twentieth century that AD become redefined as affecting late as well as early onset patients. This shift in thinking accompanied a transformation in the conceptualization of senile dementia and normal aging. The

British psychiatrist Martin Roth made a seminal contribution with his 1955 study, in which he argued that mental disorders in the elderly could be split into distinct categories, which carried very different prognoses (Roth, 1955). With senile dementia increasingly viewed as a pathological condition and distinguished from other psychiatric disorders of the elderly it could be studied in its own right, and it soon became apparent that the historical distinction from AD no longer seemed valid. In the late 1960s, Roth and his colleagues Blessed and Tomlinson demonstrated that the majority of cases of senile dementia had neurofibrillary tangles and amyloid plaques and the latter correlated with severity of cognitive impairment (Blessed *et al.*, 1968). Roth concluded in 1970 that "Traditionally the distinction between Alzheimer's disease and Senile dementia was a clear one. It rested on the occurrence in Alzheimer's disease of focal phenomena: the Parietal lobe group of features, the characteristic mixture of apraxia, agnosia, spatial disorientation and so on. In Senile dementia, on the other hand, a simple amnestic dementia was held to be the principal ingredient of the clinical picture… …German workers have recently called this distinction into question. Lauter and Meyer claim to have demonstrated focal phenomena in the senile cases. In the light of these is the distinction (between Alzheimer's disease and Senile dementia) valid clinically or pathologically, or are we left with age criteria alone?" (Whitehouse *et al.*, 2000).

With AD and senile dementia unified in a single disease concept, a line was now drawn between dementia and normal aging and it was increasingly appreciated that major cognitive impairment was not an inevitable outcome of aging. Although Glennerstedt had reported plaques in 84% of non-demented elderly people in 1933, observations that pathological features of AD may occur without dementia could be incorporated into the new framework. The work by Blessed and colleagues had demonstrated that the severity of pathology was worse in patients with dementia and, according to the psychodynamic model that was prominent among some psychiatrists working on senile dementia at the time, an individual's ability to withstand organic damage depended on a variety of personality factors, stress and life crises, as well as the underlying pathology. Once the separation between AD and senile dementia was eliminated, it was realized that AD was in fact responsible for the majority of dementia and was very common. In an editorial published in *Archives of Neurology* in 1976 entitled 'The prevalence and malignancy of Alzheimer's disease: A major killer,' Robert Katzman argued for a unifying concept of AD and senile dementia and estimated that the disease may rank as the fourth or fifth

most common cause of death in the United States (Katzman, 1976). It took some time for the distinction to be completely abandoned, with the terms 'Alzheimer's disease' and 'senile dementia of the Alzheimer type' recommended initially. However, the new conceptualisation of AD had a profound impact on public attitudes. It represented the start of AD becoming redefined as a major social and public health issue and concern for public policy.

1.1.3 Insights into the biology and genetics underlying Alzheimer's disease

Alongside the changing public perception of AD, scientific understanding of the biological basis of the disease began to grow. In the late 1970s, the cholinergic deficit in AD was identified and linked to selective degeneration of cells in the nucleus basalis of Meynert, paving the way for the subsequent development of cholinesterase inhibitors as symptomatic treatments. In 1984, George Glenner identified the Aβ protein in angiopathic blood vessels from patients with Down syndrome, and made the observation that it was homologous with that found in AD, highlighting an important possible clue to the genetic aetiology of AD. It had been recognized as early as the 1930s that there were some rare families in which multiple individuals developed AD with a pattern suggesting autosomal dominant inheritance (Lowenberg and Waggoner, 1934). The finding that individuals with AD and with full trisomy 21, who invariably develop plaques and tangles at autopsy if they live to middle age, have the same Aβ pathology put chromosome 21 in the spotlight. Aβ was subsequently identified in plaques and in 1987 the *amyloid precursor protein* (*APP*) gene was cloned and found to localize, as predicted, to chromosome 21. Direct sequencing of *APP* in a large family from Nottinghamshire with early onset AD (Dementia Research Centre (DRC) Family 23 – F23) who had volunteered to participate in research identified a mutation at codon 717, which co-segregated with disease (Goate *et al.*, 1991). Chromosome 21 linkage was not, however, identified in many of the other kindreds that were studied and it soon became clear that AD was genetically heterogeneous. Four years later, *Presenilin 1* (*PSEN1*) on chromosome 14 was identified as the major locus for autosomal dominant familial AD (FAD) (Sherrington *et al.*, 1995) and *Presenilin 2* (*PSEN2*) on chromosome 1 as the locus for a minority of cases (Levy-Lahad *et al.*, 1995). It had also recently been found that the *Apolipoprotein E4* allele was a major risk factor for sporadic early and late onset forms of AD (Corder *et al.*, 1993).

Figure 1.2 Recombinant events in DRC Family 23 localised the AD locus to a region that included *APP*

Diagram courtesy of John Hardy, Institute of Neurology, University College London (Goate *et al.*, 1991)

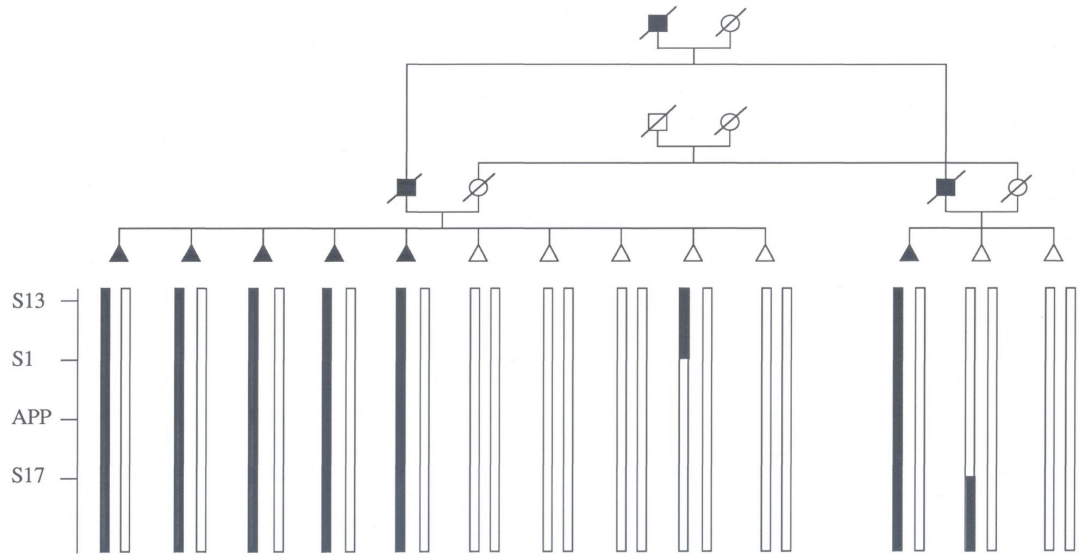

After the identification of *APOE*4 as a major risk factor for AD, almost fifteen years passed before another gene was found to be conclusively associated with the disease. However, the last decade has seen some major developments in our understanding of genetic risk factors for sporadic AD. Genome-wide association studies have identified multiple genetic loci with low risk effects for AD, including *CLU, PICALM, CR1, BIN1, MS4A6A, ABCA7, SORL1, PTK2B, EPHA1,* and *HLA-DRB5-HLA-DRB1* (Guerreiro and Hardy, 2014). The biological processes that these loci are involved in: immune and inflammatory responses; cholesterol and lipid metabolism; and endosomal vesicle recycling; have as a result been highlighted as potentially important pathways in AD pathogenesis. The role of the innate immune system was brought further to the forefront by the discovery in 2013 that rare variants in *TREM2*, a microglial surface receptor, are associated with a significantly increased risk (3x) of AD. Much as the mainstay of current symptomatic treatments for AD, the acetylcholinesterase inhibitors donepezil, rivastigmine and galantamine, can be seen to have been derived from pathological neurochemical findings of a cholinergic deficit, the current search for

disease-modifying treatments is strongly influenced by genetic findings. The biological pathways illuminated by the autosomal dominant genes and by more recent genetic studies open up further potential therapeutic avenues for drug discovery efforts in AD.

Although autosomal dominant mutations account for a very small proportion of cases of AD, the discoveries from these young onset families had, and continue to have, profound implications. The amyloid cascade hypothesis was proposed, which posits that accumulation of Aβ is the initiating event in AD pathogenesis (Hardy and Higgins, 1992). This hypothesis has had a major influence on research and motivated the development of therapies that aim to reduce production of Aβ or increase its clearance from the brain. Identification of FAD mutations also provided the information necessary to make transgenic animals in which these therapies could be tested, some with dramatic effect, before going in to a series of trials in humans. Ironically, these initial clinical trials tended to exclude the familial patients that had contributed to the ideas and models on the basis of their young age.

1.1.4 Young onset and familial Alzheimer's disease return to the spotlight

More recently, there has been a refocus on young onset AD and in particular FAD, with clinical trials belatedly turning their attention towards individuals with autosomal dominantly inherited mutations. This was largely because of changes in the view of when the disease first develops in the brain, when it is first detectable *in vivo*, and when it may be most effective to intervene. This paradigm shift has been driven by a realisation that AD has a long presymptomatic period, partly informed by the prospective study of asymptomatic individuals including those at risk of FAD. The potential for early identification and intervention has been enhanced by the development of new cerebrospinal fluid (CSF) markers and brain positron emission tomography (PET) imaging measures of amyloid and tau. More recent research diagnostic criteria for AD incorporate biomarkers and preclinical states of disease into the framework (Dubois *et al.*, 2014). Just as technological developments at the turn of the twentieth century, in the form of new histological staining methods and microscopes, facilitated the original definition of AD, advances in biomarker and imaging technology over the past decade have supported this latest conceptualization of the disease. Molecular imaging with PET tracers that bind amyloid and tau now allow us to see what

Alzheimer couldn't see: the "plaques and tangles" during life. The increasing recognition of the long preclinical period to AD coincided with a series of failures of treatment trials that included patients with mild to moderately severe dementia. The concern that emerged is that if the disease has a 10-15 year presymptomatic period (or longer) when plaques and tangles become established and widely distributed in the brain, it may be too late or at least more difficult to a slow a process that has already gathered momentum by the time a patient has established dementia. If it is possible to detect and track the extent of amyloid and tau pathology *in vivo* as well as more downstream effects such as atrophy and cognitive impairment then presymptomatic treatment trials become more feasible; offering the prospect of interventions when there has been the minimum of irreversible neuronal damage and when there is most to save in terms of function.

Hence we enter the era of presymptomatic secondary prevention trials, with studies underway to test treatments in asymptomatic individuals at risk for Alzheimer's disease by virtue of genetics, FAD or *APOE4*, or because of imaging or biochemical evidence of prodromal cerebral amyloid accumulation. The effects of therapy will be tracked with MRI, PET and CSF as well as sensitive cognitive measures, aiming to delay the onset of the symptoms that led to Auguste D's institutionalisation and that are so devastating to millions globally. Alzheimer and Auguste's contributions and the debates that surrounded them remain as relevant as ever. Observations that around a third of cognitively normal older people have positive amyloid scans have resurrected some of the century-old discussions about the relationship between dementia and normal aging, and the question of how generalizable early onset (and particularly familial) AD is to late onset disease has never been so timely. In this context, with the report in 2013 that Auguste D. had had a *PSEN1* mutation it seemed that perhaps a full circle had been reached, with treatments being tested in families that may have been her distant relatives. However, in a follow-up report the following year the mutation in Auguste D. was not validated, nor were mutations in *APP* or *PSEN2* identified (Rupp *et al.*, 2014). The rediscovery of Auguste D.'s brain sections in 1997 had allowed the pathological diagnosis of AD to be confirmed by modern immunohistochemical methods but any genetic basis for her disease (she was *APOE3* homozygous) remains, as with so many other early onset AD patients, a mystery.

The past century has seen a number of transformations in the conceptualization of AD. The 2013 G8 dementia summit recognized AD as a growing global health and economic problem, requiring serious action in terms of investment in research and development of disease-modifying therapies but also that alongside the search for prevention and treatment strategies we must invest in enabling people to live well with dementia - ensuring that patients and their families have access to early diagnosis and support that is all too often lacking. A hundred years on, Alzheimer's legacy is more relevant than ever – in fact the question of how tractable is this disease and how we care for those with it is perhaps one of the key challenges for the coming century. The concept of AD will no doubt undergo further refinements and reinventions over future decades. Reflection on the diverse factors that have shaped the concept of AD over the past century may, therefore, inform our understanding of developments in the way we perceive and respond to the disease in the years to come.

1.2 Alzheimer's disease pathogenesis and the role of genetic mutations

Since the discoveries in the early 1990s that FAD could be caused by autosomal dominantly inherited mutations in *APP, PSEN1* and *PSEN2* over two hundred variants have been described in these genes. Many are clearly established as pathogenic for AD, some are thought to represent non-pathogenic polymorphisms and in other cases, the pathogenic nature of the change is as yet unclear. In addition to trisomy 21, duplications of the *APP* gene have also been identified as a cause of FAD (Rovelet-Lecrux *et al.*, 2006). Mutations in *PSEN*1 account for the majority of cases of FAD and it is in *PSEN1* that the greatest numbers of mutations have been found, with 219 recorded to date (January 2017) compared to 51 and 16 in *APP* and *PSEN2* respectively [2]. Collectively, these mutations are thought to account for less than 1% of Alzheimer's disease cases. The degree to which FAD may be a paradigm for the much commoner, late onset, sporadic form of the disease is uncertain but the insights gleaned from the study of FAD have catalysed much of our current knowledge of the pathobiological basis of the disease. The development of cellular models and transgenic mice harbouring mutations in *APP* and the *Presenilins* has allowed the disease mechanism to be explored in detail and probed with potential therapeutic agents. As these therapies come closer to clinical application, the debate regarding how generalisable the changes of FAD are to those of

sporadic AD grows in significance. Unravelling the pathway through which specific genetic mutations translate into the manifestations of clinical AD, and how the resulting phenotypes may vary, are clearly important areas of investigation. However although much has been published describing novel FAD gene mutations and exploring their functional effects at a molecular level, there have been fewer detailed reports of the resulting clinical phenotypes (Larner and Doran, 2006, Larner and Doran, 2009, Jayadev *et al.*, 2010, Tang *et al.*, 2016). In this section of the Introduction, I review how closely the phenotype of FAD resembles and differs from that of sporadic AD. The importance of appreciating the degree of phenotypic heterogeneity that exists in both familial and sporadic AD becomes apparent and will form a major theme of this thesis. Finally, I discuss several mechanisms by which the clinical picture, and underlying pathology, may be influenced by genotype.

The pathological hallmarks of AD in both familial and sporadic cases are extracellular plaques of Aβ and intraneuronal inclusions of hyperphosphorylated tau. Although the initiating driver of pathology in sporadic AD remains unclear, it is now well recognised that mutations in all three genes known to cause FAD ultimately result in enhanced production and/or deposition of Aβ (Selkoe, 1997). The mechanisms through which they achieve this are complex and variable. APP is a transmembrane protein whose function is not yet fully determined, although it appears to play a role in neural plasticity and the regulation of synapse formation. APP may be proteolytically cleaved by α, β and γ secretases and, during its normal metabolism, it can undergo cleavage via alternative pathways. Cleavage by α-secretase is considered to be part of the non-amyloidogenic pathway in APP processing. It precludes Aβ formation as it cleaves within the segment of APP that would otherwise give rise to Aβ (see Figure 1.3) (Esch *et al.*, 1990). Upon cleavage by α-secretase, APP releases its extracellular domain, a fragment called APPsα, which is known to have neurotrophic effects. Alternatively, APP may undergo sequential cleavage by β and γ secretase. Extracellular cleavage by β-secretase (also known as BACE1: β-site of APP cleaving enzyme) generates a soluble extracellular fragment and is followed by cleavage of APP within its transmembrane domain by γ secretase. The unusual property of γ-secretase is that it may cleave APP at a variety of different sites, generating a peptide from 39-43 amino acids in length; the amyloid- β (Aβ) protein. PSEN1 forms part of the γ secretase complex (De Strooper *et al.*, 1998) and the majority of pathogenic *PSEN1* mutations are located in areas thought

to lie in the vicinity of its transmembrane domains. Under normal conditions, the majority of Aβ is in the form of a 40 amino acid long peptide "Aβ-40". There is some additional production of the longer moiety; Aβ-42, which accounts for 5-15% of the total pool of Aβ in health. Smaller quantities of other Aβs, both longer and shorter, may also be observed. Aβ peptides, particularly Aβ-42, can cause toxic effects on neuronal and synaptic function as intracellular oligomers and can also seed to form extracellular precipitates in the form of amyloid plaques. Aβ-42 is the most amyloidogenic form of the peptide; its hydrophobic nature makes it more susceptible to conformational change leading to amyloid fibrillogenesis (Jarrett *et al.*, 1993, McGowan *et al.*, 2005).

Figure 1.3 *APP* gene with mutations indicated

Diagram courtesy of Richard Crook, Mayo Clinic Jacksonville, and John Hardy, Institute of Neurology, University College London. Reprinted from (Ryan and Rossor, 2010), with permission.

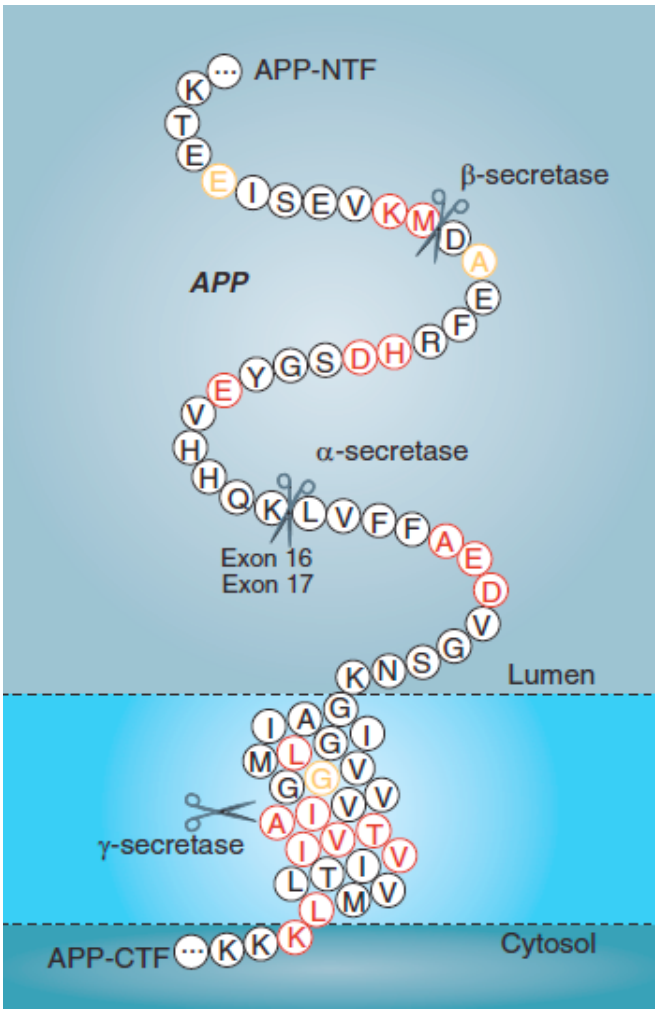

Most FAD-causing mutations were thought to either increase Aβ-40 and Aβ-42 or alter the ratio between them. However, the discovery of the 'Arctic' *APP* mutation (p.Glu693Gly) in a Swedish family, which is located away from the secretase sites, led to the suggestion of an alternative pathogenic mechanism. Aβ-40 and Aβ-42 are actually found in decreased levels with this mutation, however they have an increased propensity to form protofibrils, which may accelerate their deposition in intracellular or extracellular locations, or both (Nilsberth *et al.*, 2001). More recent kinetic studies have investigated how γ-secretase carries out a number of sequential cleavages of its substrates. There is an initial endopeptidase cleavage releasing a soluble intracellular domain, which may translocate to the nucleus to regulate gene expression. Successive carboxypeptidase-like cleavages then process the remaining transmembrane fragment. *PSEN1* mutations all appear to decrease the efficiency of this carboxypeptidase-like activity, resulting in the release of longer Aβ peptides, which are more prone to aggregation (Chavez-Gutierrez *et al.*, 2012, Szaruga *et al.*, 2015).

1.3 Clinical manifestations of Alzheimer's disease

The most obvious and striking difference between familial and sporadic AD in general is that individuals harbouring FAD mutations typically have a much younger age at onset. That the disease should manifest at an earlier age is not surprising, given the increased Aβ deposition that these mutations cause. The youngest ages at onset are seen in families with *PSEN1* mutations, which typically fall within the range 35-55 years – although cognitive symptoms may manifest as early as the third decade of life (Moehlmann *et al.*, 2002). *APP* mutations tend to give rise to symptom onset between 40-65 years and *PSEN2* mutations between 40-70 years. It has been suggested that, as well as being associated with a younger age at onset of disease, *PSEN1* mutations give rise to shorter disease durations (4.8-6.8 years) than *PSEN2* and *APP* mutations (range 4.4 – 10.8 years and 9.0 – 16 years respectively) (Holmes, 2002). However, the survival data of different series demonstrate considerable variation. Although the disease course of FAD is often considered to be more aggressive, some reports find comparable disease durations for the familial and sporadic forms of AD (Godbolt *et al.*, 2004). A large meta-analysis, which pooled information from a number of different FAD datasets, found the average disease duration in FAD (9.7 years) to be just modestly shorter than

the average disease duration in sporadic AD (11.3 years) (Ryman *et al.*, 2014). Drawing direct comparisons between disease duration in familial and sporadic AD is problematic as survival is likely to be affected by age at onset itself. Younger, healthier patients may survive longer at more severe stages of disease than older patients with sporadic AD, who are more likely to be frail and often have multiple co-morbidities. Another major difficulty in interpreting survival data is that estimates for age at symptom onset are highly subjective and unreliable. Symptoms tend to develop insidiously so, in some cases, may pass unrecognised for quite some time. On the other hand, as awareness of the heritable nature of the disease heightens with subsequent generations, symptoms are likely to be noticed at an earlier stage. This probably contributes to the range in age at onset that is witnessed both between and within families with the same mutation. However, other genetic and epigenetic factors are also likely to be important in modulating age at onset.

Possession of an *APOE*4 allele has been reported to be associated with younger symptom onset in a family with the *APP* p.Val717Ile mutation (Sorbi *et al.*, 1995), as is the case in sporadic AD, although *APOE* genotype was not found to influence age at onset in kindreds with *APP* mutations at codon 692 or 693 (Haan *et al.*, 1994). In *PSEN1* mutations, a modifying effect on age at onset by the *E*4 allele was not previously thought to occur (Van Broeckhoven *et al.*, 1994). However, when a single large Colombian kindred with the p.Glu280Ala *PSEN1* mutation was examined, the *APOE*4 allele did appear to be associated with an earlier age at onset (Pastor *et al.*, 2003). Younger ages at onset in *APOE*4 carriers have also been reported in kindreds of Volga German descent carrying the same p.Asn141Ile *PSEN2* mutation (Wijsman *et al.*, 2005). In the recent meta-analysis of pooled FAD datasets, as expected, an individual's age at symptom onset correlated strongly with their parental age at onset, the mean age at onset for their family and the mean age at onset for their mutation type (Ryman *et al.*, 2014). However, although mutation type accounted for a majority of the variance in age at symptom onset, substantial variation remained within many families and mutation types, suggesting the existence of other genetic, environmental and stochastic modifying factors (Fox *et al.*, 1997). Although there were trends towards younger ages at onset in *APOE*4 carriers and later ages at onset in *APOE*2 carriers, these did not reach significance in the pooled datasets. Pathological studies have shown that the proportion of brain tissue occupied by Aβ-42-containing plaques is significantly higher in *PSEN1*-

associated AD than sporadic AD. Although there does not appear to be a difference in the amount of tissue containing Aβ-40 between these two disease groups, both *PSEN1*-AD and sporadic AD show the same relationship between Aβ deposition and *APOE* genotype: Individuals who carry an *E*4 allele demonstrate a greater proportion of Aβ-40 deposition in both familial and sporadic disease. It has been suggested that, in the presence of the apolipoprotein *E*4 isoform, the threshold for Aβ-40 fibrillisation is decreased, fostering the deposition of Aβ-40 onto Aβ-42-containing plaques (Mann *et al.*, 2001).

1.3.1 Cognitive phenotypes

1.3.1.1 Amnestic presentations

The majority of individuals with FAD have similar clinical presentations to those with sporadic AD, comprising early impairment of episodic memory, which gradually progresses to involve multiple cognitive domains. Longitudinal group studies of individuals at risk of FAD demonstrate that the earliest neuropsychological manifestations are a subtle fall in verbal memory and performance IQ scores, occurring at least 2-3yrs presymptomatically (Fox *et al.*, 1998). The neuropsychological profile of FAD at a group level has also been found to show relatively well preserved naming, spelling and visuoperceptual skills compared with sporadic AD in the early stages (Warrington *et al.*, 2001, Godbolt *et al.*, 2004). There can therefore be a particularly long prodromal phase in FAD, where subtle memory problems are the only clinical feature for several years (Godbolt *et al.*, 2004). Presymptomatic cognitive deficits are accompanied by a range of neuroimaging changes (discussed in chapter 2) with gradually accelerating rates of whole brain and hippocampal atrophy in the five years prior to symptom onset (Scahill *et al.*, 2002) (Chan *et al.*, 2003).

The early stages of sporadic AD have been harder to study. Historically, individuals with memory concerns have tended to seek medical attention only when their symptoms are well established. However, we are currently witnessing a change in the tide of public opinion towards an appreciation of the importance of early diagnosis. There is increased recognition that most patients with sporadic AD are likely to have experienced a period of relatively isolated, usually amnestic, deficits termed mild cognitive impairment

(MCI) prior their diagnosis of AD (Petersen *et al.*, 1999). The term MCI is usually used to refer to individuals with cognitive decline which is more than anticipated from normal aging but insufficient to fulfil criteria for dementia. The term will thus be applied to a heterogeneous group, not all of whom will develop AD, and there is a great research effort aiming to improve the characterization of these individuals and refine the definition of the MCI label (Albert *et al.*, 2011, Dubois *et al.*, 2014). Nevertheless, there are now many lines of evidence supporting the notion that sporadic AD is preceded by a long prodromal stage. The canonical FAD phenotype, manifesting with early progressive impairment of episodic memory, can perhaps then be viewed as equivalent to the typical amnestic AD phenotype, preceded by MCI, that is seen commonly in sporadic disease.

Many atypical presentations of FAD have, however, been reported and there can be significant heterogeneity both between and within families regarding clinical phenotype. Heterogeneity, however, also exists within sporadic AD and as recognition of these more unusual variants increases, they may be found to occur more frequently than was previously appreciated.

1.3.1.2 Language presentations

Several *PSEN1* mutations have been reported to present with language impairment including p.Gly209Val, p.His163Tyr, p.Pro264Leu and p.Arg278Ile. The p.Pro264Leu and p.Arg278Ile mutations were detected in patients who were given initial clinical diagnoses of progressive non-fluent aphasia (Godbolt *et al.*, 2004, Mahoney *et al.*, 2013). Language deficits have been described in association with many other mutations later in the disease course, as is also often the case in sporadic AD. There is a growing body of research aiming to better characterise individuals with neurodegenerative disease who have predominant impairments of language function at presentation. Primary progressive aphasia (PPA) was traditionally thought to signify a disease in the spectrum of frontotemporal lobar degenerations. However, a 'logopenic' variant (LPA) of PPA is now also recognised, in which AD appears to be the commonest underlying pathology (Gorno-Tempini *et al.*, 2008).

1.3.1.3 Behavioural and psychiatric presentations

In sporadic AD, symptoms of agitation, depression, delusions and hallucinations occur commonly, particularly in the later stages of disease. Many *PSEN1* mutations are associated with behavioural and psychiatric symptoms during the course of the disease and these can, rarely, be the presenting features. Prominent early behavioural symptoms have also been reported in association with several *PSEN2* mutations, including pMet239Val, p.Thr122Arg and p.Tyr231Cys. (Marcon *et al.*, 2009). An underlying pathological diagnosis of AD has been obtained for some *PSEN1* mutations where a behavioural presentation has been described, including p.Val89Leu (Queralt *et al.*, 2002), p.Leu226Phe (Zekanowski *et al.*, 2006) and p.Met139Val (Rippon *et al.*, 2003). It has been suggested that a distribution of pathology involving structures in frontal-subcortical circuits, such as the thalamus and striatum, may contribute to the behavioural phenotype in some of these patients (Queralt *et al.*, 2002). Pathological confirmation for other *PSEN1* mutations such as p.Leu113Pro remains to be established. (Raux *et al.*, 2000) In some cases, the presence of behavioural and language features has been prominent enough to prompt a clinical diagnosis of frontotemporal dementia (FTD), as was the case for the *PSEN1* insArg352 genotype (Amtul *et al.*, 2002, Tang-Wai *et al.*, 2002). It was initially hypothesised that this *PSEN1* genotype may be capable of inducing a distinct neurodegenerative illness, more akin to FTD than AD. Intriguingly, not only did the members of the kindred have an FTD phenotype but when an affected individual eventually came to autopsy, ubiquitin pathology typical of FTD was found. The subsequent discovery of the *progranulin* gene as a cause of familial FTD led to a re-evaluation of this case, which was indeed found to harbour a *progranulin* mutation (Pickering-Brown *et al.*, 2006). With the benefit of hindsight, the change in *PSEN1* was then reconsidered to be a non-pathogenic polymorphism. This case highlights the importance of exercising caution when ascribing pathogenicity to rare *PSEN1* variants, especially when the phenotype is unusual.

1.3.1.4 Visual presentations

Visuospatial and visuoperceptual deficits commonly occur in the later stages of both sporadic and familial AD. In sporadic AD, a posterior cortical atrophy (PCA) variant may occur, where marked visual processing deficits are the presenting features and memory is relatively well preserved until later in the disease (Mendez *et al.*, 2002,

Tang-Wai *et al.*, 2004, Crutch *et al.*, 2012). PCA is an umbrella term for a neurodegenerative syndrome that preferentially affects parietal, occipital and occipito-temporal brain regions, characterised by progressive deterioration of higher visual processing skills and other posterior cortical functions including literacy, numeracy and praxis. Although AD is by far the most common underlying cause (Renner *et al.*, 2004), a number of different pathologies can also give to the PCA syndrome, including corticobasal degeneration (CBD), dementia with Lewy bodies (DLB), prion disease and subcortical gliosis (Victoroff *et al.*, 1994, Renner *et al.*, 2004, Tang-Wai *et al.*, 2004). Some studies comparing the distribution of pathology in AD cases with PCA and typical amnestic presentations have demonstrated higher amyloid plaque and neurofibrillary tangle burden in primary visual and visual association areas in PCA (Hof *et al.*, 1997). Others found increased neurofibrillary tangle but similar amyloid plaque density in visual areas, with fewer tangles or plaques in the hippocampus in PCA compared to typical AD (Tang-Wai *et al.*, 2004). Estimates of the overall prevalence of PCA are difficult, partly because it tends to be under-diagnosed and because different ways of describing the syndrome are used inconsistently. However, in a study of all AD patients presenting to one specialist centre, 5% were found to have had a visual and 3% an apraxic presentation (Snowden *et al.*, 2007).

Symptom onset in PCA tends to occur at a much earlier age than in AD in general: typically mid-50s to early 60s (Mendez *et al.*, 2002), although a wider age spread (40-86 years) has been reported (Tang-Wai *et al.*, 2004). Despite the young age at onset, the available cases series indicate that PCA patients do not tend to have any stronger family history of dementia than patients with typical AD. In earlier studies, PCA appeared to be associated with the same or lower *APOE4* allele frequency as typical AD (Mendez *et al.*, 2002, Tang-Wai *et al.*, 2004, Schott *et al.*, 2006, van der Flier *et al.*, 2006, Snowden *et al.*, 2007, Balasa *et al.*, 2011). More recently, in a large study of patients with a clinical diagnosis of PCA and a separate group of patients lacking clinical information who had posterior AD neuropathologically, *APOE4* did appear to be a risk factor for PCA and *CLU, BIN1* and *ABCA7* were identified as additional potential risk loci (Carrasquillo *et al.*, 2014). An international consortium to assess genetic risk factors for PCA has since been established, which confirmed that *APOE* is a risk factor for PCA (although a weaker risk factor than for typical AD), and identified *CR1, ABCA7, BIN1* and three novel loci (*SEMA3C*, *CNTNAP5* and *FAM46A*) as potential genes of interest

in PCA (Schott *et al.*, 2016). There have been only single case reports of patients with familial disease presenting with PCA – including PCA due to a *PSEN1* mutation (Sitek *et al.*, 2013) and familial prion disease due to a 5-octapeptide repeat insertion (Depaz *et al.*, 2012) in the *prion protein* gene.

1.3.2 Neurological symptoms and signs

Neurological symptoms and signs tend to be more prominent in FAD than sporadic AD, and have been recognised as a feature of the disease ever since it was first reported. Myoclonus and seizures are common. Spastic paraparesis, extrapyramidal signs and cerebellar ataxia have also been described, though less frequently. Rarely, neurological manifestations may be presenting symptoms of FAD (Appendix 11.1). All of these features seem to be particularly prominent in kindreds with very early onset of symptoms, below the age of 40 (Snider *et al.*, 2005). However, it is important to note that significant phenotypic heterogeneity is observed, both between families sharing a common mutation and within the affected individuals of a single family. Whilst all of these unusual features do appear to occur more frequently in familial than sporadic AD, the fact that younger patients often survive to more severe stages of disease may contribute in part to the trend. The preference for reporting atypical cases of FAD over those with sporadic AD may also play a role. Furthermore, atypical AD phenotypes often cause diagnostic uncertainty in sporadic disease and are less likely to be reported unless post-mortem (or other) confirmation of AD is obtained. In some reports of individuals with FAD, particularly those including longitudinal assessments, it is clear that neurological symptoms and signs developed at an early stage of the disease and there are cases where these features predate cognitive impairment. However, other reports of 'early' atypical features should be read with caution as sometimes the disease may be well established by the time a patient first presents to a clinician.

1.3.2.1 Myoclonus and seizures

Myoclonus, especially perhaps fine finger myoclonus, can be a particularly prominent and early sign in FAD, in contrast to sporadic AD where it tends to become apparent later in the course of the disease. The same pattern appears to occur with seizures,

which seem to be reported more frequently and at an earlier stage in the disease in FAD than in sporadic AD (Kennedy *et al.*, 1993, Zarea *et al.*, 2016). Myoclonus and seizures are often reported in very young onset cases of FAD. In fact, tonic-clonic seizures pre-dating the onset of cognitive impairment by several years have been reported in association with the *PSEN1* p.Leu166Pro and p.Leu235Pro mutations, both of which may cause cognitive symptoms in the third decade of life (Campion *et al.*, 1996, Moehlmann *et al.*, 2002). Fine finger myoclonus has also been noted to occur prior the onset of objective memory impairment, although it may not necessarily be apparent to the patient or their family at this mild early stage (Godbolt *et al.*, 2004). Interestingly, there is a cluster of mutations associated with early myoclonus and seizures in the region encoding transmembrane domain III of the *PSEN1* gene (p.Leu166Pro, p.Ser169Leu, p.Ser169Pro, p.Ser170Phe). Early myoclonus and seizures are also observed in individuals with *APP* mutations and particularly with *APP* duplications (see below).

1.3.2.2 Spastic paraparesis

Spastic paraparesis has been reported in association with over twenty different *PSEN1* mutations (Karlstrom *et al.*, 2008). Symptoms of spastic paraparesis may occur simultaneously with cognitive deficits or may predate them by several years. Progressive spastic paraparesis occurring for over a decade prior to the onset of cognitive impairment has been reported in association with the *PSEN1* p.Arg278Lys mutation (Assini *et al.*, 2003). In some families, individuals with spastic paraparesis have appeared to have a delayed onset of dementia compared to their relatives lacking these features (Smith *et al.*, 2001, Assini *et al.*, 2003). There is a particular association of spastic paraparesis with *PSEN1* exon 9 deletions, although not all individuals with these deletions demonstrate the phenotype (Hiltunen *et al.*, 2000). In those who do, there are frequently characteristic histological findings of large, rounded plaques in the frontal cortex known as ‘cotton wool plaques’ (Verkkoniemi *et al.*, 2000). Composed of Aβ40 and 42, cotton wool plaques usually lack a compact amyloid core and show very little neuritic change or glial cell component. The spastic paraparesis phenotype of FAD is often not associated with any specific imaging findings. However, significant white matter abnormalities on cranial MRI, presumed secondary to amyloid angiopathy, have

been observed in a family exhibiting spastic paraparesis and cotton wool plaques secondary to the p.Glu280Gly *PSEN1* mutation (O'Riordan *et al.*, 2002).

Several hypotheses have been proposed to explain why certain *PSEN1* mutations may give rise to the spastic paraparesis phenotype. The observation that most of the mutations associated with spastic paraparesis cause exceptionally high levels of Aβ42 suggests that a dosage effect may be operating (Houlden *et al.*, 2000). Intraneuronal Aβ may also play a role; this is a more frequent finding in AD patients with cotton wool plaques. As intraneuronal Aβ is known to induce only a weak immune response, it has been postulated that cotton wool plaques may result from a combination of increased Aβ production and decreased clearance (Tabira *et al.*, 2002). However, the presence of cotton wool plaques *per se* is not enough to explain the phenotype as these have also been found in patients lacking signs of spastic paraparesis (Yokota *et al.*, 2003). Furthermore, the presence of spastic paraparesis is highly variable, even between the affected individuals of a single family sharing identical mutations and similar environmental exposures. There may, therefore, be additional as yet unidentified factors operating in these patients that drive the pathology towards structures, like the corticospinal tracts and motor cortex, which are usually spared in both familial and sporadic AD.

1.3.2.3 Extrapyramidal signs

Extrapyramidal signs have been reported in association with several different *PSEN1* mutations, particularly those causing very early onset disease and other neurological signs such as spastic paraparesis (Dintchov *et al.*, 2009). A novel *PSEN2* mutation (p.Ala85Val) has also been reported where Parkinsonism was a feature (Piscopo *et al.*, 2008). In the majority of cases, the Parkinsonism does not become apparent until several years into the clinical course. However, an extrapyramidal syndrome characterised by rigidity, bradykinesia and an abnormal posture and gait was present from the onset of cognitive symptoms in the first reported kindred harbouring the *PSEN1* p.Gly217Asp mutation (Takao *et al.*, 2002). The autopsy findings in this family included, in addition to neurofibrillary tangles, amyloid angiopathy and neuritic plaques, neuronal rarefaction in the substantia nigra and numerous cotton wool plaques. These were distributed throughout the cerebral cortex but were also concentrated in

subcortical structures, particularly the striatum. As the authors suggest, the topography of pathology in these patients could account for their clinical presentations. Furthermore these cases illustrate how the separate, yet often overlapping, phenotypes of spastic paraparesis and Parkinsonism in FAD may share a common pathological substrate of cotton wool plaques located in specific anatomical areas.

Another histological feature that can underlie a Parkinsonian presentation of FAD is Lewy body pathology (LBP). Both LBP and cotton wool plaques were detected in a patient exhibiting a dopa-responsive Parkinsonian syndrome who developed cognitive symptoms seven years after the onset of his movement disorder. He was found to possess a novel three base pair deletion (p.Thr440del) in *PSEN1* (Ishikawa *et al.*, 2005). Widespread neocortical LBP has been demonstrated in a kindred with very early onset FAD secondary to a p.Ser170Phe *PSEN1* mutation, in which the age at symptom onset was as young as 26 (Snider *et al.*, 2005). In this family, myoclonus, seizures and extrapyramidal signs were features of the disease. Parkinsonism, seizures, a very early onset of disease and LBP were also reported in association with the p.Met233Val mutation in *PSEN1* (Houlden *et al.*, 2001). However, not all FAD patients with extrapyramidal signs are found to have LBP and equally, many patients with LBP do not manifest Parkinsonism clinically. In fact, concomitant LBP is a frequent finding in neuropathological examinations of patients with both familial and sporadic AD, occurring in up to 60% patients with each disease according to some series (Lippa *et al.*, 1998, Hamilton, 2000). Studies including analysis of the frequency of LBP in different FAD gene mutations have suggested that *PSEN1* mutations are significantly more likely to have associated LBP than *PSEN2* mutations (Leverenz *et al.*, 2006). Furthermore, there appear to be mutation-specific effects on the development of LBP in FAD. Certain *PSEN1* mutations such as p.Ala260Val are associated with diffuse LBP whereas in others, like p.Gly209Val, the LBP seems to occur in the amygdala only. In other *PSEN1* mutations, such as p.Ala246Glu, there tends to be very little LBP at all (Lippa *et al.*, 1998). LBP has also been observed in association with *APP* mutations and, with both the *Presenilins* and *APP*, no correlations between mutation position and the development of this pathological picture have been identified (Houlden *et al.*, 2001). It has been suggested that the presence of diffuse LBP in FAD is associated with longer durations of disease than when the LBP is restricted to limbic areas (Leverenz *et al.*, 2006). However, a detailed understanding of the significance of LBP in FAD and how

LBP relates to duration and manifestation of disease remains to be elucidated, particularly as many studies were conducted before synuclein antibodies became available.

1.3.2.4 Cerebellar signs

Variable cerebellar Aβ deposition has been observed in both familial and sporadic AD (Cole *et al.*, 1989, Larner, 1997). In several *PSEN1* mutations, particularly p.Glu280Ala (Lemere *et al.*, 1996), p.Ile143Thr (Martin *et al.*, 1991), p.Met139Val (Haltia *et al.*, 1994) and p.Gly209Val (Lampe *et al.*, 1994) severe involvement of the cerebellum by Aβ plaque deposition has been noted. This has also been found in FAD secondary to the *APP*717 mutations (Mann *et al.*, 1996) and in the brains of elderly patients with Down syndrome (Mann *et al.*, 1990, Mann and Iwatsubo, 1996). Even in cases of FAD with similar amounts of Aβ deposition to sporadic AD in the cerebellum, cerebellar Purkinje cell loss and reactive astrocytosis are significantly more severe in FAD than sporadic AD (Fukutani *et al.*, 1997). Pathological involvement of the cerebellum may occur without cerebellar signs featuring in the clinical presentation (Larner and Doran, 2006). However, progressive cerebellar ataxia has been reported as preceding cognitive impairment in the p.Ser170Phe (Piccini *et al.*, 2007) and p.Pro117Ala (Anheim *et al.*, 2007) mutations in *PSEN1*. Furthermore, cerebellar signs have been observed during the disease course in a range of other mutations in *PSEN1*, including p.Glu280Ala (Sepulveda-Falla *et al.*, 2014) and p.Leu282Val (Dermaut *et al.*, 2001). This latter mutation is notable for its association with an unusually high amount of amyloid angiopathy, which was found to involve the cerebellum in the individual manifesting cerebellar signs.

1.3.3 Influence of mutation location on pathology and phenotype

1.3.3.1 Presenilin 1 mutations

Two distinct histopathological profiles have been identified in FAD caused by *PSEN1* mutations and the type of pathology appears to be driven by the position of the mutation within the gene (Mann *et al.*, 2001). Mutations occurring before codon 200 are more frequently associated with a type 1 pattern of pathology whilst mutations beyond codon 200 tend to have type 2 pathology, which includes more severe cerebral amyloid

angiopathy (CAA). Type 1 pathology more closely resembles the pathology seen in sporadic AD, with many diffuse and cored plaques and few white matter plaques. CAA is only mild to moderate, and is usually confined to leptomeningeal vessels. In type 2 pathology, the number and distribution of diffuse and cored plaques is similar but these tend to be much larger and concentrated around amyloidotic arteries. CAA is nearly always severe, involving both leptomeningeal and intraparenchymal arteries. Aβ40 deposition tends to be increased in those with type 2 pathology, and this effect is independent of *APOE* genotype. As might be expected, the distinction between the two types of pathology is not absolute; some mutations occurring before codon 200 have been associated with widespread CAA, such as p.Glu184Asp (Yasuda *et al.*, 1997) and p.Ile83_Met84del (Steiner *et al.*, 2001). Equally, the p.Asn405Ser mutation, occurring after codon 200, appears to produce limited CAA (Yasuda *et al.*, 2000). However, overall there do appear to be clinical implications of the different histopathological signatures. Individuals with type 1 pathology have been reported to have a younger age at onset (by on average 5 years) and shorter disease duration (by around 2.5 years) than those with type 2 pathology (Mann *et al.*, 2001). The influence of *PSEN1* mutation position on the clinical phenotype of FAD is explored in more detail in chapter 3 of this thesis.

In order to explain the dichotomous manner by which the mutation site influences the development of amyloid angiopathy, it has been suggested that *PSEN1* mutations may actually act through two separate pathways (Mann *et al.*, 2001). First, they increase the production and deposition of Aβ42 and secondly, by affecting Notch signalling, they induce breakdown of the vascular epithelium. The subsequent leakage of Aβ into brain tissue may seed onto existing deposits of Aβ, producing the large plaques seen around vessels in type 2 pathology, and promoting the development of CAA. Interestingly, the residues of *PSEN1* that are thought to be functionally most important, namely aspartyl residues at the active site and *PSEN1* cleavage site, are located in the region of the gene where mutations are associated with severe amyloid angiopathy. Also important is the observation that these type 2 cases have less aggressive phenotypes, with later ages at onset and longer disease durations.

1.3.3.2 APP mutations

The majority of *APP* mutations reported to date lie in the vicinity of the β and γ secretase cleavage sites. *APP* residue 717, located just distal to the C-terminus of the Aβ domain by the γ secretase site, was recognised early on to represent a mutation hotspot. The 'London' *APP* V717I mutation was the first described (in DRC family 23), comprising valine substituted by isoleucine, but valine substituted by glycine, phenylananine or leucine at the 717 codon also results in a similar phenotype. Families with mutations at this site were found to share common features of early impairment of episodic memory, dyscalculia, lack of insight and prominent myoclonus and seizures (Rossor *et al.*, 1993). A double point mutation at *APP* 670/671 (G to T, A to C), resulting in a lysine methionine to asparagine leucine double substitution, was later identified in two Swedish families (Mullan *et al.*, 1992). This double mutation frames the other end of the Aβ domain, lying at the N-terminus by the β secretase site.

Some mutations have also been found within the Aβ coding sequence, and these appear to have specific pathological and clinical features, particularly in relation to CAA (Table 1.1). The 'Dutch mutation' in *APP*; a missense mutation resulting in a glutamate to glutamine substitution at position 693 (*APP* p.Glu693Gln) gives rise to a highly distinct phenotype (Van Broeckhoven *et al.*, 1990). These individuals have severe CAA leading to recurrent cerebral haemorrhage. The main clinical features are focal neurological symptoms and signs relating to these cerebrovascular events, although most patients do also develop dementia. Pathologically, diffuse parenchymal deposits of Aβ are observed, but the hallmark neuritic plaques and neurofibrillary tangles of AD are absent. A neighbouring mutation at residue 692 (an alanine to glycine substitution) has been reported in a separate family and labelled the Flemish mutation (Hendriks *et al.*, 1992). The affected individuals suffered either haemorrhages or a progressive dementia or both. A biopsy of a family member with haemorrhages revealed CAA with sparse neuritic plaques but no neurofibrillary tangles. Postmortem examination of mutation carriers presenting with dementia did, however, demonstrate neurofibrillary tangles, in addition to neuritic plaques and CAA (Roks *et al.*, 2000). Presymptomatic carriers of the Flemish mutation have also been investigated and found to have significantly increased periventricular and subcortical white matter lesions on cranial MRI (Roks *et al.*, 2000).

Table 1.1 Clinical and pathological features of autosomal dominant *APP* mutations lying within the Aβ coding domain

***APP* Mutation**	**CAA**	**Amyloid plaques**	**Neurofibrillary tangles**	**Clinical Phenotype**
Flemish p.Ala692Gly	Present	Present	Usually present	Recurrent cerebral haemorrhage or dementia or both
Dutch p.Glu693Gln	Present	Absent	Absent	Predominantly recurrent cerebral haemorrhage. Usually also followed by dementia
Arctic p.Glu693Gly	Present	Present, with characteristic ring-like structure	Present	Dementia only
Iowa p.Asp694Asn	Present	Present, with extensive Aβ40 deposition	Present	Dementia only

Another *APP* mutation within the Aβ sequence, known as the Iowa mutation (*APP* p.Asp694Asn) has also been found to be associated with severe CAA on pathological investigation. Widespread neurofibrillary tangles and amyloid plaques with particularly abundant Aβ40 deposition are seen with this mutation. Clinically, however, these

affected individuals lacked symptoms of recurrent cerebrovascular events and presented with progressive cognitive impairment (Grabowski *et al.*, 2001). A similar picture was found with the 'Arctic' mutation *APP* p.Glu693Gly, which has a purely cognitive phenotype, typical of AD, despite the presence of marked CAA (Basun *et al.*, 2008). The pathological findings in the Arctic mutation also include neurofibrillary tangles and abundant amyloid plaques with characteristic ring-like structures. Why the presence of CAA should have clinical manifestations with some of these mutations but not with others is intriguing. This is particularly true for the Arctic and Dutch mutations, which occur at exactly the same position (amino acid 693) but give rise to totally different phenotypes. It has been proposed that the explanation may lie in the polarity of the substituted amino acid. The Dutch mutation involves replacement of a glutamic acid with glutamine, which is polar and hydrophilic. Dutch Aβ may therefore have a greater affinity for, and propensity to disrupt, the vessel wall than Arctic Aβ, which is non-polar and hydrophobic (Basun *et al.*, 2008).

Mutations at codon 673 of *APP*, which alter the residue at position two in the Aβ peptide, also cause strikingly different effects depending on the nature of the substituted amino acid. The p.Ala673Val variant was identified in an Italian pedigree with an autosomal recessive pattern of inheritance of early onset AD (Di Fede *et al.*, 2009, Giaccone *et al.*, 2010) and only causes disease in the homozygous state. The substitution causes a shift in APP processing towards the amyloidogenic pathway through increased processing at the β-secretase site, together with enhancement of the aggregation and fibrillogenic properties of Aβ, whilst interaction between mutant and wild-type Aβ hinders amyloidogenesis in the heterozygous state. However, an alanine to threonine substitution at position 673 (p. Ala673Thr) actually protects against AD and the development of cognitive decline in elderly people without AD. The *APP* p.Ala673Thr variant was identified in whole-genome sequence data from the Icelandic population, where it was observed to be significantly more common in the healthy elderly control group than in those with AD (Jonsson *et al.*, 2012). This variant impairs APP processing at the β-secretase site, resulting in an almost 40% reduction in amyloidogenic peptide formation in vitro. The protective effect of the p.Ala673Thr variant provides proof of principle for the idea that reducing BACE1 cleavage of APP may protect against AD, supporting the notion that BACE1 inhibition may be a promising therapeutic target.

1.3.3.3 *APP* duplications

The well established link between Down syndrome and AD provided early evidence that copy number variation may play a role in AD pathogenesis and it is now well recognised that duplications of the *APP* gene can give rise to FAD (Rovelet-Lecrux *et al.*, 2006). The phenotype associated with APP duplication can be diverse, even within a single family (Guyant-Marechal *et al.*, 2008). However, characteristic features include a high frequency of seizures, up to 57% in one series, and prominent amyloid angiopathy (Rovelet-Lecrux *et al.*, 2006). An autosomal dominant family history of partial seizures present from adolescence has been reported in one *APP* duplication family (McNaughton *et al.*, 2010). The size of the duplication does not appear to influence the clinical presentation. The cognitive phenotype resembles that of typical AD, with early progressive impairment of episodic memory. In some families, the clinical presentation is solely cognitive, with no distinguishing neurological features (Kasuga *et al.*, 2009). Knowledge of the prevalence of *APP* duplications and spectrum of associated clinical features is likely to expand as increasing numbers of centres search for copy number variation in their cohorts of patients.

Interestingly, a post-mortem study of an individual with an *APP* duplication revealed diffuse neocortical LBP with additional CAA and AD pathology (Guyant-Marechal *et al.*, 2008). The clinical phenotype of this patient, comprising cognitive decline associated with visual hallucinations and extrapyramidal signs, was also compatible with a diagnosis of DLB. As the authors suggest, this case adds weight to the hypothesis that accumulation of Aβ can induce LBP. However, further work must be done in larger cohorts of patients to elucidate more about the clinical manifestations of coexistent Lewy body pathology in FAD, and to investigate the relationship between β-amyloid and alpha-synuclein in neurodegenerative disease in general.

1.3.4 Genetic modifiers of phenotype in sporadic AD

In FAD, genetic factors clearly modify the clinical phenotype in striking ways. The manifestations of sporadic AD are also likely to be influenced by genetic factors, though generally in a far subtler manner. The involvement of the *APOE* gene in sporadic AD has long been known, with possession of the *E*4 allele conferring both an increased risk of developing the disease and possibly driving the pathology towards limbic areas

(Schott *et al.*, 2006). More recently identified 'risk genes' for sporadic AD include *CLU, PICALM, CR1, BIN1, MS4A, CD2AP, CD33, EPHA1, ABCA7* (Harold *et al.*, 2009, Lambert *et al.*, 2009, Naj *et al.*, 2011) and *TREM2* (Guerreiro *et al.*, 2013, Jonsson *et al.*, 2013). An important direction for future work will be to investigate whether these variants have phenotypic associations, particularly in sporadic AD but also in familial disease.

Genes known to cause FAD may also play a role in sporadic disease. There are certain *PSEN1* polymorphisms, for example p.Glu318Gly, whose pathogenic nature remains uncertain. It has been suggested that some *PSEN1* polymorphisms may modify the phenotype of sporadic AD by altering the rate of cognitive decline (Belbin *et al.*, 2009). There is some evidence to suggest that FAD-causing gene mutations may sometimes be even more directly implicated in cases of apparently sporadic AD; through somatic and germline mosaicism (Beck *et al.*, 2004). An individual who underwent negative genetic testing on a peripheral blood sample was subsequently found to have the *PSEN1* p.Pro436Gln mutation in DNA extracted from cerebral cortex. Although this proband had no family history of dementia herself, one of her daughters subsequently developed symptoms and was found to have inherited the mutant haplotype from her mother. Interestingly, the two affected individuals had a difference in age at onset of around 15 years and strikingly different clinical phenotypes, although both featured prominent neurological signs. As the authors suggest, these findings have several important implications. Differing levels of mosaicism may account for some of the phenotypic variation seen in FAD. Furthermore, there may be many patients with AD who have pathogenic somatic mutations expressed in brain tissue that are not found on conventional sequencing of DNA extracted from blood lymphocytes. Indeed, developments in deep DNA sequencing technology have recently allowed mosaic mutations with low allelic frequency in AD-relevant genes to be detected in brain-derived DNA from a number of sporadic AD patients (Sala Frigerio *et al.*, 2015).

1.4 Future perspectives

In the decades since the identification of the first FAD mutation, significant advances have been made in our understanding of FAD at a molecular, genetic, pathological and

clinical level. The number of known mutations has risen exponentially and, with them, an expanding spectrum of clinical phenotypes has been identified. Observations of how certain symptoms and signs tend to cluster with particular mutations has led to an appreciation of how the location of a mutation within a gene can dictate the type of pathology that develops, particularly in relation to CAA. Familial and sporadic AD have been shown to share many similarities. They commonly present with identical symptoms of impaired episodic memory but can both, more rarely, have initial deficits in other cognitive domains. The factors dictating the topography of pathology in both familial and sporadic disease remain to be elucidated. However, possible mechanisms have been proposed. As has often been the case, the insights gained from studying FAD continue to inform our understanding of AD in general. With disease-modifying therapy trials now focussing interest on the earliest stages of disease, longitudinal study of the presymptomatic phase in individuals destined to develop FAD has become a major priority for AD research.

Increased recognition of how knowledge gleaned from the study of FAD has the potential to increase our understanding of AD as a whole led to the launch of the first international collaborative study of individuals carrying FAD mutations; the dominantly inherited Alzheimer network (DIAN) (Bateman *et al.*, 2011). This multicentre study collects longitudinal data to explore the clinical, imaging, neuropsychological, blood and cerebrospinal fluid changes that occur in the long period leading up to symptom onset in FAD. By establishing the largest cohort of FAD patients studied to date, it will allow some of the unresolved questions surrounding the relationship between genotype and phenotype in FAD to be addressed. Aided by initiatives like DIAN, research into FAD is likely to progress at an accelerating pace over the coming decade. The advent of disease-modifying therapy provides great momentum for driving forward this progress, as it creates an unprecedented need to understand the pathogenesis of AD in more detail. Issues such as the relationship between AD pathology and CAA, for example, have been brought to the forefront by amyloid immunotherapy trials. It has been found that, in patients treated with Aβ42 immunotherapy, removal of amyloid plaques may be accompanied by accumulation of Aβ42 in perivascular drainage pathways, with an associated transient increase in CAA (Weller *et al.*, 2009). It appears that this plaque-derived Aβ42 can be cleared, given sufficient time (Boche *et al.*, 2008). However, factors including *APOE* genotype are likely to influence how effectively this is

achieved. Understanding more about the mechanisms underlying the variable occurrence and clinical manifestation of CAA in FAD may thus have far-reaching implications. It is clear that in both familial and sporadic AD, a range of atypical clinical phenotypes can occur and by understanding more about how genetic factors modify the pathological, biomarker and clinical picture, we may find that the phenotype contains clues suggesting the most appropriate treatment for an individual.

2 Imaging biomarkers in Alzheimer's disease

2.1 Introduction

Imaging plays an increasingly important role in both clinical practice and research in AD. Clinically, there is growing appreciation that imaging provides not just exclusion of alternative pathologies, but also positive predictive, diagnostic and prognostic information in dementia. Imaging can improve specificity of diagnosis in trial populations, facilitate research on the earlier stages of disease and provide crucial information regarding drug safety and toxicity. With the advent of disease-modifying therapies, these properties acquire increasing importance. Furthermore, imaging biomarkers have the potential to serve as outcome measures of disease progression. A whole arsenal of imaging modalities has now been developed, each allowing a different aspect of the disease process to be explored. However, the limitations of each technique must also be appreciated. A multimodal approach, where imaging markers are combined, may be required to maximise the potential of imaging to enhance our understanding of AD and to help find effective therapies. In this introductory chapter, I outline the current role of neuroimaging in AD within the realms of both clinical practice and research. I discuss the potential for expansion of this role in the future and consider some of the challenges that this will entail. Finally, I review how imaging has been used to gain insights into preclinical change in AD, which forms one of the major themes of this thesis.

The idea that inspecting the structure of the brain can open a window into understanding aspects of its function has a long history. Early 19th century theories of phrenology, despite their scientific and moral flaws, were important in stimulating interest in how human cognition can be explored by examining the structure of different brain regions (Zola-Morgan, 1995). In the decades that followed, neuropathological studies of patients with lesions advanced understanding of localised cognitive function further. This drive to explore the workings of the brain through investigation of its structure was revolutionised by the development of neuroimaging. The introduction of computed tomography (CT) in the 1970s and magnetic resonance imaging (MRI) in the 1980s allowed the brain to be viewed directly, during life, for the first time. More recently, functional and molecular imaging have added to our ability to "see" the brain in life.

The capacity to examine non-invasively the processes occurring within the brain, and to investigate the variable ways in which it responds to disease and intervention, have had a huge impact on clinical practice and research within neurology. Over the past forty years an array of increasingly sophisticated neuroimaging techniques has evolved, allowing specific aspects of disease to be probed in detail. There are now techniques that assess brain activity, microstructure, perfusion, connectivity, metabolism, and even histopathological hallmarks of disease – all *in vivo*. In the field of AD, this is proving to be particularly important. Although tremendous efforts and progress have been made in our understanding of the biological basis of AD, we remain fairly ignorant about the sequence of pathological events and how they relate to the clinical manifestations of disease. As discussed in the preceding chapter, AD is heterogeneous with patients presenting in a variety of ways. It is also a diffuse disease, with amyloid plaques, neurofibrillary tangles and synapse loss affecting ineloquent as well as eloquent areas of the brain. This may be very relevant to the pathological cascade. Furthermore, we are still unclear about aspects of the underlying mechanisms by which our treatments for AD affect the pathological process. Motivated by the current trials of disease-modifying therapy for AD, this thesis includes several studies that use imaging techniques to investigate the pathological underpinnings of phenotypic heterogeneity and preclinical change in AD.

2.2 Imaging in Clinical Practice

Diagnosis in dementia is not always straightforward. Post-mortem studies have shown that, even in specialist centres, 10-15% patients thought to have AD are incorrectly diagnosed (Knopman *et al.*, 2001). Differentiating AD from other possible diagnoses such as DLB or FTD is often difficult clinically, particularly early on in the illness. However, the early stage of the disease may be precisely the time when certain therapeutic interventions are most likely to be effective and it is also the period where there is the most to save in terms of cognitive function. There is increasing evidence that the clinical manifestations of AD are preceded by a long period during which pathological changes accrue (Price and Morris, 1999). Interventions to the pathological cascade may need to be made early on in this process to be effective. Gaining an early diagnosis is also extremely important from the perspective of an individual patient and

their family. It allows them to make decisions about the future at a stage where they still have the cognitive abilities to do so, and to gain access to the services and support they need before a crisis point is reached. The concept of early diagnosis should not be confused with screening for which there is not evidence of benefit in dementia; what is clear is that once patients and their families are aware of a problem and seek medical help there are often long days in the assessment and diagnostic process which all too often remains inexact as well as slow. The fact that an early (or perhaps more precisely a timely) diagnosis is a priority for patients and carers is reflected in the importance given to improving early diagnosis by carer organisations like the Alzheimer's Association and Alzheimer's Society, and by government initiatives such as the UK's National Dementia Strategy [3].

The role of neuroimaging in the diagnosis of AD has, until recently, focussed on excluding alternative pathologies as the cause of an individual's cognitive impairment. Current diagnostic guidelines advise that all patients complaining of cognitive symptoms should have structural imaging (unenhanced CT or MRI) at least once to exclude structural causes such as tumours and haematomas (Knopman *et al.*, 2001, Waldemar *et al.*, 2007, Hort *et al.*, 2010). These surgical causes are rare and we are currently witnessing a change in thinking towards an appreciation of the positive diagnostic information that can be revealed by MRI. Patterns of atrophy offer important clues to the underlying diagnosis and in some cases, can even act as the signature for a specific molecular pathology. For example semantic dementia, one of the main clinical variants of FTD, is characterised by the distinctive imaging appearance of asymmetrical anterior dominant (usually left) temporal lobe atrophy, best seen on coronal T1-weighted MRI, and the predictable neuropathological findings of ubiquitin-positive, tau-negative neuronal inclusions (Hodges and Patterson, 2007). Investigation of the differential diagnosis in a patient with cognitive symptoms can be enhanced further by selectively employing a range of different MRI techniques. Diffusion weighted imaging (DWI), for example, often reveals characteristic areas of hyperintense signal abnormality in the cortex and putamen in patients with sporadic Creutzfold-Jakob disease (CJD) and in the pulvinar nucleus of the thalamus in variant CJD (Schroter *et al.*, 2000). These DWI changes have been shown to correlate with the histopathological spongiform and gliotic changes seen at autopsy in these individuals (Manners *et al.*, 2009). T2-weighted imaging (especially FLAIR – fluid attenuated inversion recovery –

imaging) is particularly useful for assessing vascular load and white matter disease. Although this is still a rather uncertain area, the appearances of extensive, irregular white matter signal change, multiple infarcts and/or high signal foci in the basal ganglia, thalamus and infratentorial regions can be highly suggestive of vascular dementia (Schmidt, 1992). Conversely the absence of these changes on imaging makes a vascular cause much less likely. Furthermore, the presence of an unusual pattern or significant white matter signal change in an individual who lacks vascular risk factors can provide an important warning sign to a clinician to investigate the patient for alternative and potentially reversible causes of cognitive decline such as vasculitis, metabolic or inflammatory disease or demyelination; additional investigation may include additional blood tests, CSF analysis or rarely brain biopsy (Waldemar *et al.*, 2007). As we will discuss in Chapters 4 and 5, the presence of white matter hyperintensities in posterior cortical areas (Thanprasertsuk *et al.*, 2014) and cortico-subcortical microbleeds on gradient echo (T2*-GRE) sequences (Cordonnier and van der Flier, 2011), may predict underlying CAA.

There is now a wealth of evidence that, in addition to its ability to identify surgically treatable lesions and more unusual causes of dementia, MRI can demonstrate characteristic features that positively support a diagnosis of AD (Waldemar *et al.*, 2007, Hort *et al.*, 2010). In the UK this recognition is included in guidance from the National Institute of Health and Clinical Excellence (NICE) [4]. Most established is the presence of disproportionate medial temporal lobe atrophy on MRI. By the time patients with AD present with symptoms, hippocampal volumes are already significantly reduced and the severity of AD pathology and neuronal loss correlates with the degree of hippocampal atrophy on antemortem MRI (Jack *et al.*, 2002) (Figure 2.1). Furthermore, the presence of medial temporal lobe atrophy has been shown to predict conversion from MCI to AD (DeCarli *et al.*, 2007). This atrophy can be detected by both volumetric measurements and by visual assessments of scans (Scheltens *et al.*, 1992, De Leon *et al.*, 1997). Visually rating just a single coronal slice of an MRI has been shown to have 80-85% sensitivity and sensitivity for distinguishing patients with AD from those with no cognitive impairment, and similar sensitivity and specificity levels for diagnosing amnestic MCI (Duara *et al.*, 2008). The overall pattern of cortical atrophy also provides valuable diagnostic information; studies which have included pathological confirmation of the diagnosis have shown that the combination of posterior atrophy together with

medial temporal lobe atrophy on MRI carries positive predictive value for diagnosing AD (Likeman *et al.*, 2005).

Figure 2.1 Medial temporal lobe atrophy on MRI; a sensitive marker of neurodegeneration in AD.

Reprinted from (Ryan and Fox, 2009), with permission.

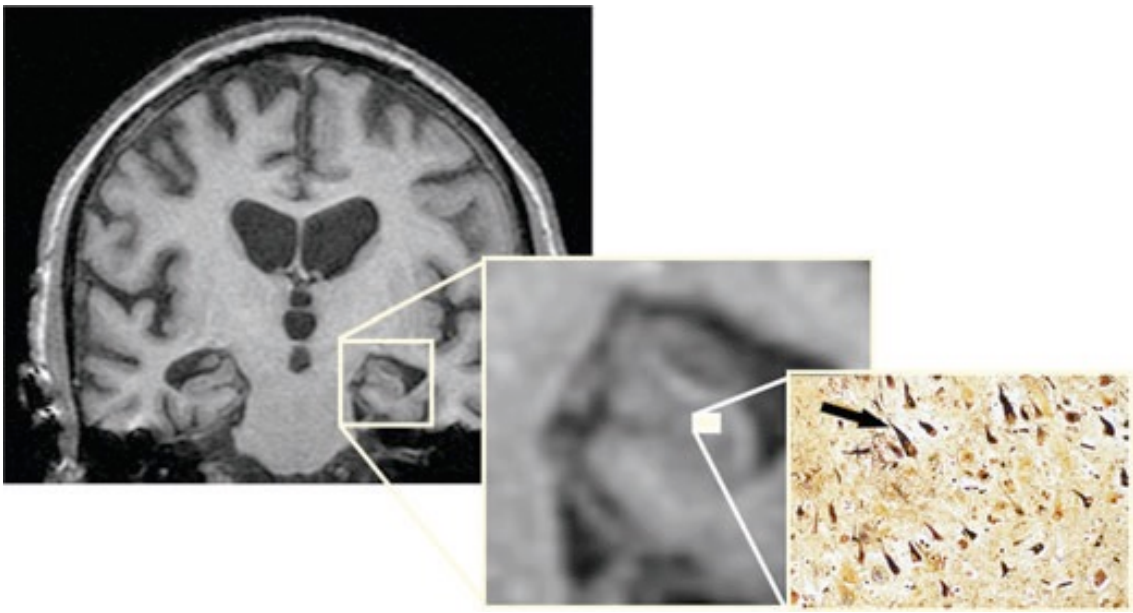

In recognition of the diagnostic value of MRI, it has been proposed that the presence of medial temporal lobe atrophy on MRI should be incorporated into new diagnostic criteria for AD (Dubois *et al.*, 2007, Albert *et al.*, 2011, Dubois *et al.*, 2014). Furthermore, it is appreciated that in cases where uncertainty about the diagnosis persists after clinical assessment and structural imaging, there can be a role for functional imaging. Single photon emission computed tomography (SPECT) studies of regional blood flow and measurements of glucose metabolism with positron emission tomography (FDG-PET) are the most frequently applied functional imaging studies in clinical practice. The most commonly described criterion for AD is a symmetrical reduction in blood flow or glucose metabolism in parieto-temporal areas. Patterns on functional imaging with FDG-PET have been reported to have levels of sensitivity and specificity of around 90% and 70% for separating AD patients from controls (Silverman *et al.*, 2001, Jagust *et al.*, 2007). Although this specificity level is only moderate, the relatively high sensitivity level means that a negative scan favours a normal outcome at

follow up. In cases where it is unclear whether a degenerative disease is present at all, this extra reassurance can be clinically helpful.

2.3 Imaging in Research

The power of imaging to enable earlier detection of disease is particularly important in the realm of clinical research; it opens a window of opportunity for conducting research on the early phase of disease and for allowing earlier intervention. Imaging measures are also attractive putative markers of disease progression for clinical trials, although they are still far from acting as surrogate outcomes in AD and are likely to require multiple results from disease-modifying trials in order for this to occur (Fox and Kennedy, 2009). However, the need for reliable biomarkers for clinical trials in AD is clearly pressing and increasingly, changes in imaging markers are included as secondary outcome measures (Cash *et al.*, 2014). Withdrawal and survival studies are difficult in a disease like AD where survival may be for as long as 15 years. The clinical scores used to assess new treatments are problematic as they are non-linear and are influenced by a multitude of factors affecting the performance of both the patient and examiner on a particular day. Furthermore, they have a limited ability to address the fundamental question of whether a treatment causes a true long-lasting disease modifying effect or simply a short-term improvement in symptoms. This distinction is crucially important; the expected duration of benefit is a factor in the decision for an individual patient of whether to embark on a new experimental treatment, especially when the side-effect profile is significant. Imaging allows repeated assessments but without the practice effects involved in repeated neuropsychology. It provides a closer reflection of the changes occurring at a pathological level than can be achieved by neuropsychological and clinical scoring alone. Furthermore, it is non-invasive, making it more likely to be acceptable to some patients than other putative biomarkers such as CSF, obtained by lumbar puncture.

Importantly, different modalities of neuroimaging can allow different aspects of brain function and disease process to be probed. Cerebral perfusion, metabolism and activation can be assessed by SPECT scanning, perfusion MRI, FDG-PET and functional MRI (fMRI). Tissue microstructural changes are indicated by changes in

diffusion imaging and magnetisation transfer. Changes in the integrity of white matter tracts connecting different brain areas can be investigated with diffusion tensor imaging (DTI). The metabolic environment of the brain can be investigated with MR spectroscopy. Certain pathological effects can be visualised by specific scanning sequences, such as microbleeds on susceptibility-weighted MRI. Finally, molecular imaging can be employed to show aspects of the pathological cascade directly. For example, deposition of fibrillar amyloid, detected using the carbon-11 (^{11}C) based PET ligand Pittsburgh compound B (PIB) and more recently fluorine-18 (^{18}F) based amyloid tracers; deposition of tau with even newer tracers such as ^{11}C-PBB3 or a number of ^{18}F-tau ligands; or loss of dopamine transport using the SPECT tracer [^{123}I]FP-CIT. In the future it may well be that a multimodal imaging approach is employed to investigate responses to treatment from several different perspectives simultaneously.

Whilst the use of imaging biomarkers as surrogate end-points may take some time to be adopted (and regulatory acceptance will require much supporting evidence), baseline imaging measurements do already have an established role in clinical trials. In recruiting individuals to trials, imaging is used to improve the specificity of diagnosis in order to create a more homogenous trial population. Trials of agents targeting specific aspects of the AD disease process are more likely to show a true effect if the individuals in the trial do actually have AD rather than non-AD pathologies such as FTD or vascular dementias. The most straightforward way of identifying individuals with a vascular cause of their cognitive impairment is by the use of MRI; similarly focal fronto-temporal atrophy suggests FTD rather than AD. As we move towards more complex, dangerous and targeted therapies this becomes increasingly important as we want to be sure that the patients we are trialling these treatments on do in fact possess the molecular targets. MRI can also open an earlier therapeutic window in clinical trials. In MCI studies, recruitment of subjects is enriched if the presence of medial temporal lobe atrophy on MRI is part of the inclusion criteria, as this atrophy is predictive of conversion from MCI to AD (Devanand *et al.*, 2007).

Amyloid imaging also shows changes very early on in AD, with high PIB-retention observed in patients with MCI who later will convert to AD (Forsberg *et al.*, 2008) (Figure 2.2). However, we are yet to determine the significance of the 20-30% of healthy controls who also demonstrate amyloid deposition (Rowe *et al.*, 2007). Whether

these individuals are those who will subsequently develop AD (and when) will only be determined with long term follow up studies.

Figure 2.2. **Amyloid imaging with PIB-PET can be positive early in AD and may predict conversion from MCI to AD**

Images courtesy of David Brooks, Imperial College, London. Reprinted from (Ryan and Fox, 2009), with permission. The "hot colours" in red and yellow indicate areas of tracer retention and therefore fibrillary amyloid; the scans illustrated are from two individuals with MCI; the image on the left shows only non-specific white-matter binding and the individual has not progressed clinically after several years; the image on the right shows extensive cortical amyloid deposition and the individual progressed to a diagnosis of AD over the following 18 months.

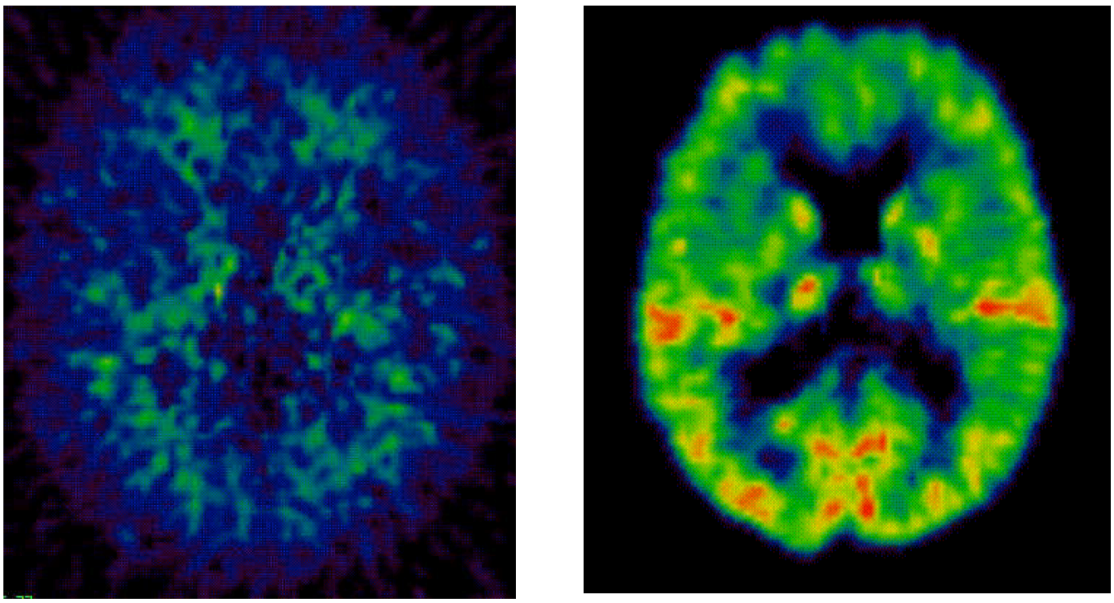

MCI non-converter **MCI converter**

Imaging, because it provides topographical information (unlike a blood or CSF marker), also has value for investigating the site of action and nature and extent of the therapeutic effect, together with potential toxicity. It can act as a sensitive maker of effects that may be clinically silent initially. In the first active immunotherapy for AD study, the side-effect of meningoencephalitis was detected on imaging (Gilman *et al.*, 2005). A subsequent passive immunotherapy trial of Bapineuzumab picked up asymptomatic changes on T2-weighted/FLAIR sequences that were initially referred to as "vasogenic

oedema" in some individuals on their safety MRI, allowing these participants to have tailored treatment with their immunotherapy being withheld until the imaging changes had resolved (Sperling *et al.*, 2012). Identification of additional cases with similar imaging abnormalities in subsequent trials led to the realisation that amyloid-modifying therapies could be associated with a spectrum of imaging changes (Coric *et al.*, 2012, Ostrowitzki *et al.*, 2012). The umbrella term 'ARIA' was coined to describe these amyloid-related imaging abnormalities, which include FLAIR signal abnormalities believed to represent cerebral oedema and sulcal effusions (ARIA-E) and abnormalities on T2*-GRE sequences thought to represent microbleeds and haemosiderosis (ARIA-H) (Sperling *et al.*, 2011). Monitoring for ARIA with safety MRI has now become an essential part of AD clinical trials and a rating scale has been developed with the aim of standardising the measures (Barkhof *et al.*, 2013). Typical protocols for MRI safety scans include a FLAIR sequence, sensitive to oedema, effusion, inflammation and infarction and T2*-GRE or susceptibility-weighted imaging (SWI) sequences to detect microbleeds and haemosiderosis.

The hope for drug discovery efforts is that biomarkers will allow disease modifying effects to be identified, and that this will be achieved with smaller sample sizes if the selection of appropriate individuals is refined by biomarkers. The size of a trial is determined by the variance of the outcome measure. The power analysis from the Alzheimer's disease neuroimaging initiative (ADNI) demonstrated that, for a 25% slope reduction in AD disease progression, many more individuals would be needed to demonstrate a difference using the ADAS-cog than if MRI-derived measures of atrophy were used (Schuff *et al.*, 2009). It may well be that personalised biomarkers prove to be the most effective approach towards monitoring AD progression. Characterising an individual's own rate of atrophy and measuring the effect of a therapy on this rate may be more valuable than comparing rates between individuals. An individual's serial MRI scans can be registered together and used to calculate an atrophy rate, either for the whole brain or for specific regions such as the hippocampus. The rate of whole brain atrophy in AD is 4-5 times the rate in normal ageing (Fox *et al.*, 2005). Much of our knowledge of the brain atrophy that occurs in the very early stage of AD comes from the study of individuals with the rare, familial form of the disease. FAD, through prospective study of individuals who are cognitively normal but genetically destined to develop the disease, provides an insight into the earliest manifestations of the

pathological process. This has helped to illuminate the long preclinical phase during which AD pathology accumulates prior to symptom onset. It has also revealed how rates of whole brain atrophy accelerate in the five years prior to symptom onset in FAD gene mutation carriers (Chan *et al.*, 2003). If disease-modifying therapies do prove to be effective, one can envisage a time in the future where these individuals who are undoubtedly going to develop AD undergo monitoring of their atrophy rate, with acceleration of this rate prompting initiation of treatment.

Although imaging clearly has the potential to provide valuable biomarkers for AD research, there is still much work to be done to refine the techniques themselves and to understand more about how they reflect the underlying pathology. Firstly, the assumption in clinical trials will be that slowing of atrophy indicates slowing of neurodegeneration, however this is yet to be proven. Furthermore, it is important to consider the possibility that the timings of change in a biomarker and in the clinical outcome it is intended to represent may not be simultaneous. For example, the AN1792 Aβ immunisation study revealed the unexpected result that patients who mounted high antibody responses showed greater atrophy rates than those who responded less, the converse of what might have been expected (Fox *et al.*, 2005). At the time several possible explanations were proposed including accelerated neuronal loss, increased clearance of amyloid from the brain with associated fluid shifts or reduced plaque-associated inflammation in antibody-responders. More recent work examining post-mortem brain tissue from AD subjects who participated in that trial has shown that there is indeed evidence that Aβ immunisation may have accelerated loss of damaged degenerating neurons (Paquet *et al.*, 2015) and resulted in reductions in associated inflammation. Whatever the underlying cause of the volume changes, this study showed that MRI could provide evidence that a treatment was reaching the target (brain) and was having an effect on brain structure, but that one cannot simply assume that a biomarker will behave in the same way in a treatment trial as it does in untreated subjects (Vellas *et al.*, 2009). Essentially, it will be important to investigate how imaging markers respond to our treatments, as well as how they respond to the disease itself, including studying imaging effects in animal models (Frisoni and Delacourte, 2009). There will also be a need to exercise caution in drawing conclusions from functional imaging. Most importantly, disease-modifying changes will need to be

distinguished from symptomatic effects. With amyloid imaging, there is the additional concern that it may prove insensitive to change once at a clinical stage for the disease, when there appears to be a ceiling effect of amyloid binding with little progression over time (Engler *et al.*, 2006). Equally a specific molecular marker may not lie on the causal pathway from pathogenesis to symptoms; amyloid imaging may demonstrate fibrillary amyloid plaques but not the oligomers, which are increasingly thought to have a fundamental role in AD pathogenesis (Selkoe, 2008).

Each imaging modality carries its own set of limitations. However, as long as these are appreciated and taken into account, imaging is likely to play a prominent part in the scientific journey to understand AD in the future, particularly if the strength of combining imaging biomarkers is realised. The role of imaging in the clinical investigation of patients with dementia is also evolving. There are always large issues to overcome in translating research into clinical practice. Methods need to be accessible, practical and have value for detection, differential diagnosis and prognosis. Imaging has the potential to fulfil all of these requirements. In the few decades that have passed since neuroimaging was first developed, considerable progress has been made in advancing the techniques and applying them to clinical problems. Although there is still much work to be done, the pressing need for reliable biomarkers in AD provides great momentum for driving this progress forwards.

2.4 Imaging presymptomatic Alzheimer's disease

It is now well established that the pathophysiological process of AD begins many years, even decades, before symptoms develop and there is currently great interest in defining and characterising the preclinical stages of the disease (Sperling *et al.*, 2011). This interest has been driven in part by the disappointing results of trials of amyloid-modifying therapies in patients with so-called "mild to moderate" AD, with at least one trial (of Solanezumab) showing in a post-hoc analysis that milder subjects appeared to do better than more affected individuals (Doody *et al.*, 2014, Karran and Hardy, 2014). The suggestion being that treatment in the majority of trials may have been "too little, too late" with the implication that treating earlier in the disease would have had greater

chances of slowing progression. The observation from some previous trials, of apparent treatment-related reductions in Aβ burden at autopsy or on amyloid imaging, have encouraged the view that disease-modification may be possible, but perhaps with only limited benefit if downstream neurodegeneration is already well established. 20-40% of cognitively normal older individuals show evidence of Aβ accumulation in both PET imaging and CSF studies and a similar proportion of healthy elderly people have been found to have AD pathology at post-mortem (Sperling *et al.*, 2011) – the percentage who are "amyloid-positive" is very age-related and is also higher in those who carry an *ApoE*4 allele. The proportion of these individuals who will or would have gone on to develop AD dementia is currently unknown, so research recommendations have proposed the term 'asymptomatic at risk state for AD' to refer to this particular preclinical stage (Dubois *et al.*, 2010). The other proposed preclinical stage of AD is 'presymptomatic AD, a term reserved for individuals with autosomal dominantly inherited mutations in the *PSEN1*, *PSEN2* and *APP* genes who will inevitably develop symptoms of FAD. In this final introductory section, I describe the insights into presymptomatic AD that have been gained through previous imaging studies of FAD mutation carriers and discuss some of the uncertainties and future challenges that remain as we enter an era of prevention trials for AD.

Understanding the timing and temporal order by which different imaging biomarkers become abnormal in presymptomatic AD is a fundamental issue for the field. The longitudinal study of healthy FAD mutation carriers with multi-modal imaging provides a unique opportunity to address this question. In recent years a number of large initiatives have been gathering such data: the DIAN study, with sites across the USA, Australia and in the UK; and the Alzheimer's Prevention Initiative (API), which studies a large Colombian kindred affected by the *PSEN1* p.Glu280Ala mutation. So far, the results reported from these studies have largely been cross-sectional but as symptoms tend to arise at a similar age within a family, the ages at which an individual's relatives became clinically affected have been used to predict how far from symptom onset a presymptomatic participant may be. On this basis, amyloid imaging with PIB-PET in DIAN and Florbetapir-PET in API have demonstrated accumulation of Aβ in mutation carriers who are as far as 15 years below their expected age at symptom onset (Bateman *et al.*, 2012, Fleisher *et al.*, 2012, Benzinger *et al.*, 2013). This confirms findings from earlier smaller studies, that Aβ deposition on PET is an early event in presymptomatic

FAD. A striking observation from the initial FAD PIB-PET studies was that Aβ deposition was most intense in the striatum (Figure 2.3); a pattern reported for a variety of *PSEN1* mutations and for *APP* mutation and duplication cases (Klunk *et al.*, 2007, Remes *et al.*, 2008, Villemagne *et al.*, 2009). This striatal predominance does not appear to be seen with the Colombian kindred *PSEN1* mutation, and other *PSEN1* mutations have subsequently been found to be associated with more prominent thalamic PIB uptake (Knight *et al.*, 2011). The topography of early amyloid deposition in FAD caused by different mutations therefore appears to be more heterogeneous than was once thought.

Figure 2.3 PIB-PET imaging showing prominent striatal amyloid deposition in a presymptomatic *PSEN1* mutation carrier approximately three years prior to anticipated age at onset.

Reprinted from 'Neuroimaging in Dementia', published by Springer, with permission.

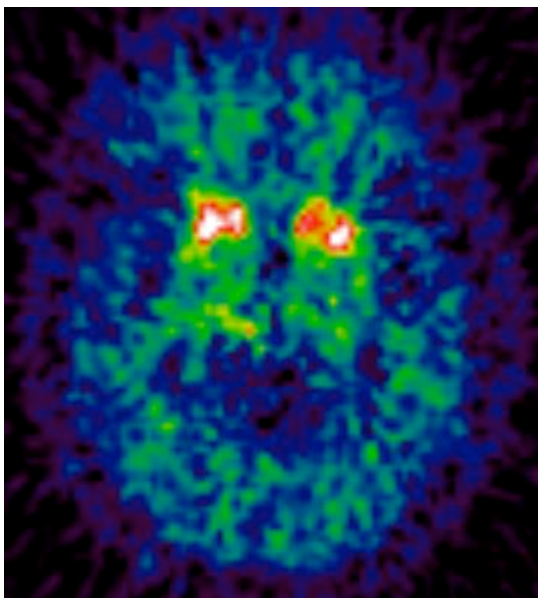

Whilst amyloid-PET imaging measures the accumulation of abnormal protein, the other imaging modalities that have been applied to presymptomatic FAD are thought to capture aspects of neurodegeneration further downstream. The most widely used of these have been FDG-PET to measure glucose metabolism and structural MRI to investigate atrophy. MR spectroscopy has also been used and found to demonstrate posterior cingulate metabolic changes in presymptomatic mutation carriers who were on

average 10 years younger than the mean age at onset for their family (Godbolt *et al.*, 2006). Using FDG-PET, widespread hypometabolism has been observed in presymptomatic FAD in a pattern similar to that seen in sporadic AD (Mosconi *et al.*, 2006). In the DIAN study, parietal hypometabolism was evident from around 10 years prior to the parental age at symptom onset. Most regions appeared to show the sequence of events predicted by theoretical biomarker models of AD, with amyloid accumulation occurring first, followed by hypometabolism followed by atrophy (Jack *et al.*, 2010) (Figure 2.4). However, the DIAN data also indicated that there may be more complexity to the trajectory of presymptomatic biomarker changes than such models at first suggest. Firstly, different brain regions appear to vary in their vulnerability to the presence of amyloid pathology. Whilst all subcortical regions showed elevated PIB uptake, hypometabolism was only evident in the hippocampus (Benzinger *et al.*, 2013). Secondly, the direction of biomarker change was not always as predicted. In very young mutation carriers who were ~25 years from expected age at onset, there was some suggestion that there might be a hypermetabolic phase in some regions including precuneus and posterior cingulate. The numbers in this subgroup were small, however, so replication of the results in a larger cohort will be required. Furthermore longitudinal studies will be critical to understanding these changes.

Structural MRI is the imaging modality that has been most thoroughly investigated in FAD and, importantly, it has been used to study mutation carriers longitudinally from a presymptomatic stage up to the actual age at onset of clinical symptoms. Accelerating hippocampal and whole brain atrophy rates have been observed at 5.5 and 3.5 years respectively before symptom onset in mutation carriers (Ridha *et al.*, 2006). Cortical thinning of precuneus and posterior cingulate cortex has been reported approximately four and three years before onset (Knight *et al.*, 2011) In these small cohort studies, longitudinal measures were able to detect presymptomatic change earlier than when a cross-sectional approach was taken. A more recent longitudinal study of a larger group of mutation carriers detected thinning of precuneus up to eight years before expected symptom onset and identified a signature pattern of cortical thinning in FAD (Weston *et al.*, 2016). Baseline thickness of this cortical signature (which comprises entorhinal cortex, supramarginal gyrus, superior frontal cortex, superior and inferior parietal cortex and precuneus) was found to predict rate of subsequent thinning and correlate with presymptomatic cognitive change. Visual rating of hippocampal atrophy in

presymptomatic FAD appears to be relatively insensitive (Ringman *et al.*, 2010); visual assessment may be less sensitive in FAD and early onset disease than in late onset AD (Ryan and Fox, 2009).

Figure 2.4 Hypothetical model of dynamic biomarkers of AD expanded to explicate the preclinical phase,

Reprinted from (Sperling *et al.*, 2011), with permission. Aβ as identified by cerebrospinal fluid $A\beta_{42}$ assay or PET amyloid imaging. Synaptic dysfunction evidenced by FDG-PET or functional magnetic resonance imaging (fMRI), with a dashed line to indicate that synaptic dysfunction may be detectable in *APOE*4 carriers before detectable Aβ deposition. Neuronal injury is evidenced by CSF tau or phospho-tau, brain structure is evidenced by structural MRI. Biomarkers change from normal to maximally abnormal (y-axis) as a function of disease stage (x-axis). The temporal trajectory of two key indicators used to stage the disease clinically, cognitive and behavioral measures, and clinical function are also illustrated. Figure adapted with permission from (Jack *et al.*, 2010).

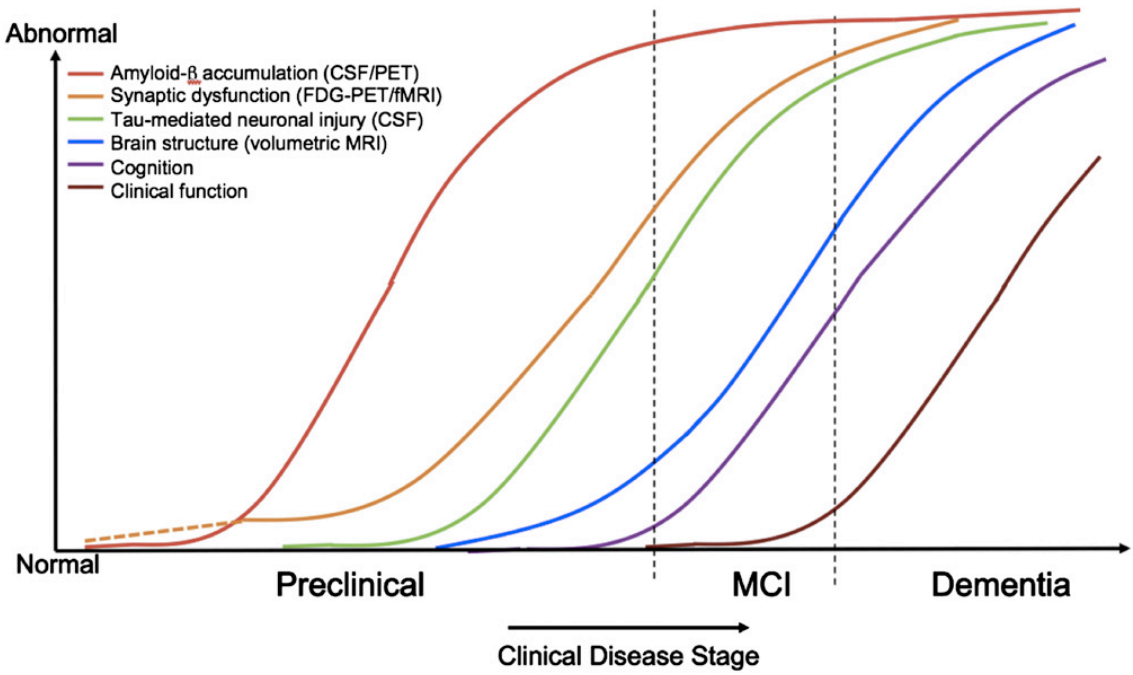

In view of the early striatal and thalamic amyloid deposition witnessed in FAD, more recent studies have also examined whether these subcortical structures undergo presymptomatic atrophy. In Chapter 6, I describe decreased volumes of thalamus and caudate in mutation carriers who were on average 5.6 years from parental age at onset, at a stage where hippocampal atrophy was not yet evident (Ryan *et al.*, 2013). Presymptomatic atrophy of thalamus, caudate and putamen has also been reported in a separate cohort of mutation carriers who were ~15 years younger than the median age of dementia diagnosis in their family (Lee *et al.*, 2013). A voxel-based morphometry (VBM) analysis of DIAN data demonstrated decreasing thalamic grey matter in presymptomatic DIAN mutation carriers closer to age at onset (Cash *et al.*, 2013). Subsequent analysis of a larger cohort from DIAN using an automated segmentation technique to assess cortical thickness and subcortical regional volumes demonstrated atrophy of the hippocampus, putamen, thalamus, amygdala and accumbens ~10 years and cortical thinning, particularly of precuneus, ~5 years before the parental age at symptom onset (Benzinger *et al.*, 2013). The lack of caudate atrophy in the DIAN data is somewhat surprising, particularly given the high amyloid burden observed in this structure. However, the caudate has been associated with a number of unexpected results in studies of presymptomatic FAD. Lee et al. found that, although caudate volumes were reduced in young presymptomatic mutation carriers, there was a trend towards increasing caudate size in symptomatic mutation carriers during the pre-dementia phase (Lee *et al.*, 2013). Another group reported increased caudate volumes and cortical thickness in precuneus and parietotemporal areas in a small number of mutation carriers who were approximately a decade younger than their family's median age at symptom onset – with the intriguing possibility that early amyloid deposition may cause volume increases perhaps due to plaque-associated inflammatory responses. (Fortea *et al.*, 2010). Like the report of hypermetabolism in very young mutation carriers, these observations of possible increases in regional volumes require replication in larger studies to ensure that they are not artefactual but they do raise the possibility that biomarkers may change in unexpected ways during the presymptomatic stages of the disease.

DTI is another modality that has been found to show some unexpected abnormalities in presymptomatic FAD. This advanced MRI technique provides insights into tissue microstructure by examining the magnitude and directionality of water diffusion within

white matter tracts and fibre-rich grey matter regions. Diffusion in white matter is described as anisotropic as it occurs preferentially along the major axis of a fibre. The three-dimensional nature of this diffusion is characterised by a diffusion tensor, from which various metrics can be extracted. Fractional anisotropy (FA) describes the overall shape of the tensor, with axial (AxD) and radial diffusivity (RD) representing diffusion in the principal direction of the tract and in the plane perpendicular to this. Mean diffusivity (MD) describes the overall magnitude of diffusion. Early DTI studies focussed on white matter FA alone and decreased FA in the fornix, interpreted as loss of structural integrity, was reported in presymptomatic mutation carriers who were on average 13 years younger than the age at dementia diagnosis in their family (Ringman *et al.*, 2007). In Chapter 6, I report a different observation; symptomatic mutation carriers were found to have the expected widespread reductions in white matter FA with increased MD, RD and AxD, however presymptomatic mutation carriers demonstrated a contrasting decrease in MD and AxD in the right cingulum (Ryan *et al.*, 2013). Reductions in AxD occur in axonal injury, which we hypothesise may be an early event in presymptomatic FAD. I also examined diffusion characteristics in grey matter regions of interest and found a corresponding reduction in MD in the right hippocampus. Reduced caudate MD has been reported in another cohort of presymptomatic *PSEN1* mutation carriers and it has been suggested that reductions in MD may reflect early pathological responses to amyloid accumulation such as microglial activation and/or swelling of neurons and glia (Fortea *et al.*, 2010). Finally, I observed increased FA in the thalamus and caudate of presymptomatic mutation carriers, which may be due to the degeneration of long-coursing white matter tracts with preservation of short interneurons within these highly connected structures. Refinement of DTI analysis methods and their application to larger cohorts, particularly those with longitudinal data, will hopefully allow these initial findings to be explored in greater depth.

Another advanced MRI technique that is starting to be applied to the study of presymptomatic FAD is fMRI. Detailed discussion of this imaging modality is outside the scope of this thesis but briefly, it has been found to detect very early differences between mutation carriers and their mutation-negative siblings. In the Colombian kindred, altered hippocampal activation during memory encoding on fMRI and decreased right parietal volume has been reported approximately two decades before the median age at onset of mild cognitive impairment for the family (Reiman *et al.*, 2012).

Another study has found decreased left hippocampal fMRI activity during memory retrieval in mutation carriers (Braskie *et al.*, 2013). In the DIAN study, resting state fMRI data has been analysed to look at functional connectivity in the default mode network; the set of brain regions whose coordinated activity during wakeful rest appears to be critical for successful memory function. Reduced connectivity in precuneus/posterior cingulate and right parietal cortex was observed in mutation carriers on average 12 years from parental age at onset, with decreasing functional connectivity observed in those closer to their expected age at onset (Chhatwal *et al.*, 2013).

One of the challenges in comparing different imaging studies of presymptomatic AD is that different groups have used different measures to estimate how far from clinical onset the mutation carriers may be. These include years from the parental age at symptom onset, the mean or median age at symptom onset for the family or the mean/median age at diagnosis of mild cognitive impairment or dementia. The latter two of these will of course occur later than the age at symptom onset and may vary according to a range of sociocultural factors surrounding presentation to health professionals. Recollections of when a relative's symptoms began are themselves subjective and can change over time. Furthermore, although symptoms appear to manifest at broadly similar ages within families, there is variability. Our understanding is currently quite limited regarding both the degree of such variability and the potential genetic or environmental modifiers that may underpin it. All of these caveats should be considered when cross-sectional studies are used to predict the temporal evolution of imaging changes in presymptomatic FAD. Comparability between studies may also be limited by differences in image analysis techniques as variability in methods, for example the approach used to segment a structure of interest like the caudate, may have an influence on the results generated. Finally, it remains uncertain how heterogeneously different FAD mutations affect imaging biomarkers in the presymptomatic phase.

Overall, the literature to date indicates that a variety of imaging biomarker abnormalities is evident in presymptomatic FAD. The use of a range of modalities has started to provide insights into the selective vulnerability of different regions to Aβ pathology, which longitudinal data should help to clarify. Longitudinal imaging will also be important for exploring the suggestion that the direction of change in some biomarkers may be dynamic at different points during the presymptomatic stage of

disease. Appreciating the possibility that imaging biomarkers may change in unpredictable ways during preclinical disease is important, particularly in light of upcoming treatment trials. Previous clinical trials have shown that treatments can also have unexpected effects on biomarkers, with the greatest volume losses in the AN1792 Aβ active immunisation trial seen in antibody-responders (Fox *et al.*, 2005). As the API and DIAN study have now both launched presymptomatic prevention trials of amyloid-modifying therapies, information about the sequence of biomarker changes during the natural history of the disease and in the context of treatment will be acquired in tandem. Study of the asymptomatic at-risk state of sporadic AD may progress in a similar fashion, with an anti-amyloid treatment trial (the A4 trial) in healthy older people with evidence of Aβ deposition on amyloid PET scans also underway (Sperling *et al.*, 2014). In this context, where imaging will be used to both define and study an at-risk state, a multi-modal approach will be important and insights from the study of presymptomatic FAD may be particularly valuable.

3 Clinical phenotype and genetic associations in autosomal dominant familial Alzheimer's disease: a case series

3.1 Introduction

Other than the younger age at symptom onset, FAD is considered to be clinically similar to sporadic AD, with progressive impairment of episodic memory characterising both forms of the disease. While atypical phenotypes are seen in both familial and sporadic AD (Ryan and Rossor, 2010, Crutch *et al.*, 2012, Shea *et al.*, 2015), relatively little is known about the proportion of individuals with FAD who present with atypical cognitive symptoms, the prevalence of additional neurological features, or the relationships between genotype and phenotype and the pathophysiological mechanisms that may underlie them.

Prevention trials for autosomal dominant FAD are underway and have stimulated important work investigating biomarker changes in preclinical disease. However, they also necessitate better understanding of the natural history of the disease in the symptomatic phase and of factors that influence age at onset. A recent meta-analysis found that mutation type accounted for a large proportion of the variance in age at onset, but substantial variation was still observed between, and even within, families with the same mutation (Ryman *et al.*, 2014). Younger ages at onset in *APOE*4 carriers have been reported in some studies analysing families with *APP*, *PSEN1* or *PSEN*2 mutations (Sorbi *et al.*, 1995, Pastor *et al.*, 2003, Wijsman *et al.*, 2005) although this association was not evident in the recent meta-analysis (Ryman *et al.*, 2014). Relatively little is known about the factors underlying variability in age at onset between different mutations within a single gene although, as will be discussed in Chapter 4, *PSEN1* mutations beyond codon 200 have been found to be associated with a later age at onset, more severe CAA and a greater burden of white matter hyperintensities on MRI than mutations located before codon 200 (Mann *et al.*, 2001, Ryan *et al.*, 2015, Shea *et al.*, 2015).

The aim of this study was to analyse the clinical phenotype data gathered on a large cohort of symptomatic individuals from FAD families studied in the UK over the past twenty-five years. We aimed to ascertain the initial cognitive symptoms and frequency of additional neurological features in the cohort, to investigate potential associations with age at symptom onset, mutation position and *APOE* genotype and to report the clinical and neuropathological features of the cases with novel mutations.

3.2 Materials and methods

3.2.1 Participants

Between July 1, 1987 and October 31, 2015, families with histories suggestive of dominantly inherited AD were referred to the Dementia Research Centre (DRC) at University College London's Institute of Neurology from clinical and research centres across the UK and Ireland. Following identification of the first *APP* mutation in one of these families (Goate *et al.*, 1991), *APP* mutations have been found in 11 of the families in our longitudinal FAD research study and *PSEN1* mutations in 55 other families. Five families with *APP* duplications have also been identified, which are not included in this study as they have been reported in detail elsewhere (McNaughton *et al.*, 2010). To date, no pathogenic *PSEN2* mutations have been identified in our cohort. Individuals with reported *APP* or *PSEN1* sequence variants of questionable pathogenicity were not included in this study.

Information regarding age at symptom onset, defined as the age at which clearly progressive symptoms of cognitive, behavioural or motor change were first noticed by someone who knew the subject well, was available for 213 individuals; 168 with *PSEN1* and 45 with *APP* mutations. Detailed contemporaneous records documenting the medical history and neurological examination findings were available for 121; 85 with *PSEN1* and 36 with *APP* mutations. Assessments were evaluated to determine the initial cognitive/behavioural symptoms and the presence of the following neurological features: myoclonus, seizures, pyramidal, extrapyramidal and cerebellar signs. Neurological features were classified as 'early' or 'late' depending on whether they were first observed before or after five years from symptom onset. *APOE* status could be established for 126 individuals; 95 with a *PSEN1* and 31 with an *APP* mutation.

Ethical approval for the study was obtained from the local institutional ethics committee and carried out in accordance with the Declaration of Helsinki; written informed consent was obtained from all participants or from their guardian if cognitive impairment prohibited written informed consent. A flow diagram detailing the number of participants involved in each component of this study and in the imaging studies reported in subsequent chapters of the thesis is shown in Figure 3.1.

Figure 3.1 Familial Alzheimer's disease study participants

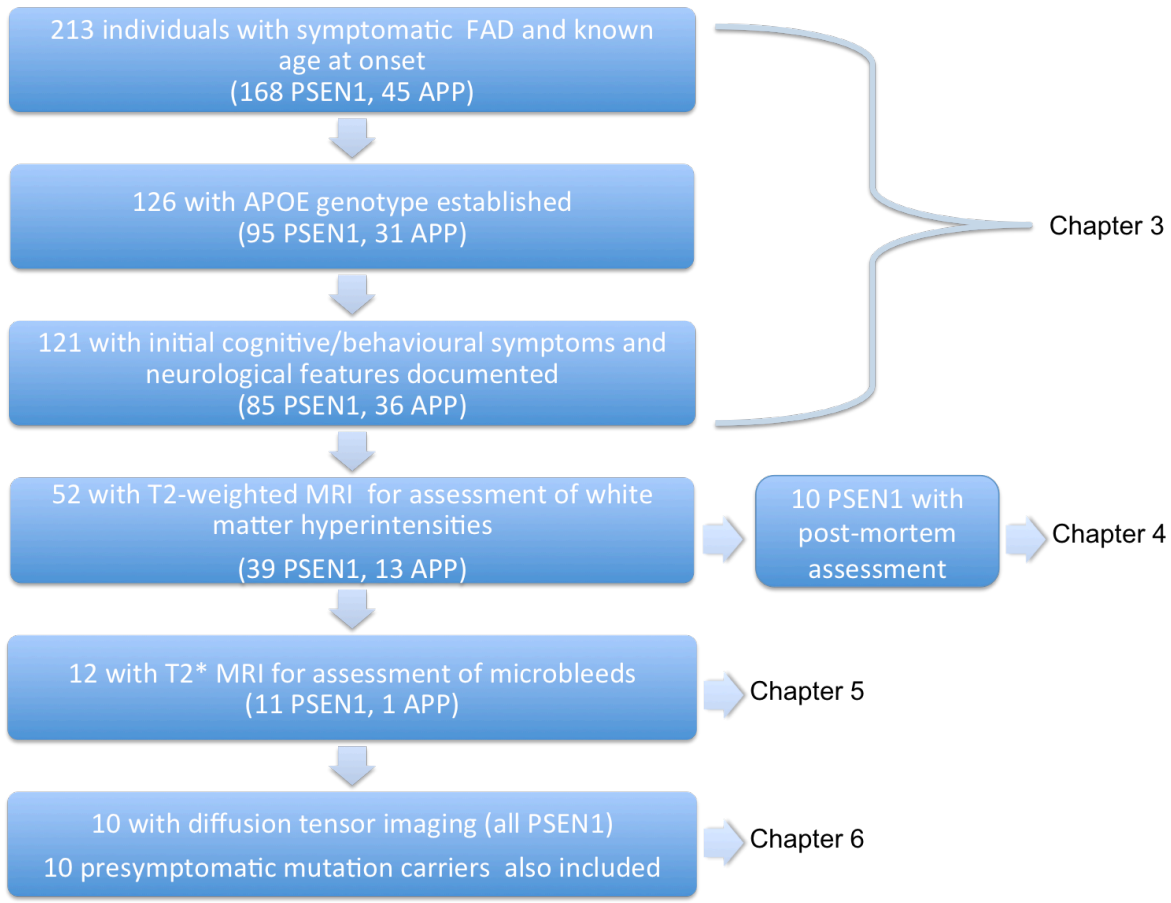

3.2.2 Procedures

Mutation analysis was carried out as described previously (Janssen *et al.*, 2003), for details see Appendix 11.2. The likely pathogenicity of novel variants was predicted using a previously published algorithm, which classifies variants as possibly, probably or definitely pathogenic (Guerreiro *et al.*, 2010). The software tools Polyphen (version

1.1.3) and Provean (version 2) were also used to predict whether the resulting amino acid substitutions were likely to impact on the biological function of the protein. Polyphen allocates a score between 0 and 1, with 1 representing the most damaging change. Provean generates a score, which predicts that the protein variant will have a "deleterious" effect if it is equal or below -2.5 and a "neutral" effect if it is above this threshold. Cases that were found to have novel variants in *PSEN1* or *APP* were then assessed for the presence of additional mutations in other dementia related genes using the Ion Torrent Dementia Chip, as described in Appendix 11.2.

Two novel variant cases underwent post-mortem brain donation to the Queen Square Brain Bank for Neurological Disorders, UCL Institute of Neurology. Aβ-positive plaque and neurofibrillary tangle pathology were assessed using Consortium to Establish a Registry for AD (CERAD) recommendations and Braak and Braak staging respectively (Mirra *et al.*, 1991, Braak *et al.*, 2006).

3.2.3 Statistical analysis

Differences in age at symptom onset between the *APP* and *PSEN1* mutation groups, between *APOE*4 carriers and noncarriers within each genetic group and between individuals with *PSEN1* mutations located before or after codon 200 were investigated using two sample *t* tests. Associations between age at onset and *PSEN1* mutation were analysed using a linear mixed effects model with random effects for mutation and family. The intraclass correlation coefficient was used to quantify the proportion of variance in age at onset explained by mutation, and by mutation and family. Groups of individuals with *APP* and *PSEN1* mutations were analysed separately to calculate the proportion of individuals presenting with amnestic symptoms; or with atypical symptoms of behavioural change, language impairment, dyscalculia or executive impairment; and the proportions with myoclonus, seizures, and pyramidal, extrapyramidal or cerebellar signs. Two sample t tests were used to investigate whether age at onset differed between those with typical and atypical presentations, or those with and without additional neurological features. Fisher's exact tests were used to investigate associations between atypical cognitive presentations or additional neurological features and *APOE*4 status, *PSEN1* exon and *PSEN1* mutation location

compared to codon 200. All results are reported as statistically significant if $p<0.05$; analyses were performed using Stata (version 12).

3.3 Results

3.3.1 Genetics

The numbers of individuals and families with each mutation are summarised in Table 3.1. One individual had a novel *APP* variant (p.Thr719Asn, NM_000484.3:c.2156C>A) and four individuals had novel *PSEN1* variants. The *PSEN1* p.Ser132Ala (NM_000021.3:c.394T>G), p.Gln222Pro (NM_000021.3:c.665A>C) and p.Phe283Leu (NM_000021.3:c.849T>G) variants were identified in three different individuals. The fourth individual had two *PSEN1* substitutions: p.Thr291Ala (NM_000021.3:c.871A>G) and p.Ala434Thr (NM_000021.3:c.1301G>A). The remainder of the cases had recognised mutations. The case with the novel *PSEN1* p.Ser132Ala variant, who had pathological confirmation of Alzheimer's disease, also had an intronic variant (NM_005910.5: rs11872014) in the *MAPT* gene. There is no consensus on the impact of the variant on MAPT splicing; it may alter an acceptor splice site and altered splicing can play a role in neurodegenerative disease (Karambataki *et al.*, 2010). However, we would not expect a *MAPT* mutation to cause Aβ pathology. In addition, this *MAPT* variant has not only been found in an elderly healthy control (unpublished data, MRC Prion Unit), but described 321 times on the Exome Aggregate Consortium (ExAC) dataset (http://exac.broadinstitute.org) with an allele frequency of 0.002952 (0.004401 in Europeans). Overall, this *MAPT* variant seems unlikely to have caused disease in this patient. No additional variants in dementia related genes were found in the other cases with novel *PSEN1* or *APP* variants.

Table 3.1 Mutations carried by the individuals in the cohort

Gene	Mutation	Exon	Number of families	Number of affected individuals (range in family size)	Mean age at onset (range)
APP	p.Ala692Gly	17	1	4	46 (39-54)
	p.Val715Ala	17	1	1	42
	p.Val717Gly	17	1	13	50 (40-59)
	p.Val717Ile	17	6	22 (1-8)	52 (39-59)
	p.Val717Leu	17	1	4	49 (48-51)
	p.Thr719Asn	17	1	1	46
PSEN1	Intron 4 (g.23024delG)	4	4	17 (1-12)	38 (35-45)
	p.Tyr115Cys	5	2	2	39 (34-44)
	p.Tyr115His	5	1	4	34 (30-36)
	p.Thr116Asn	5	1	2	34
	p.Glu120Lys	5	2	7 (2-5)	35 (31-39)
	p.Ser132Ala	5	1	3	59 (58-60)
	p.Met139Val	5	4	18 (1-9)	40 (35-48)
	p.Ile143Phe	5	1	2	56 (53-59)
	p.Met146Ile	5	2	6 (2-4)	48 (43-50)
	p.Leu153Val	5	1	3	35 (35-36)
	p.Tyr154Cys	5	1	1	41
	p.Leu166Arg	6	1	1	40
	p.Leu166del	6	1	1	38
	Delta 167 (p.Ile168del)	6	1	5	54 (43-60)
	p.Leu171Pro	6	1	5	42 (40-43)
	p.Glu184Asp	7	3	5 (1-2)	40 (37-45)
	p.Ile202Phe	7	1	2	48 (47-48)

	p.Gln222Pro	7	1	1	45
	p.Gly206Val	7	1	1	30
	p.Ile229Phe	7	1	3	33 (32-34)
	p.Leu235Val	7	1	4	52 (44-59)
	p.Phe237Leu	7	1	1	47
	p.Leu250Ser	7	1	7	52 (47-56)
	p.Ala260Val	8	1	1	40
	p.Cys263Phe	8	1	2	59 (58-59)
	p.Pro264Leu	8	2	3 (1-2)	50 (44-56)
	p.Pro267Ser	8	1	2	38
	p.Arg269His	8	3	4 (1-2)	55 (50-62)
	p.Arg278Ile	8	1	7	51 (44-59)
	p.Glu280Gly	8	3	16 (1-8)	42 (39-49)
	p.Phe283Leu	8	1	15	46 (42-48)
	p.Ser290Cys	9	1	5	42 (41-44)
	ΔE9*	9	1	1	45
	p.Arg377Met	11	1	1	38
	p.Gly378Val	11	1	5	44 (41-48)
	p.Gly394Val	11	1	1	40
	p.Pro436Ser	12	1	3	46 (44-50)
	p.Thr291Ala and p.Ala434Thr	9 and 12	1	1	42

***** The exon 9 deletion (NM_000021.3:c.869-1G>T; p.Ser290Cys;Thr291_Ser319del) commonly referred to as ΔE9.

All novel sequence variants identified were absent from 100 healthy unrelated white control patients. With the exception of p.Ser132Ala which was seen in one individual of European ancestry, none of the variants were found on the ExAC dataset. Where possible, when a novel sequence variant was found in the proband, genotyping of other affected family members was performed by sequencing the relevant exon to demonstrate co-segregation between the mutation and disease. However, this was not possible in the majority of cases as there were no other affected relatives still alive.

The case with the *APP* p.Thr719Asn variant had a family history of dementia suggesting autosomal dominant inheritance but there were no other living affected relatives in whom to demonstrate co-segregation. She developed memory symptoms from age 46 years, with additional word-finding and calculation difficulties and myoclonus. Her father was similarly affected, also from around the age of 46 years, and his father was also thought to have had dementia. Although there was no pathological confirmation of AD in this family, the proband had supportive investigations including a typical CSF profile with a raised tau concentration of 920 pg/ml (reference range 146-595 pg/ml) and reduced $A\beta_{1-42}$ concentration of 121 pg/ml (reference range 627-1322 pg/ml). The affected amino acid lies close to the gamma-secretase site, is highly conserved between species and numerous pathogenic mutations have been reported at neighbouring residues. A different substitution at this residue (p.Thr719Pro) has previously been reported as pathogenic (Ghidoni *et al.*, 2009). The variant is predicted to be probably pathogenic by our algorithm, probably damaging by Polyphen (score=1) and "neutral" by Provean (score=-1.521).

The case with the *PSEN1* p.Gln222Pro variant was adopted and knew nothing of her biological family. She developed memory impairment from age 46 years with word-finding difficulties and dyscalculia. The residue is conserved between species and *PSEN*s and a different substitution at this same residue (p.Gln222His) has been reported as pathogenic in a pathologically-confirmed FAD patient (Miklossy *et al.*, 2003). The variant is predicted to be probably pathogenic by our algorithm, probably damaging by Polyphen (score=1) and "deleterious" by Provean (score=-5.670).

The p.Phe283Leu *PSEN1* variant was identified in three affected individuals and absent in two unaffected individuals from the same family, with AD confirmed post-mortem in another two affected family members. All of the mutation cases had an amnestic presentation, with symptom onset at age 46, 47 and 50 years. The residue is completely conserved between species and there are numerous pathogenic mutations in this region of *PSEN1*. The variant is classified as definitely pathogenic by our algorithm, as segregation was demonstrated. Polyphen predicts the variant to be probably damaging (score=0.999) and Provean predicts it to be "deleterious" (score=-5.378).

The cases with the novel p.Ser123Ala and p.Thr291Ala and p.Ala434Thr substitutions are described in the final part of the results section.

3.3.2 Age at symptom onset

Mean (±SD) age at onset was significantly later in individuals with *APP* mutations (50.4 ±5.2, range 39-59, p<0.0001) than in those with *PSEN1* mutations (43.6 ±7.2, range 30-62). There was no significant association between possession of an *APOE4* allele and age at onset in either the *PSEN1* (43.6 ±7.2 *APOE4* +ve versus 42.3 ±6.7 *APOE4* –ve; p=0.385) or *APP* (50.7 ±4.2 *APOE4* +ve versus 50.7 ±5.3 *APOE4* –ve; p=0.998) cohorts. In individuals with a *PSEN1* mutation, age at onset (Table 3.1) was found to be influenced by the specific mutation, with 72% of the variance in age at onset explained by mutation (intra-class correlation coefficient, ICC=0.72). Mutation and family membership together explained 82% of the variance in age at onset (ICC=0.82). Mutations located before codon 200 had, on average, a younger age at onset (41.3 ±7.2) than mutations beyond codon 200 (45.8 ±6.4, p<0.0001), which appeared to be driven by a younger age at onset for mutations involving exons 5 and particularly 4 compared with the later exons (Figure 3.2 and Figure 3.3). Age at onset for the individual with the double substitution p.Thr291Ala and p.Ala434Thr is excluded from these figures as it is unclear whether pathogenicity is due to one or both of these amino acid substitutions. The intron 4 (NM_000021.3:c.338+1delG) mutation is classified as involving exon 4 as it is located just outside this exon. The mutation produces three different transcripts through aberrant splicing; two deletion transcripts resulting in truncated PSEN1 proteins and one insertion transcript resulting in full-length PSEN1 with an extra amino acid (Thr) inserted between codons 113 and 114 (PSEN1 Thr114-114ins), exon 5 begins at codon 114. The truncated proteins have been found to be undetectable in brain homogenates, indicating that the PSEN1 Thr113-114ins protein probably accounts for the pathogenicity of this mutation (De Jonghe *et al.*, 1999).

Figure 3.2 Age at onset for individuals with mutations involving each exon of the *PSEN1* gene.

Each dot represents an individual's age at onset. Within each exon, different colours represent each separate family and multiple families with the same mutation are indicated by different shades of the same colour (blue, green, purple or pink). Bars indicate mean age at onset for mutations involving each exon

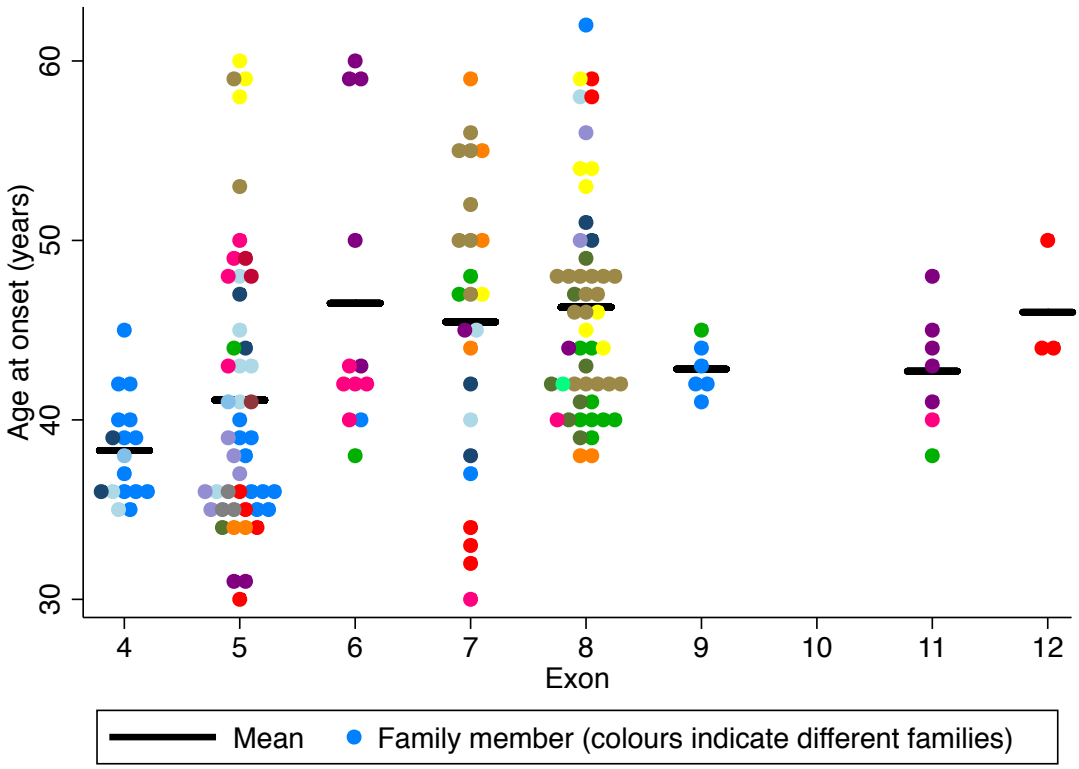

Figure 3.3 Location of the mutations present in our cohort of *PSEN1* mutation carriers, shown according to age-at-onset quartiles

Predicted membrane topology of PSEN1, with the nine transmembrane domains (dark green shaded boxes) and boundaries between coding exons indicated. The sites of amino acid substitution (or insertion in the case of Intron 4 and deletion in the case of ΔE9) are indicated by coloured circles, with the colour representing the quartile that the mean age at onset for that variant falls within. Adapted by permission from Macmillan Publishers: *Nature* (2012) (Li *et al.*, 2013). Codon 200 is shown within the fourth transmembranal domain of the protein. TM = transmembrane domain.

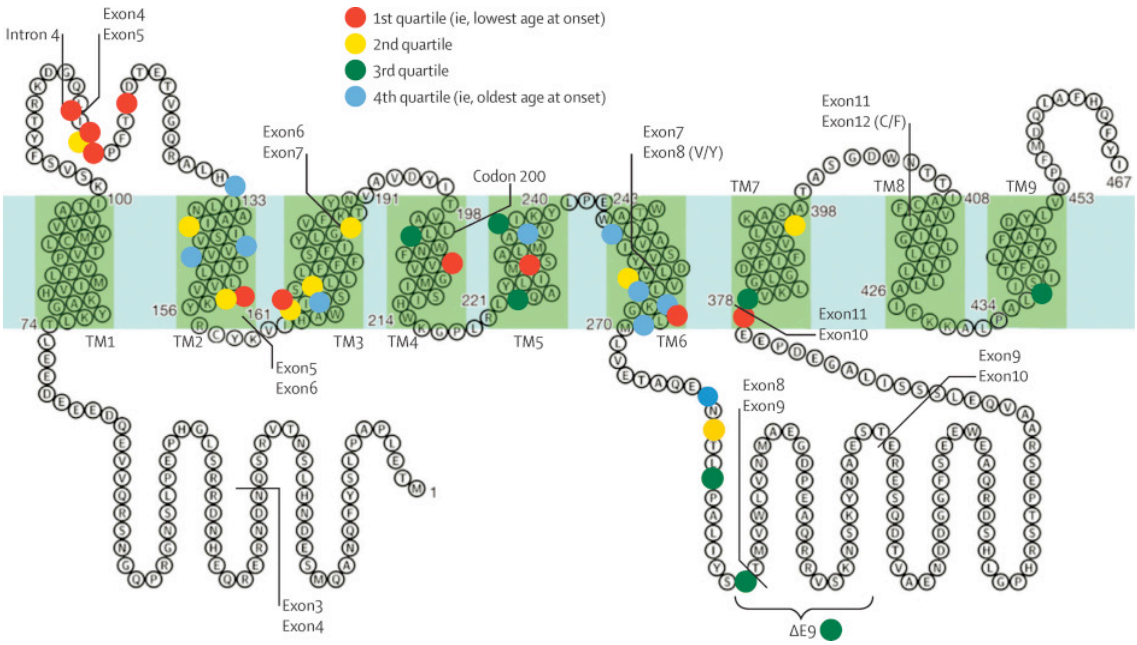

3.3.3 Cognitive-behavioural presentations

35 of 36 individuals with *APP* mutations presented with typical amnestic symptoms; the remaining individual presented with dyscalculia but developed memory problems soon after. Of the 85 individuals with *PSEN1* mutations, 71 (84%) presented with amnestic symptoms. Atypical cognitive presentations were more frequently associated with *PSEN1* than *APP* mutations (p=0.037). Of the 14 *PSEN1* mutation carriers with atypical initial cognitive features, seven (8%) presented with behavioural change, three (4%) with language impairment, two (2%) with dyscalculia and two (2%) with a dysexecutive syndrome. The *PSEN1* subgroup with atypical cognitive presentations had, on average, a somewhat later age at onset than those with typical amnestic symptoms (46.2 vs 42.0, p=0.046). Prevalence of atypical cognitive presentations differed markedly between exons, occurring in 10 of 22 (45%) individuals with exon 8 mutations, and fewer than (20%) of individuals with mutations involving other exons (Figure 3.4). As a result, atypical presentations were significantly more common in individuals whose mutation was located after codon 200 (p=0.006). Individual mutations associated with atypical cognitive presentations are listed in Table 3.2. There was no association between atypical cognitive symptoms and *APOE*4 status.

Figure 3.4 Cognitive presentations in *APP* and *PSEN1* mutation carriers in our cohort, with presenting symptoms in the *PSEN1* group shown by exon

Number of cases: 36 *APP* and 85 *PSEN1* mutation carriers

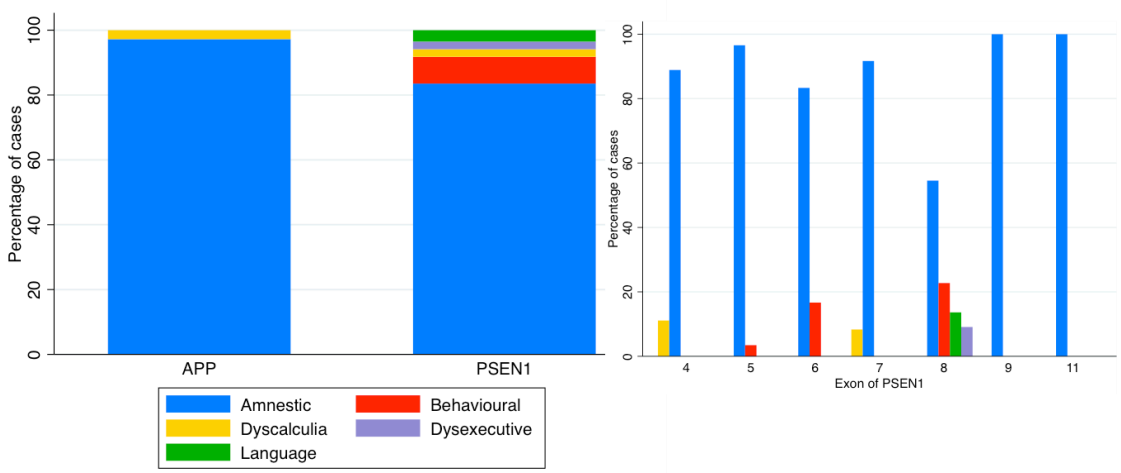

Table 3.2 Mutations associated with atypical phenotypes and additional neurological features in our cohort

Phenotype	Gene	Mutation	Patients with the phenotype (n/N)	Previous reports of the cases
Behavioural presentation	*PSEN1*	p.Met139Val	1/14	
		p.Leu166Arg	1/1	
		p.Pro264Leu	2/3	
		p.Arg269His	1/2	
		p.Arg278Ile	1/5	
		p.Glu280Gly	1/9	
Language presentation	*PSEN1*	p.Pro264Leu	1/3	(Mahoney *et al.*, 2013)
		p.Arg278Ile	2/5	(Godbolt *et al.*, 2004)
Dycalculia presentation	*PSEN1*	Intron 4 (g.23024delG)	1/9	
		p.Leu235Val	1/2	
	APP	p.Val717Ile	1/19	
Dysexecutive presentation	*PSEN1*	p.Glu280Gly	2/9	
Myoclonus	*PSEN1*	Intron 4 (g.23024delG)	6/9	
		p.Tyr115Cys	1/1	
		p.Tyr115His	1/2	
		p.Ser132Ala	1/1	
		p.Met139Val	10/14	(Kennedy *et al.*, 1995) (Fox *et al.*, 1997)
		p.Met146Ile	2/3	
		p.Glu184Asp	1/3	
		p.Ile202Phe	1/1	(Ryan *et al.*, 2014)
		p.Gly206Val	1/1	
		p.Ile229Phe	1/1	
		p.Phe237Leu	1/1	

		p.Leu250Ser	1/1	
		p.Ala260Val	1/1	
		p.Pro264Leu	1/3	
		p.Arg269His	1/2	
		p.Arg278Ile	3/5	
		p.Glu280Gly	4/9	
		p.Ser290Cys	½	
		p.Gly278Val	1/1	
		p.Gly394Val	1/1	
	APP	p.Val717Gly	5/11	(Kennedy *et al.*, 1993)
		p.Val717Ile	5/19	
		p.Val717Leu	1/4	
		p.Thr719Asn	1/1	
Seizures	*PSEN1*	Intron 4 (g.23024delG)	5/9	
		p.Tyr115Cys	1/1	
		p.Tyr115His	1/4	
		p.Met139Val	4/14	(Kennedy *et al.*, 1995) (Fox *et al.*, 1997)
		p.Met146Ile	2/3	
		p.Gly206Val	1/1	
		p.Ala260Val	1/1	
		p.Pro264Leu	2/3	
		p.Pro267Ser	1/1	
		p.Glu280Gly	2/9	
	APP	p.Ala692Gly	1/1	
		p.Val717Gly	5/11	(Kennedy *et al.*, 1993)
		p.Val717Ile	2/19	
		p.Val7171Leu	1/4	
Spastic paraparesis +/- other pyramidal signs	*PSEN1*	Intron 4 (g.23024delG)	1/9	
		p.Tyr115His	1/2	
		p.Glu120Lys	1/3	

		p.Met139Val	1/14	
		p.Met146Ile	1/3	
		p.Leu166Arg	1/1	
		p.Glu184Asp	1/3	
		p.Pro264Leu	1/3	
		p.Arg278Ile	2/5	
		p.Glu280Gly	8/9	(O'Riordan *et al.*, 2002)
		p.Gly394Val	1/1	
		p.Thr291Ala & p.Ala434Thr	1/1	
		ΔE9	1/1	
Extrapyramidal signs	*PSEN1*	p.Tyr115His	1/3	
		p.Glu120Lys	1/3	
		p.Ser132Ala	1/1	
		p.Met146Ile	1/3	
		p.Leu166Arg	1/1	
		Delta 167 (p.Ile168del)	1/2	
		p.Arg278Ile	3/5	
		p.Glu280Gly	2/9	
		p.Thr291Ala & p.Ala434Thr	1/1	
Cerebellar signs	*PSEN1*	p.Tyr115Cys	1/1	
		p.Glu280Gly	1/9	(O'Riordan *et al.*, 2002)
		p.Ser290Cys	1/2	

3.3.4 Neurological features

In the *APP* group, myoclonus and seizures were the only additional neurological features observed. In the *PSEN1* group, pyramidal, extrapyramidal and cerebellar signs were also seen. Table 3.2 shows the mutations and proportion of cases with each of these neurological features. Figure 3.5 demonstrates the proportion of cases with each neurological feature for mutations involving each exon of *PSEN1*.

Figure 3.5 Proportion of cases with each neurological feature for mutations involving each of the exons of *PSEN1*

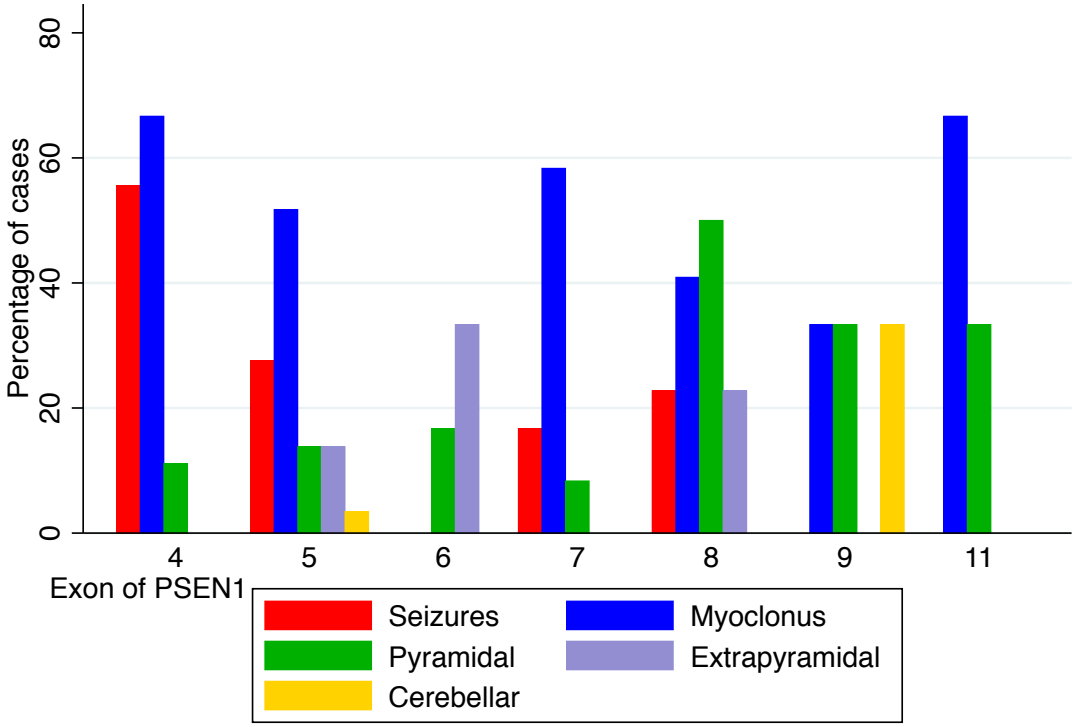

3.3.4.1 Myoclonus and seizures

The frequency of myoclonus and seizures did not differ significantly between the *PSEN1* and *APP* groups. In the *APP* group, 12 (33%) of 36 carriers had myoclonus and nine (25%) of 36 developed seizures. Of the 12 individuals with myoclonus, onset was early (≤5years from onset) in five (42%), late in two (17%), and uncertain in five (42%). Of the nine individuals with seizures, onset was early in three, late in three, and uncertain in three. In the *PSEN1* group, 40 (47%) of 85 carriers had myoclonus and 20 (24%) had seizures. Of the 40 individuals with myoclonus, onset was early in 28 (70%), late in nine (23%), and uncertain in three (7%). Of the 20 individuals with seizures, onset was early in six (30%), late in 10 (50%), and uncertain in four (20%). Individuals with myoclonus were significantly more likely to develop seizures: 40% developed seizures in the *PSEN1* group (p=0.001) and 50% in the *APP* group (p=0.036). There was no association between myoclonus or seizures and age at onset or *APOE*4 status in either the *APP* or *PSEN1* groups. There was no association between seizures or

myoclonus and *APOE*4 status, exon or mutation location with respect to codon 200 in the *PSEN1* group.

3.3.4.2 Pyramidal signs

Pyramidal signs were observed in 21 (25%) of the 85 *PSEN1* carriers. All of these individuals had spastic paraparesis, and 18 also had upper limb pyramidal signs. Of the 21 individuals with pyramidal signs, 15 (71%) developed them early, although none were reported to have these signs before onset of cognitive symptoms. The remaining six (29%) developed them late, with an absence of pyramidal signs at earlier assessments. There were no associations between pyramidal signs and age at onset or *APOE*4 status in the *PSEN1* cohort as a whole and insufficient numbers to investigate such associations at the level of individual families or mutations. Pyramidal signs were, however, observed more frequently in association with *PSEN1* mutations after codon 200 than before codon 200 (p=0.024), with particularly high frequency (50%) for mutations on exon 8 (Figure 3.5).

3.3.4.3 Extrapyramidal signs

Extrapyramidal signs were observed in 13% of the *PSEN1* group and occurred early in the illness in 67%, late in the illness in 25% and were of uncertain onset in 8%. No associations were found between extrapyramidal signs and age at onset, *APOE*4 status, exon or *PSEN1* mutation location compared to codon 200.

Of the individuals with early extrapyramidal signs, one had markedly asymmetrical features consistent with a corticobasal syndrome. Two had novel *PSEN1* variants; one presenting with a DLB phenotype. These cases are summarised below.

Corticobasal syndrome secondary to the PSEN1 p.Tyr115His mutation

This right-handed man developed memory impairment from age 34 years. Three years later, he gradually developed uncomfortable tingling sensations, involuntary jerks and stiffness of his right hand, which took up a clenched position. He then developed unsteadiness walking and lower limb stiffness, particularly on the right. On examination aged 39 years, he scored 24/30 on the MMSE and had a rigid, dystonic flexed hand with

frequent myoclonic jerks. There was a pyramidal and extrapyramidal component to the rigidity, with associated bradykinesia and limb kinetic apraxia. The lower limbs had a spastic increase in tone bilaterally, more prominent on the right, with sustained clonus. Limb reflexes were all pathologically brisk but symmetrical with flexor plantar responses. He had a spastic gait with decreased right arm swing. Brain MRI brain demonstrated strikingly focal asymmetrical left parietal atrophy. In view of the spasticity component a trial of Tizanidine was given, which caused a significant improvement in the stiffness and function of his right hand. His father had developed memory impairment aged 36 years followed by slurred speech and difficulty walking two years later.

Dementia with Lewy bodies (DLB) phenotype secondary to a novel PSEN1 mutation p.Ser132Ala

This man developed problems with episodic and topographical memory from age 59 years with early symptoms of visual perceptual impairment and difficulty learning new tasks. He sometimes failed to recognise places or experienced déjà vu in places he had never visited before. Two years later he developed visual hallucinations of people and animals and difficulty recognising his wife and daughter, at times thinking they were imposters. He subsequently developed paranoid ideation, wandering and dyspraxia. He was first examined by a neurologist aged 64 years, at which stage he had myoclonic jerks, bradykinesia and increased limb tone throughout. Limb reflexes were normal and bilateral grasp and palmomental reflexes were present. He was too severely impaired for neuropsychological testing, brain MRI showed widespread atrophy. There was no past medical history, sulpiride had been prescribed by a psychiatrist for his behavioural symptoms but stopped when he developed limb stiffness. His maternal aunt and uncle had both died aged 65 years, having developed cognitive impairment with visual hallucinations, paranoia and loss of self-care at the ages of 58 years and 60 years respectively. His mother died following a brain haemorrhage aged 61 and experienced visual hallucinations of cats whilst in hospital. His maternal grandmother died in a psychiatric hospital in her early 70s after a ten year illness. There were no affected living relatives in whom to demonstrate co-segregation. He died aged 70 years.

Post-mortem examination of the brain revealed severe neuritic plaque pathology in the CERAD consensus regions with Braak & Braak stage V neurofibrillary tangle

pathology, indicating high likelihood AD (NIA-Reagan criteria). There was also severe neocortical Lewy body pathology, Braak stage 6 (Figure 3.6). In view of the severity of the AD pathology, McKeith criteria indicate an intermediate likelihood that the pathological findings are associated with a DLB clinical syndrome (McKeith *et al.*, 2005).

Figure 3.6 Neuropathological findings in a 70 year old man with the novel *PSEN1* p.Ser132Ala mutation presenting with a Dementia with Lewy bodies phenotype

Amyloid pathology in the hippocampus of (a) cored amyloid plaques (double arrows), and (b) diffuse Aβ (arrows). (c) AT8 immunoreactivity for abnormally phosphorylated tau of neurofibrillary tangles in the CA1 sub-region of the hippocampus, and (d) of neuritic plaques in the temporal cortex (arrows). (e) Alpha-synuclein immunohistochemistry of Lewy neurites and Lewy bodies in the CA1 sub-region of the hippocampus, and (f) Lewy bodies found in the dopaminergic neurons of the substantia nigra (arrows). Bar in a represents 60µm in a, c, d and e; 20µm in f and 10µm in b.

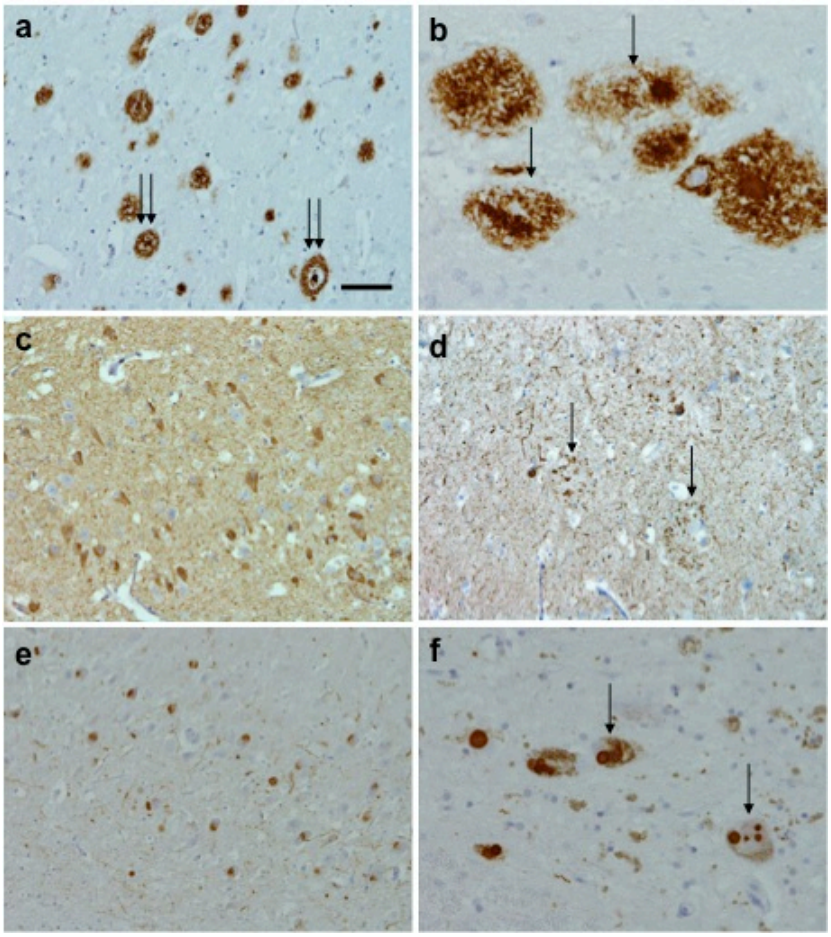

The p.Ser132Ala variant has not previously been reported. The affected amino acid is conserved between *PSEN*s and located close to the second transmembrane domain. There are several pathogenic mutations in the surrounding region, although these all fall within the second transmembrane domain. The variant is predicted to be possibly pathogenic by our algorithm, probably damaging by Polyphen (score=0.998) and "neutral" by Provean (score=-0.871).

Dementia with Parkinsonism and pyramidal signs in an individual with two PSEN1 mutations: p.Thr291Ala and p.Ala434Thr

This man of Scottish-Italian origin developed simultaneous memory symptoms and a gait disorder from age 42 years. His walking initially became unsteady and slow, with leg stiffness and frequent falls. He then developed difficulty turning and an increasingly small-stepped gait. He appeared more docile and withdrawn and neglected his self-care. From age 43 years he was noted to have slow, slurred speech and illegible handwriting. He had a history of treated hypertension and smoking. His father had died aged 34 years from a brain haemorrhage and was said to have had cognitive impairment and a shuffling gait prior to this event. Nothing else was known about the paternal side of his family. His mother died aged 73 years with no cognitive symptoms and two maternal half-siblings were well. There were no other affected relatives in whom to demonstrate co-segregation. On examination aged 44 years, he scored 17/30 on the MMSE and had clear pyramidal and extrapyramidal signs. He was hypomimic, bradyphrenic and bradykinetic with slow, dysarthric speech. Limb tone was increased throughout and reflexes were pathologically brisk with extensor plantar responses. He had truncal rigidity and walked with a stooped posture and reduced arm swing. Neuropsychometry demonstrated global memory impairment, anomia and executive dysfunction with extreme cognitive slowing, whilst visual perceptual function was intact. Brain MRI revealed extensive white matter hyperintensities with a posterior emphasis and generalised atrophy, which did not disproportionately involve the hippocampi. CSF tau concentration was 117 pg/ml, A$\beta_{1\text{-}42}$ was 279 pg/ml. He underwent a progressive decline in cognition and mobility and died aged 47 years.

Postmortem examination of the brain revealed changes of AD with tau pathology corresponding to Braak & Braak stage V. The Aβ deposition was in the form of widespread cotton wool plaques and diffuse deposits (Figure 3.7).

Figure 3.7 Neuropathological findings in a 42 year old man with a *PSEN1* double substitution, p.Thr291Ala and p.Ala434Thr, presenting with cognitive impairment, pyramidal and extrapyramidal signs

Amyloid pathology in the hippocampus of (a) cotton wool plaques and (b) capillary cerebral amyloid angiopathy (c) Diffuse deposits, shown in the granule cell layer of the cerebellum. (d) Aβ deposits in the leptomeningeal blood vessels, (e) and Aβ deposits shown to be in an amyloid conformational state using Congo red staining. (f) AT8 immunoreactivity for abnormally phosphorylated tau in the CA1 sub-region of the hippocampus, (g) and at 40X magnification detailing the neurofibrillary tangles and neuropil threads. Bar in a represents 60µm in a, c, d and g; 20µm in b and e and 200µm in f.

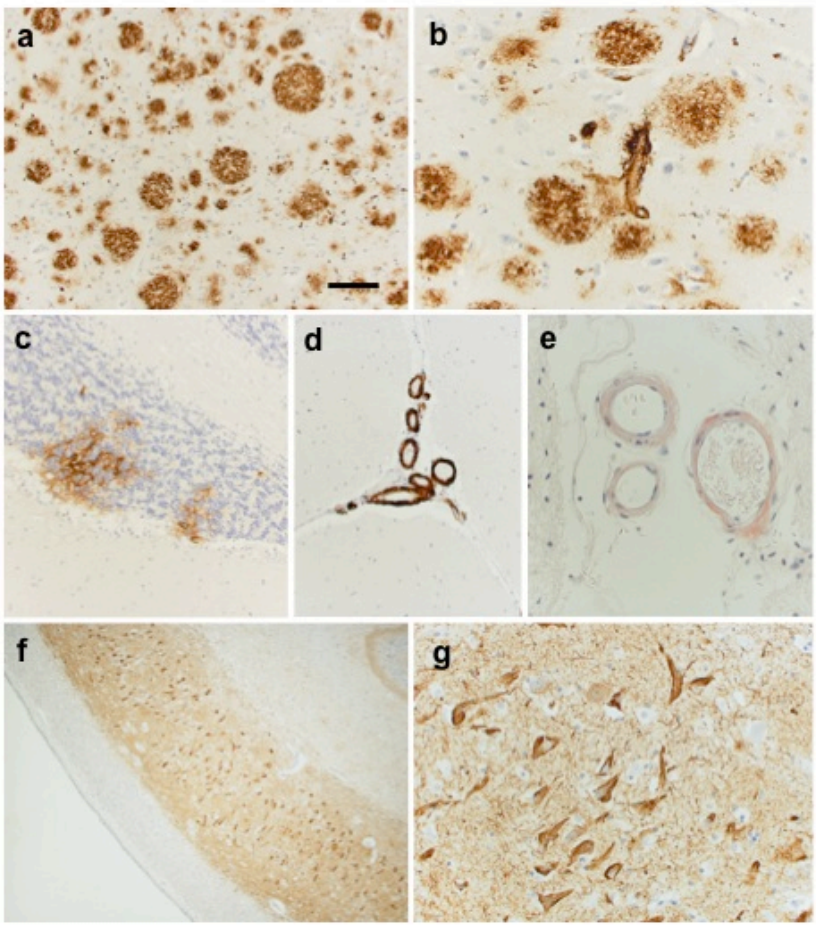

Cotton wool plaques were observed throughout neocortical regions, hippocampus, amygdala, caudate, putamen, thalamus, subthalamic nucleus and in the molecular layer of the cerebellum. There was severe CAA in leptomeningeal and cortical vessels, including capillaries. Marked gliosis and diffuse microgliosis were observed throughout the cortex and white matter. There was no α-synuclein pathology.

The p.Ala434Thr *PSEN1* mutation has been reported in a Chinese patient who presented with hallucinations and delusions, although another affected family member had a typical amnestic presentation (Jiao *et al.*, 2014). The p.Thr291Ala variant has not previously been reported. However, it affects a highly conserved amino acid and a different substitution at the same residue (p.Thr291Pro) has been reported in a French FAD patient who also had spastic paraparesis and dysarthria. This variant increases Aβ42 secretion in retrovirally transduced cells (Dumanchin *et al.*, 2006). The p.Thr291Ala variant is predicted to be possibly pathogenic by our algorithm, possibly damaging by Polyphen (score=0.674) and "neutral" by Provean (score=-1.545).

3.3.4.4 Cerebellar signs

Cerebellar signs were observed in three (4%) of the 85 *PSEN1* carriers, occurring early in two, and late in one. No associations were found with age at onset, *APOE*4 status, or exon or *PSEN1* mutation location compared to codon 200.

3.4 Discussion

This study characterises the clinical spectrum of FAD in a large case series from a single UK centre and explores some of the factors that may influence clinical heterogeneity. Significant phenotypic differences were found between *PSEN1* and *APP* mutation carriers, emphasising the potential importance of examining these groups separately in observational research and clinical trials. In addition to the well known younger age at symptom onset for *PSEN1* compared with *APP* mutations, *PSEN1* mutation carriers more frequently presented with atypical cognitive symptoms and additional neurological features. Behavioural, language and dysexecutive presentations, spastic paraparesis and other pyramidal, extrapyramidal and cerebellar signs were only

seen in the *PSEN1* cases in our cohort. Myoclonus and seizures, on the other hand, affected a similar proportion of individuals with *APP* and *PSEN1* mutations. In both genetic groups, individuals with myoclonus were significantly more likely to develop seizures than those without myoclonus, highlighting the importance for clinicians of being vigilant for symptoms of seizure activity when myoclonus is present.

Possible limitations of our study were that some atypical phenotypes, such as movement disorder presentations or much older onset, may not have been seen in our case series due to the ascertainment bias of our centre being more likely to be referred younger patients with cognitive symptoms. Also, not all individuals were followed to advanced stages of illness, so late neurological features may be more frequent than described here. With enrolment of individuals over a long period of time, there is the potential for families to have greater awareness and therefore earlier recognition of symptom onset with successive generations. The relative non-diversity of individuals seen in a single country may also limit generalizability of the findings. However, the mean age at onset in our cohort was very similar to those reported in a French case series of autosomal dominant early onset AD cases (Wallon *et al.*, 2012) and in recent systematic reviews of autosomal dominant FAD (Ryman *et al.*, 2014, Shea *et al.*, 2015). As in our case series, spastic paraparesis and extrapyramidal and cerebellar signs were seen in French *PSEN1,* but not *APP,* mutation carriers, usually manifesting within five years of symptom onset. The proportion of French individuals with *PSEN1* mutations presenting with 'frontal symptoms' (11%) was also comparable to the combined proportion of individuals in our series whose initial cognitive symptoms were behavioural (8%) or dysexecutive (2%) (Wallon *et al.*, 2012). Finally, a non-amnestic presentation was found in 16% of the autosomal dominant FAD cases reported worldwide (Shea *et al.*, 2015); the same as the proportion of *PSEN1* cases in our cohort who did not present with memory symptoms.

Whilst a significant minority of the *PSEN1* cases in our study presented with non-amnestic cognitive symptoms, all but one of the *APP* cases had initial memory symptoms. The vast majority of these mutations involve codon 717. Amnesia has been recognised as the major neuropsychological feature of mutations at this site since the earliest reports (Rossor *et al.*, 1993) and a slowly progressive pure amnestic syndrome lasting fourteen years before involvement of other cognitive domains occurred in one of these individuals with a p.Val717Gly mutation (Knight *et al.*, 2009). Dyscalculia was

also observed to be an early feature of *APP*-associated FAD in the initial case series and we found 2% of the *APP* and *PSEN1* cases to present with isolated dyscalculia, followed soon after by memory symptoms. Interestingly, none of our cases presented with a PCA syndrome. Despite the young age at onset that is typical of PCA, it has only once been reported in association with FAD secondary to a novel *PSEN1* variant p.Ile211Met (Sitek *et al.*, 2013).

There has been some evidence that phenotypic differences between *APP* and *PSEN1* mutation carriers are reflected in differences on neuroimaging and that these may provide insights into differences in underlying disease mechanisms. We have previously reported *APP* mutation carriers to have greater hippocampal atrophy than *PSEN1* carriers of similar disease severity, while *PSEN1* carriers show more extensive neocortical atrophy and white matter involvement; the latter may underlie some of the atypical features observed in *PSEN1* (Scahill *et al.*, 2013). PSEN1 forms the catalytic subunit of gamma-secretase, which processes APP, but also a large number of other substrates involved in various physiological functions including myelin repair, vascular and immune function. Gamma-secretase carries out an initial endopeptidase cleavage of its substrates followed by successive carboxypeptidase-like cleavages. *PSEN1* mutations all appear to decrease the efficiency of this carboxypeptidase-like activity, resulting in the release of longer Aβ peptides, which are more prone to aggregation. Most *PSEN1* mutations also affect the endopeptidase activity, but to various degrees, potentially impacting on the processing of other substrates in addition to APP (Chavez-Gutierrez *et al.*, 2012, Szaruga *et al.*, 2015). We speculate that altered processing of other substrates may contribute to the atypical phenotypes witnessed in association with some *PSEN1* mutations. Supporting this notion, atypical cognitive presentations and pyramidal signs in participants of this study were seen more frequently in association with *PSEN1* mutations involving exon 8. The residues encoded by exon 8 lie within the hydrophilic extended sequence between transmembrane domains six and seven of PSEN1, which is where the cleavage site processed by autocatalytic activity has been found (Bai *et al.*, 2015). Furthermore, individuals with two of the most atypical phenotypes - the corticobasal syndrome (p.Tyr115His) and DLB (p.Ser132Ala) presentations - had mutations involving hydrophilic loop 1, which has been proposed to form the initial substrate binding site in PSEN1, with Ser132 playing a critical role

(Takagi-Niidome *et al.*, 2015). Indeed, the p.Tyr115His mutation has been found to reduce endopeptidase efficiency due to substantially decreased affinity for the Notch substrate, while the affinity for APP is affected to a lesser extent (Chavez-Gutierrez *et al.*, 2012). Certain mutations may therefore differentially affect the substrate specificity of the gamma-secretase complex and investigating whether this mechanism contributes to atypical phenotypes is an important direction for future work. Also important will be studies exploring clinicopathologic correlations in FAD. It was notable that the PSEN1 p.Ser132Ala case with a DLB phenotype had severe neocortical Lewy body pathology. However, concomitant Lewy body pathology is a frequent finding in FAD (Leverenz *et al.*, 2006). Large cohort studies will be important to further investigate clinical phenotype and clinicopathologic correlations in autosomal dominant FAD, ideally with unaffected family members acting as controls.

Our results suggest that multiple factors may contribute to phenotypic heterogeneity in FAD. There was often considerable variability in the clinical features of individuals with the same mutation, even within a single family. Even so, we found that mutations before codon 200 were associated with younger age onset, whereas mutations beyond codon 200 were more frequently associated with later ages at onset, atypical cognitive presentations and pyramidal signs. Given the relatively small numbers of subjects manifesting each atypical feature, and the numbers of associations (although not independent), it is important to be cautious about nominally significant associations. Nonetheless, we felt it important to report them to allow replication in other cohorts. Indeed, a recent systematic review (Shea *et al.*, 2015) also found that *PSEN1* mutations before codon 200 had younger ages at onset and were more frequently associated with seizures and myoclonus, whilst mutations beyond codon 200 were more frequently associated with spastic paraparesis. Codon 200 is an arbitrary cut-off and mapping the mean ages at onset for different mutations to the structure of PSEN1 (Figure 3.3) suggests there may be certain areas of the protein where mutations cause particularly early-onset disease, such as the first hydrophilic loop encoded by exons four and five. This extracellular loop contributes to a key allosteric core that changes Aβ profiles through carboxypeptidase-like activity without affecting the endopeptidase function of gamma-secretase (Ohki *et al.*, 2011, Takeo *et al.*, 2014). As qualitative changes in Aβ profiles appear to underlie the pathogenicity of *PSEN1* mutations (Chavez-Gutierrez *et*

al., 2012, Szaruga *et al.*, 2015), one could speculate that they may be more dramatically altered by mutations involving this allosteric core, resulting in a more aggressive phenotype.

We have demonstrated that a subset of individuals with FAD do not have a typical amnestic presentation. As atypical presentations also occur in sporadic AD, we do not feel that our findings challenge the idea that familial cases represent a paradigm for AD, but rather highlight the importance of distinguishing and investigating atypical phenotypes in the endeavour to understand the complex underlying mechanisms that may contribute to disease. The clinical features of *PSEN1*-associated FAD may erroneously suggest a diagnosis of frontotemporal or vascular dementia, corticobasal degeneration or DLB. However, if there is a family history or if the family history is not known, we suggest that it is important to consider FAD in the differential diagnosis of patients with young onset dementia with additional neurological features. FAD detection rates have, at least historically, been lower than expected based on genetic epidemiology data and have shown considerable variability across different regions of the UK (Stevens *et al.*, 2011). Failure to identify a mutation in these families not only deprives the affected individual from a correct diagnosis and appropriate symptomatic treatment but has implications for the wider family. Individuals at risk of FAD should, if they wish, be given access to genetic counselling so that they may consider their choices in a variety of areas including predictive genetic testing and reproductive options such as pre-implantation genetic diagnosis. They may benefit from the peer support of connecting with other families affected by FAD (Walton *et al.*, 2015) and from opportunities to participate in research, including preclinical treatment trials aiming to delay or prevent the onset of symptoms.

4 Genetic determinants of white matter hyperintensities and amyloid angiopathy in familial Alzheimer's disease

4.1 Introduction

As described above, although autosomal dominantly inherited mutations in *APP*, *PSEN1* and *PSEN2* account for a small minority of AD cases, insights gained through studying FAD have contributed to our understanding of AD pathophysiology. The view that therapeutic success may only be possible with intervention very early in the disease course has motivated the development of treatment trials specifically for FAD, which offers the possibility of treating individuals at a preclinical disease stage (Reiman *et al.*, 2010, Bateman *et al.*, 2011). The young age of patients with FAD means that co-morbidities such as atherosclerotic cerebrovascular disease that can complicate clinical trials in sporadic AD are rare. However, the launch of FAD treatment trials necessitates a deeper understanding of the heterogeneity that exists within FAD, particularly with regards to CAA, which appears to be an important factor in amyloid-modifying therapeutic trials (Boche *et al.*, 2008, Sperling *et al.*, 2011, Sakai *et al.*, 2014).

As detailed in the previous chapter of this thesis there is considerable heterogeneity within FAD in the clinical phenotype; however there is also a recognition of heterogeneity at molecular and histopathological levels. Pathological findings in *PSEN1* mutation carriers have revealed considerable variability in terms of neuronal loss: the type, number and distribution of amyloid plaques; and the amount and distribution of neurofibrillary tangles (Gomez-Isla *et al.*, 1999, Maarouf *et al.*, 2008, Shepherd *et al.*, 2009). Of particular importance, marked differences in the amount of CAA have been observed that may possibly be driven by the precise location of the mutation within *PSEN1*. Intriguingly, mutations before codon 200 have been reported to be associated with many diffuse and cored plaques, few white matter plaques and only mild to moderate CAA, mainly confined to leptomeningeal blood vessels. By contrast, mutations beyond codon 200 have been described as demonstrating larger diffuse and cored plaques surrounding amyloid-laden arteries, with severe CAA that involves both leptomeningeal and intraparenchymal arteries (Mann *et al.*, 2001). The pre- or post-

codon distinction appears arbitrary but it may be an approximation for important functional differences in the PSEN1 molecule. Certainly this is the case for the APP molecule with certain *APP* mutations being associated with very severe CAA, particularly those that lie in very localised positions within the Aβ coding sequence (Revesz *et al.*, 2003, Revesz *et al.*, 2009, Shepherd *et al.*, 2009) including the Flemish (p.Ala692Gly), Dutch (p.Glu693Gln), Arctic (p.Glu693Gly) and Iowa (p.Asp694Asn) mutations. Remarkably, whilst all these mutations cause prominent CAA, the occurrence of plaques and tangles varies, as does the clinical phenotype (Ryan and Rossor, 2010). The Flemish mutation presents with haemorrhages or dementia; the Dutch mutation typically presents with recurrent cerebral haemorrhage, usually followed by dementia; and the Arctic and Iowa mutations present with dementia only.

Post-mortem studies of AD patients who participated in the initial, active, Aβ42 AN1792 immunotherapy (vaccination) trial have revealed that parenchymal amyloid removal may be accompanied by an increase in CAA, thought to be secondary to Aβ42 accumulation via perivascular drainage pathways (Boche *et al.*, 2008). The era of disease-modifying treatment trials for FAD therefore necessitates better characterisation and understanding of the variable occurrence of CAA in individuals with *APP* and *PSEN1* mutations. Radiological features of CAA include white matter hyperintensities (WMH) on T2-weighted MRI, cortico-subcortical intracerebral haemorrhages on gradient echo imaging; and atrophy best seen on T1-weighted imaging (Chao *et al.*, 2006). Whilst WMH on MRI are common in the elderly, in whom they may represent multiple pathologies, the young age of patients with FAD makes them less likely to have significant conventional vascular risk factors and MRI manifestations of atherosclerotic small vessel disease (Hopkins *et al.*, 2006). Prominent WMH in this population are therefore much more likely to be indicative of an aspect of FAD pathology. The aim of the study described in this chapter was to investigate the degree and location of WMH in symptomatic *APP* and *PSEN1* mutation carriers, together with age-matched controls, and to explore whether the reports of increased CAA in intra-domain *APP* mutations and *PSEN*1 mutations located beyond codon 200 are reflected in greater WMH burden on MRI. Pathological investigations were also carried out in 10 cases who had had post-mortem histopathological examination.

4.2 Materials and methods

4.2.1 Study Subjects

The study was conducted at the DRC, UCL Institute of Neurology at the National Hospital for Neurology and Neurosurgery. All symptomatic FAD subjects, who had a) participated in research; and b) had a confirmed pathogenic *APP* or *PSEN1* mutation; and c) had had appropriate and usable (e.g. relatively free of movement or other artefact) imaging were included in this retrospective study. Fifty-two patients were studied: 13 with *APP* mutations; and 39 with *PSEN1* mutations. In the *PSEN1* cohort, 18 subjects had pre-codon 200 mutations and 21 had post-codon 200 mutations. All FAD subjects were clinically affected and met criteria for probable AD at the time of MRI acquisition. Twenty-five healthy control subjects, mainly spouses and mutation-negative siblings, were also recruited. All subjects gave informed consent and approval was received from the local ethics committee. Mutation analysis was conducted on genomic DNA and *APOE* genotype was established for all patients. All subjects with FAD underwent clinical assessment. In most cases, a comprehensive medical history was recorded and from this, the presence or absence of hypertension, diabetes, hyperlipidaemia, stroke, transient ischaemic attack (TIA) and coronary artery disease was assessed to create a composite score for vascular risk that was the sum of the factors present, ranging from 0 to 6 (DeCarli *et al.*, 2004). This information was not available for some of the earlier historical cases and controls but could be analysed for a large subset (Table 4.1).

4.2.2 Imaging

All subjects underwent T2-weighted (T2 and/or FLAIR) and volumetric T1-weighted MRI. As this study was a retrospective analysis of individuals scanned over almost twenty years, images acquired on 1.5Tesla and 3Tesla scanners were included and there was also some variability in the parameters of the sequences used. However, an equivalent proportion of individuals were scanned at each magnetic field strength in each group.

An experienced neurologist, blinded to clinical diagnosis, visually assessed all scans. The scans were rated using the age-related white matter change (ARWMC) scale

(Wahlund *et al.*, 2001). The ARWMC scale (range 0-30) rates the degree of WMH on a four point scale for five different brain regions (frontal, parieto-occipital, temporal, infratentorial and basal ganglia including thalamus) for the right and left cerebral hemispheres separately. The ARWMC scale was chosen as it has been shown to provide robust results when applied to both CT and MRI, and therefore would be applicable to the T2-weighted MR images available in this study, which were acquired on a variety of different scanners and field strengths. T2*-weighted imaging sensitive to microbleeds was only available in the 12 most recently scanned patients (one *APP* and 11 *PSEN1* mutation carriers) and is reported in Chapter 5 (Ryan *et al.*, 2011) so was not included in the current study.

4.2.3 Pathology

Brains were donated to the Queen Square Brain Bank for Neurological Disorders, UCL Institute of Neurology. The protocol used for brain donation was approved by a London Research Ethics Committee and tissue is stored for research under a license from the Human Tissue Authority. Tissue sections (7-µm) from a number of brain regions were immunostained using commercially available antibodies as described previously and in Appendix 11.3 (Lashley *et al.*, 2008).

Quantitation of Aβ-positive mature and diffuse plaques was performed based on Consortium to Establish a Registry for Alzheimer's disease (CERAD) recommendations (Mirra *et al.*, 1991). Alzheimer-type neurofibrillary tangle pathology was determined using Braak and Braak staging (Braak *et al.*, 2006). The extent and severity of CAA was determined based on a four-tier grading system (Olichney *et al.*, 1996, Lashley *et al.*, 2008), described in Appendix 11.4. Quantitation of the immunohistochemical stains was undertaken to assess any deep white matter changes in the occipital and parietal regions. Myelin loss was assessed using myelin basic protein (MBP) immunohistochemistry (SMI94R antibody) while changes in axonal density and/or integrity were investigated using the phosphorylation dependent anti-neurofilament antibody RT97. Iba1 and CD68 immunohistochemistry was used to assess microglial response and GFAP immunohistochemistry was employed to study astrocytic response. CD3 and CD20 immunohistochemical preparations were used to assess T and B lymphocytic response, respectively. A semi-quantitative assessment of myelin loss, gliosis and microglial

expression was made, described in Appendix 11.5. Stained slides were scanned using the Leica Slide Scanner SCN400 producing digital images of the whole section. Regions of interest were marked in the deep white matter and separately in the superficial U-fibres. The latter were used as an internal control on the basis that U-fibres are relatively spared in both subcortical arteriosclerotic encephalopathy (Revesz *et al.*, 1989) and in white matter damage due to CAA (Plant *et al.*, 1990). Using x20 magnification, ten random fields from the marked areas were captured using PicPick software (www.picpick.org). The density of immunohistochemical staining (% area stained) was accessed using Image J software (www.imagej.en.softonic.com). Occipital white matter could not be analysed for the p.Arg377Met case due to an infarct and there was insufficient parietal deep white matter available for region of interest analysis for one intron 4 (g.23024delG) case.

The proportion of blood vessels affected by amyloid deposition and the severity of amyloid deposition were also determined; occipital sections immunostained with an anti-Aβ antibody were scanned and 10 random fields digitally captured as described above. The number of vessels containing Aβ in the leptomeninges and cerebral cortical parenchyma were then counted and expressed as a percentage of the total number of vessels analysed. The number of vessels classed as 'severely affected' were also counted. The criteria for this was the presence of degenerative vascular changes known to be associated with CAA (Revesz *et al.*, 2003). In both the leptomeninges and parenchyma, the diameter of the blood vessel walls were measured and averaged in 10 random fields.

4.2.4 Statistical analysis

Analysis of the association between mutation group and ARWMC score on MRI was carried out using bootstrapped regression with samples stratified by group, using 2000 replications and bias-corrected confidence intervals, implemented in STATA 11 (Stata Corporation, College Station, Texas). Due to the use of bootstrapping, exact p-values are not provided; rather, p-value ranges were inferred from whether confidence intervals excluded zero. Mutation "group" was pre-defined as either control, *APP*, *PSEN1* pre-codon 200 or *PSEN1* post-codon 200. Group differences in total ARWMC scores were assessed for each of the mutation groups compared to controls and for the two *PSEN1*

mutation groups compared to each other. Analyses were additionally adjusted for age at scan, presence of an *APOE4* allele and vascular risk score. The vascular risk scores observed in this study ranged from only 0-2 and were therefore categorised as either low (score 0) or increased (score 1-2) risk.

In the autopsy cohort, comparisons between the *PSEN1* pre-codon 200 and *PSEN1* post-codon 200 mutation groups were made for the immunohistochemical stains using t-tests for normally distributed variables and Wilcoxon rank sum testing for categorical data. Paired t-tests were used for within-subject comparisons of staining in the deep white matter and U-fibre regions of interest. In view of the skewed distribution of the ARWMC scale Kendall's tau, a non-parametric correlation coefficient, was used to investigate correlations between total ARWMC score on MRI and pathological findings in the autopsy cohort as a whole. Correlations between age at onset and the pathological findings were investigated using Kendall's tau for categorical and Pearson's pairwise correlations for continuous data. Pathological differences between *APOE*4 carriers and non-carriers were explored using the same methods as were used to compare the *PSEN1* pre and post-codon groups.

4.3 Results

4.3.1 Imaging cohort

The majority of the 52 FAD patients in this study had recognised mutations but several subjects with novel variants were also included. The *APP* cohort comprised six p.Val717Ile, four p.Val717Gly and one each of p.Val717Leu, p.Ala692Gly (Flemish) and the novel p.Thr719Asn variant. The *PSEN1* pre-codon 200 cohort comprised six intron 4 (g.23024delG) mutations, six p.Met139Val and one each of p.Ile143Phe, p.Leu166del, p.Leu166Arg, p.Glu184Asp, p.Tyr115His and p.Glu120Lys. The *PSEN1* post-codon 200 cohort comprised five p.Glu280Gly, three p.Arg278Ile, two each of p.Leu235Val and p.Pro264Leu, one each of p.Ile202Phe, p.Phe237Leu, p.Leu250Ser, p.Arg269His, p.Arg377Met, p.Gly394Val and the novel variants p.Gln222Pro and p.Phe283Leu. The final subject had pathologically confirmed AD with two post-codon 200 *PSEN1* substitutions; p.Ala434Thr (Jiao *et al.*, 2014) and the novel p.Thr291Ala variant. All novel sequence variants identified were absent from 100 healthy unrelated

white control patients and none of the variants were found in the Exome Aggregate Consortium (ExAC) browser (http://exac.broadinstitute.org). The novel variants included in this study have recently been reported (Ryan *et al.*, 2016) and their likely pathogenicity is discussed in chapter 3 of this thesis

Baseline characteristics are shown in Table 4.1, including ARWMC scores. The groups were well matched for gender. The mean age of the control group (54y) was similar to the *APP* patient group (54y). The mean age of all *PSEN1* subjects at 48 years was, as expected, younger than the *APP* group. The *PSEN1* post-codon 200 group was significantly older than the *PSEN1* pre-codon 200 group both at the time of scan (51 vs 44y; $p < 0.001$) and age at symptom onset (47 vs 39y; $p < 0.001$). The three patient groups had similar disease durations. None of the groups had clinically significant levels of conventional vascular risk factors. There was a borderline increased vascular risk score in the *PSEN1* post-codon 200 compared with *PSEN1* pre-codon 200 group ($p=0.06$), although neither group differed from controls (both $p>0.1$).

4.3.1.1 White matter hyperintensities and mutation position

Results from analyses of ARWMC score are presented in Table 4.1, with the mean total ARWMC score at each mutation position shown in Table 4.2. The *PSEN1* post-codon 200 group had a higher total ARWMC score than the *PSEN1* pre-codon 200 group (estimated difference in score 2.1 (95% CI 0.4 to 3.8), $p<0.01$) and controls (estimated difference in score 2.8 (95% CI 1.4 to 4.4), $p<0.005$), after adjusting for age. The difference between the *PSEN1* subgroups appeared to be driven by differences in the parieto-occipital ARWMC score (estimated difference in score 1.4 (95% CI 0.5 to 2.3), $0.005<p<0.01$, after adjusting for age); there was no evidence of a difference in total score after excluding this component ($p>0.1$, after adjusting for age). There was no evidence that individuals with mutations in the *APP* gene or *PSEN1* gene pre-codon 200 differed from controls in terms of their ARWMC score (both $p>0.1$, after adjusting for age). Only one *APP* subject had a mutation within the amyloid-β coding domain (p.Ala692Gly, Flemish). As expected, this individual's total ARWMC score (14) was disproportionately higher than the median score for the *APP* group (0), the remainder of which had mutations at positions 717 and 719.

Table 4.1 Subjects' characteristics and total age-related white matter change (ARWMC) scores

Subject group	**Controls**	***APP***	***PSEN1* pre-codon 200**	***PSEN1* post-codon 200**	**p-value for *PSEN1* pre-codon 200 vs post-codon 200**	**p-value for control vs *PSEN1* post-codon 200**
No. of subjects	25	13	18	21		
Gender M/F	13/12	6/7	9/9	10/11		
Age (y) at scan Mean (sd)	53.5 (10.6)	53.8 (3.5)	43.5 (7.0)	51.1 (5.9)	0.0007*	0.4*
Disease duration in years Mean (sd)	N/A	5.9 (5.6)	4.3 (1.8)	4.4 (2.5)	0.9*	N/A
Age at onset Mean (sd)	N/A	47.9 (5.3)	39.2 (6.2)	46.8 (6.1)	0.0005*	N/A
MRI scan Tesla[a] 1.5T/3T	16/9	12/1	12/6	16/5	0.5**	0.8**
Proportion carrying *APOE*4 allele	N/A	38%	22%	38%	0.3+	N/A
No. of subjects with vascular risk known	19	10	16	21		
Proportion with increased vascular risk score	21%	30%	0%	24%	0.06+	1.0+
Total ARWMC score Median Mean (interquartile range)	0 0.9 (0-1)	0 1.8 (0-2)	0 1.1 (0-1)	3 3.6 (0-7)	<0.01§	<0.005§

*T-test **Pearson chi-squared test +Fisher's exact test §Bootstrapped regression

a) One subject only (in the *PSEN1* post-codon 200 group) had a 1.0T MRI scan, so was included in the 1.5T group.

Table 4.2 Mean total white matter hyperintensity score for each *PSEN1* mutation in the cohort

***PSEN1* mutation**	**No of subjects**	**Mean total ARWMC score**
Intron 4 (g.23024delG)	6	0
p.Met139Val	6	1
p.Ile143Phe	1	0
p.Leu166del	1	2
p.Leu166Arg	1	8
p.Glu184Asp	1	1
p.Tyr115His	1	1
p.Glu120Lys	1	0
p.Ile202Phe	1	8
p.Gln222Pro	1	0
p.Leu235Val	2	5
p.Phe237Leu	1	0
p.Leu250Ser	1	0
p.Pro264Leu	2	3
p.Arg269His	1	4
p.Arg278Ile	3	8
p.Glu280Gly	5	2
p.Phe283Leu	1	4
p.Arg377Met	1	0
p.Gly394Val	1	1
p.Thr291Ala & p.Ala434Thr	1	7

Figure 4.1 shows representative MR images for subjects in the *PSEN1* cohort; some of the WMHs had an atypical appearance, with U-fibre involvement.

Figure 4.1: Example MR images from subjects with (A) p.Glu120Lys (B) Intron 4 (g.23024delG) (C) p.Met139Val (D) p.Ile202Phe (E) p.Leu235Val (F) p.Glu280Gly (G) and (H) p.Arg278Ile and (I) p.Pro264Leu mutations, whose location within the *PSEN1* gene is indicated.

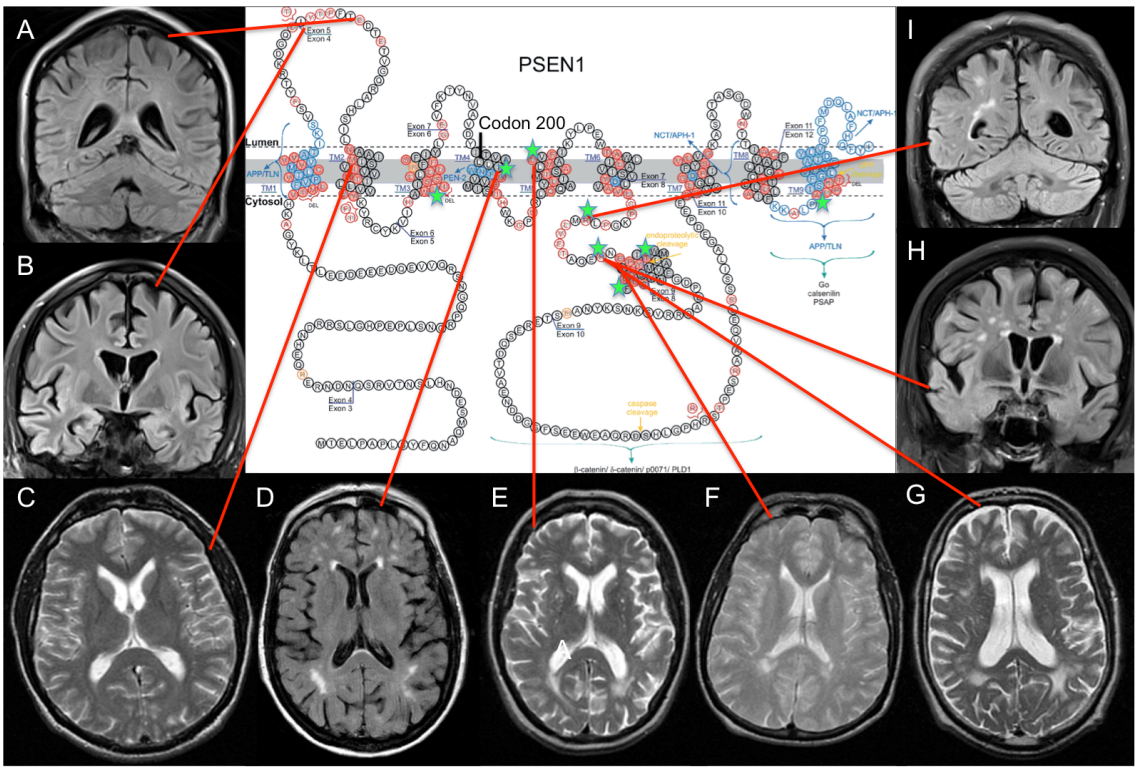

In some cases, particularly those with the p.Arg278Ile mutation (G and H), some of the WMH have an atypical appearance with extension into the U-fibres. Green stars indicate mutation positions where the mean age-related white matter change score was four or more. Figure adapted from (Dillen and Annaert, 2006) and reprinted from (Ryan *et al.*, 2015), with permission.. FAD-linked mutations are indicated in red, while non-pathogenic mutations are marked in orange. Interaction domains with APP/TLN or NCT/APH-1/PEN-2 are marked in blue, as well as the conserved residues D257 and D385 forming the putative catalytic site. Interactions of the C-terminal domain and the hydrophilic loop domain with proteins such as the brain G-protein Go, calsenilin, the

PSEN1-associated protein, b- and d-catenin, p0071 and PLD1, are shown in dark green. The endoproteolytic cleavage site separating PSEN1-NTF and -CTF in the seventh hydrophobic region, the SPP cleavage site in the ninth TMD and the caspase cleavage site in the hydrophilic loop domain are indicated by yellow arrows.

APH: Anterior pharynx-defective; CTF: C-terminal fragment; NTF: N-terminal fragment; PEN: Presenilin enhancer; PLD: Phospholipase D; NCT: Nicastrin; SPP: Signal peptide peptidase; TLN: Telencephalin; TMD: Transmembrane domain.

4.3.1.2 White matter hyperintensities and vascular risk

Accounting for vascular risk weakened the difference in ARWMC score between the *PSEN1* pre-codon 200 and *PSEN1* post-codon 200 group (estimated difference in score 1.5 (95% CI -0.3 to 3.1), $0.09<p<0.1$). However, there was still strong evidence for a difference between the *PSEN1* post-codon 200 group and controls (estimated difference in score 2.8 (95% CI 1.5 to 4.4, $p<0.005$). The model provides evidence that vascular risk and mutation position were both independent predictors of ARWMC score. Increased vascular risk score was associated with an estimated difference in ARWMC score of 2.7 (95% CI 0.5 to 5.5, $0.01<p<0.05$), after adjusting for age and mutation group.

4.3.1.3 White matter hyperintensities and *APOE4* status

There was no evidence that *APOE* status was associated with ARWMC score (after adjusting for group and age, $p>0.2$) and there was no difference in the proportion of subjects carrying an *APOE4* allele between the *PSEN1* pre-codon 200 (22%) and *PSEN1* post-codon 200 groups (38%, $p=0.3$). Only one subject in each patient group was *APOE4* homozygous: these were individuals with an *APP* p.Val717Ile mutation (ARWMC score 0): a *PSEN1* pre-codon 200 intron 4 (g.23024delG) mutation (ARWMC score 0): and a *PSEN1* post-codon 200 p.Ile202Phe mutation (Church *et al.*, 2011) (ARWMC score 8). It was the *PSEN1* p.Ile202Phe patient's baseline scan (shown in Figure 4.1) that was rated for this study. However, it should be noted that further imaging after a period of clinical deterioration three years later demonstrated floridly increased WMH with extension into the U-fibres and oedema suggesting CAA-related

inflammation (CAA-ri), which was confirmed at post-mortem and is described in Chapter 5 (Ryan et al., 2014).

4.3.2 Pathology cohort

Of the 10 subjects in the imaging study who underwent post-mortem examination, five had *PSEN1* pre-codon 200 mutations (p.Glu120Lys and four intron 4 (g.23024delG) mutations) and five had *PSEN1* post-codon 200 mutations (p.Ile202Phe, p.Leu235Val, p.Arg278Ile, p.Arg377Met and the double substitution p.Thr291Ala & p.Ala434Thr). In the autopsy subgroup, as in the larger cohort, age at onset was significantly later for those with *PSEN1* post-codon 200 compared to *PSEN1* pre-codon 200 mutations (43.6 vs 36.6y, p=0.02), although disease duration was similar (Table 4.3). The mean interval between MRI and post-mortem was five years. Three subjects in the autopsy cohort had ARWMC scores greater than 0; all were in the post-codon 200 group.

4.3.2.1 Amyloid and tau pathology

All autopsy cases demonstrated Braak stage VI tau pathology. The severity of Aβ-positive mature, diffuse or cotton wool plaques did not differ between the *PSEN1* pre-codon 200 and post-codon 200 groups. The grade of CAA showed little difference between the two groups for any region other than the cerebellum, where the median CAA score was marginally higher in the *PSEN1* post-codon 200 than pre-codon 200 group (3 vs 2, p=0.05). However, it should be noted that the average CAA grade for each region was at least 2 or 3 in both groups, and that the post-codon 200 group had an average score of 3 for all regions, reflecting widespread CAA. The mean proportion of blood vessels affected by amyloid deposition was nominally higher in the *PSEN1* post-codon 200 than pre-codon 200 group in cortical parenchyma (47.6% vs 28.6%) and leptomeninges (78.2% vs 72.2%). However, differences between the two mutation groups were not statistically significant for these, nor any other aspects of the blood vessel analysis (Table 4.3).

Table 4.3. Autopsy cohort subject demographics and results of CAA grading and blood vessel analysis

	All *PSEN1* cases (N=10)	*PSEN1* pre-codon 200 (N=5)	*PSEN1* post-codon 200 (N=5)	*p* value for *PSEN1* pre-codon 200 vs post-codon 200
Disease duration Mean (sd)	10.6 (4.6)	9.4 (4.4)	11.7 (5.1)	0.4*
Age at onset Mean (sd)	40 (5.1)	36.6 (4.2)	43.6 (3.8)	**0.02***
Years from MRI to post-mortem Mean (sd)	5.0 (3.8)	4.2 (3.2)	5.8 (4.5)	0.6
APOE status	Two 44, one 34, seven 33	One 44, four 33	One 44, one 34, three 33	1.00**
CAA grade **Median (range)**				
Frontal	2.5 (0-3)	2 (1-3)	3 (0-3)	1.0+
Temporal	2 (0-3)	2 (0-2)	3 (0-3)	0.4+
Parietal	2.5 (0-3)	2 (1-3)	3 (0-3)	1.0+
Occipital	3 (3)	3 (3)	3 (3)	.
Cerebellar	3 (2-3)	2 (2-3)	3 (3)	**0.05**+
Proportion of blood vessels affected by amyloid deposition **Mean (SD) percentage**				
Cortical	38.1 (37.3)	28.6 (41.3)	47.6 (34.5)	0.5*
Cortical 'severely affected'	27.2 (36.5)	21 (36.7)	33.4 (39.4)	0.6*
Leptomeningeal	75.2 (32.3)	72.2 (36.4)	78.2 (31.5)	0.8*
Leptomeningeal 'severely affected'	44.6 (28.5)	38.6 (29.6)	50.6 (29.3)	0.5*
Vessel diameter				
Cortical vessel diameter	19.0 (4.2)	18.1 (2.9)	19.8 (5.5)	0.6*
Leptomeningeal vessel diameter	17.1 (3.4)	17.7 (2.9)	16.5 (4.1)	0.6*

*T-test ** Fisher's exact test +Wilcoxon rank sum test

4.3.2.2 White matter pathology

Semi-quantitative assessment of myelin loss, gliosis and microglial expression in the deep white matter (Table 4.4) suggested a pattern, whereby cases with minimal or no white matter pallor tended to have more active microglia and gliosis, whereas cases with white matter pallor had minimal gliosis and activated microglia. There was some evidence that the *PSEN1* pre-codon 200 group had more white matter pallor than the *PSEN1* post-codon 200 group on HE (haematoxylin and eosin) staining of parietal (p=0.02) and occipital (p=0.07) sections, and more severe gliosis in the parietal white matter on GFAP immunohistochemistry (p=0.06). The mean density of staining (% area stained) for each immunohistochemical marker in parietal and occipital deep white matter and U-fibre regions of interest is presented in Figure 4.2.

Figure 4.2 Mean density of immunohistochemical staining in parietal and occipital white matter.

Error bars indicate standard errors. Reprinted from (Ryan *et al.*, 2015), with permission.

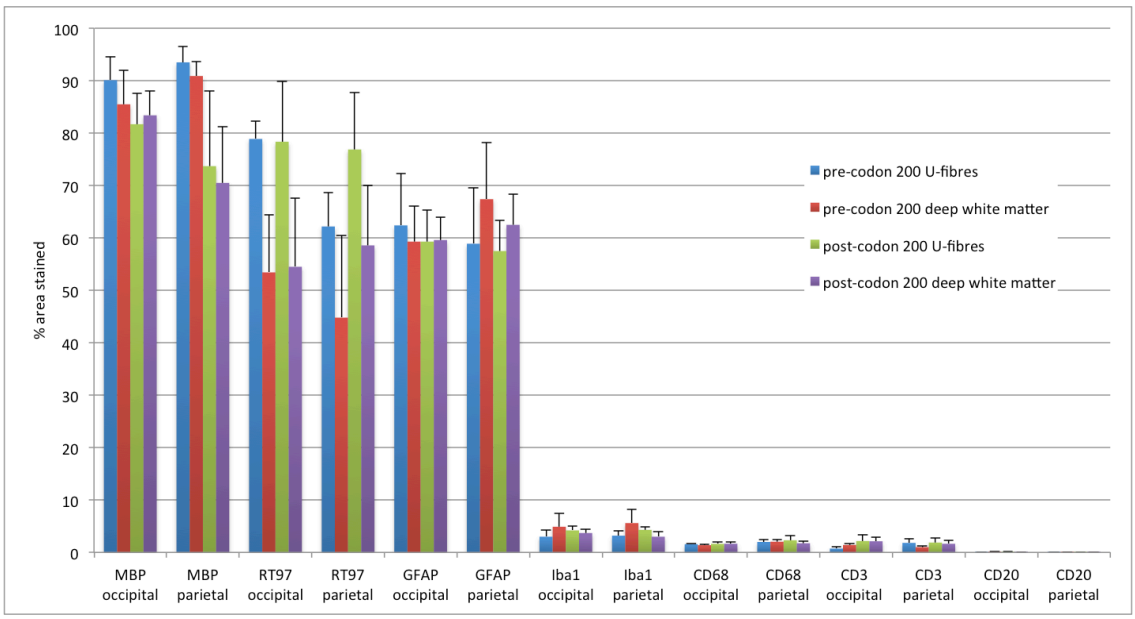

In the *PSEN1* cohort as a whole, the only differences between deep white matter and U-fibres were in RT97, which demonstrated lower axonal density/integrity in the deep white matter compared to U-fibres in occipital (53.9% vs 78.7%, p=0.02) and parietal (52.5% vs 71.3%, p=0.04) areas. When the pre-codon 200 group was analysed separately, there were still trends for the density of RT97 to be lower in deep white

matter compared to U-fibres in occipital (53.4% vs 78.9%, p=0.06) and, to a lesser extent, parietal (44.8% vs 64.3%, p=0.1) areas. There was also a slightly higher density of CD3-positive T-lymphocytes in occipital deep white matter compared to U-fibres (1.4% vs 0.7%, p=0.04) in the pre-codon 200 group. In the post-codon 200 group, none of the stains showed significant differences between deep white matter and U-fibres. However, there was weak evidence that the density of Iba1-positive microglia was somewhat higher in parietal U-fibres than deep white matter (4.3% vs 3.0%, p=0.07). Direct comparisons between the pre and post-codon 200 groups for the overall density of staining in each region and the ratio of staining in deep white matter to U-fibres demonstrated no significant differences.

4.3.2.3 Pathological features and white matter hyperintensities

In the autopsy cohort as a whole, there was a correlation between ARWMC score on MRI and grade of severity of CAA in the temporal lobe (p=0.02) and to a lesser extent frontal and parietal lobes (both p=0.09). ARWMC score was also associated with severity of cotton wool plaques in the occipital (p=0.03) and temporal, parietal and cerebellar (all p=0.04) regions (Figure 4.3). There was a trend towards a negative correlation between ARWMC score and mature plaque severity in the parietal lobe (p=0.06). Borderline associations were found between ARWMC score and the proportion of cortical blood vessels affected by amyloid deposition (p=0.07) and the proportion of leptomeningeal vessels that were classified as severely affected by CAA (p=0.09). ARWMC score was also associated with leptomeningeal blood vessel diameter (p=0.03). There was some evidence that higher ARWMC scores were associated with a lower density of CD68-positive microglia in the parietal deep white matter (p=0.04) and U-fibres (p=0.09).

4.3.2.4 Pathological features and *APOE*4 status

Three of the ten autopsy subjects carried an *APOE*4 allele; one (*E*44) in the pre-codon 200 group and two (one *E*44, one *E*34) in the post-codon 200 group. As in the larger cohort, there was no association between ARWMC score and *APOE* status. Although the *APOE*4 carrier group was very small, hence results should be interpreted with caution, the proportion of cortical blood vessels affected by amyloid deposition was

significantly greater in *APOE*4 carriers than non-carriers (84.0% vs 18.4%, p<0.002), as was the proportion of cortical vessels classified as severely affected (66.0% vs 10.6%, p=0.02). The proportion of leptomeningeal blood vessels affected by amyloid deposition was higher than the proportion of cortical blood vessels affected in both *APOE*4 carriers (99%) and non-carriers (65%) and did not significantly differ between the two *APOE* groups (p=0.13). However, there was borderline evidence that the proportion of leptomeningeal blood vessels classified as severely affected was higher in *APOE*4 carriers than non-carriers (70.0% vs 33.7%, P=0.06). The degree of parietal or occipital capillary CAA showed no association with ARWMC score and did not differ between the pre and post-codon 200 groups, nor between *APOE*4 carriers and non-carriers. *APOE*4 carriers demonstrated an increased T lymphocytic response in the parietal U-fibres (3.8% vs 1.0%, p=0.01). In contrast, *APOE*4 non-carriers demonstrated higher staining of CD68 for activated microglia in occipital U-fibres (1.9% vs 1.0%, p=0.03).

4.3.2.5 Pathological features and age at symptom onset

In the pathology cohort as a whole, there was some evidence that younger ages at onset were associated with greater immune/inflammatory responses in the deep white matter. Negative correlations were found between age at onset and density of Iba1-positive microglia in parietal deep white matter (absolute counts and ratio compared to U-fibres, both r=-0.7, p=0.03). The ratio of CD20 in occipital deep white matter compared to U-fibres also negatively correlated with age at onset (r=0.7, p=0.04) although CD20 staining was minimal in all cases. Younger ages at onset were associated with more severe gliosis on HE staining of parietal deep white matter (r=-0.5, p=0.02) and with lower axonal density/integrity in parietal deep white matter (r=0.6, p=0.06) and U-fibres (r=0.7, p=0.04) on RT97 immunohistochemistry.

Table 4.4 Semi-quantitative assessment of white matter pallor, gliosis and microglial expression in parietal and occipital deep white matter

The deep white matter in the occipital (occ) and parietal (par) lobes were semi-quantitatively assessed for white matter pallor (HE, MBP, RT97), gliosis (GFAP) and microglial expression (Iba1). This was based on a four-tier grading system where '0' represented no change in the white matter, no gliosis or microglial activation; '+' represented mild pallor of the white matter, mild gliosis and the minimal presence of activated microglia (Figure 4.3,K); '++' represented a moderate degree of white matter pallor, gliosis and microglial activation (Figure 4.3, L); '+++' represents severe pallor of the white matter, severe gliosis and severe microglial activation; '++++' represents very severe microglial activation where the majority of the microglial cells are highlighted using immunohistochemical methods (Figure 4.3, M).

Mutation	Location	Age at onset	Duration (years)	Block	HE	MBP	RT97	GFAP	Iba1
Intron 4 (g.23024delG)	Pre 200	35	16.9	Par Occ	+++ +	+ +	+ +	++ +	+ +
Intron 4 (g.23024delG)	Pre 200	39	8.1	Par Occ	+ 0	+ 0	+ 0	++ +	++ +++
Intron 4 (g.23024delG)	Pre 200	36	5.6	Par Occ	+ +	+ +	+ +	++ +	+ +
Intron 4 (g.23024delG)	Pre 200	42	9.7	Par Occ	0 +	0 0	0 0	+++ ++	++++ ++
p.Glu120Lys	Pre 200	31	6.9	Par Occ	+ 0	0 0	+ 0	+++ ++	++++ +++
p.Ile202Phe	Post 200	48	12.3	Par Occ	0 0	+ 0	+ 0	+ +	++ ++
p.Leu235Val	Post 200	44	9.3	Par Occ	0 0	0 +	0 0	+ +	++ ++

p.Arg278Ile	Post 200	46	19.6	Par Occ	0 0	0 0	0 0	++ ++	++ ++
p.Arg377Met	Post 200	38	11.6	Par	0	0	0	++	+++
p.Thr291Ala & p.Ala434Thr	Post 200	42	5.9	Par Occ	0 0	0 0	0 0	++ ++	++ +++

Figure 4.3 Pathological analysis of familial Alzheimer's disease with *PSEN1* mutations.

Aβ immunohistochemistry demonstrates prominent mature amyloid plaques (A) and mild CAA (B) in a case with a *PSEN1* mutation located before codon 200 and no white matter hyperintensities on MRI. In *PSEN1* cases with mutations beyond codon 200 and white matter hyperintensites on MRI, there was severe CAA both in the parenchyma (C), showing double barrelling, and the leptomeninges (D). Some of these post codon 200 cases also contained 'cotton wool like' Aβ plaques (E) with severe CAA involvement in the occipital cortex where Aβ deposition severely affected the capillaries (F). CD68 (G) and Iba1 (H) were used to assess any alterations in microglia response between the deep white matter and 'U' fibres. In the *PSEN1* pre-codon 200 group, lower axonal density was observed in the deep white matter (I,) compared to the 'U' fibres (J). The semiquantitative assessment suggested a trend for cases with white matter pallor to show only a minimal (K) or moderate (L) degree of microglial activation, whilst cases with normal-appearing white matter showed moderate to very severe (M) microglial activation. Reprinted from (Ryan *et al.*, 2015), with permission.

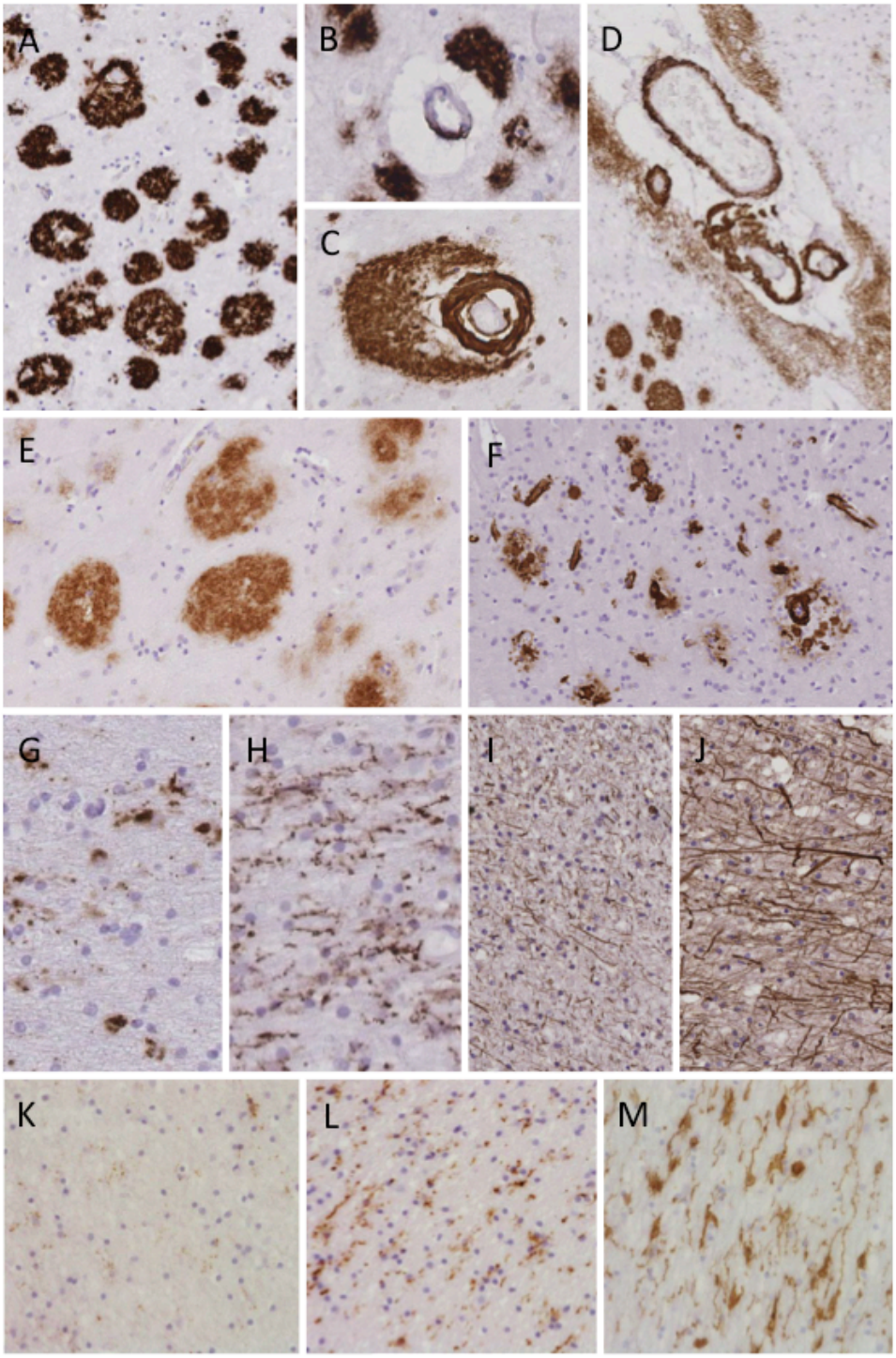
A
B
C
D
E
F
G
H
I
J
K
L
M

4.4 Discussion

Individuals with *PSEN1* post-codon 200 mutations had significantly more parieto-occipital WMH on T2-weighted MRI and also a later age at onset than those with *PSEN1* pre-codon 200 mutations. WMH may be caused by a variety of pathological processes including ischaemia, infarction, demyelination and oedema. In older patients, they commonly result from the ischaemia caused by cerebrovascular disease secondary to conventional vascular risk factors (Prins and Scheltens, 2015). Given the young age and relative lack of co-morbidities in the subjects in this study, their WMH are much more likely to reflect an aspect of FAD pathology.

It has previously been reported that *PSEN1* mutations beyond codon 200 show more prominent CAA than mutations situated pre-codon 200 (Mann *et al.*, 2001). MRI manifestations of CAA include WMH, cortico-subcortical intracerebral haemorrhages including microbleeds and atrophy (Chao *et al.*, 2006). Our finding of a greater WMH 'burden' on MRI in the *PSEN1* post-codon 200 mutation group is therefore consistent with at least a proportion of these individuals having more severe CAA. The predominantly parieto-occipital location of the WMH further supports the hypothesis that they relate to CAA. CAA, which is present to at least some degree in 70%-100% of AD brains at post-mortem (Bergeron *et al.*, 1987, Ellis *et al.*, 1996), has a particular predilection for the occipital lobes (Thal *et al.*, 2002, Alafuzoff *et al.*, 2009) and a posterior distribution of WMH has been shown to predict pathologically confirmed CAA (Thanprasertsuk *et al.*, 2014). Although only one of the *APP* subjects had a mutation within the amyloid-β coding domain, their ARWMC score was considerably higher than the median for the *APP* group, consistent with pathological reports of severe CAA in cases with intradomain *APP* mutations. There was also one outlier in the *PSEN1* pre-codon 200 group (p.Leu166Arg), whose total ARWMC score of 8 was considerably higher than the median for the group (0). This subject also carried the p.Arg62His *PSEN2* variant. It was previously unclear whether this variant represents a novel mutation or non-pathogenic polymorphism (Cruts *et al.*, 1998). Although it seems increasingly likely that it is not pathogenic (Guerreiro *et al.*, 2010), the possibility remains that it may have an influence on the clinico-pathological phenotype.

The pathology results in the patients who came to post-mortem offer some support that the WMH are related to CAA, as there was indeed a positive correlation between ARWMC score on MRI and severity of CAA in the temporal and to a lesser extent frontal and parietal lobes. Occipital CAA was the maximum grade of severity in all cases, preventing detection of any association with ARWMC score. Although the actual grade of CAA showed little difference between the pre and post-codon 200 groups for any region other than the cerebellum, where it was marginally higher in the *PSEN1* post-codon 200 group, it should be noted that in the small number of subjects with post-mortem examination, CAA was relatively severe in the majority of cases.

An alternative explanation for the increased WMH in the *PSEN1* post-codon 200 cohort is that they reflect another aspect of FAD pathology, independent of or related to CAA, which also varies according to mutation position. For example, inflammatory mediated pathology. Vascular amyloid may be associated with a variety of inflammatory reactions (Miao *et al.*, 2005, Chung *et al.*, 2011) including perivascular inflammation surrounding amyloid-laden blood vessels and granulomatous or non-granulomatous angiitis in which there is also inflammation and necrosis within the vessel wall (Eng *et al.*, 2004, Harkness *et al.*, 2004, Scolding *et al.*, 2005). The clinical and neuroradiological manifestations of these inflammatory responses do, however, appear to be relatively consistent and WMH are a common feature. WMH typically spare the U-fibres when they are caused by ischaemic cerebrovascular disease secondary to either arteriolosclerosis or CAA (Chao *et al.*, 2006). However, WMH extending into the U-fibres have been described in cases of CAA-ri (Chao *et al.*, 2006). In some of the *PSEN1* post-codon 200 cases in our study, the WMH showed a degree of extension into the U-fibres, including those with the p.Arg278Ile mutation, as demonstrated in Figure 4.1. The p.Arg278Ile mutation is associated with selective overproduction of Aβ43 and mice carrying this mutation show accelerated Aβ pathology, accompanied by an inflammatory response with massive astrocytosis surrounding amyloid plaques (Saito *et al.*, 2011).

Our alternative hypothesis that WMH may reflect secondary inflammatory mediated pathology led us to investigate microglial, astrocytic and lymphocytic responses in the autopsy cases. At a group level, there was weak evidence that the density of Iba1-stained microglia was higher in the U-fibres than deep white matter in the *PSEN1* post-

codon 200 group and the autopsy cohort included the p.Ile202Phe case with CAA-ri that has been reported elsewhere (Ryan *et al.*, 2014). However, the pathological analysis suggested that inflammatory responses might if anything be more prominent in the *PSEN1* pre-codon 200 cohort and that this may be related to the younger ages at onset. The pre-codon 200 group had more severe gliosis and a greater T lymphocytic response and decreased axonal density in deep white matter compared to U-fibres. In the pathology cohort as a whole, younger ages at onset were associated with greater immune/inflammatory responses and lower axonal density/integrity. Furthermore, higher ARWMC scores were associated with a lower density of microglia in parietal deep white matter and, on semi-quantitative assessment, cases with white matter pallor were noted to have minimal activated microglia. ARWMC scores also showed positive correlations with the severity of cotton wool plaques in occipital, parietal, temporal and cerebellar regions and a negative correlation with mature plaque severity in the parietal lobe. These observations require corroboration in larger studies but may all be connected. Cotton wool plaques are immunoreactive for Aβ but lack the dense amyloid cores, neuritic responses or microglial associations seen with mature plaques (Crook *et al.*, 1998). Their aetiology remains unknown but it has been speculated that they may result from the combination of particularly high Aβ production (Houlden *et al.*, 2000) and low clearance by the immune system (Tabira *et al.*, 2002). Of potential relevance to the imaging findings, cotton wool plaques have sometimes been noted to encroach into superficial subcortical white matter (Shrimpton *et al.*, 2007). The idea that *PSEN1* mutations located before codon 200 may be associated with a more aggressive disease course was also suggested by Mann et al., who reported younger ages at onset and shorter disease durations in these cases (Mann *et al.*, 2001).

Different genetic risk factors may interact to determine the severity and pathological consequences of CAA. In sporadic AD, the *APOE4* allele is associated with CAA severity (Greenberg *et al.*, 1995, Kalaria *et al.*, 1996, Premkumar *et al.*, 1996, Chalmers *et al.*, 2003). We found that, even in FAD, *APOE4* carriers have a greater proportion of leptomeningeal and, in particular, cortical blood vessels severely affected by CAA. *APOE*4 is also a risk factor for CAA-ri (Eng *et al.*, 2004, Kinnecom *et al.*, 2007) and for the amyloid-related imaging abnormalities (ARIA), thought to relate to vascular amyloid, observed in amyloid immunotherapy trials (Sperling *et al.*, 2011, Barakos *et*

al., 2013). It is therefore noteworthy that the only *APOE4* homozygote with a *PSEN1* post-codon 200 mutation in this study went on to develop clinical, radiological and pathological features of CAA-ri (Ryan *et al.*, 2014). In the autopsy cohort, *APOE4* carriers showed a higher T lymphocytic response in parietal U-fibres, however there was also some evidence for a greater microglial response in non-carriers so the relationship between *APOE* status and inflammation was not clear-cut. We found no association between *APOE4* status and WMH in our cohort. A previous study of sporadic AD also found that *APOE4* homozygosity was not associated with WMH, although it was associated with multiple microbleeds (Goos *et al.*, 2009). The authors of this study found particularly low ARWMC scores in *APOE4* homozygous AD patients with multiple microbleeds, prompting them to suggest that separate pathophysiological mechanisms may underpin microbleeds presenting with and without WMH. T2*-weighted imaging sensitive to microbleeds was only available in 12 of the patients in this study and is reported in Chapter 5 (Ryan *et al.*, 2011). The prevalence of one or more microbleeds in this subset of FAD patients was 25%, which is comparable to the proportion of microbleeds found in patients with sporadic AD (Cordonnier and van der Flier, 2011, Whitwell *et al.*, 2015). Interestingly, the only patient with multiple microbleeds had both a post-codon 200 *PSEN1* mutation (p.Arg269His) and the *APOE* genotype 3/4 (see Chapter 5).

CAA typically affects cortical and leptomeningeal small and medium-sized arteries and arterioles, with veins and capillaries involved less frequently (Revesz *et al.*, 2003). When the cortical capillaries are involved there are sometimes associated dyshoric changes, where amyloid deposits spread beyond the vessel wall into the surrounding neuropil (Richard *et al.*, 2010). An association has been observed between *APOE4* and capillary CAA, particularly with associated dyshoric changes (Thal *et al.*, 2002). Furthermore, capillary CAA has been found to provoke a strong inflammatory response, which does not usually occur in large vessel CAA (Richard *et al.*, 2010). This could perhaps provide a unifying explanation for how *APOE4* status appears to increase the risk of developing both microbleeds and inflammation as a consequence of CAA. Although we did not find associations between capillary CAA and *APOE* status or ARWMC score in our pathology cohort, subject numbers were small and this would be an interesting issue to explore in larger studies.

It is possible that other vascular risk factors also play a role in the manifestation of CAA in FAD. Our results suggested that increased age and the presence (albeit very minor) of conventional vascular risk factors may contribute to some of the difference in ARWMC observed between the *PSEN1* pre- and post-codon 200 groups. However, these factors could not account for the differences between the *PSEN1* post-codon 200 group and controls. It is noteworthy that the vascular risk scores in subjects with increased vascular risk were still very low - 1 or 2 at most- signifying the presence of only mild hypertension and/or hypercholesterolaemia in most cases. It seems highly unlikely that this minor increased vascular risk could wholly explain the severity of WMH seen in many of the *PSEN1* post-codon 200 patients' scans. Furthermore, the occurrence of increased vascular risk scores in the *PSEN1* post-codon 200 group could have been biased by the imaging findings themselves. Patients with FAD and WMH may be more thoroughly investigated for vascular risk factors than patients lacking such imaging features. Smoking history was not known for all of the subjects in this study. Although smoking status is not included in the system for scoring vascular risk that we used (DeCarli *et al.*, 2004), the absence of this information should be considered a limitation.

An important but inevitable limitation of this retrospective study is the lack of T2* imaging in all subjects, which is due to the fact that the scans were collected over a twenty year period, with the majority having been acquired before the introduction of gradient echo imaging to our protocol. A further limitation of the current study is that, although it is one of the largest pre-morbid imaging investigations of FAD with post-mortem neuropathological correlation, the number of autopsy cases is small. Due to the limited sample size, we did not include correction for multiple comparisons in our analysis of the data, which should be considered exploratory and requires corroboration in larger datasets.

Investigation of why *PSEN1* mutations located after codon 200 should be associated with increased CAA and/or a different inflammatory response is an important area for future research, with the potential to reveal how other functions of *PSEN1* may be affected by mutations at different sites. For example, certain post-codon 200 *PSEN1* mutations may interfere with the role of *PSEN1* in Notch processing, resulting in vulnerability of the vascular wall (Mann *et al.*, 2001). Indeed, the functionally important residues of the *PSEN1* endoproteolytic cleavage site lie at or around amino acid 298. By

contrast, recent work on γ-secretase modulators has highlighted the importance of an N-terminal, predominantly pre-codon 200 region of *PSEN1*, in the carboxypeptidase-like activity that alters Aβ profiles (Ohki *et al.*, 2011, Takeo *et al.*, 2014). One could speculate that mutations involving this allosteric core may alter more dramatically the Aβ profiles and cause a more aggressive phenotype. Another potential source of variability in the pathological consequences of different *PSEN1* mutations is their role in calcium homeostasis, which could have implications for vascular, immune and neuronal function. The function of presenilins as calcium leak channels in the endoplasmic reticulum appears to be impaired by most *PSEN1* mutations (Nelson *et al.*, 2011). However, calcium leak function is preserved with certain mutations, particularly those in a cluster located beyond codon 200 in exons 8-9 (Nelson *et al.*, 2010), which tend to be associated with cotton wool plaque pathology. Further work investigating functionally relevant differences between mutations at different sites will be important to refine our understanding of how mutation position influences pathology and phenotype, beyond the simple dichotomy of pre or post-codon 200 location.

In conclusion, we observed increased posterior WMH and later ages at onset in the *PSEN1* post-codon 200 group. WMH correlated with severity of CAA and cotton wool plaque pathology at post-mortem. In contrast, the *PSEN1* pre-codon 200 group had younger ages at onset and greater axonal loss, gliosis and T-lymphocytic response in the deep white matter. A significantly later age at onset in cases with *PSEN1* mutations beyond codon 200 cases was also reported in Mann's study (Mann *et al.*, 2001). It may suggest that some degree of protection is conferred by the source of the WMH in the post-codon 200 group, whether this is preferential deposition of amyloid in the vasculature, differing inflammatory responses, plaque species or a combination. Pathological studies have found an inverse relationship between the severity of capillary CAA and the density of amyloid plaques surrounding these capillaries, which has been interpreted as providing support for the idea that Aβ may be transported between the neuropil and circulation (Richard *et al.*, 2010). A similar observation, of increased CAA in areas of decreased amyloid plaque burden, was also made at post-mortem in brains of some of the AD patients who received Aβ immunisation (Boche *et al.*, 2008). The findings of a decrease in both CAA and plaques in immunised patients who survived longer led to the suggestion that this vascular amyloid may be cleared over time (Boche

et al., 2008). What remains an unknown and critical issue for clinical trials in FAD, is how an individual's baseline propensity for developing CAA may influence the processes by which amyloid may be cleared after immunotherapy or other amyloid depleting strategies.

5 Amyloid-related imaging abnormalities (ARIA) in familial Alzheimer's disease

The term 'ARIA' was proposed to describe the amyloid-related MRI abnormalities observed in a number of patients participating in various amyloid-modifying therapy trials for AD (Sperling *et al.*, 2011, Coric *et al.*, 2012, Ostrowitzki *et al.*, 2012, Sperling *et al.*, 2012, Salloway *et al.*, 2014). ARIA refers to a spectrum of imaging changes and may be subdivided into: ARIA-E, describing increased signal on fluid-attenuated inversion recovery (FLAIR) and other T2-weighted MRI sequences, thought to represent cerebral oedema and effusion or extravasated fluid in sulcal spaces; and ARIA-H, denoting microbleeds and superficial siderosis evident on gradient echo (T2*-GRE) sequences. Although a detailed understanding of the pathogenesis of ARIA remains to be elucidated, the imaging features are thought to reflect changes involving vascular amyloid. This chapter comprises two short reports on the subject of ARIA in FAD.

As discussed in Chapter 4, a number of strands of evidence suggest that amyloid-modifying therapy may provoke increased amyloid in the vasculature and the launch of trials of such therapy for FAD therefore raises particular interest in the imaging manifestations of CAA in mutation carriers. The previous chapter focused on white matter hyperintensities on MRI as a potential marker of CAA. Other MRI manifestations of CAA include cortical superficial siderosis, enlarged perivascular spaces in the centrum semiovale and cerebral microbleeds (Yamada, 2015). This chapter begins by considering cerebral microbleeds and describes a study investigating their prevalence in a small cohort of FAD mutation carriers. I then move from ARIA-H to ARIA-E, describing the first reported case of ARIA-E developing spontaneously during the course of *PSEN1*-associated FAD, in an *APOE4* homozygote. Potential risk factors for the development of ARIA in FAD are discussed and I argue that monitoring for ARIA and identifying individuals at increased risk of developing them should play an important role in FAD clinical trials.

5.1 Cerebral microbleeds (ARIA-H) in familial Alzheimer's disease

Determining the relevant contributions of atherosclerotic cerebrovascular disease (related to conventional risk factors including hypertension) and CAA to microbleeds identified on T2*-weighted imaging of AD patients is an important issue, which may lead to new insights into the pathology and pathogenesis of AD. However, one of the difficulties in attempting to delineate the relative contributions of conventional cerebrovascular and CAA pathology in sporadic AD is that multiple pathologies are common at more advanced ages. An alternative strategy is to study patients with FAD; such individuals can be diagnosed definitively during life and, having a younger age at symptom onset, are much more likely to have "pure" AD without co-existing cerebrovascular disease. This study is the first to assess the frequency of microbleeds in FAD.

5.1.1 Methods

All individuals with genetically confirmed FAD who had undergone T2*-weighted MRI as part of the longitudinal study of FAD at the DRC were included in this study. A total of 12 patients with FAD (mean age: 49.4, range: 35.8 – 63.4 yrs; mean disease duration: 4.0, range: 1.1 – 6.7 yrs; 75% male) were eligible. 11 patients had a mutation in the *PSEN1* gene (three Intron 4 (g.23024delG) mutations and one each of p.Leu166Arg, p.Tyr115His, p.Glu120Lys, p.Leu250Ser, p.Pro264L, p.Arg269His, p.Arg278Ile, p.Glu280Gly), and one patient carried the Val717Ile *APP* mutation. 12 controls (mean age: 59.8; range: 46.9 – 66.5 yrs; 50% male) were also studied. All mutation carriers were symptomatic and fulfilled criteria for AD dementia at the time of scanning. T2* gradient echo sequences (TR/TE 625/20ms, flip angle 20°, field of view 240x240, matrix 256x320, slice thickness 5mm) were acquired on the same 3T Siemens MRI scanner. All subjects gave written informed consent according to the Declaration of Helsinki, and the study was approved by the local ethics committee. All scans were assessed by one experienced neuroradiologist, blinded to mutation status, to evaluate the presence, number and location of microbleeds. Microbleeds were defined as small (2-10mm diameter), round and homogenous foci of low signal intensity on T2*-weighted MRI. Microbleed mimics including basal ganglia mineralization, vessel flow voids in

the subarachnoid space and artefacts at air-bone interfaces were excluded in line with standardized criteria (Gregoire *et al.*, 2009). The number and location of microbleeds was assessed in the following regions: cortical/cortico-subcortical (frontal, temporal or parieto-occipital), infratentorial (brainstem and cerebellum) and the basal ganglia (including thalamus).

5.1.2 Results

Microbleeds were found in three out of 12 patients and in none of the control subjects. Two *PSEN1* mutation carriers had 1 microbleed each (p.Leu166Arg right parieto-occipital; Intron 4 (g.23024delG) left infratentorial). Only one patient had multiple, predominantly cortical/cortico-subcortical microbleeds (over 30 in total) and fulfilled Boston Criteria for probable CAA (Greenberg *et al.*, 1996, van Rooden *et al.*, 2009). This individual, a 59-year-old man harbouring the p.Arg269His *PSEN1* mutation, had a one-year history of cognitive decline at the time of referral and recruitment to the study. He was adopted and had no siblings. There was no significant past history and no hypertension or other vascular risk factors. The neurological examination revealed finger myoclonus but was otherwise unremarkable. The MMSE was 24/30. Cognitive testing revealed him to have little insight into his problems, a pronounced dysexecutive syndrome, mild episodic memory impairment, and relative preservation of parietal lobe function. 3D-T1-weighted images showed mild generalised volume loss without predominance of medial temporal lobe atrophy. T2 FLAIR MRI depicted mild-moderate white matter disease (Figure 5.1). T2*-weighted imaging revealed prominent cerebellar, parieto-occipital and temporal lobar microbleeds (Figure 5.2).

5.1.3 Discussion

Although CAA is found at post-mortem in up to 90% of patients with sporadic AD, only around 23% of patients with AD have identifiable microbleeds on MRI (Cordonnier and van der Flier, 2011). It is possible that microbleeds only occur when CAA is particularly severe; or it may be that patients with AD and microbleeds represent a subgroup in whom the pathological process is somewhat different.

Pathological studies of FAD confirm that whilst CAA is seen in the context of mutations in *APP, PSEN1* and *PSEN2* and also in *APP* duplications, the degree of pathological CAA in FAD is also highly variable. Thus for example in *PSEN1*-associated FAD, mutations beyond codon 200 appear to be associated with particularly severe CAA (Mann *et al.*, 2001). CAA, when present, may also be associated with different clinical correlates: some mutations within the Aβ coding domain of *APP* leading to significant pathological CAA burden are associated with recurrent cerebral haemorrhage, whilst others can present with a purely cognitive phenotype (Ryan and Rossor, 2010) (see Chapter 1.3).

Figure 5.1 3T T2-weighted FLAIR coronal MRI shows white matter lesions, but no significant medial temporal lobe atrophy in a patient with the p.Arg269His *PSEN1* mutation.

Reprinted from (Ryan *et al.*, 2012), with permission.

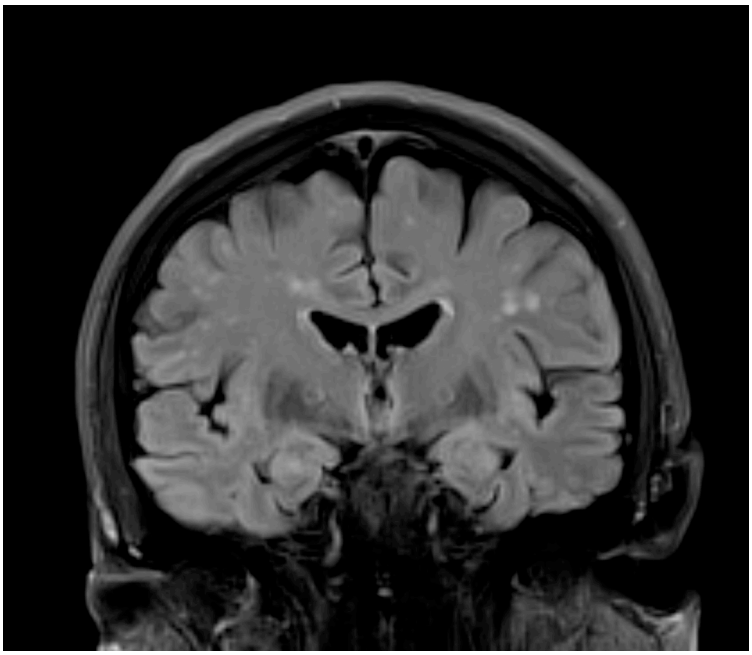

Our data confirm that microbleeds are not an inevitable feature of even "pure" genetically confirmed AD. Although numbers are small, the 25% prevalence of one or more microbleed in our series is comparable with the pooled proportion of 23% reported in a meta-analysis of studies of microbleeds in sporadic AD (Cordonnier and van der Flier, 2011). It is striking that only one individual with a *PSEN1* mutation had

microbleeds sufficient to fulfil criteria for probable CAA, and that this patient had a mutation (p.Arg269His) which has been associated both with relatively late age at onset and with conspicuous amyloid overproduction (Gomez-Isla *et al.*, 1997). We hypothesize that the atypical phenotype with a prominent early dysexecutive syndrome in this case might in part relate to the presence of significant CAA (Arvanitakis *et al.*, 2011).

Figure 5.2 3T T2* MRI shows multiple lobar hypointensities consistent with microbleeds in a patient with the p.Arg269His *PSEN1* mutation.

Reprinted from (Ryan *et al.*, 2012), with permission.

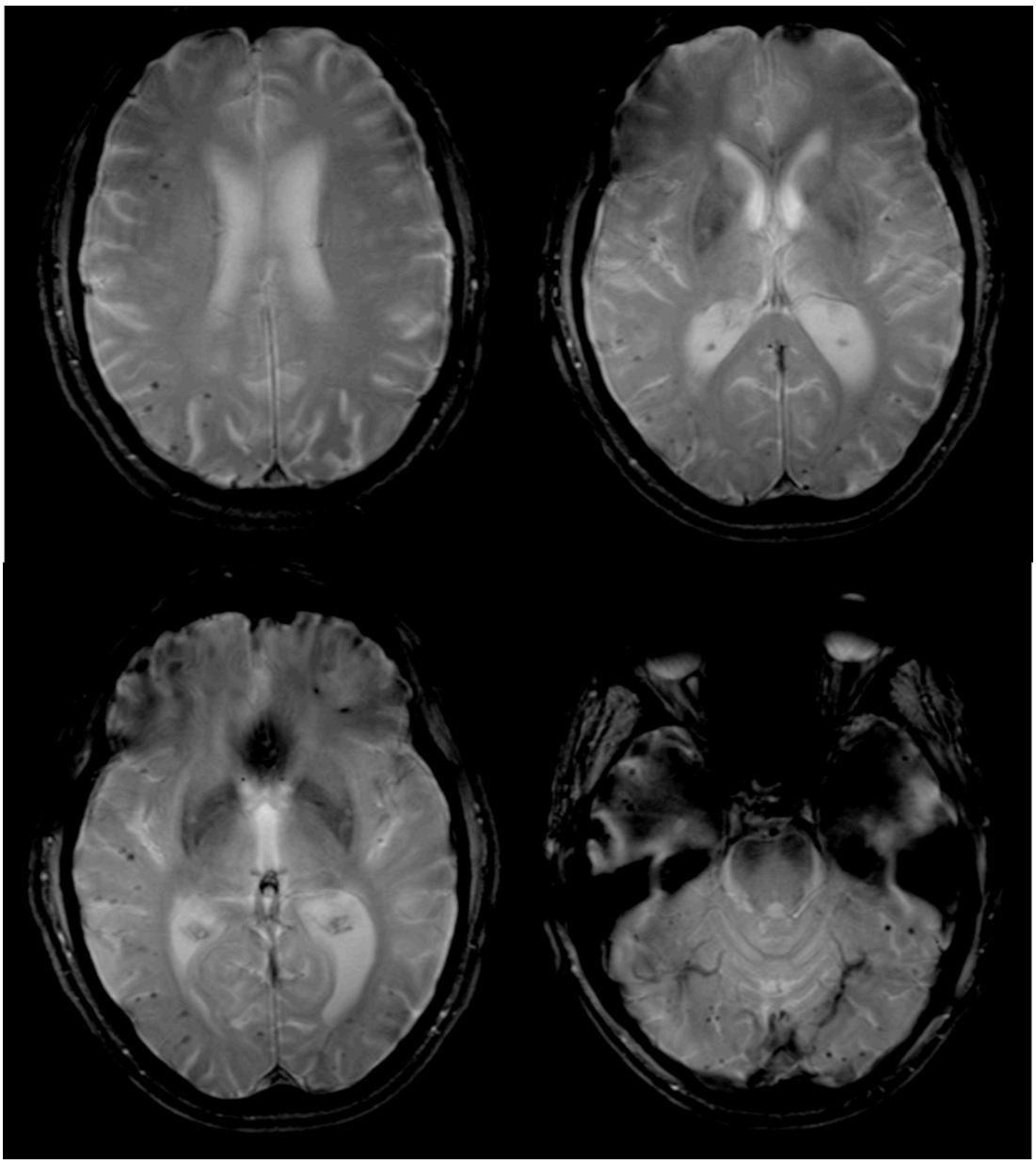

Interest in the relationship between AD and microbleeds is particularly timely in light of the findings of amyloid immunotherapy trials for AD, which have indicated that Aβ immunotherapy may lead to accumulation of Aβ42 in perivascular drainage pathways, with an associated increase in CAA and cerebral microbleeds (Boche *et al.*, 2008). It seems that clearance of this plaque-derived Aβ42 can occur over time, but both the efficacy of the process and risk of vasogenic oedema varies and may be influenced by the degree of pre-existing CAA. With the recent launch of prevention trials for presymptomatic mutation carriers (Bateman *et al.*, 2011), a deeper understanding of the relationship between CAA and microbleeds in different FAD mutations becomes increasingly relevant. Large, multi-centre studies of FAD such as DIAN, and newer scan sequences such as susceptibility-weighted imaging (SWI), potentially more sensitive to microbleeds, will be ideally placed to address these issues.

5.2 Spontaneous ARIA-E and cerebral amyloid angiopathy related inflammation in *PSEN1*-associated familial Alzheimer's disease

Although a detailed understanding of the pathogenesis of ARIA remains to be elucidated, the imaging appearances are certainly thought to reflect changes involving vascular amyloid. Recognition that the clinical and neuroimaging features of ARIA are similar, although in general milder, to those of the spontaneously occurring condition CAA-related inflammation (CAA-ri), supports the hypothesis that an immunological response to vascular amyloid, with increased vascular permeability, may be a common underlying pathophysiological mechanism (Piazza *et al.*, 2013). The observation of changes resembling ARIA-E in a small number of cases undergoing screening for clinical trials or participating in longitudinal imaging research studies suggests that it may rarely occur during the natural history of AD (Carlson *et al.*, 2011, Raman *et al.*, 2014). Its prevalence, however, is unknown and to our knowledge this is the first reported case of ARIA-E developing spontaneously during the course of *PSEN1*-associated FAD.

5.2.1 Case Report of ARIA-E in *PSEN1*-FAD

The patient developed gradual impairment of episodic memory from age 48. She was an ex-smoker with a history of treated hypercholesterolaemia and depression. On initial assessment, aged 53, she had finger myoclonus bilaterally and scored 25/30 on the MMSE. Neuropsychological assessment revealed significant impairment of immediate and delayed recall memory with language function at the lower limit of normal. Visuospatial and executive functions were relatively intact. A lumbar puncture (LP) demonstrated acellular CSF with a protein level of 0.4g/L. As a similar illness had affected her father from the age of 67 and two of her sisters from their early 50s, genetic testing was carried out. This identified the novel *PSEN1* p.Ile202Phe mutation in the patient and her affected siblings (Church *et al.*, 2011). Her *APOE* genotype was *e*4 homozygous. She was treated with a cholinesterase inhibitor and the first nine years of her illness followed a gradually progressive course. At the age of 57, she underwent a sub-acute deterioration in cognition and behaviour over a period of several weeks, becoming more emotionally labile and losing the ability to dress herself or hold a conversation. There were no associated headaches, seizures or signs of systemic infection. An MRI scan at this stage demonstrated florid white matter hyperintensities, particularly in a parieto-occipital distribution where they extended to involve the U-fibres and were associated with marked focal loss of sulcal spaces suggestive of oedema (Figure 5.3). The imaging abnormalities were bilateral but more prominent in the left hemisphere. T2*-GRE sequences were not acquired. The prospect of a further LP and steroid treatment was discussed with her family but a conservative approach was chosen. Her agitation improved on quetiapine and the course of her cognitive impairment appeared to return to the gradual rate of decline which it had previously followed. A follow up MRI nine months later showed that there had been some spontaneous improvement in the severity of white matter change and oedema. Unfortunately, she was unable to tolerate scanning long enough to acquire T2-FLAIR and T2*-GRE sequences on this occasion. Two months after the final scan she developed visual hallucinations and misperceptions, motor stereotypies and worsened agitation. An empirical trial of Prednisolone was given for a month; the family felt that this was associated with some functional improvement initially but it was not sustained and she couldn't tolerate increased doses. She continued to deteriorate, developed

seizures and was admitted to a Nursing Home. She died 10 months after her final scan and 11 years after the onset of her illness.

Figure 5.3 Serial MRI scans demonstrating the appearance and then subsequent partial resolution of ARIA

Reprinted from (Ryan *et al.*, 2014), with permission from IOS press.

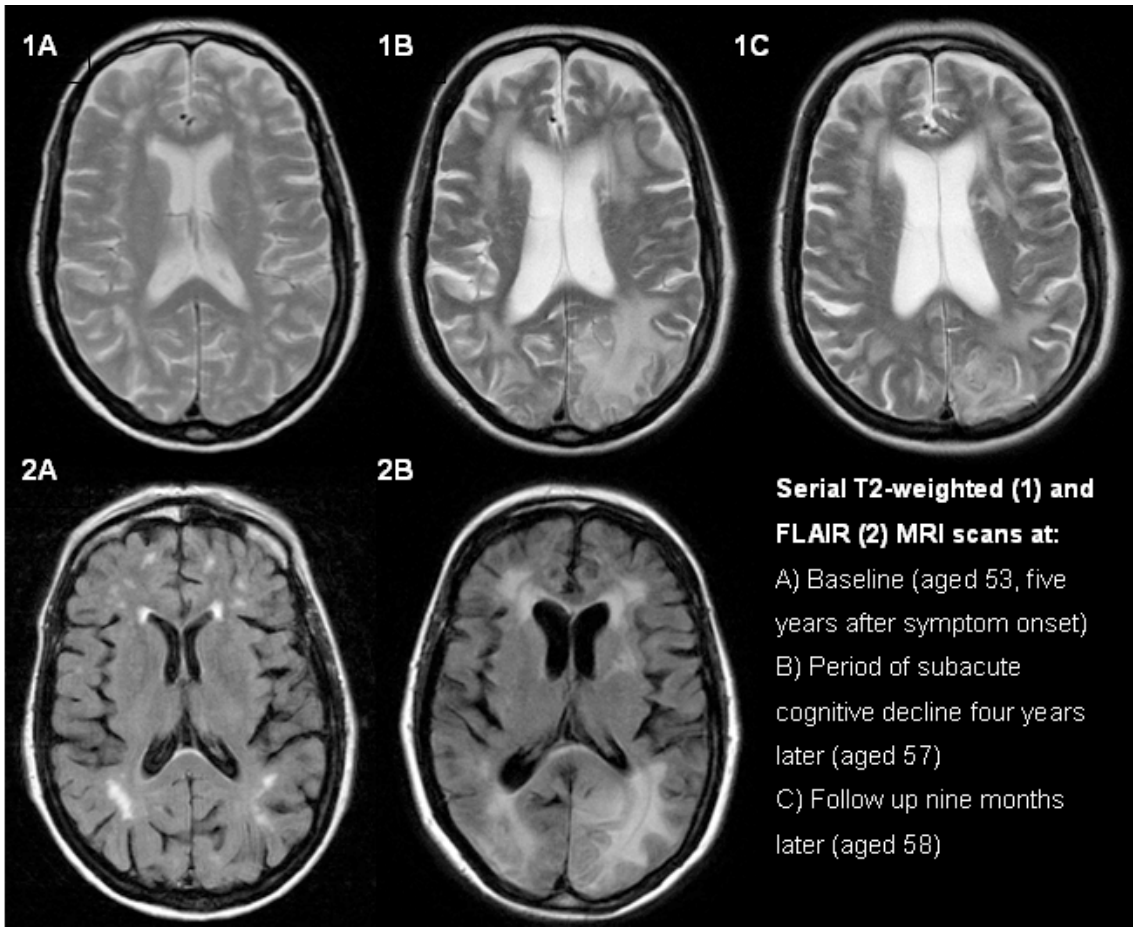

Her brain was donated to the Queen Square Brain Bank for Neurological Disorders where tissue is stored under a licence from the Human Tissue Authority. Brain weight was 1038g and macroscopic investigation confirmed severe cerebral atrophy, reduction in bulk of the hemispheric white matter, marked reduction in size of the hippocampus and amygdala and pallor of the locus coeruleus. Microscopic investigation of histological slides from representative regions of the right hemisphere of the brain demonstrated end-stage AD pathology with severe neurofibrillary tangle pathology (Braak and Braak stage VI) and extensive mature and diffuse Aβ-positive parenchymal

plaques (Thal phase 5). Tau immunohistochemistry confirmed the presence of 'frequent' neuritic plaques in all CERAD (Consortium to Establish a Registry for AD) cortical regions. Aβ immunohistochemistry also revealed 'severe' CAA with focal collections of mononuclear inflammatory cells, mostly CD3-positive T lymphocytes and CD68-positive macrophages, around some of the leptomeningeal and cortical blood vessels. One leptomeningeal small arteriole showed invasion of its thickened walls by CD3-positive T-cells (Figure 5.4), but no multinucleated giant cells were identified. Using special staining (MSB method) no fibrinoid necrosis of the walls of this or other leptomeningeal or cortical blood vessels could be demonstrated. A sparse diffuse chronic inflammatory cell infiltrate was present in the leptomeninges. In addition, there was marked diffuse increase of CD68-positive microglia/macrophages in the parenchyma of both cerebral cortex and subcortical white matter, which was slightly more severe in the temporal, parietal and occipital areas than in the frontal region. No haemorrhagic changes were seen. Some of the macrophages were observed to contain pigment, however this was negative for haemosiderin on Perls stain. As the MRI changes were more prominent in the left hemisphere, frozen tissue from the left parietal and occipital cortices was also examined. This demonstrated a small, cavitating infarct in the left occipital cortex and subcortical white matter invaded by macrophages and T lymphocytes. Macrophages and microglia were focally numerous in the surrounding brain parenchyma surrounding the infarct. a-Synuclein immunohistochemistry demonstrated amygdala predominant Lewy pathology.

Figure 5.4 Neuropathological analysis

Macroscopic observation of coronal slices confirmed cerebral atrophy and dilatation of the lateral ventricle with a reduction in bulk of the deep white matter and size of the hippocampus (A; arrow). Aβ immunohistochemistry showed numerous plaques (B) both cored (C) and diffuse. Severe CAA was found in the parenchyma (B, arrow) and leptomeninges (D) and was also found to affect capillaries in the occipital cortex (E). Numerous neurofibrillary tangles and neuropil threads were highlighted with tau immunohistochemistry (F) in the CA1 hippocampal subregion. Severe gliosis was observed throughout all cortical regions with GFAP immunohistochemistry (G) together with increased numbers of reactive microglia (H). Additional Lewy body and Lewy neurite pathology was seen in the amygdala (I). Some leptomeningeal blood vessels

were surrounded by focal collections of mononuclear inflammatory cells, mostly CD3-positive T lymphocytes and CD68-positive macrophages (K), with one leptomeningeal small arteriole showing invasion of its thickened walls by CD3-positive T-cells (L). B-I and K and L are immunohistochemical preparations, B-E: Ab peptide; F: Tau (AT8 antibody); G: GFAP; H and K: CD68; I: a-Synuclein; L: CD3; J: Haematoxylin and eosin. Bar in B represents 100μm in B, D; 50 μm in H, J, K and L; 20μm in C,E, F and I. Reprinted from (Ryan *et al.*, 2014), with permission from IOS press.

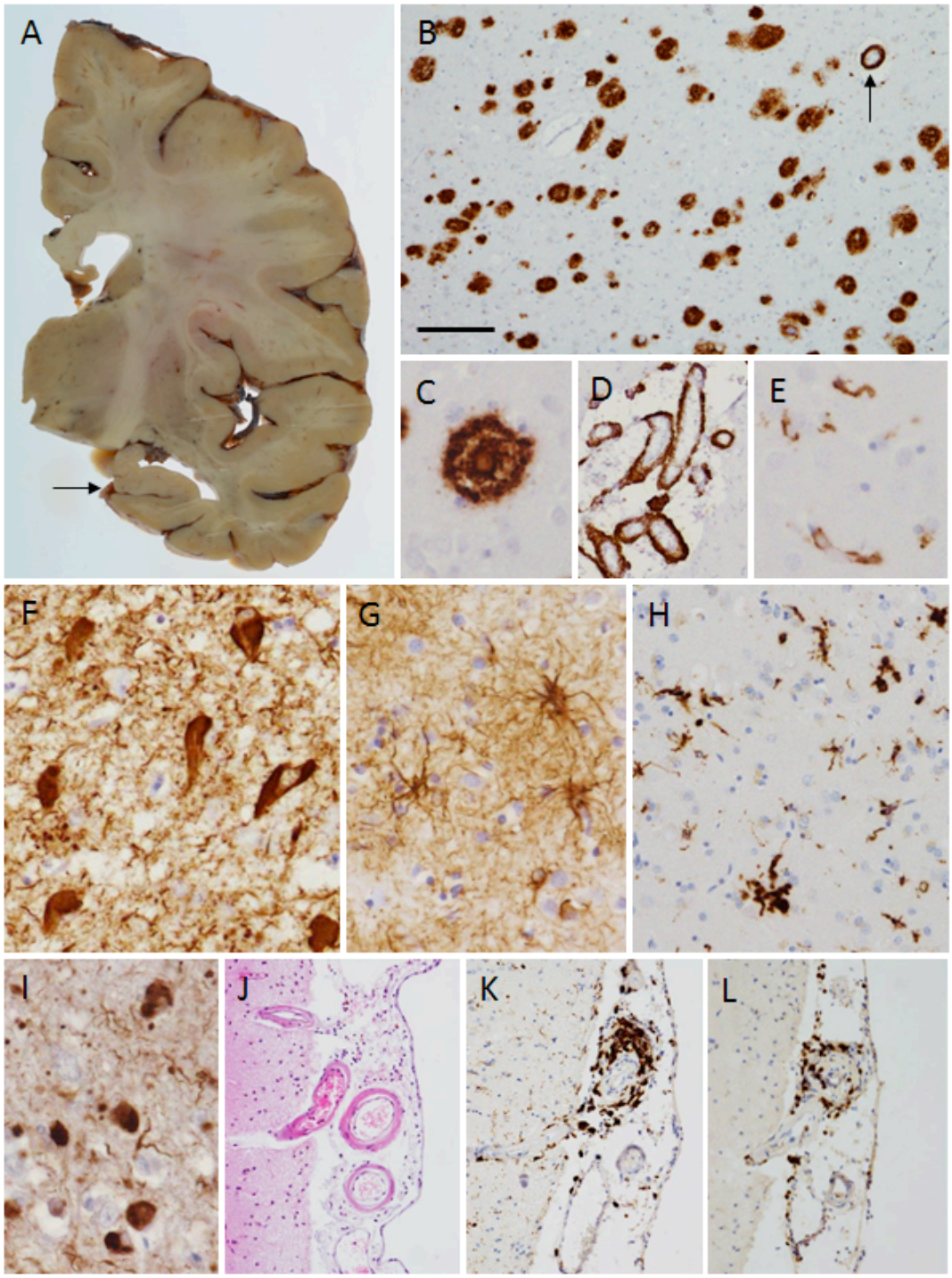
A
B
C
D
E
F
G
H
I
J
K
L

5.2.2 Discussion

The appearance of ARIA-E in this patient coincided with a period of clinical deterioration. As there was an interval of almost two years between this episode and the post-mortem examination, the exact cause of the imaging abnormalities can only be hypothesised. However, the pathological findings do support the idea that an immune/inflammatory response to vascular amyloid was implicated. There was severe CAA, with a chronic inflammatory infiltrate surrounding some of the cortical and leptomeningeal blood vessels. One leptomeningeal arteriole also showed transmural inflammation indicative of vasculitis. This case therefore adds further support to a growing body of literature linking CAA-ri to radiological features described as ARIA (Greenberg and Frosch, 2011). Whilst the precise underlying pathogenetic mechanisms are not yet fully understood, previous observations of $CD68^+$ macrophages and $CD4^+$ T-cell recruitment at sites of Aβ-related angiitis (Melzer *et al.*, 2012, Bogner *et al.*, 2014) and CSF anti-Aβ autoantibodies in patients with spontaneous CAA-ri (DiFrancesco *et al.*, 2011, Piazza *et al.*, 2013) support the notion of an autoimmune response against vascular Aβ, which may act to trigger a posterior reversible encephalopathy syndrome (Greenberg and Frosch, 2011).

Several factors may have predisposed the patient to developing this complication. *PSEN1* mutations located beyond codon 200 have been reported to cause particularly severe CAA (Mann *et al.*, 2001), and her *APOE-e*4 homozygosity may have increased her risk of developing CAA-ri. In clinical trials of the humanized anti-Aβ antibody bapineuzumab, the frequency of ARIA-E increased with *APOE-e*4 gene dose (Sperling *et al.*, 2012, Salloway *et al.*, 2014) and spontaneous CAA-ri is also associated with *APOE-e*4 homozygosity (Eng *et al.*, 2004, Kinnecom *et al.*, 2007). Capillary CAA, observed in the occipital cortex of this patient, may play an important role here as it has been found to both associate with the *APOE-e*4 allele (Thal *et al.*, 2002) and to provoke a particularly strong inflammatory response, unlike larger vessel CAA (Richard *et al.*, 2010). This individual's vascular risk factors may have rendered her further vulnerable to developing blood-brain barrier dysfunction and increased vascular permeability.

The development of ARIA-E should be further evaluated as a possible cause of sub-acute deterioration in patients with established AD. Recognition that it may arise spontaneously during the course of FAD is particularly timely with amyloid-modifying therapy trials for FAD underway. Although many of the participants in these trials will be presymptomatic, certain genetic factors may increase the risk of developing ARIA, even prior to the onset of clinical disease. This has been illustrated by a case report of ARIA developing spontaneously in a cognitively normal *APP* duplication carrier (Chamard *et al.*, 2013). Monitoring for ARIA, investigating the underlying pathophysiological mechanisms and identifying individuals at increased risk of developing them will be a crucial part of both natural history studies and treatment trials in AD.

6 MRI evidence for presymptomatic change in thalamus and caudate in familial Alzheimer's disease

6.1 Introduction

A wealth of evidence now indicates that the symptoms of AD are preceded by a long period of gradual accrual of pathological change (Price and Morris, 1999, Bateman *et al.*, 2012). FAD, although rare, provides a unique opportunity to gain insights into the earliest stages of the disease, through prospective study of mutation carriers (MCs), who are genetically destined to develop the disease. FAD MCs also represent a cohort in whom treatment may be initiated at a presymptomatic stage and a number of such trials are currently underway (Reiman *et al.*, 2010, Bateman *et al.*, 2011). As the individuals participating in these trials will have little or no cognitive impairment, there is a need to understand the trajectory of biomarker changes in presymptomatic FAD, in order to both assess disease progression and look for therapeutic effects.

Results from the large international DIAN study indicate that CSF biomarker changes are evident over two decades before an individual's expected age at symptom onset, as determined by their parental age at onset (Bateman *et al.*, 2012). Reduced concentrations of CSF amyloid-beta $(A\beta)_{42}$ and increased concentrations of CSF tau were detected at 25 and 15 years from expected symptom onset respectively. Aβ deposition on PIB-PET scans (Klunk *et al.*, 2004) and hippocampal volume loss were apparent at 15 years and cerebral hypometabolism at 10 years prior to expected symptom onset. Presymptomatic hippocampal atrophy has also been detected in longitudinal studies, which have followed smaller cohorts through the presymptomatic stage to age at symptom onset. At a group level, MCs showed hippocampal and whole brain volume loss compared with controls at three and one year before symptom onset (Ridha *et al.*, 2006). However, longitudinal measures were able to detect changes earlier, with differences in hippocampal and whole brain atrophy rates observed at 5.5 and 3.5 years before symptom onset in MCs (Ridha *et al.*, 2006, Knight *et al.*, 2011).

Prior volumetric imaging studies have mainly focussed on the neocortex and hippocampus, in view of the well-recognised roles that these structures play in higher

cognitive functions and memory, and their apparent vulnerability to AD pathology. However, PIB-PET studies have indicated that prominent amyloid deposition first appears in the striatum and thalamus in presymptomatic FAD (Klunk *et al.*, 2007, Knight *et al.*, 2011). These subcortical structures have received relatively little attention from volumetric imaging studies in AD. They are known to be significantly atrophied mild-moderate sporadic AD but it is not known how early this atrophy occurs (de Jong *et al.*, 2008). A previous FAD study reported decreased volumes of thalamus, caudate and putamen in presymptomatic mutation carriers (PMCs) who were on average 15 years younger than their family's median age at dementia diagnosis, with a trend towards increasing caudate size in those with memory deficits who were ten years younger (Lee *et al.*, 2013). Increased caudate volumes were reported in another cohort of PMCs who were approximately a decade younger than their expected age at symptom onset (Fortea *et al.*, 2010). This study also included diffusion imaging and found associated changes in mean diffusivity in the caudate of PMCs.

Although the thalamus and striatum are structures that are not conventionally associated with AD, it has long been known that they are affected by AD pathology (Braak and Braak, 1990, Braak and Braak, 1991). It is also becoming increasingly recognised that, given their dense connections with the cortex, they are involved in a variety of neural networks subserving complex cognitive and behavioural functions (Middleton and Strick, 2000). The caudate, for example, appears to play a key role in supporting the planning and execution of behaviour needed to achieve complex goals (Grahn *et al.*, 2008), whilst thalamic nuclei are involved in declarative memory function at a number of different levels (Van der Werf *et al.*, 2003). There is a growing appreciation of the idea that AD, and indeed neurodegenerative diseases in general, should be considered as network disorders in which there is selective degeneration of vulnerable neuronal circuits (Warren *et al.*, 2012). It therefore seems appropriate to investigate the subcortical grey matter regions involved in such networks, as well as the cortical areas and their connecting white matter.

DTI allows assessment of alterations in tissue microstructure in specific brain regions and can be used to examine the integrity of connecting white matter pathways (Basser *et al.*, 1994). DTI exploits the fact that water molecules show preferential diffusion along the major axis of a white matter fibre bundle (anisotropy), due to barriers hindering

perpendicular diffusion including axonal membranes and the myelin sheath. The effects of a pathological process on white matter tracts can be explored by investigating whether there are associated changes in the overall magnitude of diffusion (mean diffusivity; MD) or the degree of its directionality (fractional anisotropy; FA). Examining the component eigenvalues of the diffusion tensor, from which FA is derived, provides further information on how diffusion is altered in both the principal direction of the tract (axial diffusivity; AxD) and in the plane perpendicular to this (radial diffusivity; RD). If there are changes in AxD and RD which are proportional, there will be no corresponding change in FA, making it important to examine these components separately (Acosta-Cabronero *et al.*, 2010). DTI can be used to characterise grey matter microstructure too (Bozzali *et al.*, 2002, McKinstry *et al.*, 2002) with MD a commonly used metric (Benedetti *et al.*, 2006). In fibre-rich structures such as the thalamus and striatum, FA may also be a useful indicator of pathological change (Ciccarelli *et al.*, 2001, Tovar-Moll *et al.*, 2009, Bohanna *et al.*, 2011). Many DTI studies of sporadic AD have now been published, reporting decreased FA and increased MD in various tracts, most notably the cingulum, corpus callosum and white matter of the parahippocampal gyrus (Chua *et al.*, 2008, Stebbins and Murphy, 2009). There has been just one previous DTI study of presymptomatic FAD, which examined FA only and found it to be globally reduced in the white matter of PMCs, most strikingly in the fornix (Ringman *et al.*, 2007).

The study reported in this chapter investigates a cohort of *PSEN1* PMCs who are relatively close to their expected age at symptom onset, together with groups of symptomatic MCs (SMCs) and controls. Region of interest (ROI) analyses are used to examine volumetric and diffusivity differences in the subcortical structures that are the main focus of this study, and altered diffusivity in white matter tracts of interest. Automated whole brain analysis techniques; voxel-based morphometry (VBM) and tract-based spatial statistics (TBSS), are also used to provide whole-brain assessments of group differences in volume and DTI indices respectively.

6.2 Materials and methods

6.2.1 Subjects

20 *PSEN1* MCs were included in this study, all of whom had pathogenic mutations which have previously been reported elsewhere. Ten of these were PMCs: three p.Met146Ile, two p.Glu184Asp and one each of p.Met139Val, p.Tyr115Cys, Intron 4 (g.23024delG), p.Leu171Pro, p.Leu262Phe. Ten were SMCs: three Intron 4 (g.23024delG), two p.Glu280Gly and one each of p.Tyr115His, p.Glu120Lys, p.Pro264Leu, p.Arg269His, p.Arg278Ile. A group of 20 healthy controls (including two gene-negative siblings) was also studied. All subjects in the study underwent assessment with the Mini-Mental State Examination (MMSE). The *PSEN1* MCs also underwent neurological examination and detailed neuropsychological assessment. The neuropsychological test battery comprised measures of general intellectual functioning (Wechsler Abbreviated Scale of Intelligence (WASI)), estimated premorbid IQ (National Adult Reading Test (NART); verbal and visual recognition memory (recognition memory test (RMT) for words and faces); naming (Graded Naming Test (GNT)); calculation (Graded Difficulty Arithmetic Test (GDA)); visuoperceptual skills (object decision test from the Visual Object and Space Perception battery); speed and executive function (Stroop Test). All MCs identified a close informant who was interviewed separately to gain a collateral history; specific enquiry was made regarding cognitive symptoms in each domain, anxiety and depression. MCs were defined as symptomatic if consistent symptoms of cognitive decline were reported by the subject and/or their close informant. If there was a discrepancy between the opinion of the subject and their informant, the perspective of the informant was favoured as insight may not always be preserved in FAD. Estimated time to onset was calculated for the PMCs by subtracting the participant's current age from the age at which their parent first developed symptoms of progressive cognitive decline. The participants were recruited from an ongoing longitudinal study of FAD at the Dementia Research Centre, UCL Institute of Neurology. Some of the subjects had participated in our prior imaging studies of FAD (Ridha *et al.*, 2006, Knight *et al.*, 2011, Knight *et al.*, 2011) but the data used for this study have not been reported elsewhere. All of the subjects in this study were aware of their mutation status, having undergone clinical diagnostic or predictive genetic testing at approved clinical centres separately to their involvement in research. All subjects gave written informed consent according to the Declaration of Helsinki and

approval was received from the local ethics committee. Consent was taken by a clinician experienced in the assessment of patients with cognitive impairment and all subjects were considered to have capacity to consent according to the Mental Capacity Act of 2005. Subject demographics are detailed in Table 6.1.

6.2.2 MRI acquisition

All subjects were scanned on the same 3T Siemens TIM Trio scanner using a 32-channel phased array head-coil (Siemens, Erlangen, Germany). A sagittal 3D magnetisation prepared rapid gradient echo T1 weighted volumetric MRI (TE/TR/TI = 2.9/2200/900ms, dimensions of 256x256x208, voxel size of 1.1x1.1x1.1mm) and a coronal T2 FLAIR sequence (TE/TR/TI = 87/9000/2500 ms, voxel size of 0.9375x0.9375x5mm) were acquired. Two 64-direction DTI sequences were acquired with a single shot, spin-echo echo planar imaging (EPI) sequence (FOV 240 mm; matrix 96x96; yielding an isotropic voxel size of 2.5x2.5x2.5mm; 55 contiguous axial slices; TR: 6800 ms; TE: 91 ms; b value: 1000 s/mm^2), augmented with parallel imaging acceleration (GRAPPA). Nine acquisitions without diffusion weighting were acquired (b = 0 s/mm^2). For all subjects, volumetric T1, DTI and T2 FLAIR images were assessed visually in all planes to ensure adequate coverage and to exclude significant motion, artefacts or unexpected pathology.

6.2.3 Grey matter region of interest volumetric analysis

ROI segmentation in T1-weighted space was used to investigate the volumes of the subcortical structures of interest in this study; namely the thalamus, caudate, putamen and hippocampus. The Multi-Atlas Propagation and Segmentation (MAPS) technique was used (Keihaninejad *et al.*, 2011), which was previously developed for hippocampal segmentation and has been used in brain extraction (Leung *et al.*, 2010, Leung *et al.*, 2011). In MAPS, all of the atlases in a template library are first compared to the target image. Our template library consisted of 30 subjects (median age of 31 ± 8 years, 15 women) whose MRI scans had been manually segmented into 83 anatomical structures (Hammers *et al.*, 2003). Multiple best-matched atlases are then selected, and the labels in the selected atlases are propagated to the target image after non-linear image registration. Label fusion is then applied to combine the labels from different atlases to

create a consensus segmentation in the target image. We applied MAPS to 30 atlas images in a leave-one-out approach in order to determine the number of best-matched atlases (7-9) and the optimal label fusion technique (simultaneous truth and performance level estimation (STAPLE)) (Warfield *et al*., 2004) required to produce accurate individual ROIs by comparing them to the manually delineated regions. We used the optimised MAPS technique to generate individual ROIs for each subject in our data set (Figure 6.1). The anatomical validity of the segmentations was confirmed by two consultant neuroradiologists.

Figure 6.1 Regions of interest

Grey matter regions of interest (top): Segmentations of thalamus (blue), caudate (green), putamen (pink) and hippocampus (purple) overlaid on the T1 image of a single subject. White matter tracts of interest (bottom): Segmentations of the fornix (pale blue), right cingulum (purple), left cingulum (green), genu (yellow), body (red) and splenium (dark blue) of the corpus callosum, overlaid on the study-specific template. Reprinted from (Ryan *et al.*, 2013), with permission.

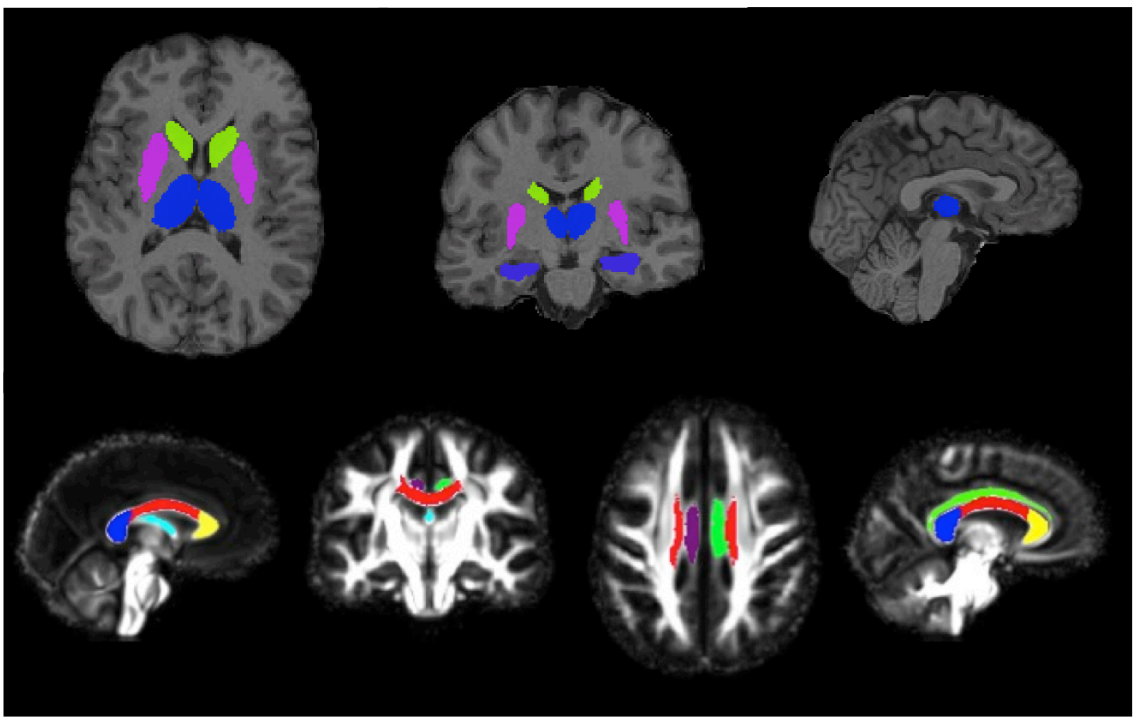

6.2.4 Grey matter region of interest diffusion tensor imaging analysis

All DTI acquisitions were registered to the first b=0 image using 12 degrees of freedom FLIRT (FSL) (Jenkinson *et al.*, 2002) for motion and eddy current correction and realigning diffusion-weighting directions appropriately. Tensor fitting was performed using Camino (Cook *et al.*, 2006). For each subject, the T1-weighted image was registered to the first (b=0) DTI image using a 12-parameter affine registration algorithm (Ourselin *et al.*, 2001). The ROIs defined using MAPS were transferred to the DTI space using nearest-neighbour interpolation. The overall average FA and MD values were calculated by averaging values for the entire individual ROI.

6.2.5 White matter tract of interest diffusion tensor imaging analysis

White matter tract of interest analysis was performed using DTI-TK to create a study-specific template using iterative tensor-based registration, which takes into account local fiber orientation (Zhang *et al.*, 2006, Keihaninejad *et al.*, 2012). In particular, all linear and non-linear registrations on the tensor images were performed using DTI-TK, which has been shown to outperform more conventional tools (Wang *et al.*, 2011). FA, mean, axial and radial diffusivity maps were created for the study-specific template and registered images. The ICBM-DTI-81 white matter labels and tracts atlas, developed by Johns Hopkins University (JHU) was used to locate the white matter tracts of interest (Mori *et al.*, 2005). The FA map of the JHU atlas was linearly and non-linearly registered to the study-specific template FA map (Ourselin *et al.*, 2001, Modat *et al.*, 2010). This transformation was used to warp the labels from the white matter atlas to the template FA image through nearest neighbour interpolation. In this study, we focused on six white matter tracts of interest: the genu, body, and splenium of the corpus callosum, fornix and left and right cingulum (Figure 6.1).

6.2.6 Statistical tests for non-voxelwise analyses

Baseline characteristics and neuropsychological test results (which were converted to z scores, based on published normative data) were compared using t-tests for normally distributed variables and Wilcoxon ranksum testing for the MMSE. Linear regression was used to factor out age effects on neuropsychological tests where no detailed age corrections were available (RMT, GNT, GDA and Object Decision). For the ROI

analyses, groups were compared using separate linear regressions for each outcome measure, in each ROI. The ROI volumetric analyses were adjusted for age, gender and total intracranial volume (TIV). The ROI DTI analyses for grey and white matter were adjusted for age and gender. TIV correction is not required for DTI as it assesses microstructural properties that are not expected to be associated with macroscopic head size. All results are reported as statistically significant if $p < 0.05$.

6.2.7 Voxel-based morphometry analysis of volumetric imaging

VBM processing was carried out using SPM8 (Statistical Parametric Mapping, version 8; Wellcome Trust Centre for Neuroimaging, London, UK). The T1-weighted scans were segmented into grey and white matter using the new segment toolbox with default settings (Weiskopf *et al.*, 2011). Segmentations were produced with rigid alignment to standard space (Montreal Neurological Institute (MNI) space) and re-sampled to 1.5mm isotropic voxels for use with DARTEL (Ashburner, 2007). DARTEL then iteratively registered the grey and white matter segments to an evolving estimate of their group-wise average (Ashburner and Friston, 2009). The native space tissue segments were then normalised to MNI space using the DARTEL transformations, modulated to account for volume changes. A smoothing kernel of 6mm full width at half maximum was applied. TIV was calculated for each subject using Jacobian integration of deformation fields created by the new segment toolbox (Ridgway *et al.*, 2011). Voxel-wise statistical analysis was performed with non-parametric permutation-testing using the FSL randomise programme (as used for the TBSS statistical analysis, described below). Grey and white matter images were modelled separately in terms of group (control, presymptomatic, symptomatic), age, gender and TIV (all mean centred). Statistical significance of differences between groups was assessed using threshold-free cluster enhancement (TFCE) (Smith and Nichols, 2009), controlling family-wise error (FWE). Results for symptomatic patients are shown thresholded at FWE $p < 0.05$; presymptomatic differences are shown at a less stringent level of FWE $p < 0.1$, with effect-maps (difference between adjusted group means as a percentage of the control mean) provided for a fuller characterization of the atrophy pattern.

6.2.8 Voxel-wise diffusion tensor imaging analysis using tract-based spatial statistics

The DTI data were also analysed with TBSS to investigate whole-brain white matter microstructural abnormalities (Smith *et al.*, 2006). In this study the modified TBSS protocol was used by incorporating a group-wise atlas as the registration target; GW-TBSS (Keihaninejad *et al.*, 2012). In the GW-TBSS pipeline, a group-wise atlas is first created based on the subset subjects' FA images using the method described in Keihaninejad *et al*., 2012. The voxel-wise statistical analysis was performed by the FSL randomise program (5000 random permutations) with correction for multiple comparisons to control FWE ($p < 0.05$) using TFCE. Age and gender were entered into the analysis as covariates.

6.3 Results

The subjects' demographic, neuropsychological and clinical data are summarised in Table 6.1. The presymptomatic (PMC) group was, as expected, younger than the symptomatic (SMC) group, and was on average 5.6 years below the expected age at symptom onset. The mean age of the control group (44.3) fell between that of the PMCs (37.8) and the SMCs (49.0) and age was used as a covariate in all analyses, as was gender. There was no clinically relevant difference in MMSE score between the controls and PMCs; SMCs had significantly lower MMSE scores than both groups as expected. The PMC and SMC groups were well matched for educational level and estimated pre-morbid IQ. Figure 6.2 shows mean and standard error z scores for the PMC and SMC groups on neuropsychological tests. The PMC group showed no significant deficit on any neuropsychological measure. The SMC group had significantly poorer performance than the PMC group on all tests except naming (GNT) and object perception.

The clinical data showed that neuropsychiatric symptoms were common in the SMC group; 40% had anxiety and 60% had depression. In the PMC group, 10% had anxiety and 20% had depression. The two PMCs with symptoms of anxiety and/or depression were both within two years of their expected age at onset; both had a long history of

recurrent psychiatric symptoms since their teenage years and required psychiatric review and medication changes at the time of their current assessment. None of the subjects had seizures but 60% of the SMCs and 40% of the PMCs had myoclonus on neurological examination. Myoclonus was the only abnormal sign present on examination of the PMCs but 20% of the SMCs had extrapyramidal signs and 60% had pyramidal signs, typically a symmetrical spastic increase in lower limb tone with hyper-reflexia.

Figure 6.2 Mean and standard error z scores for presymptomatic and symptomatic mutation carriers on standard neuropsychological tests.

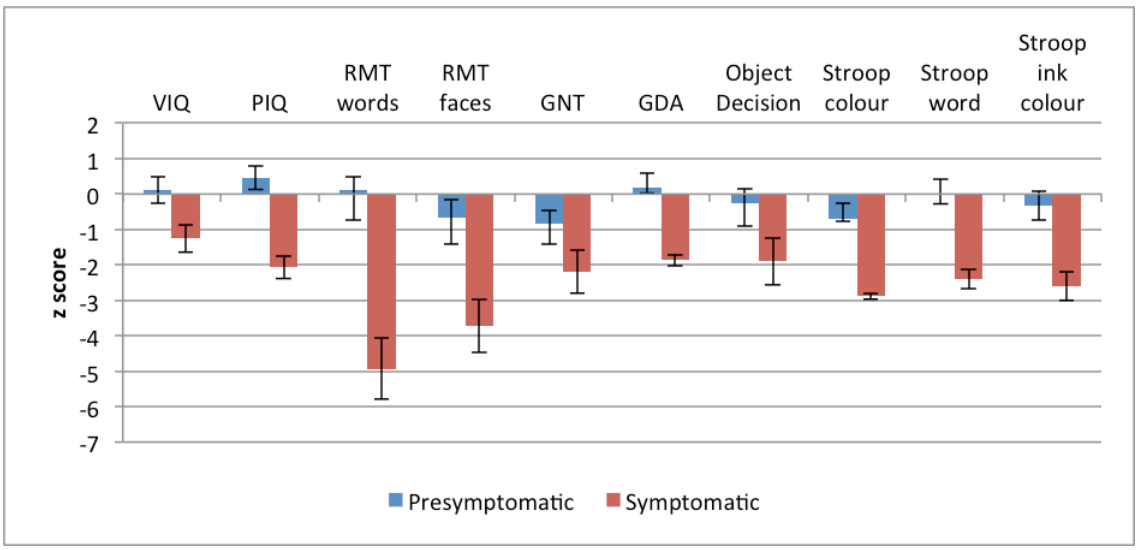

Table 6.1 Subject demographics, neuropsychological and clinical data.

Mean (SD)

	Presymptomatic MCs (4M, 6F)	Symptomatic MCs* (6M, 4F)	Control (9M, 11F)	*p* value
Age/ yrs	37.8 (4.7)	49 (9.4)	44.3 (12.7)	0.27 [a] (SMC vs control) 0.04 [a] (PMC vs control) < 0.01 [a] (PMC vs SMC)
Years from estimated age at onset	5.6 (7)	N/A	N/A	
Disease duration/ yrs	N/A	4.3 (1.7)	N/A	
MMSE/ 30 (range)	29 (28-30)	19 (13-24)	29.9 (29-30)	<0.01 [b] (SMC vs control 0.02 [b] (PMC vs control) <0.01 [b] (PMC vs SMC)
Years of education	13 (2.5)	12 (1.7)	N/A	0.20 [a]
NEUROPSYCHOLOGY				
NART estimated IQ	100.2 (12.9)	100.1 (12.5)	N/A	0.98 [a]
WASI Verbal IQ	101.7 (18.0)	81.2 (17.5)	N/A	0.02 [a]
WASI Performance IQ	106.7 (17.1)	69.0 (15.0)	N/A	<0.01 [a]
RMT words (/50)	45.9 (3.5)	30.0 (8.1)	N/A	<0.01 [c]
RMT faces (/50)	42.6 (5.3)	32.4 (7.5)	N/A	<0.01 [c]
Graded naming test (/30)	19.0 (5.0)	13.1 (7.8)	N/A	0.5 [c]
Graded difficulty arithmetic (/24)	12.9 (6.4)	2.4 (2.4)	N/A	<0.01 [c]
Object decision (/20)	18.2 (2.1)	15.6 (3.2)	N/A	0.06 [c]
Stroop colour (s)	36.2 (14.8)	63.3 (18.3)	N/A	<0.01 [a]
Stroop word (s)	23.1 (8.4)	49.1 (22.1)	N/A	<0.01 [a]
Stroop ink colour (s)	58.7 (20.5	124.4 (30.9	N/A	<0.01 [a]

*CLINICAL***				
Anxiety	10%	40%	N/A	
Depression	20%	60%	N/A	
Seizures	0%	0%	N/A	
Myoclonus	40%	60%	N/A	
Pyramidal signs	0%	60%	N/A	
Extrapyramidal signs	0%	20%	N/A	

**n* = 9 for all neuropsychological measures except WASI PIQ (N=10), NART (N=7) and Stroop colour ink interference (*n* = 5), with all reductions in *n* reflecting participants being untestable on specific tasks. Data for the complete cohort were available for all other statistical tests.

****Percentage in group manifesting the clinical feature

[a] Unpaired t-test, 2-tailed test [b] Wilcoxon ranksum test

[c] Linear regression with group and age as independent variables

The grey matter ROI volumetric analysis demonstrated significant atrophy of the left thalamus in PMCs compared with controls ($p = 0.023$), together with significant atrophy of both left caudate ($p = 0.025$) and right caudate ($p = 0.001$) (See Table 6.2 for all the grey matter ROI volumetric and DTI results). No areas of significant grey or white matter volume loss were seen in the PMC group versus controls in the VBM analysis after correction for multiple comparisons at the conventional level of FWE $p<0.05$. However, atrophy in the bilateral thalamic region was near significant (FWE $p = 0.061$, at MNI coordinates of [4.5, -13.5, 12] mm). Results thresholded at FWE $p<0.1$, together with an unthresholded effect map are shown in Figure 6.3. All of the grey matter ROIs were significantly atrophied in the SMC group compared to controls. The VBM results for the SMC versus control group comparison demonstrated grey matter volume loss in bilateral hippocampus and posterior cortical areas but the most significant volume loss was seen in the region of bilateral striatum and thalamus. Extensive loss of white matter volume was also observed in the SMCs compared with controls (Figure 6.4).

Figure 6.3 VBM results showing (top left) areas of grey matter reduction in PMCs compared with controls after correction for multiple comparisons at FWE < 0.1 and the effect-map for the PMC versus control group comparison.

In the effect-map, regions showing reduced grey matter in the PMC group are shown in red and in controls in blue. Differences between the two adjusted group-means are overlaid on a mean study-specific template. Images shown in radiological convention (right on left). Reprinted from (Ryan *et al.*, 2013), with permission.

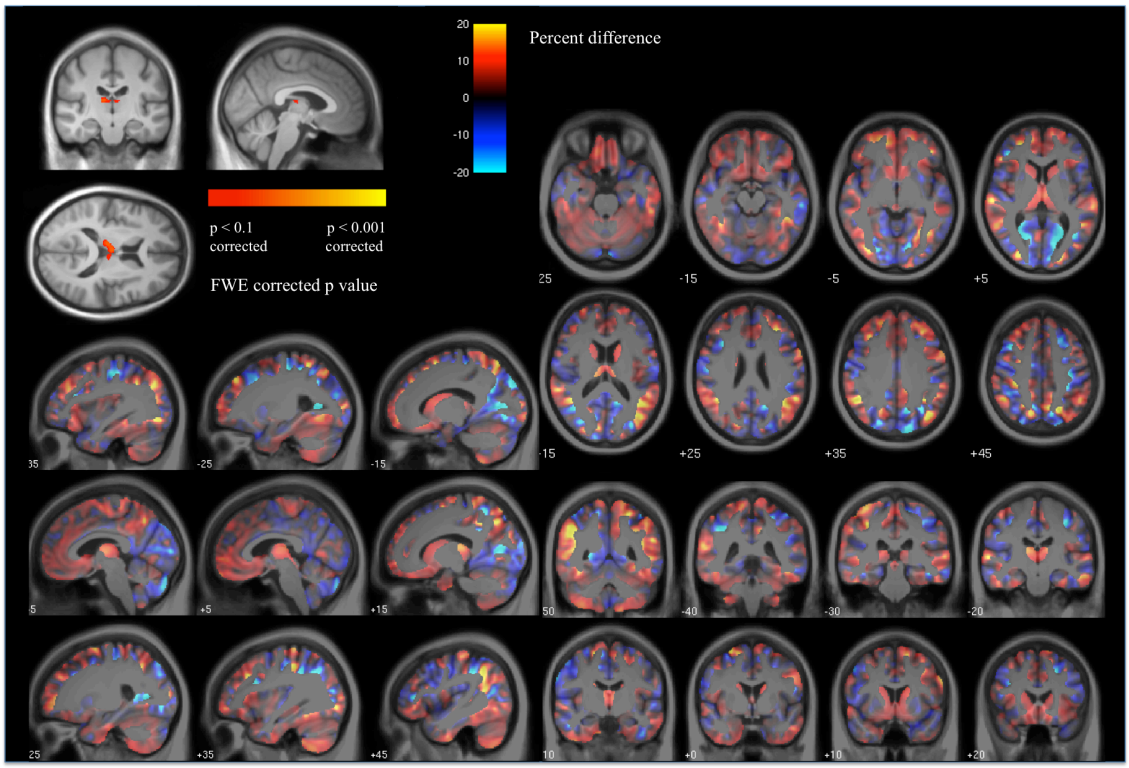

Figure 6.4. VBM results showing (top) grey matter reduction and (bottom) white matter reduction in SMCs compared with controls.

Results are shown overlaid on a mean study-specific template and are FWE- corrected for multiple comparisons. Images shown in radiological convention (right on left). Reprinted from (Ryan *et al.*, 2013), with permission.

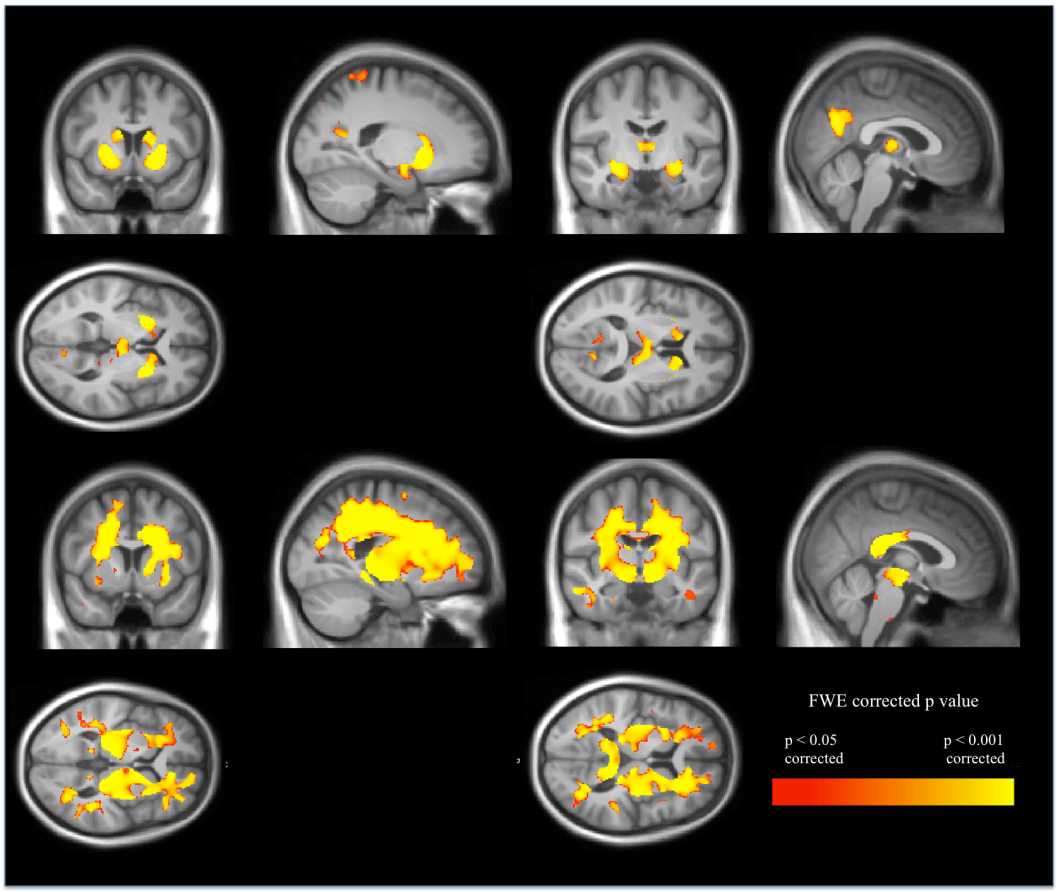

In the presymptomatic group, no significant hippocampal atrophy was evident, although the right hippocampus did show significantly decreased MD (p = 0.046) in the grey matter ROI DTI analysis relative to controls. Although not reaching significance, there was also a trend towards decreased MD in all the other subcortical structures in PMCs. This contrasts with the findings in the SMCs, who demonstrated increased MD in all the subcortical grey matter structures assessed; the pattern of change in diffusivity that is more typically observed in neurodegenerative disease. In the PMCs, FA was increased in the left thalamus (p = 0.016), right thalamus (p = 0.036) and left caudate (p = 0.004). FA was also increased in SMCs in left putamen (p = 0.032) and right putamen (p = 0.020), but did not differ significantly from controls in the other grey matter structures

assessed. In the white matter tract of interest analysis, PMCs demonstrated decreased MD (p = 0.043) and AxD (p = 0.011) in the right cingulum only (Table 6.3). Significantly decreased FA with increased MD, AxD and RD was seen in all the white matter tracts of interest in the SMCs. The TBSS analysis demonstrated widespread decreased FA and increased MD, AxD and RD in the white matter of SMCs. As demonstrated in Figure 6.5, the fall in FA in the fornix and cingulum of the SMC group appeared to be driven by an increase in radial diffusivity; very little difference in AxD was seen in these structures between the SMCs and controls. No significant differences in any of the DTI indices were seen in the TBSS analysis for PMCs vs controls.

Figure 6.5 TBSS results demonstrating areas of significantly decreased FA and significantly increased axial, radial and mean diffusivity in SMCs compared to controls.

Results are FWE-corrected for multiple comparisons using TFCE. Reprinted from (Ryan *et al.*, 2013), with permission.

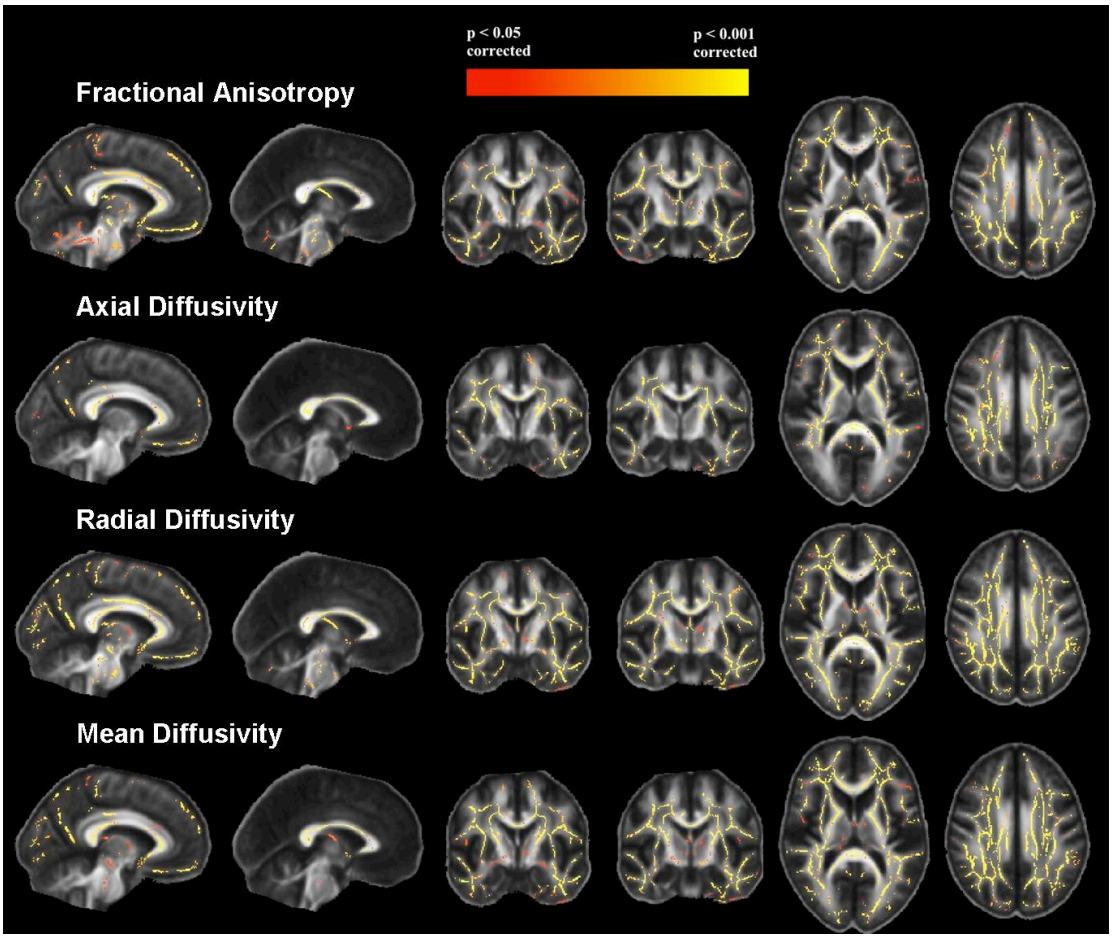

Table 6.2 Mean ± sd volumes and diffusivity indices in the grey matter regions of interest.

The differences in adjusted means between the MC and control group (95% confidence interval) are shown in italics. Significant results at $p < 0.05$ are indicated by an asterisk in the shaded cells.

	Controls	Pre-symptomatic MCs	Symptomatic MCs
Volume Right Thalamus (mm^3)	7792 ± 550	7676 ± 747 *275 (-152, 703)*	6103 ± 543 *1620 (1294 ,1947)**
Volume Left Thalamus (mm^3)	7177 ± 652	6962 ± 604 *428 (64, 792)**	5520 ± 404 *1533 (1216, 1849)**
Volume Right Caudate (mm^3)	4689 ± 512	4273 ± 553 *605 (293, 917)**	3832 ± 525 *746 (438, 1053)**
Volume Left Caudate (mm^3)	4743 ± 506	4376 ± 610 *466 (63, 868)**	3748 ± 588 *940 (537, 1343)**
Volume Right Putamen (mm^3)	5210 ± 656	5234 ± 695 *144 (-250, 537)*	4228 ± 473 *920 (555, 1285)**
Volume Left Putamen (mm^3)	5035 ± 680	4989 ± 775 *194 (-232, 620)*	3847 ± 655 *1142 (736, 1548)**
Volume Right Hippocampus (mm^3)	3131 ± 304	3153 ± 483 *-1.76 (-233, 230)*	2295 ± 477 *868 (632, 1103)**
Volume Left Hippocampus (mm^3)	3014 ± 278	3118 ± 423 *-116 (-345, 112)*	2302 ± 459 *769 (546, 991)**
FA Right Thalamus	.352 ± .017	.367 ± .019 *-.017 (-.032, -.001)**	.346 ± .031 *.006 (-.014,.025)*
FA Left Thalamus	.332 ± .013	.343 ± .008 *-.013 (-.023, -.003)**	.327 ± .031 *.007 (-.011,.025)*

FA Right Caudate	.229 ± .024	.239 ± .030 *-.017 (-.038,.004)*	.243 ± .034 *-.013 (-.037,.010)*
FA Left Caudate	.226 ± .017	.248 ± .026 *-.025 (-.041, -.009)**	.236 ± .027 *-.011 (-.029,.008)*
FA Right Putamen	.222 ± .016	.227 ± .013 *-.009 (-.021,.003)*	.242 ± .020 *-.017 (-.031, -.003)**
FA Left Putamen	.212 ± .011	.214 ± .010 *-.005 (-.013,.003)*	.228 ± .021 *-.014 (-.027, -.001)**
FA Right Hippocampus	.184 ± .016	.193 ± .022 *-.006 (-.0214,.009)*	.176 ± .032 *.004 (-.014,.023)*
FA Left Hippocampus	.178 ± .019	.192 ± .020 *-.012 (-.029,.005)*	.167 ± .033 *.007 (-.013,.028)*
MD Right Thalamus	.824 ± .030	.794 ± .043 *.022 (-.006 ,.049)*	.912 ± .089 *-.075 (-.119,-.032)**
MD Left Thalamus	.838 ± .029	.815 ± .037 *.016 (-.010, .042)*	.915 ± .069 *-.070 (-.108,-.032)**
MD Right Caudate	.956 ± .071	.949 ± .068 *.005 (-.057, .066)*	1.075 ± .111 *-.113 (-.185,-.040)**
MD Left Caudate	.993 ± .081	.955 ± .066 *.013 (-.045, .071)*	1.058 ± .072 *-.052 (-.112, .008)*
MD Right Putamen	.761 ± .026	.740 ± .028 *.016 (-.006, .038)*	.840 ± .060 *-.075 (-.108,-.041)**
MD Left Putamen	.773 ± .040	.752 ± .021 *.012 (-.016, .039)*	.838 ± .061 *-.061 (-.010,-.022)**
MD Right Hippocampus	.958 ± .033	.907 ± .073 *.044 (.002, .087)**	1.094 ± .073 *-.139 (-.181,-.096)**
MD Left Hippocampus	.952 ± .052	.921 ± .053 *.027 (-.017, .072)*	1.113 ± .096 *-.163 (-.221,-.104)**

Table 6.3. **Mean ± sd diffusivity indices in the white matter tracts of interest.**

The differences in adjusted means between the MC and control group (95% confidence interval) are shown in italics. Significant results at $p < 0.05$ are indicated by an asterisk in the shaded cells.

	Control	Presymptomatic MCs	Symptomatic MCs
FA Genu of corpus callosum	.610 ± .026	.621 ± .040 *.010 (-.017, .037)*	.570 ± .010 *-.040 (-.059, -.021)**
FA Body of corpus callosum	.612 ± .026	.613 ± .045 *-.000(-.029, .028)*	.559 ± .012 *-.054 (-.074,-.034)**
FA Splenium of corpus callosum	.684 ± .020	.691 ± .028 *.005 (-.015, .025)*	.639 ± .020 *-.045 (-.063,-.027)**
FA Fornix	.426 ± .044	.458 ± .094 *.017 (-.036, .069)*	.332 ± .046 *-.092 (-.130,-.054)**
FA Right Cingulum	.481 ± .033	.503 ± .059 *.018 (-.018, .054)*	.402 ± .019 *-.078 (-.102, -.054)**
FA Left Cingulum	.457 ± .035	.467 ± .050 *.011 (-.023, .044)*	.385 ± .018 *-.073 (-.098,-.047)**
MD Genu of corpus callosum	.849 ± .043	.835 ± .057 *.010 (-.031, .052)*	.942 ± .026 *.090 (.058 ,.122)**
MD Body of corpus callosum	.858 ± .039	.855 ± .052 *-.000(-.038, .037)*	.966 ± .041 *.105 (.071, .139)**
MD Splenium of corpus callosum	.855 ± .040	.847 ± .068 *.002 (-.042, .046)*	.974 ± .068 *.117 (.073, .160)**
MD Fornix	1.718 ± .199	1.642 ± .388 *.007 (-.214, .229)*	2.107 ± .147 *.369 (.215, .523)**
MD Right Cingulum	.821 ± .043	.776 ± .047 *.040 (.001, .078)**	.980 ± .049 *.157 (.119, .196)**
MD Left Cingulum	.776 ± .050	.752 ± .062 *.019 (-.028, .066)*	.911 ± .040 *.132 (.092, .172)**

AxD Genu of corpus callosum	1.543 ±.038	1.528 ± .041 *.010 (-.023, .044)*	1.636 ± .031 *.088 (.059,.118)**
AxD Body of corpus callosum	1.569 ±.040	1.562 ± .021 *.003 (-.027,.033)*	1.661 ± .041 *.087 (.054,.120)**
AxD Splenium of corpus callosum	1.662 ±.043	1.653 ± .075 *.004 (-.044, .052)*	1.795 ± .078 *.130 (.082,.178)**
AxD Fornix	2.536 ±.188	2.454 ± .335 *.021 (-.177,.219)*	2.832 ± .136 *.279 (.134,.424*)*
AxD Right Cingulum	1.291 ± .046	1.248 ± .020 *.042 (.010,.074)**	1.394 ± .054 *.102 (.062,.142)**
AxD Left Cingulum	1.188 ±.049	1.161 ± .039 *.018 (-.021,.057)*	1.281 ± .043 *.088 (.049,.128)**
RD Genu of corpus callosum	.503 ± .048	.488 ± .068 *.010 (-.037, .057)*	.595 ± .026 *.090 (.055,.125)**
RD Body of corpus callosum	.503 ± .043	.502 ± .069 *-.002 (-.047, .043)*	.618 ± .042 *.114 (.078,.151)**
RD Splenium of corpus callosum	.451 ± .041	.444 ± .066 *.001 (-.042,.044)*	.563 ± .064 *.110 (.068,.152)**
RD Fornix	1.310 ± .206	1.236 ± .416 *.001 (-.234, .235)*	1.744 ± .155 *.415 (.255, .575)**
RD Right Cingulum	.585 ± .050	.540 ± .073 *.039 (-.012, .089)*	.772 ± .048 *.185 (.143,.227)**
RD Left Cingulum	.569 ± .057	.547 ± .079 *.019 (-.036, .075)*	.725 ± .043 *.154 (.109, .198)**

As a supplemental analysis, ROI measures for the PMC versus SMC groups were compared. Significantly decreased FA with increased MD, AxD and RD was found in all white matter ROIs in SMCs. All grey matter ROIs except from the caudates had significantly smaller volumes in SMCs compared to PMCs. Whereas FA did not differ,

MD was significantly increased in all grey matter ROIs of SMCs except right thalamus and left caudate, where the increase was of borderline significance ($p = 0.061$ and $p = 0.075$ respectively).

6.4 Discussion

It has been established from PIB-PET imaging studies that the striatum and thalamus are affected early in the presymptomatic stage of FAD by amyloid deposition (Klunk *et al.*, 2007, Knight *et al.*, 2011). We demonstrated atrophy of the caudate and thalamus in a cohort of PMCs who were on average 5.6 years prior to their expected age at onset. It is therefore likely that many if not all would be expected to have amyloid deposition in these regions. In fact half of these PMCs had participated in a prior PIB-PET study, which found increased thalamic and striatal amyloid deposition compared to controls (Knight *et al.*, 2011). The findings of presymptomatic FAD studies will clearly depend on how far from symptom onset the individuals in the study are. A previous study examining the caudate in presymptomatic FAD interestingly demonstrated an unexpected increase in the volume of the caudate, precuneus and parietotemporal areas in PMCs who were on average 9.9 years from expected age at onset (Fortea *et al.*, 2010). The authors of this paper speculated that reactive neuronal hypertrophy and/or inflammatory processes early in the presymptomatic stage may account for an initial increase in the volume of these structures, which then undergo progressive atrophy as the disease progresses. Although their findings, like ours, need to be replicated in larger longitudinal studies, it is quite possible that pathological processes early in the presymptomatic stage cause dynamic changes in the volume of affected structures, which alter in terms of the direction of change as symptom onset is approached. Their DTI results, like ours, showed a widespread increase in MD in SMCs and a contrasting decrease in MD in the PMCs.

Increased MD and decreased FA are thought to reflect loss of integrity of cellular structures and are commonly observed in neurodegenerative diseases, as was the case with the SMCs in our study. The PMCs, on the other hand, showed significantly decreased MD in the right hippocampus and a trend towards decreased MD in the other subcortical structures studied. Decreased MD may reflect earlier pathological changes

in the pathway towards neurodegeneration, such as microglial activation/accumulation and swelling of neurons and glia. In a triple transgenic mouse model of AD the appearance of neuritic plaques is associated with hippocampal astrogliosis and microglial activation and is preceded by an increase in the density of resting microglia (Olabarria *et al.*, 2010, Rodriguez *et al.*, 2010). A DTI study of the APPsw transgenic mouse found that the time of significant amyloid plaque accumulation coincided with a fall in the magnitude of diffusion in hippocampus and cerebral cortex (Sun *et al.*, 2005). Microglial activation PET studies have demonstrated increased thalamic binding following traumatic brain injury (Ramlackhansingh *et al.*, 2011) and middle cerebral artery infarction (Pappata *et al.*, 2000), with decreased thalamic MD seen initially in acute stroke (Herve *et al.*, 2005), perhaps supporting the hypothesis that gliosis accounts for the low MD observed in PMCs. Microglia undergo persistent activation at sites of white matter damage (Wilson *et al.*, 2004), which may explain why they are observed in densely connected subcortical structures. In animal models of axonal injury, APP is upregulated in white matter at the site of trauma but is later seen in the dorsal thalamus (Spain *et al.*, 2010), where neuronal atrophy, but not cell death, has been observed (Lifshitz *et al.*, 2007). Support for the idea that subtle, subclinical but widely-distributed neuronal injury may result in microglial activation in the thalamus comes from an early microglial activation PET study, which demonstrated an age-dependent increase in thalamic binding of the tracer PK11195 in healthy controls (Cagnin *et al.*, 2001). By contrast, sporadic AD patients in this study showed increased regional PK11195 binding in the entorhinal, cingulate and temporoparietal cortex.

The PMC group in our study showed increased FA in bilateral thalamus and left caudate and, in the SMC group, increased putamen FA was seen bilaterally. FA reflects the degree of directionality (anisotropy) of diffusion of water molecules within a structure; it is therefore highest in white matter tracts, lower in grey matter and lowest in CSF. The anisotropy of the thalamus and striatum is probably due to their compartmentalised cytoarchitectural organisation, together with the large number of white matter fibres passing through them (Wiegell *et al.*, 2000). Similar to our findings, a pattern of increased FA in the thalamus and basal ganglia has been observed in patients with multiple sclerosis (MS) (Ciccarelli *et al.*, 2001, Tovar-Moll *et al.*, 2009). It has been suggested that this may be due to the selective degeneration of white matter fibres connecting these subcortical structures with cortical areas combined with the relative

preservation of anisotropic intrinsic connections between the structures themselves. This may result in an overall increase in the FA of the subcortical structures. By the same presumed mechanism, increased FA was found in a group of patients with mild cognitive impairment compared with controls in the centrum semiovale, due to degeneration of association fibres of the superior longitudinal fasciculus where they cross with intact motor projection fibres (Douaud *et al.*, 2011).

Decreased MD and AxD were observed in the right cingulum of the PMC group, whereas increased MD, AxD and RD occurred in all white matter ROIs of the SMCs. This pattern of events also conforms with the findings of pathological studies of axonal damage. Axonal injury initially causes swelling, beading and fragmentation of axons with an associated fall in AxD, probably because intracellular diffusion is hindered by the damaged membranes whilst axonal swelling and beading impedes diffusion in both the intracellular and extracellular space (Budde and Frank, 2010). Following subsequent clearance of membrane fragments, the decreased axonal density permits increased parallel diffusion in the extra-axonal space and therefore increased AxD, together with increased RD secondary to myelin degradation (Song *et al.*, 2003, Concha *et al.*, 2006). In the APPsw transgenic mouse DTI study, decreased AxD was seen diffusely in the white matter from the time of amyloid plaque accumulation, with increased RD occurring in the corpus callosum at a later stage (Sun *et al.*, 2005). Although each variable was examined separately the TBSS results in our study suggest a more prominent increase in RD than AxD in SMCs compared to controls, particularly in the fornix and cingulum, which may be because of this gradual transition of AxD from decreased to increased with advancing axonal degeneration. Other studies of early AD have also found more prominent increases in RD than AxD, with AxD decreased in some tracts (Huang *et al.*, 2007).

Several pathogenic pathways are likely to contribute to the axonal degeneration witnessed in AD, including defects in fast axonal transport resulting from enhanced production of Aβ (Kanaan *et al.*, 2013). Neurons, having longer dendrites and axons than any other cell type, are particularly vulnerable to impaired fast axonal transport, which may be why FAD-causing mutations selectively affect neurons despite being ubiquitously expressed in cells throughout the body. It may also explain why short interneurons tend to be relatively spared in AD compared to long projection neurons

(Mattson and Magnus, 2006), an observation which could well underlie our finding of increased FA in the thalamus and caudate in presymptomatic FAD. The cingulum bundle, where we observed presymptomatic diffusivity changes, is composed of particularly long-coursing white matter tracts, arising from the thalamus, cingulate gyrus and cortical association areas. It is the major route for projections from the anterior thalamus to cingulate cortex, hippocampus and retrohippocampal regions; a network that is thought to play a key role in memory and spatial orientation (Neave *et al.*, 1997). These cognitive functions are often impaired early in AD, perhaps because neurons lose their functional connections with increasing axonal damage. Eventually, once the damage has reached a stage where trophic signalling is no longer available, overt neurodegeneration may occur.

A number of strands of evidence suggest that a network of limbic neurons undergoes selective degeneration in early AD, including PET findings of hypometabolism in the thalamus, mamillary bodies, hippocampus and posterior cingulate (Nestor *et al.*, 2003). Along with the cingulum findings, our observation of presymptomatic thalamic atrophy and increased thalamic FA in FAD adds further support to this notion. The few pathological studies of thalamic involvement in AD have demonstrated extracellular amyloid deposits in almost all thalamic nuclei (Braak and Braak, 1991) and significant thalamic atrophy, thought largely to be due to loss of axons, dendrites and synaptic structures or glial cell changes (Xuereb *et al.*, 1991).

The striatum of AD patients at post-mortem has also been found to contain abundant amyloid deposits with loss of large cholinergic neurons (Oyanagi *et al.*, 1987, Braak and Braak, 1990), which potentially underlies our findings of striatal atrophy in FAD. The majority of striatal nerve cells appear to resist the development of neuritic change (Braak and Braak, 1990) despite the presence of abundant amyloid, which is intriguing given that striatal involvement on PIB-PET scans is evident over a decade prior to symptom onset in FAD. One possible hypothesis relates to differences in mechanisms of calcium homeostasis in different neuronal populations. It has been found that Presenilins act as calcium leak channels in the endoplasmic reticulum (ER) of hippocampal neurons and many *PSEN1* mutations impair this leak function, resulting in ER calcium overload and supranormal calcium release. In medium spiny striatal neurons (the major neuronal cell type in the striatum), the ER is much less leaky for

calcium and Presenilins show less involvement in calcium homeostasis (Nelson *et al.*, 2010).

The idea that widespread white matter degeneration occurs in FAD is supported by the imaging findings in our SMC cohort. Volume loss of the white matter appeared to be more widespread than that of the grey matter in the VBM analysis, and the TBSS results showed very diffuse microstructural white matter abnormalities in the SMC cohort. A variety of *PSEN1* mutations are known to be associated with spastic paraparesis and some individuals with the phenotype have white matter hyperintensities visible on brain MRI (O'Riordan *et al.*, 2002, Ryan and Rossor, 2010). It would not, therefore, be surprising if microstructural damage to the white matter gave rise to more subtle pyramidal signs and our observation that 60% of the SMCs had lower limb spasticity and hyper-reflexia may well relate to this white matter pathology. It is not clear whether there are clinical correlates of the presymptomatic thalamic and caudate changes we observed. Although extrapyramidal signs, often associated with striatal pathology, were seen in 20% of the SMCs they were not seen presymptomatically. Presymptomatic myoclonus was observed, as has been detected in prior studies (Godbolt *et al.*, 2004). The origin of this myoclonus is unknown but it is possible that thalamocortical networks are implicated, as they are in other conditions such as juvenile myoclonic epilepsy (Gerschlager and Brown, 2009).

Neuropsychologically, the SMC cohort showed deficits in widespread domains at the time they were studied, with verbal recognition memory worst affected and perhaps some relative preservation of naming and object perception, as has been observed previously (Warrington *et al.*, 2001, Godbolt *et al.*, 2004). No significant neuropsychological deficits were observed in the PMC group, although 20% of these subjects and 60% of the SMCs had symptoms of depression and/or anxiety. Anxiety and depression are relatively common in both sporadic and familial AD and it is understandable that these symptoms may occur in PMCs who are aware of their mutation status and approaching the age at which they saw their parent develop symptoms. However, it is worth noting that limbic circuits are well known to be involved in emotional expression and lesions to anterior thalamic nuclei have been found to cause a variety of neuropsychiatric symptoms including sadness, agitation and flattened affect, in addition to amnesia (Schmahmann, 2003). Disentangling whether

presymptomatic psychiatric symptoms are related more to psychological factors or disease effects will require longitudinal study of large cohorts of at risk individuals, comprising both mutation positive and negative individuals, who are unaware of their mutation status but exposed to the same anxieties about the possibility of developing symptoms. Collaborative studies such as DIAN will be ideally placed to address these issues and ascertain whether our findings are reproducible in larger FAD cohorts. The relatively small number of subjects was an important limitation of our study, as it limits power and may have accounted for the fact that reduced thalamic volume and increased caudate FA only reached statistical significance on the left in the PMC ROI analysis. Larger cohorts will be required to investigate whether the onset of subcortical imaging changes is indeed asymmetrical.

In summary, we demonstrated presymptomatic thalamic and caudate volume loss and increased FA, with decreased mean diffusivity in the right hippocampus and cingulum, in *PSEN1* MCs who were approximately 5.6 years from expected age at onset. We propose that axonal degeneration is an early event in FAD pathogenesis and that amyloid accumulation, atrophy and diffusivity changes are seen early on in the thalamus and striatum due to the large number of white matter tracts that these structures are connected with. Involvement of a subcortical structure like the thalamus, which forms a key node in a vulnerable neuronal network, could potentiate the propagation of pathology through that network. The most striking degeneration may then be observed in connected neuronal populations, such as those of the hippocampus. How generalizable our findings are to sporadic AD is an important question. There is some evidence of early white matter tract degeneration in sporadic AD from DTI studies of MCI (Chua *et al.*, 2008, Stebbins and Murphy, 2009) and thalamic atrophy has also been demonstrated in MCI (Pedro *et al.*, 2012). In healthy controls at increased risk of sporadic AD due to possession of an *APOE4* allele, decreased FA has been found in several white matter tracts including the cingulum (Smith *et al.*, 2010) and volume loss of the hippocampus, but not thalamus or striatum, has been observed (O'Dwyer *et al.*, 2012). The same neuronal network appears to disintegrate in both sporadic and familial AD but it may be that different nodes of this circuit are particularly vulnerable to different risk factors for the disease. The development of more sensitive diffusion imaging techniques such as high-angular-resolution diffusion imaging (HARDI) (Haroon *et al.*, 2011) and neurite orientation dispersion and density imaging (NODDI)

(Zhang *et al.*, 2012), and their application to the longitudinal study of individuals at risk of both familial and sporadic AD, may allow us to further investigate just how early microstructural abnormalities become evident and when is the optimal time for therapeutic intervention.

7 Thesis summary and conclusions

7.1 Summary

This thesis describes studies of FAD undertaken with the broad objectives of investigating heterogeneity in the clinical and neuroimaging features of FAD, and exploring imaging changes in the preclinical phase of FAD, in order to gain insights into underlying disease mechanisms. The work was strongly motivated by the launch of presymptomatic treatment trials for FAD, which necessitate characterisation of the full clinical spectrum of the disease, investigation of factors contributing to phenotypic heterogeneity and identification of presymptomatic biomarkers of the disease. In this final chapter, the main findings of the thesis are described and discussed, along with limitations of the studies, implications for clinical practice and future directions for FAD research.

Introductory chapters 1 and 2 reviewed the literature on the clinical phenotype of FAD and on imaging biomarkers of AD, particularly presymptomatic FAD. In chapter 3, the clinical spectrum of FAD was investigated through analysis of all symptomatic cases studied at our centre since identification of the first mutation twenty-five years ago. Significant phenotypic differences between individuals with *PSEN1* and *APP* mutations were identified, highlighting the potential importance of considering these genetic groups separately in clinical research and trials. In addition to having younger ages at symptom onset, *PSEN1* mutation carriers were much more likely to have a non-amnestic cognitive presentation, which occurred in 16% of *PSEN1* cases. Additional neurological features of pyramidal, extrapyramidal and cerebellar signs were only observed in the *PSEN1* group and there could be considerable phenotypic variability between different *PSEN1* mutations. Atypical cognitive presentations, pyramidal signs and later ages at symptom onset were seen more frequently in association with *PSEN1* mutations located beyond codon 200. A previous study had reported that neuropathological differences may also be evident between *PSEN1* mutations located before and after codon 200, with more severe CAA seen in association with post codon 200 mutations (Mann *et al.*, 2001). In chapter 4, potential differences between pre and post codon 200 *PSEN1* mutations were further investigated with an imaging study of

white matter hyperintensities (WMH) on MRI, which are a key imaging manifestation of CAA. This study demonstrated increased posterior WMH in the *PSEN* post-codon 200 mutation group and found that, in the subset of cases with post-mortem examination, WMH burden correlated with the severity of CAA and cotton wool plaque pathology. In contrast, the *PSEN1* pre-codon 200 group had younger ages at onset and greater axonal loss, gliosis and T-lymphocytic response in the deep white matter. These studies demonstrate that mutation site contributes to the phenotypic and pathological heterogeneity witnessed in FAD and motivate future work investigating functional differences between mutations at different sites of *PSEN1*. Chapter 5 continued to explore the topic of CAA in FAD with reference to 'ARIA', the term coined to describe amyloid-related imaging abnormalities' of microbleeds (ARIA-H) on T2*-GRE MRI and oedema or extravasated fluid on T2-FLAIR MRI (ARIA-E), which have been observed in amyloid-modifing therapy trials for AD and are thought to reflect vascular amyloid. A study of microbleeds in symptomatic subjects with FAD mutations is described, which is the first to assess the prevalence of microbleeds in FAD and finds this to be similar to that reported in sporadic AD. The first reported case of ARIA-E developing spontaneously during the course of *PSEN1*-associated FAD is then presented. The post-mortem findings of CAA-related inflammation (CAA-ri) in this case add further support to a growing body of literature linking CAA-ri to ARIA, and suggest that *APOE*4 homozygosity and a post-codon 200 *PSEN1* mutation may have rendered the individual particularly vulnerable to developing this complication. Monitoring for ARIA and identifying risk factors for their development will form a crucial part of preclinical treatment trials for FAD. These trials drive a need to better understand the trajectory of biomarker changes prior to symptom onset in FAD and Chapter 6 investigates volumetric and diffusivity changes in subcortical grey matter structures and their connecting white matter tracts in presymptomatic and symptomatic mutation carriers. The thalamus and striatum are included as regions of interest as they show early amyloid deposition in FAD and the study finds that they do indeed demonstrate atrophy and altered diffusivity in the presymptomatic phase. Altered diffusivity in the cingulum and hippocampus are also seen, but at a stage when hippocampal atrophy is not evident. Axonal degeneration may therefore be an early event in presymptomatic FAD and it may be owing to their dense connectivity that imaging changes are seen first in the thalamus and striatum, which then progress to involve other regions in a vulnerable neuronal network.

7.2 Imaging manifestations of familial Alzheimer's disease pathology

Work described in this thesis contributes to a growing interest in the imaging manifestations of AD pathology, particularly in the preclinical stage of the disease, and highlights a number of unresolved issues. Firstly, brain atrophy on MRI is typically thought to be a biomarker of neuronal loss, which is considered to be a very downstream element in the amyloid cascade hypothesis of AD pathogenesis. Our finding of caudate and thalamic atrophy in presymptomatic FAD mutation carriers, at a stage when hippocampal atrophy was not yet evident, therefore raises a number of questions. What is the relationship between this atrophy and the early striatal and thalamic amyloid deposition observed on PIB-PET imaging of FAD mutation carriers? Does the atrophy represent neuronal injury induced by amyloid or by amyloid independent mechanisms? Is the atrophy due to neuronal injury at all, or does it reflect non-neuronal cellular changes, for example involving the glia? Furthermore, our observations highlight the broader issue that it is not yet clear what pathological processes do account for the volume or other MRI-based changes that may be witnessed in the presymptomatic phase of AD. Whilst there are numerous clinicopathological studies correlating atrophy on MRI with neuronal loss, Braak neurofibrillary tangle stage and tau burden in patients with established symptomatic AD (Zarow *et al.*, 2005, Whitwell *et al.*, 2008) this information is lacking for the presymptomatic stage. Various different processes may give rise to changes in the volume of brain structures, some of which may be dynamic. There may potentially be both increases in volume (for example, relating to inflammation) and decreases in volume (for example, due to neuronal loss), and this uncertainty should be taken into account in hypothetical biomarker models of presymptomatic AD.

I speculate in chapter 6 that axonal injury and subsequent degeneration may account for the thalamic and caudate atrophy observed in our cohort of presymptomatic mutation carriers. Support for this hypothesis came from the associated changes in diffusivity indices found in these subcortical grey matter structures and in the cingulum and from one of the few autopsy studies to have specifically examined the thalamus in AD (Xuereb *et al.*, 1991). Xuereb et al. noted that, although there was significant loss of thalamic volume in cases with Alzheimer's disease, the amount of neuronal loss was

insufficient to account for the degree of atrophy. They suggested that the atrophy must instead be due to loss of axons, dendrites and synaptic structures or to glial cell changes. In the Discussion of chapter 6, I mainly focused on the potential role that axonal degeneration may play in the development of subcortical atrophy. However, it is also important to consider the possibility that glial cell changes may contribute to the volumetric MRI changes evident in presymptomatic FAD. Studies in a triple transgenic mouse model of AD have revealed complex changes in astroglial morphology during the early stages of the disease. Prior to the appearance of neuritic amyloid plaques hippocampal astrocytes have been observed to undergo atrophy, but once the plaques arise, those in close vicinity become gliotic whilst those further away remain atrophied (Olabarria *et al.*, 2010). One can envisage that altering glial numbers or morphology might be reflected in dynamic changes in the volume and diffusion characteristics of the affected brain structures when studied with MRI at different time-points in the presymptomatic stage. If immune-mediated mechanisms do play a role that is reflected in dynamic regional brain volume changes this could therefore potentially explain the contrasting findings from a previous study of caudate enlargement in presymptomatic FAD mutation carriers (Fortea *et al.*, 2010). A recent longitudinal multitracer PET imaging study of FAD mutation carriers offers some indirect support for this idea (Rodriguez-Vieitez *et al.*, 2016). Astrocytosis was measured using the PET tracer ^{11}C-deuterium-L-deprenyl (^{11}C-DED), which binds specifically to monoamine oxidase B (MAOB) located primarily in activated astrocytes. In this study, striatal amyloid deposition detected using PIB-PET imaging was evident approximately 17 years prior to expected age at symptom onset in mutation carriers, with astrocytosis significantly elevated around this time. With disease progression, there was an increase in amyloid deposition accompanied by a decline in astrocytosis, with the steepest decline in astrocytosis observed in the caudate and thalamus (Rodriguez-Vieitez *et al.*, 2016).

Another important question that follows on from our work is how specific to the autosomal dominant familial form of AD are early striatal and thalamic imaging changes and, if they are not such a feature of sporadic AD, what may these differences in the topography of pathology teach us about differences in the underlying disease process? It is logistically harder to study the preclinical stage of sporadic AD as individuals who will go on to develop the disease could not, until recently, be identified with a high degree of certainty. However, some studies of MCI patients who

subsequently converted to AD have demonstrated atrophy of the thalamus (Morbelli *et al.*, 2010, Dukart *et al.*, 2013) or caudate (Liu *et al.*, 2010, Madsen *et al.*, 2010), but at a stage when volume loss involving the hippocampus and/or parahippocampal cortex was also evident. Similarly, striatal amyloid deposition has been seen on PIB-PET imaging of MCI patients who subsequently converted to AD (Koivunen *et al.*, 2011, Koivunen *et al.*, 2012) and of cognitively normal *APOE*4 carriers with a family history of AD (Reiman *et al.*, 2009), but the striatal deposition has not appeared to be more prominent than the amyloid deposition also observed in cortical areas in these subjects. In contrast, individuals with Down syndrome, who invariably develop AD pathology if they live long enough, have been found to have prominent early striatal amyloid deposition on PIB-PET imaging (Handen *et al.*, 2012, Lao *et al.*, 2016). In Down syndrome, the striatum is the first brain region to become PIB-positive, at around 40 years of age, and the appearance of abnormal PIB retention is strongly associated with cognitive decline (Annus *et al.*, 2016). The long period of latency between the appearance of striatal amyloid and the onset of clinical symptoms seen in FAD due to autosomal dominant mutations may be reduced in Down syndrome, and it has been speculated that this may relate to reduced cognitive reserve in these individuals (Annus *et al.*, 2016).

In FAD due to autosomal dominantly inherited mutations and Down syndrome the presumed shared mechanism of amyloid deposition is overproduction of longer aggregation-prone species of Aβ, whereas impaired clearance may be a more relevant mechanism in sporadic AD. The striatal predominance on amyloid imaging studies of FAD and Down syndrome but not sporadic AD suggests that the striatum may be particularly vulnerable to developing amyloid deposition in conditions of overproduction. To investigate this issue, enzyme-linked immunosorbent assays (ELISA) have been used to assess the regional distribution of Aβ accumulation and molecules related to Aβ metabolism in post-mortem brain tissue from individuals with familial and sporadic AD (Shinohara *et al.*, 2014). This study found that there was disproportionate accumulation of $A\beta_{42}$ in subcortical areas in FAD compared with sporadic AD and that in FAD, the regional pattern of $A\beta_{42}$ deposition correlated with the normal distribution of APP and β-C-terminal fragment of APP. Disproportionate accumulation of tau was also observed in the striatum in FAD compared with sporadic AD. As the authors of this study speculate, this may suggest that the regional

distribution of APP and its processing drives the disproportionate subcortical accumulation of $A\beta_{42}$ and subsequently tau in FAD (Shinohara *et al.*, 2014).

There have been relatively few detailed histopathological studies of thalamic and striatal involvement in AD. Those that have focussed on the thalamus have shown that extracellular amyloid deposits are observed in almost all thalamic nuclei and that the thalamus undergoes significant atrophy in AD, but that the only nucleus to show striking nerve cell loss is the anterodorsal nucleus (Braak and Braak, 1991, Xuereb *et al.*, 1991). In addition to being the only thalamic nucleus to show nerve cell loss, the anterodorsal nucleus appears to be the most severely affected by neurofibrillary tangles. This nucleus receives its main input from the subiculum; both directly through the fornix and indirectly via the mamillothalamic tract, it projects to the retrosplenial limbic area, which in turn projects to the presubiculum. The entorhinal region receives presubicular inputs and itself projects to the hippocampus. The anterodorsal nucleus therefore occupies a central role in the so-called circuit of Papez. A key unresolved question for future research is what renders the neurons in this network vulnerable to AD and, in the case of the thalamus, why does neurofibrillary tangle formation and cell loss only occur in certain nuclei when amyloid deposits are seen so diffusely? Recent work has demonstrated further how the pattern of neurofibrillary tangle pathology in the thalamus reflects the nuclei with reciprocal projections to the hippocampus and in fact mirrors the distribution of cytoskeletal pathology in interconnected cortical areas (Rub *et al.*, 2016). Limbic nuclei of the thalamus were consistently found to have severe tau immunoreactive cytoskeletal pathology in AD, whilst nuclei involved in associative networks were only mildly affected and motor and sensory nuclei tended to be spared (Rub *et al.*, 2016). Studies of the striatum have also found that regions connected with the limbic system seem to be particularly vulnerable to AD pathology. Amyloid deposits are abundant in the striatum of AD patients but are mainly diffuse and non-neuritic (Braak and Braak, 1990). The density of diffuse plaques has been found to be consistently higher in the caudal putamen, which connects with limbic and prefrontal regions, than in the rostral putamen, which receives input from sensorimotor cortex (Brilliant *et al.*, 1997). Compact amyloid deposits and dystrophic neurites, when present, tend to be concentrated in the ventral striatum, which receives dense projections from the amygdala and hippocampus (Suenaga *et al.*, 1990).

7.3 White matter involvement in familial Alzheimer's disease

Observations from post-mortem studies add support to the idea that AD should perhaps be viewed as a network disorder in which there is selective degeneration of vulnerable neuronal circuits, with critical involvement of the limbic thalamus (Aggleton *et al.*, 2016). The notion that neurodegenerative diseases result from disintegration of distributed neural networks is a popular theme in contemporary neuroscience. The term 'molecular nexopathy' has been proposed to describe the conjunction of pathogenic protein and intrinsic network characteristics that may give rise to the specific network involvement of different neurodegenerative diseases (Warren *et al.*, 2013). According to this paradigm, pathogenic proteins may promote degeneration of a neuronal network by a variety of different mechanisms including disrupting the function or maintenance of synapses, disturbing axonal transport or repair and interfering with cellular signalling or trophic support. The resulting disease effects depend on specific characteristics of the network involved, such as patterns of protein expression or the nature of interactions across neuronal circuits. For example, short-range dendritic or interneuronal connections may be particularly vulnerable to certain molecular insults whilst long-range widely distributed projections may be more sensitive to others. Long-coursing white matter tracts appear to be particularly sensitive to defects in axonal transport and it has been shown in transgenic animal models that intraneuronal accumulation of Aβ not only triggers neuronal loss but also causes an axonopathy with disturbed neuronal trafficking, which is apparent even when signs of tau pathology are absent (Wirths *et al.*, 2006). White matter tract degeneration may therefore be an early event in AD pathogenesis; a hypothesis that is supported by our finding of altered diffusivity in the cingulum in presymptomatic *PSEN1* mutation carriers, reported in chapter 6 (Ryan *et al.*, 2013). Altered white matter integrity has also been found in cognitively normal individuals who have evidence of presymptomatic amyloid pathology: amyloid deposition on PIB-PET imaging (Rieckmann *et al.*, 2016) or reduced CSF $A\beta_{42}$ (Molinuevo *et al.*, 2014). A variety of different mechanisms may contribute to white matter damage in AD, including neuroinflammation, microvascular changes and Wallerian degeneration. The relative importance of these different processes and the temporal relationship between degeneration of grey matter regions and their associated white matter tracts is still a matter of debate. What is clear, however, is that AD is not

exclusively a grey matter disease and that white matter degeneration is a feature of both familial and sporadic AD. Furthermore, microstructural damage to the white matter revealed by DTI typically appears to be far more extensive than may be expected based on the degree of cortical atrophy (Caso *et al.*, 2015, Caso *et al.*, 2016).

With increased appreciation of the importance of white matter pathology, there has been growing interest in the role of white matter hyperintensities (WMH) in the disease. It has long been recognised that WMH on MRI are associated with increased risk, and progression, of AD in sporadic disease, although typically they are thought to reflect atherosclerotic small vessel disease and had historically been presumed to contribute to cognitive impairment in an independent albeit additive manner. However, the study described in chapter 4 of this thesis contributes to a growing body of evidence that WMH can reflect AD pathology (Ryan *et al.*, 2015). Further supporting this notion, a large study from the Dominantly Inherited Alzheimer Network (DIAN) has recently reported greater WMH burden (volume of WMH) in FAD mutation carriers; WMH burden appears to increase around six years prior to expected age at symptom onset (Lee *et al.*, 2016). As in our data, these effects were most prominent in the parietal and occipital lobes, raising the possibility that they reflect CAA, which shows a predilection for posterior brain regions. The precise pathological basis for WMH in CAA remains undetermined and is likely heterogeneous. As the increased signal on T2 or FLAIR MRI that accounts for WMH simply represents an increase in free tissue water content, it may have a variety of pathological substrates, including loss of axons and myelin, dilated perivascular spaces and gliosis. One hypothesis is that WMH arise because damage to small medullary perforating arteries results in ischaemic injury and blood-brain barrier breakdown in the vulnerable deep white matter regions that they supply. Another explanation that has been proposed is that WMH reflect impaired perivascular drainage of interstitial fluid from the white matter, due to deposition of Aβ in the basement membranes of cerebral arteries (Weller *et al.*, 2015). APOE is thought to act as a transport molecule for Aβ and there is some evidence that Aβ transport along perivascular pathways is less efficient in the presence of APOE4 than APOE3 (Hawkes *et al.*, 2012), potentially explaining why *APOE*4 carriers appear to have more severe CAA and are therefore more susceptible to side-effects from therapeutic efforts to remove Aβ from the brain.

7.4 Heterogeneity in the familial Alzheimer's disease phenotype

Interest in how genetic variability within FAD influences heterogeneity in the neuropathological, imaging and clinical manifestations of the disease has emerged as a central theme of this thesis. One of the benefits of studying individuals with FAD is that, as they are generally young, they tend not to have major co-morbidities or significant cerebrovascular disease due to conventional vascular risk factors, which can impact upon the clinical presentation. One therefore has the opportunity to study "pure" disease, and phenotypic differences observed between carriers of different mutation types may offer genuine insights into differences in underlying disease mechanism. For example, a striking difference that we observed in the clinical phenotype of FAD due to autosomal dominant *APP* and *PSEN1* mutations was that spastic paraparesis only appears to develop in association with *PSEN1* mutations. This was the case in the study of our FAD cohort reported in chapter 3 of this thesis (Ryan *et al.*, 2016) and also in a systematic review of the world literature (Shea *et al.*, 2015). *APP* and *PSEN1* mutations share a common underlying disease mechanism of causing qualitative shifts in the Aβ profiles generated from APP and, if this process underpinned the pathogenesis of spastic paraparesis, one might expect that this neurological sign would sometimes be seen in the context of *APP* mutations. On the other hand, some mutations in *PSEN1* (but not *APP*) appear to affect processing of substrates in addition to APP (Chavez-Gutierrez *et al.*, 2012) so a possible hypothesis for the specific association of spastic paraparesis with *PSEN1* mutations is that it results from effects of *PSEN1* mutations on substrates other than APP. Our observation that spastic paraparesis shows a particular association with mutations involving exon 8 of *PSEN1* further supports this idea as the residues encoded by exon 8 lie in the region of PSEN1 where the cleavage site processed by autocatalytic activity resides. Additional substrates of PSEN1, such as Notch, N-cadherin, ErbB4 and the B cell maturation antigen (BCMA), are involved in diverse physiological processes including myelination, vascular and immune function. Perturbation of the processing of these additional substrates in the context of a PSEN1 mutation could, therefore, well be envisaged to have detrimental effects upon the white matter.

7.5 Limitations

In drawing conclusions from the work presented in this thesis, it is important to consider potential limitations of the studies undertaken. In chapter 3 I investigated the clinical phenotype of autosomal dominant FAD in a large UK case series, which included patient data gathered since identification of the first mutation over 25 years ago. Although this is, to our knowledge, one of the largest single centre studies of FAD, which included families recruited from across the UK and Ireland, it is possible that some atypical phenotypes may not have been seen due to ascertainment issues. As our clinical and research centre specialises in young onset dementia, we may not have been referred individuals with more atypical phenotypes such as presentation with movement disorders, stroke or late onset cognitive symptoms. Nonetheless, having demonstrated the wide clinical spectrum of familial Alzheimer's disease (Ryan *et al.*, 2016), we hope that our work will contribute to increased awareness amongst clinicians of the possible atypical presentations of the disease. With increased genetic testing for FAD mutations in patients with atypical dementia syndromes, we may find that the phenotype broadens further.

An important limitation of the imaging studies reported in this thesis was the relatively small number of subjects, particularly for the studies that utilised newer MR acquisitions of T2*-GRE and diffusion tensor imaging. This is an inevitable issue when studying a rare genetic condition and is the motivation for our current international collaboration with other centres in the DIAN study. Despite the small number of subjects, the imaging studies reported in this thesis have demonstrated a number of insights into FAD, which have subsequently been replicated in larger studies utilising DIAN data. Our finding of presymptomatic thalamic atrophy, reported in chapter 6 (Ryan *et al.*, 2013), was followed by a voxel-based morphometry study of the DIAN cohort demonstrating a trend for decreased grey matter in the thalamus for mutation carriers closer to their expected age at onset (Cash *et al.*, 2013). Both of these studies have the limitation that parental age at onset was used to estimate how far from symptom onset the mutation carriers were. Although age at onset does correlate with parental age at onset, there can be substantial variation in some families (Ryman *et al.*, 2014), so it is important to remember that this metric does only provide an estimate of

how far through the preclinical stage an individual is at the time of scanning. Longitudinal studies that follow mutation carriers long enough to ascertain their actual age at symptom onset will be important to understand the time course of presymptomatic volumetric changes in more detail. The other finding reported in this thesis (chapter 4), which has subsequently been replicated in DIAN data, is that autosomal dominant FAD can be associated with prominent white matter hyperintensities (WMH), particularly in a parieto-occipital distribution (Ryan *et al.*, 2015, Lee *et al.*, 2016). Our study was a retrospective analysis of all FAD mutation carriers who had undergone appropriate imaging for the assessment of WMH. As this included data collected over a long period of time, a limitation was that there was some variability in the scanning sequences used. However, a strength was that some of the more historical cases had subsequently undergone post-mortem examination, allowing correlation of imaging and pathological features.

7.6 Clinical implications

Research reported in this thesis has a number of important clinical implications. Our observation of the wide clinical spectrum of autosomal dominant FAD, presented in chapter 3, highlights the importance for clinicians of considering genetic testing in young patients with dementia and additional neurological features, particularly when there is a family history or when the family history is censored. Furthermore, our findings reported in chapter 4 indicate that the appearance of prominent WMH on imaging should alert a clinician to the possibility of FAD, particularly if vascular risk factors are lacking. As discussed in chapter 5, MRI with gradient echo (T2*-GRE) sequences can provide valuable additional information in the investigation of patients with young onset dementia as the presence of cortical microbleeds may indicate that there is underlying CAA and that testing for FAD mutations is warranted. However, as microbleeds only appear to be present in around 25% of patients with familial or sporadic AD, their absence should not dissuade a clinician from making a diagnosis of AD.

Findings presented in this thesis also highlight some potential problems that may arise in patients with established FAD, which clinicians should be aware of in order to allow

appropriate investigation and management. Seizures were found to be relatively common, affecting around a quarter of individuals with *APP* or *PSEN1* mutations in our cohort. In both genetic groups, individuals with myoclonus were significantly more likely to develop seizures than those without myoclonus, highlighting the importance of being vigilant for symptoms of seizure activity when myoclonus is present. In chapter 5, I reported a case of ARIA-E arising during the course of FAD and argued that these imaging changes may have reflected the development of CAA-related inflammation (CAA-ri), and that this should be further evaluated as a possible cause of sub-acute deterioration in patients with established AD. Recent work focussed on characterising patients with the spontaneously occurring condition CAA-ri has validated clinico-radiological criteria and emphasised the importance of making this diagnosis in clinical practice due to the high response rate to prompt immunosuppressive treatment (Auriel *et al.*, 2016). An important direction for future research will be to investigate possible areas of overlap and difference in the pathogenic mechanisms underlying CAA-ri and the ARIA that have been observed in AD immunotherapy trials and, more rarely, have arisen spontaneously during the natural history of sporadic or familial AD.

Finally, our imaging findings of early thalamic atrophy and white matter involvement in FAD may have clinical implications regarding the neuropsychological tests that are used in clinical and research assessments of individuals at risk of FAD. The imaging evidence that these areas of the brain undergo changes during the presymptomatic phase indicates that sensitive assessment of the cognitive functions they subserve may be needed in order to detect subtle signs of clinical impairment. In this context, it is noteworthy that a study reporting the baseline neuropsychological characteristics of individuals in the DIAN study found that performance by cognitively normal mutation carriers who were closer to their expected age of symptom onset was poorer on both immediate and delayed recall of logical memory, the digit symbol test and the switch block of trials from a test of attention (Storandt *et al.*, 2014). These test scores may be capturing subtle deficits in episodic memory, speed of cognition and executive function respectively, perhaps reflecting early pathological involvement of subcortical regions and/or white matter in addition to the hippocampus. In further work, it would be interesting to investigate potential correlations between these separate neuropsychological tests scores and different imaging measures such as hippocampal, thalamic and WMH volume and DTI metrics. Reliable automated methods for

segmenting WMH have now been developed (Sudre *et al.*, 2015), and it is increasingly feasible to analyse longitudinal data quantitatively in order to study the relationship between WMH accrual and the progression of regional brain volume and cognitive changes in presymptomatic FAD.

7.7 Directions for future research

Work reported in this thesis opens up a number of different avenues for future research. From an imaging perspective, it would of great interest to further investigate the thalamic atrophy we observed in presymptomatic FAD mutation carriers by examining whether volume loss is driven by loss of grey or white matter and whether specific nuclei show differential involvement on imaging, as has been indicated by studies of post-mortem tissue. Advances are being made in multi-modal segmentation techniques, which incorporate information from both T1 MRI and diffusion-weighted imaging, in order to segment and parcellate structures of interest like the thalamus and it's constituent nuclei and white matter tracts (Stough *et al.*, 2014). Furthermore, advanced diffusion MRI techniques such as neurite orientation dispersion and density imaging (NODDI) are allowing the microstructural complexity of neurites to be probed in greater detail (Zhang *et al.*, 2012). Applying such methods to the study of presymptomatic FAD would be an exciting direction for future research. This would be particularly informative if the same participants were to also undergo molecular imaging of amyloid and tau deposition using PET. Insights into the temporal and spatial relationships between amyloid and tau deposition in presymptomatic FAD will be anxiously awaited by the field. Ultimately, it is likely to be the longitudinal analysis of multiple time-point multimodal data and ascertainment of rates of change that will reveal the most information about underlying pathological mechanisms.

Further investigation of the neuropathological and molecular mechanisms underlying phenotypic variability between different mutations is another important direction for future work. Forty-three FAD patients from families assessed at the Dementia Research Centre have now come to post-mortem, providing a unique opportunity to investigate neuropathological underpinnings of phenotypic heterogeneity. We plan to assess how the severity and type of amyloid plaque

(cored, diffuse and cotton wool), CAA (cortical and leptomeningeal), tau pathology, white matter degeneration (axonal loss and demyelination) and microglial response varies between different *PSEN1* and *APP* mutations and whether these pathological features associate with particular mutation positions, *APOE* genotypes, disease duration, age at symptom onset and specific neurological features such as spastic paraparesis. It will also be of interest to analyse whether different plaque species observed in FAD are associated with specific Aβ isoform profiles, whether these vary between different brain regions and how they relate to clinical presentation.

Future studies of the molecular mechanisms involved in FAD will be aided by, and may further inform, recent developments in our understanding of the function and atomic structure of gamma-secretase (Bai *et al.*, 2015, Szaruga *et al.*, 2015). In chapter 3, our exploration of clinical heterogeneity between different *PSEN1* mutations suggested that mutation position may have an influence on phenotype. Particularly early ages at onset were observed for a cluster of mutations before codon 200 involving PSEN1's first hydrophilic loop, which is known to contribute to the carboxypeptidase-like activity of PSEN1 that alters Aβ profiles. Mapping mutations to the 3-dimensional structure of PSEN1 could extend these observations further. This would allow visualisation of whether mutations associated with particularly early onset of disease do indeed involve the site where Aβ undergoes successive carboxypeptidase cleavages when the protein takes up its 3-dimensional conformation. We also found that atypical cognitive presentations and spastic paraparesis were associated with *PSEN1* mutations beyond codon 200, particularly involving exon 8. I speculated that this may relate to involvement of this region of PSEN1 in the endopeptidase activity of gamma-secretase, which processes APP and a variety of substrates. In future experimental work, this hypothesis could be tested by analysing how different *PSEN1* mutations impact upon gamma-secretase processing of a variety of substrates. Detergent resistant membranes (DRMs) prepared from brain tissue are a source of gamma-secretase for in vitro activity assays where, importantly, the lipid composition of its native environment (the membrane) is maintained. Analysing gamma-secretase activity in brain tissue from individuals who manifested specific phenotypic features during life may therefore offer valuable insights into how different mutations alter processing of APP and

other substrates (Szaruga *et al.*, 2015). Gamma-secretase processing can also be analysed in DRMs extracted from induced pluripotent stem cell-derived neurons, which have been generated from patient fibroblasts. We have been developing a unique resource of skin biopsies harvested from individuals with FAD mutations to establish fibroblast cell lines carrying specific *PSEN1* and *APP* mutations (Wray *et al.*, 2012). This will allow future investigation of numerous processes, including differential Aβ isoform production and gamma-secretase processing of substrates involved in myelin repair, vascular and immune function in cells derived from FAD patients with specific clinical and pathological features.

7.8 Implications for clinical trials

As discussed in the opening chapter of this thesis, FAD families have played a profound role in shaping the concept of AD that exists today, with the discovery of an *APP* mutation as the first genetic cause of AD contributing to the "amyloid cascade hypothesis" of AD pathogenesis (Ryan *et al.*, 2015). However, as also discussed in chapter 1, concepts of disease are dynamic and constantly evolving; influenced by developments in the forms of knowledge and technology available at the time and by the objectives of the various groups in society who are interested in a disease. The amyloid cascade hypothesis, which posits that Aβ accumulation is the initiating event in AD pathogenesis and direct cause of progressive neurodegeneration, has provided the main theoretical foundation for AD research for over 20 years. It has also motivated, and continued to justify, ongoing efforts by the pharmaceutical industry to develop drugs targeting Aβ, with the hope that removing Aβ from the brain may slow or prevent neurodegeneration. A series of high profile drug trial failures, most recently of Solanezumab in patients with mild AD, have fostered the view that treatment may need to be extremely early in the disease process in order to be effective and results from the ongoing DIAN-TU (currently of Solanezumab and Gantenerumab in presymptomatic and mildly affected FAD mutation carriers) will be anxiously awaited. With the disappointing results of AD immunotherapy trials, some researchers have urged the field to take a more holistic view of the disease. Arguing that the model provided by the amyloid cascade hypothesis is too linear and neuron-centric, they have called for a shift in focus towards the prodromal "cellular phase of AD", when complex responses and

interactions between neuronal networks, microglia, astroglia, oligodendrocytes and the vasculature allow the brain to compensate for decades until homeostasis can no longer be maintained and the clinical phase of the disease ensues (De Strooper and Karran, 2016). In this view, Aβ and tau accumulation would be considered risk factors; proteopathic stressors that initiate the cellular phase of AD, in which additional cellular factors then determine evolution towards the clinical phase. The hope is that studying AD from this conceptual framework could shed light on new drug targets in addition to Aβ, with the possibility that multiple therapeutic strategies may be needed to address different aspects of the disease.

7.9 Applying findings from familial Alzheimer's disease to sporadic Alzheimer's disease

Some might argue that a theoretical construct for AD that moves focus beyond the amyloid cascade hypothesis might challenge the idea that familial cases represent a paradigm for AD. On the contrary, work presented in this thesis highlights the degree of heterogeneity that exists within FAD and the possible contributions of diverse processes, including white matter degeneration, vascular and immune responses, to clinical presentation. Observations from FAD may not always necessarily generalise to sporadic AD. However, sporadic AD is itself a heterogeneous disease. Gaining insights into the variable mechanisms by which different FAD mutations cause disease may therefore have relevance for understanding clinical and pathological heterogeneity in sporadic AD. It may also have relevance for the interpretation of FAD treatment trials as different mutations may vary in their response to certain therapeutic interventions. Moreover, investigating the influence of genotype on neuropathological, neuroimaging and clinical manifestations of disease may potentially inform our understanding of factors influencing the efficacy, and associated risks, of different treatment strategies in sporadic AD.

In future work, in order to further explore a more holistic conceptualisation of AD that gives prominence to a prodromal "cellular phase", it will be important to study FAD mutation carriers with a variety of biomarkers in addition to amyloid and tau imaging and CSF measures of amyloid and tau. Advances in technology often lay the ground for

new ways of thinking about diseases. For example, DTI is now allowing AD to be studied as a disorder of distributed neuronal networks and, with increasing methodological developments, it may allow us to gain deeper insights into the nature of microstructural change in different cellular compartments. Work described in this thesis has demonstrated how a variety of MRI sequences can shed light on different aspects of AD pathogenesis and multi-modal MRI is likely to continue playing a central role in the investigation of presymptomatic AD. Given that immune and vascular mechanisms appear to be involved in both the early disease process, and in strategies used to combat it with amyloid-immunomodulatory agents, particular effort should perhaps be invested in understanding how such processes can be imaged, and how they affect other imaging biomarkers. A variety of techniques may play a role here including microglial and astrocyte activation studies, as may the insights gained from imaging of animal models. Much valuable work has been done to formulate hypothetical models of AD biomarkers using evidence gathered from studies of sporadic AD, MCI and normal ageing (Jack *et al.*, 2013), but we must keep an open mind to the complex and potentially unpredictable changes that may occur during the prodromal phase of AD. The challenge now is to use longitudinal studies of FAD mutation carriers, combined with insights from neuropathology and molecular biology, to better understand the temporal evolution of biomarker changes during the whole natural history of FAD, so that hypothetical models may be further refined and the optimal time for therapeutic intervention may be guided.

8 Publications

This section details papers that have been published based on the work in this thesis.

Chapter 1. Introduction

Alzheimer's disease in the one hundred years since Alzheimer's death
Ryan NS, Rossor, MN, Fox NC. Brain. 2015 Dec; 138(Pt 12): 3816-21.

Correlating familial Alzheimer's disease gene mutations with clinical phenotype **Ryan NS**, Rossor MN. Biomarkers in Medicine. 2010 Feb; 4(1):99-112.

Chapter 2. Imaging biomarkers in Alzheimer's disease

Imaging biomarkers in Alzheimer's Disease **Ryan NS**, Fox NC. Annals of the New York Academy of Science. 2009 Oct; 1180:20-7.

Imaging presymptomatic Alzheimer's disease. **Ryan NS**, Fox NC, Advances in Clinical Neuroscience and Rehabilitation. 2014 June; V14(2):6-9

Chapter 3. Clinical phenotype and genetic associations in autosomal dominant familial Alzheimer's disease: a case series

Clinical phenotype and genetic associations in autosomal dominant familial Alzheimer's disease: a case series **Ryan NS**, Nicholas JM, Weston PS, Liang Y, Lashley T, Guerreiro R, Adamson G, Kenny J, Beck J, Chavez-Gutierrez L, de Strooper B, Revesz T, Holton J, Mead S, Rossor MN, Fox NC. Lancet Neurology. 2016 Dec; 15(13):1326-1335.

Chapter 4. Genetic determinants of white matter hyperintensities and amyloid angiopathy in familial Alzheimer's disease

Genetic determinants of white matter hyperintensities and amyloid angiopathy in familial Alzheimer's disease. **Ryan NS**, Biessels GJ, Kim L, Nicholas JM, Barber PA, Walsh P, Gami P, Morris HR, Bastos-Leite AJ, Schott JM, Beck J, Mead S, Chavez-Gutierrez L, De Strooper B, Rossor MN, Revesz T, Lashley T, Fox NC. Neurobiol Aging. 2015 Dec; 36(12):3140-51

Chapter 5. Amyloid-related imaging abnormalities (ARIA) in familial Alzheimer's disease

Cerebral microbleeds in familial Alzheimer's disease **Ryan NS**, Bastos-Leite A, Rohrer JD, Werring DJ, Rossor MN, Fox NC, Schott JM. Brain 2012 Jan;135(Pt1):e201.

Spontaneous ARIA (Amyloid-Related Imaging Abnormalities) and Cerebral Amyloid Angiopathy Related Inflammation in Presenilin 1-Associated Familial Alzheimer's Disease. **Ryan NS**, Lashley T, Revesz T, Dantu K, Fox NC, Morris HR. J Alzheimers Dis. 2015; 44(4):1069-74.

Chapter 6. MRI evidence for presymptomatic change in thalamus and caudate in familial Alzheimer's disease

Magnetic resonance imaging evidence for presymptomatic change in thalamus and caudate in familial Alzheimer's disease. **Ryan NS**, Keihaninejad S, Shakespeare TJ, Lehmann M, Crutch SJ, Malone IB, Thornton JS, Mancini L, Hyare H, Yousry T, Ridgway GR, Zhang H, Modat M, Alexander DC, Rossor MN, Ourselin S, Fox NC. Brain. 2013 May;136 (Pt 5):1399-414.

Reply: Implications of presymptomatic change in thalamus and caudate in Alzheimer's disease. **Ryan NS**, Fox NC. Brain. 2013 Jul 3.

Other publications

Other publications that I authored, or contributed to, during the course of my PhD are listed below.

Brain imaging evidence of early involvement of subcortical regions in familial and sporadic Alzheimer's disease. Tentolouris-Piperas V, **Ryan NS**, Thomas DL, Kinnunen KM. Brain Res. 2016 Nov 12. pii: S0006-8993(16)30751-X.

Presymptomatic cortical thinning in familial Alzheimer disease: A longitudinal MRI study. Weston PS, Nicholas JM, Lehmann M, **Ryan NS**, Liang Y, Macpherson K, Modat M, Rossor MN, Schott JM, Ourselin S, Fox NC. Neurology. 2016 Nov 8; 87(19):2050-2057.

White matter hyperintensities are a core feature of Alzheimer's disease: Evidence from the dominantly inherited Alzheimer network. Lee S, Viqar F, Zimmerman ME, Narkhede A, Tosto G, Benzinger TL, Marcus DS, Fagan AM, Goate A, Fox NC, Cairns NJ, Holtzman DM, Buckles V, Ghetti B, McDade E, Martins RN, Saykin AJ, Masters CL, Ringman JM, **Ryan NS**, Förster S, Laske C, Schofield PR, Sperling RA, Salloway S, Correia S, Jack C Jr, Weiner M, Bateman RJ, Morris JC, Mayeux R, Brickman AM; Dominantly Inherited Alzheimer Network. Ann Neurol. 2016 Jun; 79(6):929-39.

Genetic risk factors for the posterior cortical atrophy variant of Alzheimer's disease. Schott JM, Crutch SJ, Carrasquillo MM, Uphill J, Shakespeare TJ, **Ryan NS**, Yong KX, Lehmann M, Ertekin-Taner N, Graff-Radford NR, Boeve BF, Murray ME, Khan QU, Petersen RC, Dickson DW, Knopman DS, Rabinovici GD, Miller BL, González AS, Gil-Néciga E, Snowden JS, Harris J, Pickering-Brown SM, Louwersheimer E, van der Flier WM, Scheltens P, Pijnenburg YA, Galasko D, Sarazin M, Dubois B, Magnin E, Galimberti D, Scarpini E, Cappa SF, Hodges JR, Halliday GM, Bartley L, Carrillo MC, Bras JT, Hardy J, Rossor MN, Collinge J, Fox NC, Mead S. Alzheimers Dement. 2016 Aug; 12(8):862-71.

Gamma-secretase dysfunction in the brains of familial Alzheimer's disease patients. Szaruga M, Veugelen S, Benurwar M, Lismont S, Sepulveda-Falla D, Lleo A, **Ryan**

NS, Lashley T, Fox NC, Murayama S, Gijsen H, De Strooper B, Chavez-Gutierrez L. Journal of Experimental Medicine. 2015 Nov 16; 212(12): 2003-13.

Developmental regulation of tau splicing is disrupted in stem cell-derived neurons from frontotemporal dementia patients with the 10 + 16 splice-site mutation in MAPT. Sposito T, Preza E, Mahoney CJ, Setó-Salvia N, **Ryan NS**, Morris HR, Arber C, Devine MJ, Houlden H, Warner TT, Bushell TJ, Zagnoni M, Kunath T, Livesey FJ, Fox NC, Rossor MN, Hardy J, Wray S. Hum Mol Genet. 2015 Sep 15;24(18):5260-5269.

Diffusion imaging changes in grey matter in Alzheimer's disease: a potential marker of early degeneration. Weston PS, Simpson IJ, **Ryan NS**, Ourselin S, Fox NC, Alzheimer's Res Ther. 2015 Jul:7(1):47.

Abnormalities of fixation, saccade and pursuit in posterior cortical atrophy Shakespeare TJ, Kaski D, Yong KX, Paterson RW, Slattery CF, **Ryan NS**, Schott JM, Crutch SJ. Brain. 2015 Jul;138(Pt 7):1976-91.

Motor features in posterior cortical atrophy and their imaging correlates. **Ryan NS**, Shakespeare TJ, Lehmann M, Keihaninejad S, Nicholas JM, Leung KK, Fox NC, Crutch SJ. Neurobiol Aging. 2014 Dec;35(12):2845-57.

Imaging endpoints for clinical trials in Alzheimer's disease. Cash DM, Rohrer JD, **Ryan NS**, Ourselin S, Fox NC. Alzheimer's Res Ther. 2014 Dec 20;6(9):87.

The pattern of atrophy in familial Alzheimer's disease: Volumetric MRI results from the DIAN study. Cash DM, Ridgway GR, Liang Y, **Ryan NS**, Kinnunen KM, Yeatman T, Malone IB, Benzinger TL, Jack CR Jr, Thompson PM, Ghetti BF, Saykin AJ, Masters CL, Ringman JM, Salloway SP, Schofield PR, Sperling RA, Cairns NJ, Marcus DS, Xiong C, Bateman RJ, Morris JC, Rossor MN, Ourselin S, Fox NC; Dominantly Inherited Alzheimer Network (DIAN). Neurology. 2013 Oct 15;81 (16):1425-33.

Homozygosity for the C9orf72 GGGGCC repeat expansion in frontotemporal dementia. Fratta P, Poulter M, Lashley T, Rohrer JD, Polke JM, Beck J, **Ryan N**, Hensman D,

Mizielinska S, Waite AJ, Lai MC, Gendron TF, Petrucelli L, Fisher EM, Revesz T, Warren JD, Collinge J, Isaacs AM, Mead S. Acta Neuropathol. 2013 Sep;126(3):401-9.

An unbiased longitudinal analysis framework for tracking white matter changes using diffusion tensor imaging with application to Alzheimer's disease. Keihaninejad S, Zhang H, **Ryan NS**, Malone IB, Modat M, Cardoso MJ, Cash DM, Fox NC, Ourselin S. Neuroimage. 2013 May 15;72:153-63.

Genetic influences on atrophy patterns in familial Alzheimer's Disease: a comparison of APP and PSEN1 mutations. Scahill RI, Ridgway GR, Bartlett JW, Barnes J, **Ryan NS**, Mead S, Beck J, Clarkson MJ, Crutch SJ, Schott JM, Ourselin S, Warren JD, Hardy J, Rossor MN, Fox NC. J Alzheimers Dis. 2013 Jan 1;35(1):199-212.

White matter tract signatures of the progressive aphasias Mahoney CJ, Malone IB, Ridgway GR, Buckley AH, Downey LE, Golden HL, **Ryan NS**, Ourselin S, Schott JM, Rossor MN, Fox NC, Warren JD. Neurobiol Aging. 2013 Jun;34(6):1687-99.

Shining a light on posterior cortical atrophy Crutch SJ, Schott JM, Rabinovici GD, Boeve BF, Cappa SF, Dickerson BC, Dubois B, Graff-Radford NR, Krolak-Salmon P, Lehmann M, Mendez MF, Pijnenburg Y, **Ryan NS**, Scheltens P, Shakespeare T, Tang-Wai DF, van der Flier WM, Bain L, Carrillo MC, Fox NC. Alzheimers Dement. 2013 Jul;9(4):463-5.

Imaging the Onset and Progression of Alzheimer's Disease: Implications for Prevention Trials Liang Y, **Ryan NS**, Schott JM, Fox NC. J Alzheimers Dis. 2013;33 Suppl 1:S305-12. Review.

The importance of group-wise registration in tract based spatial statistics study of neurodegeneration: a simulation study in Alzheimer's disease Keihaninejad S, **Ryan NS**, Malone IB, Modat M, Cash D, Ridgway GR, Zhang H, Fox NC, Ourselin S. PLoS One. 2012;7(11).

Creation of an open-access, mutation-defined fibroblast resource for neurological disease research Wray S, Self M; NINDS Parkinson's Disease iPSC Consortium; NINDS Huntington's Disease iPSC Consortium; NINDS ALS iPSC Consortium, Lewis PA, Taanman JW, **Ryan NS**, Mahoney CJ, Liang Y, Devine MJ, Sheerin UM, Houlden H, Morris HR, Healy D, Marti-Masso JF, Preza E, Barker S, Sutherland M, Corriveau RA, D'Andrea M, Schapira AH, Uitti RJ, Guttman M, Opala G, Jasinska-Myga B, Puschmann A, Nilsson C, Espay AJ, Slawek J, Gutmann L, Boeve BF, Boylan K, Stoessl AJ, Ross OA, Maragakis NJ, Van Gerpen J, Gerstenhaber M, Gwinn K, Dawson TM, Isacson O, Marder KS, Clark LN, Przedborski SE, Finkbeiner S, Rothstein JD, Wszolek ZK, Rossor MN, Hardy J. PLoS One. 2012;7(8)

Global gray matter changes in posterior cortical atrophy: A serial imaging study Lehmann M, Barnes J, Ridgway GR, **Ryan NS**, Warrington EK, Crutch SJ, Fox NC. Alzheimers Dement. 2012 Nov;8(6):502-12.

Identifying cortical visual dysfunction in posterior cortical atrophy Shakespeare TJ, **Ryan NS**, Petrushkin H, Crutch SJ. Optometry in Practice 2012: 13(4).

Posterior cerebral atrophy in the absence of medial temporal atrophy in pathologically-confirmed Alzheimer's disease Lehmann M, Koedam EL, Barnes J, Bartlett JW, **Ryan NS**, Pijnenburg Y, Barkhof F, Wattjes M, Scheltens P, Fox NC. Neurobiology of Aging 2012 Mar;33(3):627.

Duplication of amyloid precursor protein (APP) but not prion protein (PRNP) is a significant cause of early onset dementia in a large UK series McNaughton D, Knight W, Guerreiro R, **Ryan N**, Lowe J, Poulter M, Nicholl DJ, Hardy J, Revesz T, Lowe J, Rossor M, Collinge J, Mead S. Neurobiology of Aging. 2012 Feb;33(2):426.e13-21.

Defining and describing the pre-dementia stages of familial Alzheimer's disease **Ryan NS**, Rossor MN. Alzheimers Res Ther. 2011 Sep 27; 3(5):29.

Familial Alzheimer's disease and inherited prion disease in the UK are poorly ascertained Stevens JC, Beck J, Lukic A, **Ryan N,** Abbs S, Collinge J, Fox NC, Mead S. J Neurol Neurosurg Psychiatry. 2011 Sep;82(9):1054-7.

Carbon-11-Pittsburgh compound B positron emission tomography imaging of amyloid deposition in presenilin 1 mutation carriers Knight WD, Okello AA, **Ryan NS,** Turkheimer FE, Rodríguez Martinez de Llano S, Edison P, Douglas J, Fox NC, Brooks DJ, Rossor MN. Brain. 2011 Jan;134(Pt 1):293-300

Abnormal visual phenomena in posterior cortical atrophy Crutch SJ, Lehmann M, Gorgoraptis N, Kaski D, **Ryan N**, Husain M, Warrington EK. Neurocase. 2010 Sep 2:1-18.

Alzheimer Disease: Visual rating of atrophy aids diagnostic accuracy **Ryan NS**, Fox NC. Nature Reviews Neurology. 2009 May; 5(5):243-4.

9 Division of labour

I carried out the work described in this thesis in collaboration with researchers based at the Dementia Research Centre (DRC), at other departments within UCL and at other collaborating institutions. I am grateful to everyone who was involved in this work for their contributions, which are detailed below. Collaborators who were based outside the DRC when the work was carried out are marked with superscript letters and their affiliations are listed on page 174.

NSR, Natalie S Ryan; MNR, Martin N Rossor; NCF, Nick C Fox; PSJW, Philip SJ Weston, YL, Yuying Liang. TL, Tammaryn Lashley[a]; TR, Tamas Revesz[a]; JH, Janice Holton[a]; GA, Gary Adamson[b]; JB, Jon Beck[b]; SM, Simon Mead[b]; JMN, Jennifer M Nicholas; RG, Rita Guerreiro[c]; JK, Janna Kenny[b]; LCG, Lucia Chavez-Gutierrez[d]; BDS, Bart de Strooper[d]; GJB, Geert-Jan Biessels; PAB, Philip A Barber; PW, Phoebe Walsh[a]; PG, Priya Gami[a]; LK, Lois Kim; JMS, Jonathan M Schott, JDR, Jonathan D Rohrer; ABL, Antonio Bastos-Leite; HRM, Huw R Morris[e]; KD, Kiran Dantu[f]; ML, Manja Lehmann; SC, Sebastian Crutch; SK, Shiva Keihaninejad; JST, John S Thornton[g]; LM, Laura Mancini[g]; DCS, Daniel C Alexander[h]; SO, Sebastian Ourselin[h], TJS, Timothy J Shakespeare; HH, Harpreet Hyare[b]; TY, Tarek Yousry[g]; GRR, Gerard R Ridgway[i]; IBM, Ian B Malone, HZ, Hui Zhang[h]; MM, Marc Modat[h].

Chapter 3: Clinical phenotype and genetic associations in autosomal dominant familial Alzheimer's disease: a case series

NSR, MNR and NCF designed the study. NSR, PSJW, YL, MNR and NCF contributed to subject recruitment and clinical assessment. NSR analysed the clinical data. TL, TR and JH analysed the neuropathological data. GA, JB, SM analysed the genetic data. NSR carried out the statistical analysis with support from JMN. NSR, RG, GA, JK, SM, LCG and BDS contributed to interpretation of the genotype and phenotype data. NSR wrote the initial version of the report, all authors contributed to revision and editing of the report.

Chapter 4: Genetic determinants of white matter hyperintensities and amyloid angiopathy in familial Alzheimer's disease

NSR, GJB and NCF designed the study. NSR, MNR and NCF contributed to subject recruitment and clinical assessment. GJB carried out the visual ratings of white matter hyperintensity burden on MRI, blinded to clinical diagnosis. NSR, PAB, PW, PG, TL and TR contributed to analysis of the neuropathological data. NSR, LK and JMN contributed to the statistical analysis. JB and SM analysed the genetic data. NSR wrote the initial version of the report, all authors contributed to revision and editing of the report.

Chapter 5.1: Cerebral microbleeds (ARIA-H) in familial Alzheimer's disease

NSR and JMS designed the study. NSR, JDR and JMS contributed to subject recruitment and data collection. ABL carried out the visual assessment of microbleeds, blinded to clinical diagnosis. NSR analysed the data and wrote the initial version of the report, all authors contributed to revision and editing of the report.

Chapter 5.2: Spontaneous ARIA-E and cerebral amyloid angiopathy related inflammation in *PSEN1*-associated familial Alzheimer's disease

NSR, NCF and HRM conceived of the report. NSR, KD and HRM contributed to clinical assessment and data collection. TL and TR analysed the neuropathological data. NSR wrote the initial version of the report, all authors contributed to revision and editing of the report.

Chapter 6: Magnetic resonance imaging evidence for presymptomatic change in thalamus and caudate in familial Alzheimer's disease.

NSR and NCF designed the study. NSR carried out subject recruitment, clinical assessment and data collection. ML and SC carried out the neuopsychological assessments and analysed the neuropsychological data. JST, LM, DCA and SO contributed to development of the DTI acquisition protocol. NSR, SK, TJS, ML, HH, TY and GRR contributed to analysis of the volumetric MRI data. NSR, SK, IBM, HZ,

MM, DCA and SO contributed to analysis of the DTI data. NSR wrote the initial version of the report, all authors contributed to revision and editing of the report.

a) Queen Square Brain Bank, Department of Molecular Neuroscience, UCL Institute of Neurology
b) MRC Prion Unit, Department of Neurodegenerative Diseases, UCL Institute of Neurology
c) Department of Molecular Neuroscience, UCL Institute of Neurology
d) VIB Center for the Biology of Disease, Leuven and Center for Human Genetics and Leuven Institute for Neurodegenerative Diseases, University of Leuven, Leuven, Belgium.
e) Department of Clinical Neuroscience, UCL Institute of Neurology
f) Department of Old Age Psychiatry, Ysbyty Ystrad Fawr Hospital, Hengoed, Wales
g) Neuroradiological Academic Unit, UCL Institute of Neurology and Lysholm Department of Neuroradiology, National Hospital for Neurology and Neurosurgery, UCLH NHS Foundation Trust
h) Centre for Medical Image Computing, UCL
i) Wellcome Trust Centre for Neuroimaging, UCL Institute of Neurology

10 Acknowledgements

Thank you to all of the people mentioned above for their help with different aspects of the work described in this thesis and in particular to my supervisors Nick Fox and Jason Warren for their continued support. I am grateful to all my colleagues at the DRC who shared their wisdom and expertise with me. I thank my collaborators for assisting with the neuropathological and genetic analyses and for insightful discussions, from which I have learnt so much.

I extend my thanks to present and past staff at the DRC for their contribution to our ongoing longitudinal study of FAD; and to clinical colleagues across the UK for referring patients to this. Above all, I would like to thank all the individuals from families affected by FAD, whose generous participation in research made this work possible. Their dedication was a constant source of inspiration.

I am grateful for the funding I received to carry out this work, from a MRC Clinical Research Training Fellowship and a Brain Exit Fellowship.

Finally, I would like to thank my friends and my family, which has grown with the arrival of my two children since embarking on this PhD. In your very different ways, you have all supported, encouraged and inspired me, and for this I am forever grateful.

11 Appendix

11.1 Neurological presentations of familial Alzheimer's disease

Neurological symptoms and signs occur commonly in FAD and may, more rarely, represent the initial clinical features. This table summarises mutations that were reported to present with neurological features, identified from a literature review undertaken when work towards this thesis began (Ryan and Rossor, 2010).

Clinical Feature	Mutation	Unusual pathology
Seizures and myoclonus	*PSEN1* p.Asn135Ser	
	PSEN1 p.Leu166Pro	
	PSEN1 p.Leu235Pro	
	APP p.Val717Ile	
	APP p.Thr714Ala	
	APP duplication	Cerebral amyloid angiopathy & Lewy body pathology
Spastic paraparesis	*PSEN1* p.Ile83_Met84del	Cotton wool plaques
	PSEN1 Δexon9	Cotton wool plaques
	PSEN1 p.Tyr154Asn	
	PSEN1 p.Phe237Ile	
	PSEN1 p.Val261Phe	
	PSEN1 p.Pro264Leu	Cotton wool plaques
	PSEN1 p.Gly266Ser	
	PSEN1 p.Arg278Lys	
	PSEN1 p.Arg278Thr	
	PSEN1 p.Glu280Gly	Cotton wool plaques
	PSEN1 p.Pro284Leu	Cotton wool plaques
	PSEN1 p.Pro436Gln	Cotton wool plaques

Extrapyramidal signs	*PSEN1* p.Ser170Phe	Lewy body pathology
	PSEN1 p.Gly217Asp	Cotton wool plaques & cerebral amyloid angiopathy
	PSEN1 p.Met223Val	Lewy body pathology
	PSEN1 p.Thr440del	Cotton wool plaques & Lewy body pathology
	PSEN2 p.Ala85Val	Lewy body pathology
Cerebellar signs	*PSEN1* p.Pro117Ala *PSEN1* p.Ser170Phe *PSEN1* p.Glu280Ala	Severe Purkinje cell loss
Focal neurological symptoms & signs	*APP* p.Glu693Gln *APP* p.Ala692Gly	Cerebral amyloid angiopathy with recurrent cerebral haemorrhages

11.2 Genetics methods

Genomic DNA was prepared from peripheral blood leukocytes using a Nucleon BACC3 extraction kit (GE Healthcare). Mutation analysis was done on genomic DNA by direct sequencing of both strands of PCR-amplified coding exons. Primer sequences were designed according to Genbank entries and are available on request. Amplification was done using a standard protocol and PCR products were purified using MicroClean (Microzone). Sequencing reactions were carried out using the BigDye® Terminator v1.1 Cycle Sequencing Kit (Life Technologies) the products were run out on the 3730xl DNA Analyzer (Life Technologies). Confirmation of missense mutations was carried out by differential enzymatic restriction digests, by an allele discrimination method using TaqMan 5' nuclease assay (Life Technologies) or by allele-specific oligo hybridisation.

Cases that were found to have novel variants in *PSEN1* or *APP* were then assessed for the presence of additional mutations in other dementia related genes using the Ion Torrent Dementia Chip. For this, sequencing was carried out using Ion Torrent(tm)

technology (Thermo Fisher Scientific): A custom primer panel was designed using Ion AmpliSeq(tm) Designer comprising 17 dementia related genes including exon flanking regions and some untranslated sequence. Sample libraries were prepared using Ion AmpliSeq(tm) kits, transferred to the Ion OneTouch(tm) 2 system for template preparation (emulsion PCR) and then sequenced using the Personal Genome Machine(r) System. Assessment of C9orf72 gene expansions and alteration of the octapeptide repeat motif of PRNP was carried out by repeat-primed PCR and DNA size fractionation respectively.

List of sequenced genes:

APP
*C9ORF72**
CHMP2B
CSF1R
FUS
GRN
ITM2B
MAPT
NOTCH3
PRNP
PSEN1
PSEN2
SERPINI1
SQSTM1
TARDBP
TREM2
TYROBP
VCP

*Gene not sequenced but simply assessed for expansions using repeat-primed PCR.

11.3 Immunohistochemical methods in the pathology cohort

Paraffin sections were dewaxed in xylene. Endogenous peroxidase activity was blocked with 0.3% H_2O_2 in methanol and non-specific binding with 10% dried milk solution. Immunohistochemistry required pressure cooker pretreatment in citrate buffer (pH 6.0) for all antibodies unless otherwise stated. Tissue sections were incubated with the primary antibodies for one hour at room temperature, followed by biotinylated anti-rabbit IgG (1:200, 30 min; Dako) or biotinylated anti-mouse IgG (1:200, 30 min; Dako) and Avidin–biotin complex (30 min; Dako). Colour was developed with di-aminobenzidine/H_2O_2. Antibodies to the following proteins were used: amyloid-β (Aβ) (Dako, 1:100), requiring formic acid pretreatment before pressure cooking; tau (AT8 clone; Autogen Bioclear, 1:600); Iba1 (Wako, 1:1000); glial fibrillary acidic protein (Dako, 1:1000); Myelin Basic Protein (MBP, Covance, 1:500) and RT-97 (Vector, 1:20), CD3 (Dako, 1:100); CD20 (Dako, 1:200) and CD68 (Dako, 1:150). Sections were also stained with routine haematoxylin and eosin (HE) stains to evaluate any structural or cellular abnormalities in the cases being examined.

11.4 Grading system used to assess severity of cerebral amyloid angiopathy

Score 0 was given to vessels devoid of amyloid deposition, while score 1 reflected trace to scattered distribution of amyloid in leptomeningeal or cortical blood vessels. A score of 2 indicated that at least some vessels demonstrated circumferential amyloid deposition. A score of 3 corresponded to widespread, circumferential staining of many leptomeningeal and superficial cortical vessels. A score of 4 indicated severe amyloid deposition accompanied by projection of amyloid into the adjacent parenchyma or the presence of amyloid deposition in capillaries (Olichney *et al.*, 1996). The severity of CAA was graded in frontal, temporal, parietal and occipital cortex and cerebellum.

11.5 Semi-quantitative assessment of myelin loss, gliosis and microglial expression.

The deep white matter in the occipital and parietal lobes were semi-quantitatively assessed for white matter pallor, gliosis and microglial expression, through examination by eye down the microscope. This was based on a four-tier grading system where ‘0’ represented no change in the white matter, no gliosis or microglial activation; ‘+’

represented mild pallor of the white matter, mild gliosis and the minimal presence of activated microglia (Figure 4.3,K); '++' represented a moderate degree of white matter pallor, gliosis and microglial activation (Figure 4.3, L); '+++' represents severe pallor of the white matter, severe gliosis and severe microglial activation; '++++' represents very severe microglial activation where the majority of the microglial cells are highlighted using immunohistochemical methods (Figure 4.3, M).

12 Bibliography

Websites

[1] https://yougov.co.uk/news/2015/07/26/alzheimers-greatest-concern-over-60s/
[2] http://www.molgen.ua.ac.be/admutations/
[3] https://www.gov.uk/government/publications/living-well-with-dementia-a-national-dementia-strategy
[4] https://www.nice.org.uk/guidance/cg42

Reference List

Acosta-Cabronero J, Williams GB, Pengas G, Nestor PJ. Absolute diffusivities define the landscape of white matter degeneration in Alzheimer's disease. Brain. 2010;133(Pt 2):529-39.

Aggleton JP, Pralus A, Nelson AJ, Hornberger M. Thalamic pathology and memory loss in early Alzheimer's disease: moving the focus from the medial temporal lobe to Papez circuit. Brain. 2016;139(Pt 7):1877-90.

Alafuzoff I, Thal DR, Arzberger T, Bogdanovic N, Al Sarraj S, Bodi I, et al. Assessment of beta-amyloid deposits in human brain: a study of the BrainNet Europe Consortium. Acta Neuropathol. 2009;117(3):309-20.

Albert MS, DeKosky ST, Dickson D, Dubois B, Feldman HH, Fox NC, et al. The diagnosis of mild cognitive impairment due to Alzheimer's disease: recommendations from the National Institute on Aging-Alzheimer's Association workgroups on diagnostic guidelines for Alzheimer's disease. AlzheimersDement. 2011;7(3):270-9.

Albert MS, DeKosky ST, Dickson D, Dubois B, Feldman HH, Fox NC, et al. The diagnosis of mild cognitive impairment due to Alzheimer's disease: recommendations from the National Institute on Aging-Alzheimer's Association workgroups on diagnostic

guidelines for Alzheimer's disease. Alzheimer's & dementia : the journal of the Alzheimer's Association. 2011;7(3):270-9.

Amtul Z, Lewis PA, Piper S, Crook R, Baker M, Findlay K, et al. A presenilin 1 mutation associated with familial frontotemporal dementia inhibits gamma-secretase cleavage of APP and notch. Neurobiol Dis. 2002;9(2):269-73.

Anheim M, Hannequin D, Boulay C, Martin C, Campion D, Tranchant C. Ataxic variant of Alzheimer's disease caused by Pro117Ala PSEN1 mutation. J Neurol Neurosurg Psychiatry. 2007;78(12):1414-5.

Annus T, Wilson LR, Hong YT, Acosta-Cabronero J, Fryer TD, Cardenas-Blanco A, et al. The pattern of amyloid accumulation in the brains of adults with Down syndrome. Alzheimer's & dementia : the journal of the Alzheimer's Association. 2016;12(5):538-45.

Arvanitakis Z, Leurgans SE, Wang Z, Wilson RS, Bennett DA, Schneider JA. Cerebral amyloid angiopathy pathology and cognitive domains in older persons. Ann Neurol. 2011;69(2):320-7.

Ashburner J. A fast diffeomorphic image registration algorithm. Neuroimage. 2007;38(1):95-113.

Ashburner J, Friston KJ. Computing average shaped tissue probability templates. Neuroimage. 2009;45(2):333-41.

Assini A, Terreni L, Borghi R, Giliberto L, Piccini A, Loqui D, et al. Pure spastic paraparesis associated with a novel presenilin 1 R278K mutation. Neurology. 2003;60(1):150.

Auriel E, Charidimou A, Gurol ME, Ni J, Van Etten ES, Martinez-Ramirez S, et al. Validation of Clinicoradiological Criteria for the Diagnosis of Cerebral Amyloid Angiopathy-Related Inflammation. JAMA neurology. 2016;73(2):197-202.

Bai XC, Yan C, Yang G, Lu P, Ma D, Sun L, et al. An atomic structure of human gamma-secretase. Nature. 2015;525(7568):212-7.

Balasa M, Gelpi E, Antonell A, Rey MJ, Sanchez-Valle R, Molinuevo JL, et al. Clinical features and APOE genotype of pathologically proven early-onset Alzheimer disease. Neurology. 2011;76(20):1720-5.

Barakos J, Sperling R, Salloway S, Jack C, Gass A, Fiebach JB, et al. MR imaging features of amyloid-related imaging abnormalities. AJNR American journal of neuroradiology. 2013;34(10):1958-65.

Barkhof F, Daams M, Scheltens P, Brashear HR, Arrighi HM, Bechten A, et al. An MRI rating scale for amyloid-related imaging abnormalities with edema or effusion. AJNR American journal of neuroradiology. 2013;34(8):1550-5.

Basser PJ, Mattiello J, LeBihan D. MR diffusion tensor spectroscopy and imaging. Biophysical journal. 1994;66(1):259-67.

Basun H, Bogdanovic N, Ingelsson M, Almkvist O, Naslund J, Axelman K, et al. Clinical and neuropathological features of the arctic APP gene mutation causing early-onset Alzheimer disease. Arch Neurol. 2008;65(4):499-505.

Bateman RJ, Aisen PS, De Strooper B, Fox NC, Lemere CA, Ringman JM, et al. Autosomal-dominant Alzheimer's disease: a review and proposal for the prevention of Alzheimer's disease. AlzheimersResTher. 2011;3(1):1.

Bateman RJ, Xiong C, Benzinger TL, Fagan AM, Goate A, Fox NC, et al. Clinical and biomarker changes in dominantly inherited Alzheimer's disease. The New England journal of medicine. 2012;367(9):795-804.

Beck JA, Poulter M, Campbell TA, Uphill JB, Adamson G, Geddes JF, et al. Somatic and germline mosaicism in sporadic early-onset Alzheimer's disease. HumMolGenet. 2004;13(12):1219-24.

Belbin O, Beaumont H, Warden D, Smith AD, Kalsheker N, Morgan K. PSEN1 polymorphisms alter the rate of cognitive decline in sporadic Alzheimer's disease patients. Neurobiol Aging. 2009;30(12):1992-9.

Benedetti B, Charil A, Rovaris M, Judica E, Valsasina P, Sormani MP, et al. Influence of aging on brain gray and white matter changes assessed by conventional, MT, and DT MRI. Neurology. 2006;66(4):535-9.

Benzinger TL, Blazey T, Jack CR, Jr., Koeppe RA, Su Y, Xiong C, et al. Regional variability of imaging biomarkers in autosomal dominant Alzheimer's disease. Proceedings of the National Academy of Sciences of the United States of America. 2013;110(47):E4502-9.

Bergeron C, Ranalli PJ, Miceli PN. Amyloid angiopathy in Alzheimer's disease. CanJ Neurol Sci. 1987;14(4):564-9.

Blessed G, Tomlinson BE, Roth M. The association between quantitative measures of dementia and of senile change in the cerebral grey matter of elderly subjects. The British journal of psychiatry : the journal of mental science. 1968;114(512):797-811.

Boche D, Zotova E, Weller RO, Love S, Neal JW, Pickering RM, et al. Consequence of Abeta immunization on the vasculature of human Alzheimer's disease brain. Brain. 2008;131(Pt 12):3299-310.

Bogner S, Bernreuther C, Matschke J, Barrera-Ocampo A, Sepulveda-Falla D, Leypoldt F, et al. Immune activation in amyloid-beta-related angiitis correlates with decreased parenchymal amyloid-beta plaque load. Neuro-degenerative diseases. 2014;13(1):38-44.

Bohanna I, Georgiou-Karistianis N, Egan GF. Connectivity-based segmentation of the striatum in Huntington's disease: vulnerability of motor pathways. Neurobiol Dis. 2011;42(3):475-81.

Bozzali M, Cercignani M, Sormani MP, Comi G, Filippi M. Quantification of brain gray matter damage in different MS phenotypes by use of diffusion tensor MR imaging. AJNR American journal of neuroradiology. 2002;23(6):985-8.

Braak H, Alafuzoff I, Arzberger T, Kretzschmar H, Del Tredici K. Staging of Alzheimer disease-associated neurofibrillary pathology using paraffin sections and immunocytochemistry. Acta Neuropathol. 2006;112(4):389-404.

Braak H, Braak E. Alzheimer's disease: striatal amyloid deposits and neurofibrillary changes. Journal of neuropathology and experimental neurology. 1990;49(3):215-24.

Braak H, Braak E. Alzheimer's disease affects limbic nuclei of the thalamus. Acta Neuropathol. 1991;81(3):261-8.

Braskie MN, Medina LD, Rodriguez-Agudelo Y, Geschwind DH, Macias-Islas MA, Thompson PM, et al. Memory performance and fMRI signal in presymptomatic familial Alzheimer's disease. Human brain mapping. 2013;34(12):3308-19.

Brilliant MJ, Elble RJ, Ghobrial M, Struble RG. The distribution of amyloid beta protein deposition in the corpus striatum of patients with Alzheimer's disease. Neuropathology and applied neurobiology. 1997;23(4):322-5.

Budde MD, Frank JA. Neurite beading is sufficient to decrease the apparent diffusion coefficient after ischemic stroke. Proceedings of the National Academy of Sciences of the United States of America. 2010;107(32):14472-7.

Cagnin A, Brooks DJ, Kennedy AM, Gunn RN, Myers R, Turkheimer FE, et al. In-vivo measurement of activated microglia in dementia. Lancet. 2001;358(9280):461-7.

Campion D, Brice A, Dumanchin C, Puel M, Baulac M, De LS, V, et al. A novel presenilin 1 mutation resulting in familial Alzheimer's disease with an onset age of 29 years. Neuroreport. 1996;7(10):1582-4.

Carlson C, Estergard W, Oh J, Suhy J, Jack CR, Jr., Siemers E, et al. Prevalence of asymptomatic vasogenic edema in pretreatment Alzheimer's disease study cohorts from phase 3 trials of semagacestat and solanezumab. Alzheimer's & dementia : the journal of the Alzheimer's Association. 2011;7(4):396-401.

Carrasquillo MM, Khan Q, Murray ME, Krishnan S, Aakre J, Pankratz VS, et al. Late-onset Alzheimer disease genetic variants in posterior cortical atrophy and posterior AD. Neurology. 2014;82(16):1455-62.

Cash DM, Ridgway GR, Liang Y, Ryan NS, Kinnunen KM, Yeatman T, et al. The pattern of atrophy in familial Alzheimer disease: volumetric MRI results from the DIAN study. Neurology. 2013;81(16):1425-33.

Cash DM, Rohrer JD, Ryan NS, Ourselin S, Fox NC. Imaging endpoints for clinical trials in Alzheimer's disease. Alzheimer's research & therapy. 2014;6(9):87.

Caso F, Agosta F, Filippi M. Insights into White Matter Damage in Alzheimer's Disease: From Postmortem to in vivo Diffusion Tensor MRI Studies. Neuro-degenerative diseases. 2016;16(1-2):26-33.

Caso F, Agosta F, Mattavelli D, Migliaccio R, Canu E, Magnani G, et al. White Matter Degeneration in Atypical Alzheimer Disease. Radiology. 2015:142766.

Chalmers K, Wilcock GK, Love S. APOE epsilon 4 influences the pathological phenotype of Alzheimer's disease by favouring cerebrovascular over parenchymal accumulation of A beta protein. Neuropathology and applied neurobiology. 2003;29(3):231-8.

Chamard L, Wallon D, Pijoff A, Berger E, Viennet G, Hannequin D, et al. Amyloid-related imaging abnormalities in AbetaPP duplication carriers. Journal of Alzheimer's disease : JAD. 2013;37(4):789-93.

Chan D, Janssen JC, Whitwell JL, Watt HC, Jenkins R, Frost C, et al. Change in rates of cerebral atrophy over time in early-onset Alzheimer's disease: longitudinal MRI study. Lancet. 2003;362(9390):1121-2.

Chao CP, Kotsenas AL, Broderick DF. Cerebral amyloid angiopathy: CT and MR imaging findings. Radiographics. 2006;26(5):1517-31.

Chavez-Gutierrez L, Bammens L, Benilova I, Vandersteen A, Benurwar M, Borgers M, et al. The mechanism of gamma-Secretase dysfunction in familial Alzheimer disease. The EMBO journal. 2012;31(10):2261-74.

Chhatwal JP, Schultz AP, Johnson K, Benzinger TL, Jack C, Jr., Ances BM, et al. Impaired default network functional connectivity in autosomal dominant Alzheimer disease. Neurology. 2013;81(8):736-44.

Chua TC, Wen W, Slavin MJ, Sachdev PS. Diffusion tensor imaging in mild cognitive impairment and Alzheimer's disease: a review. CurrOpinNeurol. 2008;21(1):83-92.

Chung KK, Anderson NE, Hutchinson D, Synek B, Barber PA. Cerebral amyloid angiopathy related inflammation: three case reports and a review. J Neurol Neurosurg Psychiatry. 2011;82(1):20-6.

Church A, Prescott J, Lillis S, Rees J, Chance P, Williamson K, et al. A novel presenilin 1 mutation, I202F occurring at a previously predicted pathogenic site causing autosomal dominant Alzheimer's disease. Neurobiol Aging. 2011;32(3):556-2.

Ciccarelli O, Werring DJ, Wheeler-Kingshott CA, Barker GJ, Parker GJ, Thompson AJ, et al. Investigation of MS normal-appearing brain using diffusion tensor MRI with clinical correlations. Neurology. 2001;56(7):926-33.

Cole G, Williams P, Alldryck D, Singharo S. Amyloid plaques in the cerebellum in Alzheimer's disease. Clin Neuropathol. 1989;8(4):188-91.

Concha L, Gross DW, Wheatley BM, Beaulieu C. Diffusion tensor imaging of time-dependent axonal and myelin degradation after corpus callosotomy in epilepsy patients. Neuroimage. 2006;32(3):1090-9.

Cook PA, Bai Y, Nedjati-Gilani S, Seunarine KK, Hall MG, Parker GJ, et al. Camino: Open-Source Diffusion-MRI Reconstruction and Processing. Proc Int Soc Mag Reson Med. 2006;14:Abstract.

Corder EH, Saunders AM, Strittmatter WJ, Schmechel DE, Gaskell PC, Small GW, et al. Gene dose of apolipoprotein E type 4 allele and the risk of Alzheimer's disease in late onset families. Science. 1993;261(5123):921-3.

Cordonnier C, van der Flier WM. Brain microbleeds and Alzheimer's disease: innocent observation or key player? Brain. 2011;134(Pt 2):335-44.

Coric V, van Dyck CH, Salloway S, Andreasen N, Brody M, Richter RW, et al. Safety and tolerability of the gamma-secretase inhibitor avagacestat in a phase 2 study of mild to moderate Alzheimer disease. Arch Neurol. 2012;69(11):1430-40.

Crook R, Verkkoniemi A, Perez-Tur J, Mehta N, Baker M, Houlden H, et al. A variant of Alzheimer's disease with spastic paraparesis and unusual plaques due to deletion of exon 9 of presenilin 1. Nature medicine. 1998;4(4):452-5.

Crutch SJ, Lehmann M, Schott JM, Rabinovici GD, Rossor MN, Fox NC. Posterior cortical atrophy. Lancet Neurol. 2012;11(2):170-8.

Cruts M, van Duijn CM, Backhovens H, Van den BM, Wehnert A, Serneels S, et al. Estimation of the genetic contribution of presenilin-1 and -2 mutations in a population-based study of presenile Alzheimer disease. HumMolGenet. 1998;7(1):43-51.

de Jong LW, van der Hiele K, Veer IM, Houwing JJ, Westendorp RG, Bollen EL, et al. Strongly reduced volumes of putamen and thalamus in Alzheimer's disease: an MRI study. Brain. 2008;131(Pt 12):3277-85.

De Jonghe C, Cruts M, Rogaeva EA, Tysoe C, Singleton A, Vanderstichele H, et al. Aberrant splicing in the presenilin-1 intron 4 mutation causes presenile Alzheimer's disease by increased Abeta42 secretion. Human molecular genetics. 1999;8(8):1529-40.

De Leon MJ, George AE, Golomb J, Tarshish C, Convit A, Kluger A, et al. Frequency of hippocampal formation atrophy in normal aging and Alzheimer's disease. Neurobiol Aging. 1997;18(1):1-11.

De Strooper B, Karran E. The Cellular Phase of Alzheimer's Disease. Cell. 2016;164(4):603-15.

De Strooper B, Saftig P, Craessaerts K, Vanderstichele H, Guhde G, Annaert W, et al. Deficiency of presenilin-1 inhibits the normal cleavage of amyloid precursor protein. Nature. 1998;391(6665):387-90.

DeCarli C, Frisoni GB, Clark CM, Harvey D, Grundman M, Petersen RC, et al. Qualitative estimates of medial temporal atrophy as a predictor of progression from mild cognitive impairment to dementia. Arch Neurol. 2007;64(1):108-15.

DeCarli C, Mungas D, Harvey D, Reed B, Weiner M, Chui H, et al. Memory impairment, but not cerebrovascular disease, predicts progression of MCI to dementia. Neurology. 2004;63(2):220-7.

Depaz R, Haik S, Peoc'h K, Seilhean D, Grabli D, Vicart S, et al. Long-standing prion dementia manifesting as posterior cortical atrophy. Alzheimer Dis Assoc Disord. 2012;26(3):289-92.

Dermaut B, Kumar-Singh S, De Jonghe C, Cruts M, Lofgren A, Lubke U, et al. Cerebral amyloid angiopathy is a pathogenic lesion in Alzheimer's disease due to a novel presenilin 1 mutation. Brain. 2001;124(Pt 12):2383-92.

Devanand DP, Pradhaban G, Liu X, Khandji A, De Santi S, Segal S, et al. Hippocampal and entorhinal atrophy in mild cognitive impairment: prediction of Alzheimer disease. Neurology. 2007;68(11):828-36.

Di Fede G, Catania M, Morbin M, Rossi G, Suardi S, Mazzoleni G, et al. A recessive mutation in the APP gene with dominant-negative effect on amyloidogenesis. Science. 2009;323(5920):1473-7.

DiFrancesco JC, Brioschi M, Brighina L, Ruffmann C, Saracchi E, Costantino G, et al. Anti-Abeta autoantibodies in the CSF of a patient with CAA-related inflammation: a case report. Neurology. 2011;76(9):842-4.

Dillen K, Annaert W. A two decade contribution of molecular cell biology to the centennial of Alzheimer's disease: are we progressing toward therapy? International review of cytology. 2006;254:215-300.

Dintchov TL, Mehrabian S, Van den BM, Radoslavova RM, Cruts M, Kirilova JA, et al. Novel PSEN1 mutation in a bulgarian patient with very early-onset Alzheimer's disease, spastic paraparesis, and extrapyramidal signs. Am J AlzheimersDis Other Demen. 2009;24(5):404-7.

Doody RS, Thomas RG, Farlow M, Iwatsubo T, Vellas B, Joffe S, et al. Phase 3 trials of solanezumab for mild-to-moderate Alzheimer's disease. The New England journal of medicine. 2014;370(4):311-21.

Douaud G, Jbabdi S, Behrens TE, Menke RA, Gass A, Monsch AU, et al. DTI measures in crossing-fibre areas: increased diffusion anisotropy reveals early white matter alteration in MCI and mild Alzheimer's disease. Neuroimage. 2011;55(3):880-90.

Duara R, Loewenstein DA, Potter E, Appel J, Greig MT, Urs R, et al. Medial temporal lobe atrophy on MRI scans and the diagnosis of Alzheimer disease. Neurology. 2008;71(24):1986-92.

Dubois B, Feldman HH, Jacova C, Cummings JL, DeKosky ST, Barberger-Gateau P, et al. Revising the definition of Alzheimer's disease: a new lexicon. Lancet Neurol. 2010;9(11):1118-27.

Dubois B, Feldman HH, Jacova C, DeKosky ST, Barberger-Gateau P, Cummings J, et al. Research criteria for the diagnosis of Alzheimer's disease: revising the NINCDS-ADRDA criteria. Lancet Neurol. 2007;6(8):734-46.

Dubois B, Feldman HH, Jacova C, Hampel H, Molinuevo JL, Blennow K, et al. Advancing research diagnostic criteria for Alzheimer's disease: the IWG-2 criteria. Lancet Neurol. 2014;13(6):614-29.

Dukart J, Mueller K, Villringer A, Kherif F, Draganski B, Frackowiak R, et al. Relationship between imaging biomarkers, age, progression and symptom severity in Alzheimer's disease. Neuroimage Clin. 2013;3:84-94.

Dumanchin C, Tournier I, Martin C, Didic M, Belliard S, Carlander B, et al. Biological effects of four PSEN1 gene mutations causing Alzheimer disease with spastic paraparesis and cotton wool plaques. Human mutation. 2006;27(10):1063.

Ellis RJ, Olichney JM, Thal LJ, Mirra SS, Morris JC, Beekly D, et al. Cerebral amyloid angiopathy in the brains of patients with Alzheimer's disease: the CERAD experience, Part XV. Neurology. 1996;46(6):1592-6.

Eng JA, Frosch MP, Choi K, Rebeck GW, Greenberg SM. Clinical manifestations of cerebral amyloid angiopathy-related inflammation. Ann Neurol. 2004;55(2):250-6.

Engler H, Forsberg A, Almkvist O, Blomquist G, Larsson E, Savitcheva I, et al. Two-year follow-up of amyloid deposition in patients with Alzheimer's disease. Brain. 2006;129(Pt 11):2856-66.

Esch FS, Keim PS, Beattie EC, Blacher RW, Culwell AR, Oltersdorf T, et al. Cleavage of amyloid beta peptide during constitutive processing of its precursor. Science. 1990;248(4959):1122-4.

Fleisher AS, Chen K, Quiroz YT, Jakimovich LJ, Gomez MG, Langois CM, et al. Florbetapir PET analysis of amyloid-beta deposition in the presenilin 1 E280A autosomal dominant Alzheimer's disease kindred: a cross-sectional study. Lancet Neurol. 2012;11(12):1057-65.

Forsberg A, Engler H, Almkvist O, Blomquist G, Hagman G, Wall A, et al. PET imaging of amyloid deposition in patients with mild cognitive impairment. Neurobiol Aging. 2008;29(10):1456-65.

Fortea J, Sala-Llonch R, Bartres-Faz D, Bosch B, Llado A, Bargallo N, et al. Increased cortical thickness and caudate volume precede atrophy in PSEN1 mutation carriers. JAlzheimersDis. 2010;22(3):909-22.

Fox NC, Black RS, Gilman S, Rossor MN, Griffith SG, Jenkins L, et al. Effects of Abeta immunization (AN1792) on MRI measures of cerebral volume in Alzheimer disease. Neurology. 2005;64(9):1563-72.

Fox NC, Kennedy AM, Harvey RJ, Lantos PL, Roques PK, Collinge J, et al. Clinicopathological features of familial Alzheimer's disease associated with the M139V mutation in the presenilin 1 gene. Pedigree but not mutation specific age at onset provides evidence for a further genetic factor. Brain. 1997;120 (Pt 3):491-501.

Fox NC, Kennedy J. Structural imaging markers for therapeutic trials in Alzheimer's disease. J NutrHealth Aging. 2009;13(4):350-2.

Fox NC, Petersen RC. The G8 Dementia Research Summit--a starter for eight? Lancet. 2013;382(9909):1968-9.

Fox NC, Warrington EK, Seiffer AL, Agnew SK, Rossor MN. Presymptomatic cognitive deficits in individuals at risk of familial Alzheimer's disease. A longitudinal prospective study. Brain. 1998;121 (Pt 9):1631-9.

Frisoni GB, Delacourte A. Neuroimaging outcomes in clinical trials in Alzheimer's disease. J NutrHealth Aging. 2009;13(3):209-12.

Fukutani Y, Cairns NJ, Rossor MN, Lantos PL. Cerebellar pathology in sporadic and familial Alzheimer's disease including APP 717 (Val-->Ile) mutation cases: a morphometric investigation. J Neurol Sci. 1997;149(2):177-84.

Gerschlager W, Brown P. Myoclonus. Current opinion in neurology. 2009;22(4):414-8.

Ghidoni R, Albertini V, Squitti R, Paterlini A, Bruno A, Bernardini S, et al. Novel T719P AbetaPP mutation unbalances the relative proportion of amyloid-beta peptides. Journal of Alzheimer's disease : JAD. 2009;18(2):295-303.

Giaccone G, Morbin M, Moda F, Botta M, Mazzoleni G, Uggetti A, et al. Neuropathology of the recessive A673V APP mutation: Alzheimer disease with distinctive features. Acta Neuropathol. 2010;120(6):803-12.

Gilman S, Koller M, Black RS, Jenkins L, Griffith SG, Fox NC, et al. Clinical effects of Abeta immunization (AN1792) in patients with AD in an interrupted trial. Neurology. 2005;64(9):1553-62.

Goate A, Chartier-Harlin MC, Mullan M, Brown J, Crawford F, Fidani L, et al. Segregation of a missense mutation in the amyloid precursor protein gene with familial Alzheimer's disease. Nature. 1991;349(6311):704-6.

Godbolt AK, Beck JA, Collinge J, Garrard P, Warren JD, Fox NC, et al. A presenilin 1 R278I mutation presenting with language impairment. Neurology. 2004;63(9):1702-4.

Godbolt AK, Cipolotti L, Watt H, Fox NC, Janssen JC, Rossor MN. The natural history of Alzheimer disease: a longitudinal presymptomatic and symptomatic study of a familial cohort. Arch Neurol. 2004;61(11):1743-8.

Godbolt AK, Waldman AD, MacManus DG, Schott JM, Frost C, Cipolotti L, et al. MRS shows abnormalities before symptoms in familial Alzheimer disease. Neurology. 2006;66(5):718-22.

Gomez-Isla T, Growdon WB, McNamara MJ, Nochlin D, Bird TD, Arango JC, et al. The impact of different presenilin 1 andpresenilin 2 mutations on amyloid deposition, neurofibrillary changes and neuronal loss in the familial Alzheimer's disease brain: evidence for other phenotype-modifying factors. Brain. 1999;122 (Pt 9):1709-19.

Gomez-Isla T, Wasco W, Pettingell WP, Gurubhagavatula S, Schmidt SD, Jondro PD, et al. A novel presenilin-1 mutation: increased beta-amyloid and neurofibrillary changes. Ann Neurol. 1997;41(6):809-13.

Goos JD, Kester MI, Barkhof F, Klein M, Blankenstein MA, Scheltens P, et al. Patients with Alzheimer disease with multiple microbleeds: relation with cerebrospinal fluid biomarkers and cognition. Stroke. 2009;40(11):3455-60.

Gorno-Tempini ML, Brambati SM, Ginex V, Ogar J, Dronkers NF, Marcone A, et al. The logopenic/phonological variant of primary progressive aphasia. Neurology. 2008;71(16):1227-34.

Grabowski TJ, Cho HS, Vonsattel JP, Rebeck GW, Greenberg SM. Novel amyloid precursor protein mutation in an Iowa family with dementia and severe cerebral amyloid angiopathy. Ann Neurol. 2001;49(6):697-705.

Grahn JA, Parkinson JA, Owen AM. The cognitive functions of the caudate nucleus. Progress in neurobiology. 2008;86(3):141-55.

Greenberg SM, Finklestein SP, Schaefer PW. Petechial hemorrhages accompanying lobar hemorrhage: detection by gradient-echo MRI. Neurology. 1996;46(6):1751-4.

Greenberg SM, Frosch MP. Life imitates art: anti-amyloid antibodies and inflammatory cerebral amyloid angiopathy. Neurology. 2011;76(9):772-3.

Greenberg SM, Rebeck GW, Vonsattel JP, Gomez-Isla T, Hyman BT. Apolipoprotein E epsilon 4 and cerebral hemorrhage associated with amyloid angiopathy. Ann Neurol. 1995;38(2):254-9.

Gregoire SM, Chaudhary UJ, Brown MM, Yousry TA, Kallis C, Jager HR, et al. The Microbleed Anatomical Rating Scale (MARS): reliability of a tool to map brain microbleeds. Neurology. 2009;73(21):1759-66.

Guerreiro R, Hardy J. Genetics of Alzheimer's disease. Neurotherapeutics : the journal of the American Society for Experimental NeuroTherapeutics. 2014;11(4):732-7.

Guerreiro R, Wojtas A, Bras J, Carrasquillo M, Rogaeva E, Majounie E, et al. TREM2 variants in Alzheimer's disease. The New England journal of medicine. 2013;368(2):117-27.

Guerreiro RJ, Baquero M, Blesa R, Boada M, Bras JM, Bullido MJ, et al. Genetic screening of Alzheimer's disease genes in Iberian and African samples yields novel mutations in presenilins and APP. Neurobiol Aging. 2010;31(5):725-31.

Guyant-Marechal I, Berger E, Laquerriere A, Rovelet-Lecrux A, Viennet G, Frebourg T, et al. Intrafamilial diversity of phenotype associated with app duplication. Neurology. 2008;71(23):1925-6.

Haan J, Van Broeckhoven C, van Duijn CM, Voorhoeve E, van Harskamp F, van Swieten JC, et al. The apolipoprotein E epsilon 4 allele does not influence the clinical expression of the amyloid precursor protein gene codon 693 or 692 mutations. Ann Neurol. 1994;36(3):434-7.

Haltia M, Viitanen M, Sulkava R, Ala-Hurula V, Poyhonen M, Goldfarb L, et al. Chromosome 14-encoded Alzheimer's disease: genetic and clinicopathological description. Ann Neurol. 1994;36(3):362-7.

Hamilton RL. Lewy bodies in Alzheimer's disease: a neuropathological review of 145 cases using alpha-synuclein immunohistochemistry. Brain Pathol. 2000;10(3):378-84.

Hammers A, Allom R, Koepp MJ, Free SL, Myers R, Lemieux L, et al. Three-dimensional maximum probability atlas of the human brain, with particular reference to the temporal lobe. Human brain mapping. 2003;19(4):224-47.

Handen BL, Cohen AD, Channamalappa U, Bulova P, Cannon SA, Cohen WI, et al. Imaging brain amyloid in nondemented young adults with Down syndrome using Pittsburgh compound B. Alzheimer's & dementia : the journal of the Alzheimer's Association. 2012;8(6):496-501.

Hardy JA, Higgins GA. Alzheimer's disease: the amyloid cascade hypothesis. Science. 1992;256(5054):184-5.

Harkness KA, Coles A, Pohl U, Xuereb JH, Baron JC, Lennox GG. Rapidly reversible dementia in cerebral amyloid inflammatory vasculopathy. Eur J Neurol. 2004;11(1):59-62.

Harold D, Abraham R, Hollingworth P, Sims R, Gerrish A, Hamshere ML, et al. Genome-wide association study identifies variants at CLU and PICALM associated with Alzheimer's disease. NatGenet. 2009;41(10):1088-93.

Haroon HA, Reynolds H, Carter SF, Embleton KV, Herholz KG, Parker GJ. HARDI-based microstructural complexity mapping reveals distinct subcortical and cortical grey

matter changes in mild cognitive impairment and Alzheimer's disease. Proc Int Soc Mag Reson Med. 2011;682.

Hawkes CA, Sullivan PM, Hands S, Weller RO, Nicoll JA, Carare RO. Disruption of arterial perivascular drainage of amyloid-beta from the brains of mice expressing the human APOE epsilon4 allele. PloS one. 2012;7(7):e41636.

Hendriks L, van Duijn CM, Cras P, Cruts M, Van Hul W, Van Harskamp F, et al. Presenile dementia and cerebral haemorrhage linked to a mutation at codon 692 of the beta-amyloid precursor protein gene. NatGenet. 1992;1(3):218-21.

Herve D, Molko N, Pappata S, Buffon F, LeBihan D, Bousser MG, et al. Longitudinal thalamic diffusion changes after middle cerebral artery infarcts. J Neurol Neurosurg Psychiatry. 2005;76(2):200-5.

Hiltunen M, Helisalmi S, Mannermaa A, Alafuzoff I, Koivisto AM, Lehtovirta M, et al. Identification of a novel 4.6-kb genomic deletion in presenilin-1 gene which results in exclusion of exon 9 in a Finnish early onset Alzheimer's disease family: an Alu core sequence-stimulated recombination? Eur J HumGenet. 2000;8(4):259-66.

Hodges JR, Patterson K. Semantic dementia: a unique clinicopathological syndrome. Lancet Neurol. 2007;6(11):1004-14.

Hof PR, Vogt BA, Bouras C, Morrison JH. Atypical form of Alzheimer's disease with prominent posterior cortical atrophy: a review of lesion distribution and circuit disconnection in cortical visual pathways. Vision research. 1997;37(24):3609-25.

Holmes C. Genotype and phenotype in Alzheimer's disease. BrJ Psychiatry. 2002;180:131-4.

Hopkins RO, Beck CJ, Burnett DL, Weaver LK, Victoroff J, Bigler ED. Prevalence of white matter hyperintensities in a young healthy population. Journal of neuroimaging : official journal of the American Society of Neuroimaging. 2006;16(3):243-51.

Hort J, O'Brien JT, Gainotti G, Pirttila T, Popescu BO, Rektorova I, et al. EFNS guidelines for the diagnosis and management of Alzheimer's disease. Eur J Neurol. 2010;17(10):1236-48.

Houlden H, Baker M, McGowan E, Lewis P, Hutton M, Crook R, et al. Variant Alzheimer's disease with spastic paraparesis and cotton wool plaques is caused by PS-1 mutations that lead to exceptionally high amyloid-beta concentrations. Ann Neurol. 2000;48(5):806-8.

Houlden H, Crook R, Dolan RJ, McLaughlin J, Revesz T, Hardy J. A novel presenilin mutation (M233V) causing very early onset Alzheimer's disease with Lewy bodies. Neurosci Lett. 2001;313(1-2):93-5.

Huang J, Friedland RP, Auchus AP. Diffusion tensor imaging of normal-appearing white matter in mild cognitive impairment and early Alzheimer disease: preliminary evidence of axonal degeneration in the temporal lobe. AJNR American journal of neuroradiology. 2007;28(10):1943-8.

Huppert FA, Brayne C, O'Connor DW. Dementia and normal aging. Cambridge: Cambridge Univerity Press; 1994.

Ishikawa A, Piao YS, Miyashita A, Kuwano R, Onodera O, Ohtake H, et al. A mutant PSEN1 causes dementia with Lewy bodies and variant Alzheimer's disease. Ann Neurol. 2005;57(3):429-34.

Jack CR, Jr., Dickson DW, Parisi JE, Xu YC, Cha RH, O'Brien PC, et al. Antemortem MRI findings correlate with hippocampal neuropathology in typical aging and dementia. Neurology. 2002;58(5):750-7.

Jack CR, Jr., Knopman DS, Jagust WJ, Petersen RC, Weiner MW, Aisen PS, et al. Tracking pathophysiological processes in Alzheimer's disease: an updated hypothetical model of dynamic biomarkers. Lancet Neurol. 2013;12(2):207-16.

Jack CR, Jr., Knopman DS, Jagust WJ, Shaw LM, Aisen PS, Weiner MW, et al. Hypothetical model of dynamic biomarkers of the Alzheimer's pathological cascade. Lancet Neurol. 2010;9(1):119-28.

Jagust W, Reed B, Mungas D, Ellis W, Decarli C. What does fluorodeoxyglucose PET imaging add to a clinical diagnosis of dementia? Neurology. 2007;69(9):871-7.

Janssen JC, Beck JA, Campbell TA, Dickinson A, Fox NC, Harvey RJ, et al. Early onset familial Alzheimer's disease: Mutation frequency in 31 families. Neurology. 2003;60(2):235-9.

Jarrett JT, Berger EP, Lansbury PT, Jr. The carboxy terminus of the beta amyloid protein is critical for the seeding of amyloid formation: implications for the pathogenesis of Alzheimer's disease. Biochemistry. 1993;32(18):4693-7.

Jayadev S, Leverenz JB, Steinbart E, Stahl J, Klunk W, Yu CE, et al. Alzheimer's disease phenotypes and genotypes associated with mutations in presenilin 2. Brain. 2010;133(Pt 4):1143-54.

Jenkinson M, Bannister P, Brady M, Smith S. Improved optimization for the robust and accurate linear registration and motion correction of brain images. Neuroimage. 2002;17(2):825-41.

Jiao B, Tang B, Liu X, Xu J, Wang Y, Zhou L, et al. Mutational analysis in early-onset familial Alzheimer's disease in Mainland China. Neurobiol Aging. 2014;35(8):1957 e1-6.

Jonsson T, Atwal JK, Steinberg S, Snaedal J, Jonsson PV, Bjornsson S, et al. A mutation in APP protects against Alzheimer's disease and age-related cognitive decline. Nature. 2012;488(7409):96-9.

Jonsson T, Stefansson H, Steinberg S, Jonsdottir I, Jonsson PV, Snaedal J, et al. Variant of TREM2 associated with the risk of Alzheimer's disease. The New England journal of medicine. 2013;368(2):107-16.

Kalaria RN, Cohen DL, Premkumar DR. Apolipoprotein E alleles and brain vascular pathology in Alzheimer's disease. Annals of the New York Academy of Sciences. 1996;777:266-70.

Kanaan NM, Pigino GF, Brady ST, Lazarov O, Binder LI, Morfini GA. Axonal degeneration in Alzheimer's disease: when signaling abnormalities meet the axonal transport system. Experimental neurology. 2013;246:44-53.

Karambataki M, Malousi A, Maglaveras N, Kouidou S. Synonymous polymorphisms at splicing regulatory sites are associated with CpGs in neurodegenerative disease-related genes. Neuromolecular medicine. 2010;12(3):260-9.

Karlstrom H, Brooks WS, Kwok JB, Broe GA, Kril JJ, McCann H, et al. Variable phenotype of Alzheimer's disease with spastic paraparesis. J Neurochem. 2008;104(3):573-83.

Karran E, Hardy J. Antiamyloid therapy for Alzheimer's disease--are we on the right road? The New England journal of medicine. 2014;370(4):377-8.

Kasuga K, Shimohata T, Nishimura A, Shiga A, Mizuguchi T, Tokunaga J, et al. Identification of independent APP locus duplication in Japanese patients with early-onset Alzheimer disease. J Neurol Neurosurg Psychiatry. 2009;80(9):1050-2.

Katzman R. Editorial: The prevalence and malignancy of Alzheimer disease. A major killer. Arch Neurol. 1976;33(4):217-8.

Keihaninejad S, Ryan N, Malone I, Leung K, Hyare H, Ourselin S, et al. Automated segmentation of the thalamus for measurement of MRI diffusion indices: evaluation and application to familial Alzheimer's disease. Alzheimer's and Dementia. 2011;7(4):S50. Abstract.

Keihaninejad S, Ryan NS, Malone IB, Modat M, Cash D, Ridgway GR, et al. The importance of group-wise registration in tract based spatial statistics study of neurodegeneration: a simulation study in Alzheimer's disease. PloS one. 2012;7(11):e45996.

Kennedy AM, Newman S, McCaddon A, Ball J, Roques P, Mullan M, et al. Familial Alzheimer's disease. A pedigree with a mis-sense mutation in the amyloid precursor protein gene (amyloid precursor protein 717 valine-->glycine). Brain. 1993;116 (Pt 2):309-24.

Kennedy AM, Newman SK, Frackowiak RS, Cunningham VJ, Roques P, Stevens J, et al. Chromosome 14 linked familial Alzheimer's disease. A clinico-pathological study of a single pedigree. Brain. 1995;118 (Pt 1):185-205.

Kinnecom C, Lev MH, Wendell L, Smith EE, Rosand J, Frosch MP, et al. Course of cerebral amyloid angiopathy-related inflammation. Neurology. 2007;68(17):1411-6.

Klunk WE, Engler H, Nordberg A, Wang Y, Blomqvist G, Holt DP, et al. Imaging brain amyloid in Alzheimer's disease with Pittsburgh Compound-B. Ann Neurol. 2004;55(3):306-19.

Klunk WE, Price JC, Mathis CA, Tsopelas ND, Lopresti BJ, Ziolko SK, et al. Amyloid deposition begins in the striatum of presenilin-1 mutation carriers from two unrelated pedigrees. J Neurosci. 2007;27(23):6174-84.

Knight WD, Ahsan RL, Jackson J, Cipolotti L, Warrington EK, Fox NC, et al. Pure progressive amnesia and the APPV717G mutation. Alzheimer Dis Assoc Disord. 2009;23(4):410-4.

Knight WD, Kim LG, Douiri A, Frost C, Rossor MN, Fox NC. Acceleration of cortical thinning in familial Alzheimer's disease. Neurobiol Aging. 2011;32(10):1765-73.

Knight WD, Okello AA, Ryan NS, Turkheimer FE, Rodriguez Martinez de Llano S, Edison P, et al. Carbon-11-Pittsburgh compound B positron emission tomography imaging of amyloid deposition in presenilin 1 mutation carriers. Brain. 2011;134(Pt 1):293-300.

Knopman DS, DeKosky ST, Cummings JL, Chui H, Corey-Bloom J, Relkin N, et al. Practice parameter: diagnosis of dementia (an evidence-based review). Report of the

Quality Standards Subcommittee of the American Academy of Neurology. Neurology. 2001;56(9):1143-53.

Koivunen J, Karrasch M, Scheinin NM, Aalto S, Vahlberg T, Nagren K, et al. Cognitive decline and amyloid accumulation in patients with mild cognitive impairment. Dement Geriatr Cogn Disord. 2012;34(1):31-7.

Koivunen J, Scheinin N, Virta JR, Aalto S, Vahlberg T, Nagren K, et al. Amyloid PET imaging in patients with mild cognitive impairment: a 2-year follow-up study. Neurology. 2011;76(12):1085-90.

Lambert JC, Heath S, Even G, Campion D, Sleegers K, Hiltunen M, et al. Genome-wide association study identifies variants at CLU and CR1 associated with Alzheimer's disease. NatGenet. 2009;41(10):1094-9.

Lampe TH, Bird TD, Nochlin D, Nemens E, Risse SC, Sumi SM, et al. Phenotype of chromosome 14-linked familial Alzheimer's disease in a large kindred. Ann Neurol. 1994;36(3):368-78.

Lao PJ, Betthauser TJ, Hillmer AT, Price JC, Klunk WE, Mihaila I, et al. The effects of normal aging on amyloid-beta deposition in nondemented adults with Down syndrome as imaged by carbon 11-labeled Pittsburgh compound B. Alzheimer's & dementia : the journal of the Alzheimer's Association. 2016;12(4):380-90.

Larner AJ. The cerebellum in Alzheimer's disease. Dement Geriatr Cogn Disord. 1997;8(4):203-9.

Larner AJ, Doran M. Clinical phenotypic heterogeneity of Alzheimer's disease associated with mutations of the presenilin-1 gene. J Neurol. 2006;253(2):139-58.

Larner AJ, Doran M. Genotype-phenotype relationships of presenilin-1 mutations in Alzheimer's disease: an update. J AlzheimersDis. 2009;17(2):259-65.

Lashley T, Holton JL, Gray E, Kirkham K, O'Sullivan SS, Hilbig A, et al. Cortical alpha-synuclein load is associated with amyloid-beta plaque burden in a subset of Parkinson's disease patients. Acta Neuropathol. 2008;115(4):417-25.

Lee GJ, Lu PH, Medina LD, Rodriguez-Agudelo Y, Melchor S, Coppola G, et al. Regional brain volume differences in symptomatic and presymptomatic carriers of familial Alzheimer's disease mutations. J Neurol Neurosurg Psychiatry. 2013;84(2):154-62.

Lee S, Viqar F, Zimmerman ME, Narkhede A, Tosto G, Benzinger TL, et al. White matter hyperintensities are a core feature of Alzheimer's disease: Evidence from the dominantly inherited Alzheimer network. Ann Neurol. 2016;79(6):929-39.

Lemere CA, Lopera F, Kosik KS, Lendon CL, Ossa J, Saido TC, et al. The E280A presenilin 1 Alzheimer mutation produces increased A beta 42 deposition and severe cerebellar pathology. NatMed. 1996;2(10):1146-50.

Leung KK, Barnes J, Modat M, Ridgway GR, Bartlett JW, Fox NC, et al. Brain MAPS: an automated, accurate and robust brain extraction technique using a template library. Neuroimage. 2011;55(3):1091-108.

Leung KK, Barnes J, Ridgway GR, Bartlett JW, Clarkson MJ, Macdonald K, et al. Automated cross-sectional and longitudinal hippocampal volume measurement in mild cognitive impairment and Alzheimer's disease. Neuroimage. 2010;51(4):1345-59.

Leverenz JB, Fishel MA, Peskind ER, Montine TJ, Nochlin D, Steinbart E, et al. Lewy body pathology in familial Alzheimer disease: evidence for disease- and mutation-specific pathologic phenotype. Arch Neurol. 2006;63(3):370-6.

Levy-Lahad E, Wasco W, Poorkaj P, Romano DM, Oshima J, Pettingell WH, et al. Candidate gene for the chromosome 1 familial Alzheimer's disease locus. Science. 1995;269(5226):973-7.

Li X, Dang S, Yan C, Gong X, Wang J, Shi Y. Structure of a presenilin family intramembrane aspartate protease. Nature. 2013;493(7430):56-61.

Lifshitz J, Kelley BJ, Povlishock JT. Perisomatic thalamic axotomy after diffuse traumatic brain injury is associated with atrophy rather than cell death. Journal of neuropathology and experimental neurology. 2007;66(3):218-29.

Likeman M, Anderson VM, Stevens JM, Waldman AD, Godbolt AK, Frost C, et al. Visual assessment of atrophy on magnetic resonance imaging in the diagnosis of pathologically confirmed young-onset dementias. Arch Neurol. 2005;62(9):1410-5.

Lippa CF, Fujiwara H, Mann DM, Giasson B, Baba M, Schmidt ML, et al. Lewy bodies contain altered alpha-synuclein in brains of many familial Alzheimer's disease patients with mutations in presenilin and amyloid precursor protein genes. Am J Pathol. 1998;153(5):1365-70.

Liu Y, Paajanen T, Zhang Y, Westman E, Wahlund LO, Simmons A, et al. Analysis of regional MRI volumes and thicknesses as predictors of conversion from mild cognitive impairment to Alzheimer's disease. Neurobiol Aging. 2010;31(8):1375-85.

Lowenberg K, Waggoner RW. Familial organic psychosis (Alzheimer's type). Archives of Neurology and Psychiatry. 1934;31(4):737-54.

Maarouf CL, Daugs ID, Spina S, Vidal R, Kokjohn TA, Patton RL, et al. Histopathological and molecular heterogeneity among individuals with dementia associated with Presenilin mutations. MolNeurodegener. 2008;3:20.

Madsen SK, Ho AJ, Hua X, Saharan PS, Toga AW, Jack CR, Jr., et al. 3D maps localize caudate nucleus atrophy in 400 Alzheimer's disease, mild cognitive impairment, and healthy elderly subjects. Neurobiol Aging. 2010;31(8):1312-25.

Mahoney CJ, Downey LE, Beck J, Liang Y, Mead S, Perry RJ, et al. The presenilin 1 P264L mutation presenting as non-fluent/agrammatic primary progressive aphasia. Journal of Alzheimer's disease : JAD. 2013;36(2):239-43.

Mann DM, Iwatsubo T. Diffuse plaques in the cerebellum and corpus striatum in Down's syndrome contain amyloid beta protein (A beta) only in the form of A beta 42(43). Neurodegeneration. 1996;5(2):115-20.

Mann DM, Iwatsubo T, Ihara Y, Cairns NJ, Lantos PL, Bogdanovic N, et al. Predominant deposition of amyloid-beta 42(43) in plaques in cases of Alzheimer's disease and hereditary cerebral hemorrhage associated with mutations in the amyloid precursor protein gene. Am J Pathol. 1996;148(4):1257-66.

Mann DM, Jones D, Prinja D, Purkiss MS. The prevalence of amyloid (A4) protein deposits within the cerebral and cerebellar cortex in Down's syndrome and Alzheimer's disease. Acta Neuropathol. 1990;80(3):318-27.

Mann DM, Pickering-Brown SM, Takeuchi A, Iwatsubo T. Amyloid angiopathy and variability in amyloid beta deposition is determined by mutation position in presenilin-1-linked Alzheimer's disease. Am J Pathol. 2001;158(6):2165-75.

Manners DN, Parchi P, Tonon C, Capellari S, Strammiello R, Testa C, et al. Pathologic correlates of diffusion MRI changes in Creutzfeldt-Jakob disease. Neurology. 2009;72(16):1425-31.

Marcon G, Di Fede G, Giaccone G, Rossi G, Giovagnoli AR, Maccagnano E, et al. A novel Italian presenilin 2 gene mutation with prevalent behavioral phenotype. J AlzheimersDis. 2009;16(3):509-11.

Martin JJ, Gheuens J, Bruyland M, Cras P, Vandenberghe A, Masters CL, et al. Early-onset Alzheimer's disease in 2 large Belgian families. Neurology. 1991;41(1):62-8.

Mattson MP, Magnus T. Ageing and neuronal vulnerability. Nature reviews Neuroscience. 2006;7(4):278-94.

McGowan E, Pickford F, Kim J, Onstead L, Eriksen J, Yu C, et al. Abeta42 is essential for parenchymal and vascular amyloid deposition in mice. Neuron. 2005;47(2):191-9.

McKeith IG, Dickson DW, Lowe J, Emre M, O'Brien JT, Feldman H, et al. Diagnosis and management of dementia with Lewy bodies: third report of the DLB Consortium. Neurology. 2005;65(12):1863-72.

McKinstry RC, Mathur A, Miller JH, Ozcan A, Snyder AZ, Schefft GL, et al. Radial organization of developing preterm human cerebral cortex revealed by non-invasive water diffusion anisotropy MRI. Cerebral cortex. 2002;12(12):1237-43.

McNaughton D, Knight W, Guerreiro R, Ryan N, Lowe J, Poulter M, et al. Duplication of amyloid precursor protein (APP), but not prion protein (PRNP) gene is a significant cause of early onset dementia in a large UK series. Neurobiol Aging. 2010;33(2):426.e13-21.

Melzer N, Harder A, Gross CC, Wolfer J, Stummer W, Niederstadt T, et al. CD4(+) T cells predominate in cerebrospinal fluid and leptomeningeal and parenchymal infiltrates in cerebral amyloid beta-related angiitis. Arch Neurol. 2012;69(6):773-7.

Mendez MF, Ghajarania M, Perryman KM. Posterior cortical atrophy: clinical characteristics and differences compared to Alzheimer's disease. Dement Geriatr Cogn Disord. 2002;14(1):33-40.

Miao J, Xu F, Davis J, Otte-Holler I, Verbeek MM, Van Nostrand WE. Cerebral microvascular amyloid beta protein deposition induces vascular degeneration and neuroinflammation in transgenic mice expressing human vasculotropic mutant amyloid beta precursor protein. Am J Pathol. 2005;167(2):505-15.

Middleton FA, Strick PL. Basal ganglia output and cognition: evidence from anatomical, behavioral, and clinical studies. Brain and cognition. 2000;42(2):183-200.

Miklossy J, Taddei K, Suva D, Verdile G, Fonte J, Fisher C, et al. Two novel presenilin-1 mutations (Y256S and Q222H) are associated with early-onset Alzheimer's disease. Neurobiol Aging. 2003;24(5):655-62.

Mirra SS, Heyman A, McKeel D, Sumi SM, Crain BJ, Brownlee LM, et al. The Consortium to Establish a Registry for Alzheimer's Disease (CERAD). Part II. Standardization of the neuropathologic assessment of Alzheimer's disease. Neurology. 1991;41(4):479-86.

Modat M, Ridgway GR, Taylor ZA, Lehmann M, Barnes J, Hawkes DJ, et al. Fast free-form deformation using graphics processing units. Computer methods and programs in biomedicine. 2010;98(3):278-84.

Moehlmann T, Winkler E, Xia X, Edbauer D, Murrell J, Capell A, et al. Presenilin-1 mutations of leucine 166 equally affect the generation of the Notch and APP intracellular domains independent of their effect on Abeta 42 production. Proceedings of the National Academy of Sciences of the United States of America. 2002;99(12):8025-30.

Molinuevo JL, Ripolles P, Simo M, Llado A, Olives J, Balasa M, et al. White matter changes in preclinical Alzheimer's disease: a magnetic resonance imaging-diffusion tensor imaging study on cognitively normal older people with positive amyloid beta protein 42 levels. Neurobiol Aging. 2014;35(12):2671-80.

Morbelli S, Piccardo A, Villavecchia G, Dessi B, Brugnolo A, Piccini A, et al. Mapping brain morphological and functional conversion patterns in amnestic MCI: a voxel-based MRI and FDG-PET study. Eur J Nucl Med Mol Imaging. 2010;37(1):36-45.

Mori S, Wakana S, Nagae-Poetscher L, van Zijl P. MRI atlas of human white matter. Amsterdam: Elsevier 2005.

Mosconi L, Sorbi S, de Leon MJ, Li Y, Nacmias B, Myoung PS, et al. Hypometabolism exceeds atrophy in presymptomatic early-onset familial Alzheimer's disease. J NuclMed. 2006;47(11):1778-86.

Mullan M, Crawford F, Axelman K, Houlden H, Lilius L, Winblad B, et al. A pathogenic mutation for probable Alzheimer's disease in the APP gene at the N-terminus of beta-amyloid. NatGenet. 1992;1(5):345-7.

Naj AC, Jun G, Beecham GW, Wang LS, Vardarajan BN, Buros J, et al. Common variants at MS4A4/MS4A6E, CD2AP, CD33 and EPHA1 are associated with late-onset Alzheimer's disease. Nat Genet. 2011;43(5):436-41.

Neave N, Nagle S, Aggleton JP. Evidence for the involvement of the mammillary bodies and cingulum bundle in allocentric spatial processing by rats. Eur J Neurosci. 1997;9(5):941-55.

Nelson O, Supnet C, Liu H, Bezprozvanny I. Familial Alzheimer's disease mutations in presenilins: effects on endoplasmic reticulum calcium homeostasis and correlation with clinical phenotypes. J AlzheimersDis. 2010;21(3):781-93.

Nelson O, Supnet C, Tolia A, Horre K, De Strooper B, Bezprozvanny I. Mutagenesis mapping of the presenilin 1 calcium leak conductance pore. J BiolChem. 2011;286(25):22339-47.

Nestor PJ, Fryer TD, Smielewski P, Hodges JR. Limbic hypometabolism in Alzheimer's disease and mild cognitive impairment. Ann Neurol. 2003;54(3):343-51.

Nilsberth C, Westlind-Danielsson A, Eckman CB, Condron MM, Axelman K, Forsell C, et al. The 'Arctic' APP mutation (E693G) causes Alzheimer's disease by enhanced Abeta protofibril formation. NatNeurosci. 2001;4(9):887-93.

O'Dwyer L, Lamberton F, Matura S, Tanner C, Scheibe M, Miller J, et al. Reduced hippocampal volume in healthy young ApoE4 carriers: an MRI study. PloS one. 2012;7(11):e48895.

O'Riordan S, McMonagle P, Janssen JC, Fox NC, Farrell M, Collinge J, et al. Presenilin-1 mutation (E280G), spastic paraparesis, and cranial MRI white-matter abnormalities. Neurology. 2002;59(7):1108-10.

Ohki Y, Higo T, Uemura K, Shimada N, Osawa S, Berezovska O, et al. Phenylpiperidine-type gamma-secretase modulators target the transmembrane domain 1 of presenilin 1. The EMBO journal. 2011;30(23):4815-24.

Olabarria M, Noristani HN, Verkhratsky A, Rodriguez JJ. Concomitant astroglial atrophy and astrogliosis in a triple transgenic animal model of Alzheimer's disease. Glia. 2010;58(7):831-8.

Olichney JM, Hansen LA, Galasko D, Saitoh T, Hofstetter CR, Katzman R, et al. The apolipoprotein E epsilon 4 allele is associated with increased neuritic plaques and cerebral amyloid angiopathy in Alzheimer's disease and Lewy body variant. Neurology. 1996;47(1):190-6.

Ostrowitzki S, Deptula D, Thurfjell L, Barkhof F, Bohrmann B, Brooks DJ, et al. Mechanism of amyloid removal in patients with Alzheimer disease treated with gantenerumab. Arch Neurol. 2012;69(2):198-207.

Ourselin S, Roche A, Subsol G, Pennec X, Ayache N. Reconstructing a serial structure from serial histological sections. Image and Vision Computing. 2001;19:25-31.

Oyanagi K, Takahashi H, Wakabayashi K, Ikuta F. Selective involvement of large neurons in the neostriatum of Alzheimer's disease and senile dementia: a morphometric investigation. Brain research. 1987;411(2):205-11.

Pappata S, Levasseur M, Gunn RN, Myers R, Crouzel C, Syrota A, et al. Thalamic microglial activation in ischemic stroke detected in vivo by PET and [11C]PK1195. Neurology. 2000;55(7):1052-4.

Paquet C, Amin J, Mouton-Liger F, Nasser M, Love S, Gray F, et al. Effect of active Abeta immunotherapy on neurons in human Alzheimer's disease. The Journal of pathology. 2015;235(5):721-30.

Pastor P, Roe CM, Villegas A, Bedoya G, Chakraverty S, Garcia G, et al. Apolipoprotein Eepsilon4 modifies Alzheimer's disease onset in an E280A PS1 kindred. Ann Neurol. 2003;54(2):163-9.

Pedro T, Weiler M, Yasuda CL, D'Abreu A, Damasceno BP, Cendes F, et al. Volumetric brain changes in thalamus, corpus callosum and medial temporal structures: mild Alzheimer's disease compared with amnestic mild cognitive impairment. Dement Geriatr Cogn Disord. 2012;34(3-4):149-55.

Petersen RC, Smith GE, Waring SC, Ivnik RJ, Tangalos EG, Kokmen E. Mild cognitive impairment: clinical characterization and outcome. Arch Neurol. 1999;56(3):303-8.

Piazza F, Greenberg SM, Savoiardo M, Gardinetti M, Chiapparini L, Raicher I, et al. Anti-amyloid beta autoantibodies in cerebral amyloid angiopathy-related inflammation: implications for amyloid-modifying therapies. Ann Neurol. 2013;73(4):449-58.

Piccini A, Zanusso G, Borghi R, Noviello C, Monaco S, Russo R, et al. Association of a presenilin 1 S170F mutation with a novel Alzheimer disease molecular phenotype. Arch Neurol. 2007;64(5):738-45.

Pickering-Brown SM, Baker M, Gass J, Boeve BF, Loy CT, Brooks WS, et al. Mutations in progranulin explain atypical phenotypes with variants in MAPT. Brain. 2006;129(Pt 11):3124-6.

Piscopo P, Marcon G, Piras MR, Crestini A, Campeggi LM, Deiana E, et al. A novel PSEN2 mutation associated with a peculiar phenotype. Neurology. 2008;70(17):1549-54.

Plant GT, Revesz T, Barnard RO, Harding AE, Gautier-Smith PC. Familial cerebral amyloid angiopathy with nonneuritic amyloid plaque formation. Brain. 1990;113 (Pt 3):721-47.

Premkumar DR, Cohen DL, Hedera P, Friedland RP, Kalaria RN. Apolipoprotein E-epsilon4 alleles in cerebral amyloid angiopathy and cerebrovascular pathology associated with Alzheimer's disease. The American journal of pathology. 1996;148(6):2083-95.

Price JL, Morris JC. Tangles and plaques in nondemented aging and "preclinical" Alzheimer's disease. Ann Neurol. 1999;45(3):358-68.

Prince M, Bryce R, Albanese E, Wimo A, Ribeiro W, Ferri CP. The global prevalence of dementia: a systematic review and metaanalysis. Alzheimer's & dementia : the journal of the Alzheimer's Association. 2013;9(1):63-75 e2.

Prins ND, Scheltens P. White matter hyperintensities, cognitive impairment and dementia: an update. Nature reviews Neurology. 2015.

Queralt R, Ezquerra M, Lleo A, Castellvi M, Gelpi J, Ferrer I, et al. A novel mutation (V89L) in the presenilin 1 gene in a family with early onset Alzheimer's disease and marked behavioural disturbances. J Neurol Neurosurg Psychiatry. 2002;72(2):266-9.

Raman MR, Wiste HJ, Senjem ML, Ward CP, Jack CR, Jr., Kantarci K. Spontaneous amyloid-related imaging abnormalities in a cognitively normal adult. Neurology. 2014;83(19):1771-2.

Ramlackhansingh AF, Brooks DJ, Greenwood RJ, Bose SK, Turkheimer FE, Kinnunen KM, et al. Inflammation after trauma: microglial activation and traumatic brain injury. Ann Neurol. 2011;70(3):374-83.

Raux G, Gantier R, Thomas-Anterion C, Boulliat J, Verpillat P, Hannequin D, et al. Dementia with prominent frontotemporal features associated with L113P presenilin 1 mutation. Neurology. 2000;55(10):1577-8.

Reiman EM, Chen K, Liu X, Bandy D, Yu M, Lee W, et al. Fibrillar amyloid-beta burden in cognitively normal people at 3 levels of genetic risk for Alzheimer's disease. Proceedings of the National Academy of Sciences of the United States of America. 2009;106(16):6820-5.

Reiman EM, Langbaum JB, Tariot PN. Alzheimer's prevention initiative: a proposal to evaluate presymptomatic treatments as quickly as possible. BiomarkMed. 2010;4(1):3-14.

Reiman EM, Quiroz YT, Fleisher AS, Chen K, Velez-Pardo C, Jimenez-Del-Rio M, et al. Brain imaging and fluid biomarker analysis in young adults at genetic risk for autosomal dominant Alzheimer's disease in the presenilin 1 E280A kindred: a case-control study. Lancet Neurol. 2012;11(12):1048-56.

Remes AM, Laru L, Tuominen H, Aalto S, Kemppainen N, Mononen H, et al. Carbon 11-labeled pittsburgh compound B positron emission tomographic amyloid imaging in patients with APP locus duplication. Arch Neurol. 2008;65(4):540-4.

Renner JA, Burns JM, Hou CE, McKeel DW, Jr., Storandt M, Morris JC. Progressive posterior cortical dysfunction: a clinicopathologic series. Neurology. 2004;63(7):1175-80.

Revesz T, Ghiso J, Lashley T, Plant G, Rostagno A, Frangione B, et al. Cerebral amyloid angiopathies: a pathologic, biochemical, and genetic view. J Neuropathol ExpNeurol. 2003;62(9):885-98.

Revesz T, Hawkins CP, du Boulay EP, Barnard RO, McDonald WI. Pathological findings correlated with magnetic resonance imaging in subcortical arteriosclerotic encephalopathy (Binswanger's disease). J Neurol Neurosurg Psychiatry. 1989;52(12):1337-44.

Revesz T, Holton JL, Lashley T, Plant G, Frangione B, Rostagno A, et al. Genetics and molecular pathogenesis of sporadic and hereditary cerebral amyloid angiopathies. Acta Neuropathol. 2009;118(1):115-30.

Richard E, Carrano A, Hoozemans JJ, van Horssen J, van Haastert ES, Eurelings LS, et al. Characteristics of dyshoric capillary cerebral amyloid angiopathy. J Neuropathol ExpNeurol. 2010;69(11):1158-67.

Ridgway GR, Barnes J, Pepple T, Fox N. Estimation of total intracranial volume; a comparison of methods. Alzheimer's and Dementia. 2011;7(4):S62. Abstract.

Ridha BH, Barnes J, Bartlett JW, Godbolt A, Pepple T, Rossor MN, et al. Tracking atrophy progression in familial Alzheimer's disease: a serial MRI study. Lancet Neurol. 2006;5(10):828-34.

Rieckmann A, Van Dijk KR, Sperling RA, Johnson KA, Buckner RL, Hedden T. Accelerated decline in white matter integrity in clinically normal individuals at risk for Alzheimer's disease. Neurobiol Aging. 2016;42:177-88.

Ringman JM, O'Neill J, Geschwind D, Medina L, Apostolova LG, Rodriguez Y, et al. Diffusion tensor imaging in preclinical and presymptomatic carriers of familial Alzheimer's disease mutations. Brain. 2007;130(Pt 7):1767-76.

Ringman JM, Pope W, Salamon N. Insensitivity of visual assessment of hippocampal atrophy in familial Alzheimer's disease. J Neurol. 2010;257(5):839-42.

Rippon GA, Crook R, Baker M, Halvorsen E, Chin S, Hutton M, et al. Presenilin 1 mutation in an african american family presenting with atypical Alzheimer dementia. Arch Neurol. 2003;60(6):884-8.

Rodriguez JJ, Witton J, Olabarria M, Noristani HN, Verkhratsky A. Increase in the density of resting microglia precedes neuritic plaque formation and microglial activation in a transgenic model of Alzheimer's disease. Cell death & disease. 2010;1:e1.

Rodriguez-Vieitez E, Saint-Aubert L, Carter SF, Almkvist O, Farid K, Scholl M, et al. Diverging longitudinal changes in astrocytosis and amyloid PET in autosomal dominant Alzheimer's disease. Brain. 2016;139(Pt 3):922-36.

Roks G, Van Harskamp F, De K, I, Cruts M, De Jonghe C, Kumar-Singh S, et al. Presentation of amyloidosis in carriers of the codon 692 mutation in the amyloid precursor protein gene (APP692). Brain. 2000;123 (Pt 10):2130-40.

Rosenberg CE, Golden J. Framing Disease: Studies in Cultural History. New Brunswick, New Jersey: Rutgers University Press; 1992.

Rossor MN, Newman S, Frackowiak RS, Lantos P, Kennedy AM. Alzheimer's disease families with amyloid precursor protein mutations. Ann N YAcadSci. 1993;695:198-202.

Roth M. The natural history of mental disorder in old age. The Journal of mental science. 1955;101(423):281-301.

Rovelet-Lecrux A, Hannequin D, Raux G, Le Meur N, Laquerriere A, Vital A, et al. APP locus duplication causes autosomal dominant early-onset Alzheimer disease with cerebral amyloid angiopathy. NatGenet. 2006;38(1):24-6.

Rowe CC, Ng S, Ackermann U, Gong SJ, Pike K, Savage G, et al. Imaging beta-amyloid burden in aging and dementia. Neurology. 2007;68(20):1718-25.

Rub U, Stratmann K, Heinsen H, Del Turco D, Ghebremedhin E, Seidel K, et al. Hierarchical Distribution of the Tau Cytoskeletal Pathology in the Thalamus of Alzheimer's Disease Patients. Journal of Alzheimer's disease : JAD. 2016;49(4):905-15.

Rupp C, Beyreuther K, Maurer K, Kins S. A presenilin 1 mutation in the first case of Alzheimer's disease: revisited. Alzheimer's & dementia : the journal of the Alzheimer's Association. 2014;10(6):869-72.

Ryan NS, Bastos-Leite AJ, Rohrer JD, Werring DJ, Fox NC, Rossor MN, et al. Cerebral microbleeds in familial Alzheimer's disease. Brain. 2011;135(Pt 1):e201.

Ryan NS, Bastos-Leite AJ, Rohrer JD, Werring DJ, Fox NC, Rossor MN, et al. Cerebral microbleeds in familial Alzheimer's disease. Brain. 2012;135(Pt 1):e201; author reply e2.

Ryan NS, Biessels GJ, Kim L, Nicholas JM, Barber PA, Walsh P, et al. Genetic determinants of white matter hyperintensities and amyloid angiopathy in familial Alzheimer's disease. Neurobiol Aging. 2015;36(12):3140-51.

Ryan NS, Fox NC. Alzheimer disease: Visual rating of atrophy aids diagnostic accuracy. Nature reviews Neurology. 2009;5(5):243-4.

Ryan NS, Fox NC. Imaging biomarkers in Alzheimer's disease. Annals of the New York Academy of Sciences. 2009;1180:20-7.

Ryan NS, Keihaninejad S, Shakespeare TJ, Lehmann M, Crutch SJ, Malone IB, et al. Magnetic resonance imaging evidence for presymptomatic change in thalamus and caudate in familial Alzheimer's disease. Brain. 2013;136(Pt 5):1399-414.

Ryan NS, Lashley T, Revesz T, Dantu K, Fox NC, Morris HR. Spontaneous ARIA (Amyloid-Related Imaging Abnormalities) and Cerebral Amyloid Angiopathy Related Inflammation in Presenilin 1-Associated Familial Alzheimer's Disease. Journal of Alzheimer's disease : JAD. 2014;44(4):1069-74.

Ryan NS, Nicholas JM, Weston PS, Liang Y, Lashley T, Guerreiro R, et al. Clinical phenotype and genetic associations in autosomal dominant familial Alzheimer's disease: a case series. Lancet Neurol. 2016.

Ryan NS, Rossor MN. Correlating familial Alzheimer's disease gene mutations with clinical phenotype. BiomarkMed. 2010;4(1):99-112.

Ryan NS, Rossor MN, Fox NC. Alzheimer's disease in the 100 years since Alzheimer's death. Brain. 2015;138(Pt 12):3816-21.

Ryman DC, Acosta-Baena N, Aisen PS, Bird T, Danek A, Fox NC, et al. Symptom onset in autosomal dominant Alzheimer disease: a systematic review and meta-analysis. Neurology. 2014;83(3):253-60.

Saito T, Suemoto T, Brouwers N, Sleegers K, Funamoto S, Mihira N, et al. Potent amyloidogenicity and pathogenicity of Abeta43. NatNeurosci. 2011;14(8):1023-32.

Sakai K, Boche D, Carare R, Johnston D, Holmes C, Love S, et al. Abeta immunotherapy for Alzheimer's disease: effects on apoE and cerebral vasculopathy. Acta Neuropathol. 2014;128(6):777-89.

Sala Frigerio C, Lau P, Troakes C, Deramecourt V, Gele P, Van Loo P, et al. On the identification of low allele frequency mosaic mutations in the brains of Alzheimer's disease patients. Alzheimer's & dementia : the journal of the Alzheimer's Association. 2015;11(11):1265-76.

Salloway S, Sperling R, Fox NC, Blennow K, Klunk W, Raskind M, et al. Two phase 3 trials of bapineuzumab in mild-to-moderate Alzheimer's disease. The New England journal of medicine. 2014;370(4):322-33.

Scahill RI, Ridgway GR, Bartlett JW, Barnes J, Ryan NS, Mead S, et al. Genetic influences on atrophy patterns in familial Alzheimer's disease: a comparison of APP and PSEN1 mutations. Journal of Alzheimer's disease : JAD. 2013;35(1):199-212.

Scahill RI, Schott JM, Stevens JM, Rossor MN, Fox NC. Mapping the evolution of regional atrophy in Alzheimer's disease: unbiased analysis of fluid-registered serial MRI. Proc NatlAcadSciUSA. 2002;99(7):4703-7.

Scheltens P, Leys D, Barkhof F, Huglo D, Weinstein HC, Vermersch P, et al. Atrophy of medial temporal lobes on MRI in "probable" Alzheimer's disease and normal ageing: diagnostic value and neuropsychological correlates. J Neurol Neurosurg Psychiatry. 1992;55(10):967-72.

Schmahmann JD. Vascular syndromes of the thalamus. Stroke. 2003;34(9):2264-78.

Schmidt R. Comparison of magnetic resonance imaging in Alzheimer's disease, vascular dementia and normal aging. Eur Neurol. 1992;32(3):164-9.

Schott JM, Crutch SJ, Carrasquillo MM, Uphill J, Shakespeare TJ, Ryan NS, et al. Genetic risk factors for the posterior cortical atrophy variant of Alzheimer's disease. Alzheimer's & dementia : the journal of the Alzheimer's Association. 2016;12(8):862-71.

Schott JM, Ridha BH, Crutch SJ, Healy DG, Uphill JB, Warrington EK, et al. Apolipoprotein e genotype modifies the phenotype of Alzheimer disease. Arch Neurol. 2006;63(1):155-6.

Schroter A, Zerr I, Henkel K, Tschampa HJ, Finkenstaedt M, Poser S. Magnetic resonance imaging in the clinical diagnosis of Creutzfeldt-Jakob disease. Arch Neurol. 2000;57(12):1751-7.

Schuff N, Woerner N, Boreta L, Kornfield T, Shaw LM, Trojanowski JQ, et al. MRI of hippocampal volume loss in early Alzheimer's disease in relation to ApoE genotype and biomarkers. Brain. 2009;132(Pt 4):1067-77.

Scolding NJ, Joseph F, Kirby PA, Mazanti I, Gray F, Mikol J, et al. Abeta-related angiitis: primary angiitis of the central nervous system associated with cerebral amyloid angiopathy. Brain. 2005;128(Pt 3):500-15.

Selkoe DJ. Alzheimer's disease: genotypes, phenotypes, and treatments. Science. 1997;275(5300):630-1.

Selkoe DJ. Soluble oligomers of the amyloid beta-protein impair synaptic plasticity and behavior. Behavioural brain research. 2008;192(1):106-13.

Sepulveda-Falla D, Barrera-Ocampo A, Hagel C, Korwitz A, Vinueza-Veloz MF, Zhou K, et al. Familial Alzheimer's disease-associated presenilin-1 alters cerebellar activity and calcium homeostasis. The Journal of clinical investigation. 2014;124(4):1552-67.

Shea YF, Chu LW, Chan AO, Ha J, Li Y, Song YQ. A systematic review of familial Alzheimer's disease: Differences in presentation of clinical features among three mutated genes and potential ethnic differences. Journal of the Formosan Medical Association = Taiwan yi zhi. 2015;115(2):67-75.

Shepherd C, McCann H, Halliday GM. Variations in the neuropathology of familial Alzheimer's disease. Acta Neuropathol. 2009;118(1):37-52.

Sherrington R, Rogaev EI, Liang Y, Rogaeva EA, Levesque G, Ikeda M, et al. Cloning of a gene bearing missense mutations in early-onset familial Alzheimer's disease. Nature. 1995;375(6534):754-60.

Shinohara M, Fujioka S, Murray ME, Wojtas A, Baker M, Rovelet-Lecrux A, et al. Regional distribution of synaptic markers and APP correlate with distinct clinicopathological features in sporadic and familial Alzheimer's disease. Brain. 2014;137(Pt 5):1533-49.

Shrimpton AE, Schelper RL, Linke RP, Hardy J, Crook R, Dickson DW, et al. A presenilin 1 mutation (L420R) in a family with early onset Alzheimer disease, seizures and cotton wool plaques, but not spastic paraparesis. Neuropathology : official journal of the Japanese Society of Neuropathology. 2007;27(3):228-32.

Silverman DH, Small GW, Chang CY, Lu CS, Kung De Aburto MA, Chen W, et al. Positron emission tomography in evaluation of dementia: Regional brain metabolism and long-term outcome. Jama. 2001;286(17):2120-7.

Sitek EJ, Narozanska E, Peplonska B, Filipek S, Barczak A, Styczynska M, et al. A patient with posterior cortical atrophy possesses a novel mutation in the presenilin 1 gene. PloS one. 2013;8(4):e61074.

Smith CD, Chebrolu H, Andersen AH, Powell DA, Lovell MA, Xiong S, et al. White matter diffusion alterations in normal women at risk of Alzheimer's disease. Neurobiol Aging. 2010.

Smith MJ, Kwok JB, McLean CA, Kril JJ, Broe GA, Nicholson GA, et al. Variable phenotype of Alzheimer's disease with spastic paraparesis. Ann Neurol. 2001;49(1):125-9.

Smith SM, Jenkinson M, Johansen-Berg H, Rueckert D, Nichols TE, Mackay CE, et al. Tract-based spatial statistics: voxelwise analysis of multi-subject diffusion data. Neuroimage. 2006;31(4):1487-505.

Smith SM, Nichols TE. Threshold-free cluster enhancement: addressing problems of smoothing, threshold dependence and localisation in cluster inference. Neuroimage. 2009;44(1):83-98.

Snider BJ, Norton J, Coats MA, Chakraverty S, Hou CE, Jervis R, et al. Novel presenilin 1 mutation (S170F) causing Alzheimer disease with Lewy bodies in the third decade of life. Arch Neurol. 2005;62(12):1821-30.

Snowden JS, Stopford CL, Julien CL, Thompson JC, Davidson Y, Gibbons L, et al. Cognitive phenotypes in Alzheimer's disease and genetic risk. Cortex; a journal devoted to the study of the nervous system and behavior. 2007;43(7):835-45.

Song SK, Sun SW, Ju WK, Lin SJ, Cross AH, Neufeld AH. Diffusion tensor imaging detects and differentiates axon and myelin degeneration in mouse optic nerve after retinal ischemia. Neuroimage. 2003;20(3):1714-22.

Sorbi S, Nacmias B, Forleo P, Piacentini S, Latorraca S, Amaducci L. Epistatic effect of APP717 mutation and apolipoprotein E genotype in familial Alzheimer's disease. Ann Neurol. 1995;38(1):124-7.

Spain A, Daumas S, Lifshitz J, Rhodes J, Andrews PJ, Horsburgh K, et al. Mild fluid percussion injury in mice produces evolving selective axonal pathology and cognitive deficits relevant to human brain injury. Journal of neurotrauma. 2010;27(8):1429-38.

Sperling R, Salloway S, Brooks DJ, Tampieri D, Barakos J, Fox NC, et al. Amyloid-related imaging abnormalities in patients with Alzheimer's disease treated with bapineuzumab: a retrospective analysis. Lancet Neurol. 2012;11(3):241-9.

Sperling RA, Aisen PS, Beckett LA, Bennett DA, Craft S, Fagan AM, et al. Toward defining the preclinical stages of Alzheimer's disease: recommendations from the National Institute on Aging-Alzheimer's Association workgroups on diagnostic guidelines for Alzheimer's disease. AlzheimersDement. 2011;7(3):280-92.

Sperling RA, Jack CR, Jr., Black SE, Frosch MP, Greenberg SM, Hyman BT, et al. Amyloid-related imaging abnormalities in amyloid-modifying therapeutic trials: Recommendations from the Alzheimer's Association Research Roundtable Workgroup. AlzheimersDement. 2011;7(4):367-85.

Sperling RA, Rentz DM, Johnson KA, Karlawish J, Donohue M, Salmon DP, et al. The A4 Study: Stopping AD Before Symptoms Begin? Science translational medicine. 2014;6(228):228fs13.

Stebbins GT, Murphy CM. Diffusion tensor imaging in Alzheimer's disease and mild cognitive impairment. Behavioural neurology. 2009;21(1):39-49.

Steiner H, Revesz T, Neumann M, Romig H, Grim MG, Pesold B, et al. A pathogenic presenilin-1 deletion causes abberrant Abeta 42 production in the absence of congophilic amyloid plaques. J BiolChem. 2001;276(10):7233-9.

Stevens JC, Beck J, Lukic A, Ryan N, Abbs S, Collinge J, et al. Familial Alzheimer's disease and inherited prion disease in the UK are poorly ascertained. J Neurol Neurosurg Psychiatry. 2011;82(9):1054-7.

Storandt M, Balota DA, Aschenbrenner AJ, Morris JC. Clinical and psychological characteristics of the initial cohort of the Dominantly Inherited Alzheimer Network (DIAN). Neuropsychology. 2014;28(1):19-29.

Stough JV, Glaister J, Ye C, Ying SH, Prince JL, Carass A. Automatic method for thalamus parcellation using multi-modal feature classification. Medical image computing and computer-assisted intervention : MICCAI International Conference on Medical Image Computing and Computer-Assisted Intervention. 2014;17(Pt 3):169-76.

Sudre CH, Cardoso MJ, Bouvy WH, Biessels GJ, Barnes J, Ourselin S. Bayesian model selection for pathological neuroimaging data applied to white matter lesion segmentation. IEEE transactions on medical imaging. 2015;34(10):2079-102.

Suenaga T, Hirano A, Llena JF, Yen SH, Dickson DW. Modified Bielschowsky stain and immunohistochemical studies on striatal plaques in Alzheimer's disease. Acta Neuropathol. 1990;80(3):280-6.

Sun SW, Song SK, Harms MP, Lin SJ, Holtzman DM, Merchant KM, et al. Detection of age-dependent brain injury in a mouse model of brain amyloidosis associated with Alzheimer's disease using magnetic resonance diffusion tensor imaging. Experimental neurology. 2005;191(1):77-85.

Szaruga M, Veugelen S, Benurwar M, Lismont S, Sepulveda-Falla D, Lleo A, et al. Qualitative changes in human gamma-secretase underlie familial Alzheimer's disease. The Journal of experimental medicine. 2015;212(12):2003-13.

Tabira T, Chui DH, Nakayama H, Kuroda S, Shibuya M. Alzheimer's disease with spastic paresis and cotton wool type plaques. J Neurosci Res. 2002;70(3):367-72.

Takagi-Niidome S, Sasaki T, Osawa S, Sato T, Morishima K, Cai T, et al. Cooperative roles of hydrophilic loop 1 and the C-terminus of presenilin 1 in the substrate-gating mechanism of gamma-secretase. J Neurosci. 2015;35(6):2646-56.

Takao M, Ghetti B, Hayakawa I, Ikeda E, Fukuuchi Y, Miravalle L, et al. A novel mutation (G217D) in the Presenilin 1 gene (PSEN1) in a Japanese family: presenile

dementia and parkinsonism are associated with cotton wool plaques in the cortex and striatum. Acta Neuropathol. 2002;104(2):155-70.

Takeo K, Tanimura S, Shinoda T, Osawa S, Zahariev IK, Takegami N, et al. Allosteric regulation of gamma-secretase activity by a phenylimidazole-type gamma-secretase modulator. Proceedings of the National Academy of Sciences of the United States of America. 2014;111(29):10544-9.

Tang M, Ryman DC, McDade E, Jasielec MS, Buckles VD, Cairns NJ, et al. Neurological manifestations of autosomal dominant familial Alzheimer's disease: a comparison of the published literature with the Dominantly Inherited Alzheimer Network observational study (DIAN-OBS). Lancet Neurol. 2016;15(13):1317-25.

Tang-Wai D, Lewis P, Boeve B, Hutton M, Golde T, Baker M, et al. Familial frontotemporal dementia associated with a novel presenilin-1 mutation. Dement Geriatr Cogn Disord. 2002;14(1):13-21.

Tang-Wai DF, Graff-Radford NR, Boeve BF, Dickson DW, Parisi JE, Crook R, et al. Clinical, genetic, and neuropathologic characteristics of posterior cortical atrophy. Neurology. 2004;63(7):1168-74.

Thal DR, Ghebremedhin E, Rub U, Yamaguchi H, Del Tredici K, Braak H. Two types of sporadic cerebral amyloid angiopathy. J Neuropathol ExpNeurol. 2002;61(3):282-93.

Thanprasertsuk S, Martinez-Ramirez S, Pontes-Neto OM, Ni J, Ayres A, Reed A, et al. Posterior white matter disease distribution as a predictor of amyloid angiopathy. Neurology. 2014.

Tovar-Moll F, Evangelou IE, Chiu AW, Richert ND, Ostuni JL, Ohayon JM, et al. Thalamic involvement and its impact on clinical disability in patients with multiple sclerosis: a diffusion tensor imaging study at 3T. AJNR American journal of neuroradiology. 2009;30(7):1380-6.

Van Broeckhoven C, Backhovens H, Cruts M, Martin JJ, Crook R, Houlden H, et al. APOE genotype does not modulate age of onset in families with chromosome 14 encoded Alzheimer's disease. Neurosci Lett. 1994;169(1-2):179-80.

Van Broeckhoven C, Haan J, Bakker E, Hardy JA, Van Hul W, Wehnert A, et al. Amyloid beta protein precursor gene and hereditary cerebral hemorrhage with amyloidosis (Dutch). Science. 1990;248(4959):1120-2.

van der Flier WM, Schoonenboom SN, Pijnenburg YA, Fox NC, Scheltens P. The effect of APOE genotype on clinical phenotype in Alzheimer disease. Neurology. 2006;67(3):526-7.

Van der Werf YD, Jolles J, Witter MP, Uylings HB. Contributions of thalamic nuclei to declarative memory functioning. Cortex; a journal devoted to the study of the nervous system and behavior. 2003;39(4-5):1047-62.

van Rooden S, van der Grond J, van den Boom R, Haan J, Linn J, Greenberg SM, et al. Descriptive analysis of the Boston criteria applied to a Dutch-type cerebral amyloid angiopathy population. Stroke. 2009;40(9):3022-7.

Vellas B, Black R, Thal LJ, Fox NC, Daniels M, McLennan G, et al. Long-term follow-up of patients immunized with AN1792: reduced functional decline in antibody responders. CurrAlzheimer Res. 2009;6(2):144-51.

Verkkoniemi A, Somer M, Rinne JO, Myllykangas L, Crook R, Hardy J, et al. Variant Alzheimer's disease with spastic paraparesis: clinical characterization. Neurology. 2000;54(5):1103-9.

Victoroff J, Ross GW, Benson DF, Verity MA, Vinters HV. Posterior cortical atrophy. Neuropathologic correlations. Arch Neurol. 1994;51(3):269-74.

Villemagne VL, Ataka S, Mizuno T, Brooks WS, Wada Y, Kondo M, et al. High striatal amyloid beta-peptide deposition across different autosomal Alzheimer disease mutation types. Arch Neurol. 2009;66(12):1537-44.

Wahlund LO, Barkhof F, Fazekas F, Bronge L, Augustin M, Sjogren M, et al. A new rating scale for age-related white matter changes applicable to MRI and CT. Stroke. 2001;32(6):1318-22.

Waldemar G, Dubois B, Emre M, Georges J, McKeith IG, Rossor M, et al. Recommendations for the diagnosis and management of Alzheimer's disease and other disorders associated with dementia: EFNS guideline. Eur J Neurol. 2007;14(1):e1-26.

Wallon D, Rousseau S, Rovelet-Lecrux A, Quillard-Muraine M, Guyant-Marechal L, Martinaud O, et al. The French series of autosomal dominant early onset Alzheimer's disease cases: mutation spectrum and cerebrospinal fluid biomarkers. Journal of Alzheimer's disease : JAD. 2012;30(4):847-56.

Walton J, Ryan N, Crutch S, Rohrer JD, Fox N. The importance of dementia support groups. Bmj. 2015;351:h3875.

Wang Y, Gupta A, Liu Z, Zhang H, Escolar ML, Gilmore JH, et al. DTI registration in atlas based fiber analysis of infantile Krabbe disease. Neuroimage. 2011;55(4):1577-86.

Warfield SK, Zou KH, Wells WM. Simultaneous truth and performance level estimation (STAPLE): an algorithm for the validation of image segmentation. IEEE transactions on medical imaging. 2004;23(7):903-21.

Warren JD, Rohrer JD, Hardy J. Disintegrating brain networks: from syndromes to molecular nexopathies. Neuron. 2012;73(6):1060-2.

Warren JD, Rohrer JD, Schott JM, Fox NC, Hardy J, Rossor MN. Molecular nexopathies: a new paradigm of neurodegenerative disease. Trends Neurosci. 2013;36(10):561-9.

Warrington EK, Agnew SK, Kennedy AM, Rossor MN. Neuropsychological profiles of familial Alzheimer's disease associated with mutations in the presenilin 1 and amyloid precursor protein genes. J Neurol. 2001;248(1):45-50.

Weiskopf N, Lutti A, Helms G, Novak M, Ashburner J, Hutton C. Unified segmentation based correction of R1 brain maps for RF transmit field inhomogeneities (UNICORT). Neuroimage. 2011;54(3):2116-24.

Weller RO, Boche D, Nicoll JA. Microvasculature changes and cerebral amyloid angiopathy in Alzheimer's disease and their potential impact on therapy. Acta Neuropathol. 2009;118(1):87-102.

Weller RO, Hawkes CA, Kalaria RN, Werring DJ, Carare RO. White matter changes in dementia: role of impaired drainage of interstitial fluid. Brain pathology. 2015;25(1):63-78.

Weston PS, Nicholas JM, Lehmann M, Ryan NS, Liang Y, Macpherson K, et al. Presymptomatic cortical thinning in familial Alzheimer disease: A longitudinal MRI study. Neurology. 2016;87(19):2050-7.

Whitehouse P, Maurer K, Ballenger JF. Concepts of Alzheimer's Disease: Biological, Clinical and Cultural Perspectives. Baltimore, Maryland: John Hopkins University Press; 2000.

Whitwell JL, Josephs KA, Murray ME, Kantarci K, Przybelski SA, Weigand SD, et al. MRI correlates of neurofibrillary tangle pathology at autopsy: a voxel-based morphometry study. Neurology. 2008;71(10):743-9.

Whitwell JL, Kantarci K, Weigand SD, Lundt ES, Gunter JL, Duffy JR, et al. Microbleeds in Atypical Presentations of Alzheimer's Disease: A Comparison to Dementia of the Alzheimer's Type. Journal of Alzheimer's disease : JAD. 2015.

Wiegell MR, Tuch DS, Larsson HBW, Wedeen VJ. Angular differentiation of thalamic nuclei by quantitative DTI. Proc Int Soc Mag Reson Med. 2000;8(481.):Abstract.

Wijsman EM, Daw EW, Yu X, Steinbart EJ, Nochlin D, Bird TD, et al. APOE and other loci affect age-at-onset in Alzheimer's disease families with PS2 mutation. American journal of medical genetics Part B, Neuropsychiatric genetics : the official publication of the International Society of Psychiatric Genetics. 2005;132B(1):14-20.

Wilson S, Raghupathi R, Saatman KE, MacKinnon MA, McIntosh TK, Graham DI. Continued in situ DNA fragmentation of microglia/macrophages in white matter weeks and months after traumatic brain injury. Journal of neurotrauma. 2004;21(3):239-50.

Wirths O, Weis J, Szczygielski J, Multhaup G, Bayer TA. Axonopathy in an APP/PS1 transgenic mouse model of Alzheimer's disease. Acta Neuropathol. 2006;111(4):312-9.

Wray S, Self M, Consortium NPsDi, Consortium NHsDi, Consortium NAi, Lewis PA, et al. Creation of an open-access, mutation-defined fibroblast resource for neurological disease research. PloS one. 2012;7(8):e43099.

Xuereb JH, Perry RH, Candy JM, Perry EK, Marshall E, Bonham JR. Nerve cell loss in the thalamus in Alzheimer's disease and Parkinson's disease. Brain. 1991;114 (Pt 3):1363-79.

Yamada M. Cerebral amyloid angiopathy: emerging concepts. Journal of stroke. 2015;17(1):17-30.

Yasuda M, Maeda K, Ikejiri Y, Kawamata T, Kuroda S, Tanaka C. A novel missense mutation in the presenilin-1 gene in a familial Alzheimer's disease pedigree with abundant amyloid angiopathy. Neurosci Lett. 1997;232(1):29-32.

Yasuda M, Maeda S, Kawamata T, Tamaoka A, Yamamoto Y, Kuroda S, et al. Novel presenilin-1 mutation with widespread cortical amyloid deposition but limited cerebral amyloid angiopathy. J Neurol Neurosurg Psychiatry. 2000;68(2):220-3.

Yokota O, Terada S, Ishizu H, Ujike H, Ishihara T, Namba M, et al. Variability and heterogeneity in Alzheimer's disease with cotton wool plaques: a clinicopathological study of four autopsy cases. Acta Neuropathol. 2003;106(4):348-56.

Zarea A, Charbonnier C, Rovelet-Lecrux A, Nicolas G, Rousseau S, Borden A, et al. Seizures in dominantly inherited Alzheimer disease. Neurology. 2016;87(9):912-9.

Zarow C, Vinters HV, Ellis WG, Weiner MW, Mungas D, White L, et al. Correlates of hippocampal neuron number in Alzheimer's disease and ischemic vascular dementia. Ann Neurol. 2005;57(6):896-903.

Zekanowski C, Golan MP, Krzysko KA, Lipczynska-Lojkowska W, Filipek S, Kowalska A, et al. Two novel presenilin 1 gene mutations connected with frontotemporal dementia-like clinical phenotype: genetic and bioinformatic assessment. ExpNeurol. 2006;200(1):82-8.

Zhang H, Schneider T, Wheeler-Kingshott CA, Alexander DC. NODDI: practical in vivo neurite orientation dispersion and density imaging of the human brain. Neuroimage. 2012;61(4):1000-16.

Zhang H, Yushkevich PA, Alexander DC, Gee JC. Deformable registration of diffusion tensor MR images with explicit orientation optimization. Medical image analysis. 2006;10(5):764-85.

Zola-Morgan S. Localization of brain function: the legacy of Franz Joseph Gall (1758-1828). Annual review of neuroscience. 1995;18:359-83.

13 Glossary

AAO: Age at onset

Aβ: amyloid-beta

ABCA7: ATP-binding cassette, sub-family A, member 7 gene

AD: Alzheimer's disease

ADAS-Cog: Alzheimer's disease assessment scale, cognitive subscale

ApoE: Apolipoprotein E

APP: Amyloid precursor protein

API: Alzheimer's Prevention Initiative

ARIA: Amyloid-related imaging abnormalities

ARWMC: Age-related white matter change

AxD: Axial diffusivity

BACE-1: β-site amyloid precursor protein cleaving enzyme

BIN1: Bridging integrator 1

CAA: Cerebral amyloid angiopathy

CAA-ri: CAA-related inflammation

CBD: Corticobasal degeneration

CERAD: Consortium to Establish a Registry for Alzheimer's disease

CJD: Creutzfold-Jakob disease

CLU: Clusterin

CNTNAP5: Contactin-associated protein-like 5

CR1: Complement receptor type 1

CSF: Cerebrospinal fluid

CT: Computed tomography

DARTEL: Diffeomorphic anatomical registration through exponentiated lie algebra

DIAN: Dominantly inherited Alzheimer network

DLB: Dementia with Lewy bodies

DRC: Dementia Research Centre

DTI: Diffusion tensor imaging

DTI-TK: Diffusion tensor imaging toolkit

DWI: Diffusion-weighted imaging

EPHA1: EPH receptor A1

FA: Fractional anisotropy

FAD: Familial Alzheimer's disease

FAM46A: Family with sequence similarity 46, member A1

FDG-PET: Fluorodeoxyglucose positron emission tomography

FLAIR: Fluid-attenuated inversion recovery

FLIRT: FMRIB's (Oxford centre for functional magnetic resonance imaging of the brain) linear image registration tool

fMRI: Functional magnetic resonance imaging

FTD: Frontotemporal dementia

FWE: Family-wise error

GDA: Graded difficulty arithmetic test

GFAP: Glial fibrillary acidic protein

GNT: Graded naming test

GRE: Gradient echo

HLA-DRB5-HLA-DRB1: Major histocompatibility complex, class II, DR beta 5 and DR beta 1

ICC: Intra-class correlation co-efficient

IQ: Intelligence quotient

LBP: Lewy body pathology

LP: Lumbar puncture

LPA: Logopenic progressive aphasia

MAPS: Multi-atlas propogation and segmentation

MAPT: Microtubule-associated protein tau

MBP: Myelin basic protein

MC: Mutation carrier

MCI: Mild cognitive impairment

MD: Mean diffusivity

MMSE: Mini-mental state examination

MPRAGE: Magnetization-prepared rapid acquisition with gradient echo

MRI: Magnetic resonance imaging

MS4A6A: Membrane-spanning 4-domains, subfamily A, member 6A

PCA: Posterior cortical atrophy

PCR: Polymerase chain reaction

PET: Positron emission tomography

PIB: Pittsburgh compound B

PICALM: Phosphatidylinositol binding clathrin assembly protein

PMC: Presymptomatic mutation carrier

PPA: Primary progressive aphasia

PRNP: Prion protein

PSEN1: Presenilin 1

PSEN2: Presenilin 2

PTK2B: Protein tyrosine kinase 2 beta

RD: Radial diffusivity

RMT: Recognition memory test

ROI: Region of interest

SD: Standard deviation

SEMA3C: Semaphorin 3C

SMC: Symptomatic mutation carrier

SORL1: Sortilin-related receptor with A-type repeats

SPECT: Single photon emission computed tomography

SWI: Susceptibility-weighted imaging

TBSS: Tract-based spatial statistics

TFCE: Threshold-free cluster enhancement

TIV: Total intracranial volume

TREM2: Triggering receptor expressed on myeloid cells 2

VBM: Voxel-based morphometry

WMH: White matter hyperintensity